# Functional Characterization of Prostate Cancer Biomarkers

Dissertation

zur

Erlangung der naturwissenschaftlichen Doktorwürde

(Dr. sc. nat.)

vorgelegt der

Mathematisch-naturwissenschaftlichen Fakultät

der

Universität Zürich

von

**JOSEFINE GERHARDT**

aus

Deutschland

Promotionskomitee

Prof. Dr. Roland Wenger (Vorsitz)

Prof. Dr. Glen Kristiansen (Leitung der Dissertation)

Prof. Dr. Burkhard Becher

Zürich, 2011

Meinen Liebsten

# Acknowledgements

This page is dedicated to all the people who contributed to the successful completion of this thesis.

I would particularly like to thank Prof. Dr. Glen Kristiansen for supervision of this thesis, for his enthusiasm and for giving me the required freedom to complete the project.
I would like to thank Prof. Dr. Roland Wenger for chairing the thesis committee and for his stimulating suggestions during the committee meetings and, if necessary, beyond.
Furthermore, I thank Prof. Dr. Burkhard Becher for being committee member and for his valuable scientific input during the committee meetings.
I thank Prof. Dr. Lars-Christian Horn for the external review of this thesis.

Special thanks go to Oralea Büchi for excellent, efficient and patient performance of the instructed experiments.
I would like to thank Annette Bohnert for excellent technical assistance.
I would like to further acknowledge Matteo Montani, Corinna Steinbrech, Florian Fritzsche, Silvia Behnke, Martina Storz, Heike Liewen, Frank Stenner, the people from the division of cytology, Peter Wild, Ashkan Mortezavi, Irina Hofmann, Marc Beer, Fabian Huber, Thomas Hermanns, Michael Müntener, Manfred Dietel, Klaus Jung, Carsten Stephan and Britta Beyer for providing data or patient material or for collaborating on experiments that were included in this thesis.

I would like to thank the people in our and in neighbouring labs Verena Tischler, Gunther Boysen, Van-Duc Luu, Markus Rechsteiner, Peter Schraml, Dorothee Pflüger, Anna Nowicka, Laura Morra, Silvia Casagrande, Martina Storz, Susanne Dettwiler, Adriana von Teichmann, Sonja Brun-Schmid, Marion Bawohl, Friederike Böhm, Nicole Grosse, Polina Furmanova and Katrin Orlowski for experimental support and a nice working atmosphere.

Außerdem möchte ich Birgit, Marion, Estelle, Noemi, Juliane, Nicole, André, Melanie Birke und Duc, Gunther, Jeannette, Verena, Georg und allen Volleyballern danken für die schöne Zeit, die wir gemeinsam in Züri verbracht haben. Euch allen wünsche ich alles Gute für die Zukunft, auf ein baldiges Wiedersehen!
Besonderer Dank gilt Sabrina, Marion, Thomas, Estelle, Juliane und Dorothee, bei denen ich immer willkommen war.

Ein großes Dankeschön geht an meine Eltern und meine Familie, die mich auf dem langen Weg begleitet, unterstützt und immer wieder ermutigt haben.
Die letzten Zeilen sind für Steffen reserviert. Ich danke dir für die große Unterstützung in allen Belangen vor und hinter den Kulissen.

Thank you very much! Vielen Dank! Merci beaucoup! Mille grazie! Merci vielmal!

# Declaration

Herewith I declare that I have written this thesis myself and that I have only used the explicitly quoted references. Several text passages and figures have been taken from [1] and [2], in case of the manuscript from Montani and Gerhardt *et al.* with agreement of M. Montani. Further, I declare that all experiments have been performed by myself with assistance from Oralea Büchi and Annette Bohnert with the exceptions given in **Tab. 1**. These experiments were conducted in cooperation with the listed persons.

**Tab. 1 Experiments that were performed in cooperation with the listed persons.**

| Experiment | Persons |
|---|---|
| Collection of samples and patient data | |
| tissue | Peter Wild[1], Ashkan Mortezavi[1], Irina Hofmann[1], Marc Beer[1], Fabian Huber[1], Thomas Hermanns[2], Michael Müntener[2], Glen Kristiansen[1,3], Florian Fritzsche[1,3], Manfred Dietel[3], Klaus Jung[4], Carsten Stephan[5], |
| sera | Heike Liewen[6], Frank Stenner[6] |
| TMA construction | |
| TMA #1 | Martina Storz[1] |
| TMA #2 | Britta Beyer[3], Glen Kristiansen[1,3] |
| Immunohistochemistry | Silvia Behnke[1] |
| Immunofluorescence | Silvia Behnke[1] |
| Evaluation of staining intensities | |
| TMA #1 | |
| CANT1 | Florian Fritzsche[1,3], Glen Kristiansen[1,3] |
| FOXA1 | Matteo Montani[7], Glen Kristiansen[1,3] |
| TMA #2 | Corinna Steinbrech[1], Glen Kristiansen[1,3] |
| Statistical analyses of TMA data | |
| CANT1 | Corinna Steinbrech[1], Glen Kristiansen[1,3] |
| FOXA1 | Matteo Montani[7], Glen Kristiansen[1,3] |
| Generation of cell blocks | Division of cytology[1] |
| ELISA | Heike Liewen[6], Frank Stenner[6] |

[1] Department of Surgical Pathology, UniversitätsSpital Zürich, Zurich, Switzerland
[2] Department of Urology, UniversitätsSpital Zürich, Zurich, Switzerland
[3] Institute of Pathology, Charité–Universitätsmedizin Berlin, Berlin, Germany
[4] Berlin Institute for Urologic Research, Berlin, Germany
[5] Department of Urology, Charité–Universitätsmedizin Berlin, Berlin, Germany
[6] Clinic and Policlinic for Oncology, UniversitätsSpital Zürich, Zurich, Switzerland
[7] Institute of Pathology, University of Bern, Switzerland

Josefine Gerhardt, Zurich, Switzerland

# Index

# Summary

With the onset of prostate-specific antigen (PSA) screening two decades ago the number of prostate cancer suspicious cases has markedly increased. Due to the lack of specificity men with elevated PSA levels need to be biopsied to confirm the diagnosis. In order to reduce the number of the unnecessary taking of biopsies, new specific and non-invasive biomarkers are required to facilitate prostate cancer diagnosis. Here, we suggest calcium-activated nucleotidase (CANT) 1 as a novel serum marker candidate for further validation.

As a result of serum PSA measurement, also the number of confirmed prostate cancer cases has risen. Especially more insignificant carcinomas are detected, which would never have affected the patients' life. Thus, overtreatment of these cases and the therapy-induced morbidity is a big issue in clinical prostate cancer management. Within this study, we identify two potential prognostic biomarkers to predict the risk of disease recurrence. This risk is reduced in patients with very high CANT1 protein levels in their prostatectomy specimens. Applying the histochemical score to quantify CANT1 protein levels, CANT1 is shown to be an independent prognostic biomarker. In contrast, strong forkhead box (FOX) A1 expression is prognostically unfavourable. Since an ideal prognostic marker should be applied to pre-treatment samples, analysis of both immunohistochemical markers in large biopsy cohorts is strongly recommended.

Once the tumor has recurred, progression to castration-resistance is likely. Further elucidation of the underlying mechanisms is necessary to progress in the development of life-prolonging therapies for these patients. Here, we show that despite ubiquitous overexpression of Golgi membrane protein (GOLM) 1 in prostate carcinomas, this protein has no functional relevance for the analyzed cancer cells. In contrast, knockdown of FOXA1 reduces *in vitro* tumorigenicity. Moreover, FOXA1 expression increases with prostate cancer progression and is associated with poor prognosis, especially in cases with low androgen receptor levels. Thus, we conclude that FOXA1 upregulation is a novel mechanism of castration-resistance for prostate cancer cells. Additionally, we reveal that CANT1 expression is already elevated in the precursor lesion prostatic intraepithelial neoplasia. *In vitro* experiments establish the secretion of CANT1 as well as the reduction of *in vitro* tumorigenicity accompanied by G1 cell cycle arrest upon CANT1 knockdown. Furthermore, induction of selected unfolded protein response target genes and enhancement of CANT1 mRNA expression upon stress induction in the endoplasmic reticulum (ER) are indicated. We thus propose that CANT1 is upregulated in prostate carcinomas to counteract tumor-associated ER stress. According to our model, this might be achieved by the interplay

between soluble truncated CANT1, which prevents calcium release from the ER, and full-length CANT1, which regulates protein folding. Since knockdown of CANT1 heavily impaired proliferation of the hormone-independent cell line PC-3, which is a model for castration-resistant prostate carcinomas, CANT1 might be an interesting therapeutic target for this group of prostate carcinomas.

# Zusammenfassung

Seit Beginn des prostata-spezifischen Antigen (PSA)-Screenings vor zwei Jahrzehnten ist die Zahl der Prostatakrebs-Verdachtsfälle deutlich angestiegen. Aufgrund der fehlenden Spezifität müssen Männer mit einem erhöhten PSA-Level biopsiert werden, um die Diagnose zu bestätigen. Zur Reduktion der unnötigen Entnahmen von Biopsien werden neue spezifische und nicht-invasive Biomarker benötigt, die die Prostatakrebsdiagnose vereinfachen. In der vorliegenden Arbeit schlagen wir Calcium-aktivierte Nukleotidase (CANT) 1 als neuen Serummarkerkandidaten für die weitere Evaluierung vor.

Als Folge der Serum-PSA-Messung ist auch die Zahl bestätigter Prostatakarzinomfälle gestiegen. Dabei werden hauptsächlich mehr insignifikante Karzinome detektiert, die niemals das Leben der Patienten beeinträchtigt hätten. Daher ist die Überbehandlung dieser Fälle und die therapieinduzierte Morbidität ein großes Thema im klinischen Management von Prostatakrebs. In dieser Studie identifizieren wir zwei potentielle prognostische Biomarker zur Vorhersage des Rezidivrisikos. Dieses Risiko ist in Patienten, deren Prostatektomie-präparate sehr hohe CANT1-Proteinmengen aufweisen, reduziert. Es wird gezeigt, dass CANT1 unter Anwendung des histochemischen Scores für die Quantifizierung von CANT1-Proteinmengen ein unabhängiger prognostischer Biomarker ist. Im Gegensatz dazu ist eine starke Expression von Forkhead Box (FOX) A1 prognostisch ungünstig. Da ein idealer prognostischer Marker an Proben, die vor der ersten Behandlung entnommen wurden, angewendet werden sollte, wird die Analyse von beiden immunhistochemischen Markern in großen Biopsiekohorten empfohlen.

Sobald ein Rezidiv des Tumors auftritt, ist die Progression zur Kastrationsresistenz sehr wahrscheinlich. Die weitere Aufklärung der darunterliegenden Mechanismen ist notwendig, um die Entwicklung lebensverlängernder Therapien für diese Patienten voranzutreiben. Hier zeigen wir, dass Golgimembranprotein (GOLM) 1 trotz ubiquitärer Überexpression in Prostatakarzinomen keine funktionelle Relevanz für die analysierten Krebszellen hat. Im Gegensatz dazu reduziert die Herunterregulierung von FOXA1 die *in vitro*-Tumorigenität. Darüber hinaus steigt die Expression von FOXA1 mit der Progression des Prostatakarzinoms und ist mit einer schlechten Prognose assoziiert, besonders in Fällen mit niedrigen Androgenrezeptormengen. Daher schlussfolgern wir, dass FOXA1-Aufregulation einen neuartigen Mechanismus der Kastrationsresistenz von Prostatakrebszellen darstellt. Zusätzlich weisen wir eine erhöhte CANT1-Expression schon in der Vorläuferläsion der prostatischen intraepithelialen Neoplasie nach. *In vitro*-Experimente zeigen die Sekretion von CANT1 sowie eine Reduktion der *in vitro*-Tumorigenität nach CANT1-Herunterregulierung,

die von einem G1-Zellzyklusarrest begleitet wird. Weiterhin deutet sich eine Induktion von ausgewählten Zielgenen der sogenannten „unfolded protein response“ sowie eine Verstärkung der CANT1-mRNA-Expression nach Stressinduktion im endoplasmatischen Retikulum (ER) an. Daher postulieren wir, dass CANT1 in Prostatakarzinomen aufreguliert ist, um dem tumorassoziierten ER-Stress entgegenzuwirken. Unserem Modell zufolge könnte dies erreicht werden durch ein Zusammenspiel zwischen löslichem abgespaltenem CANT1, welches die Calcium-Freisetzung im ER verhindert, und membranverankertem CANT1, welches die Proteinfaltung reguliert. Da die Herunterregulierung von CANT1 die Proliferation der hormonunabhängigen Zelllinie PC-3, welche als Modell für kastrationsresistente Prostatakarzinome gilt, sehr stark beeinträchtigt, könnte CANT1 ein interessantes therapeutisches Zielprotein für diese Gruppe von Prostatakarzinomen sein.

# 1 Introduction

## *1.1 The clinical aspects of prostate cancer*

### 1.1.1 An overview of prostate histology

The prostate surrounds the urethra and the healthy organ weighs 30 to 40 g in adult men. It is organized in three zones, the inner transition zone and the outer peripheral and central zones. Histologically, the prostate contains epithelial and stromal parts, whereas the epithelial cells are arranged in glands. These consist of ducts that branch out from the urethra. Each gland is framed by a secretory (inner) and basal (outer) cell layer. Prostatic intraepithelial neoplasia (PIN), which is believed to be the precursor lesion of prostate cancer [3, 4], is characterized by a benign architecture with large and branched glands. However, nuclei are atypic, they are enlarged and hyperchromatic and have prominent nucleoli.

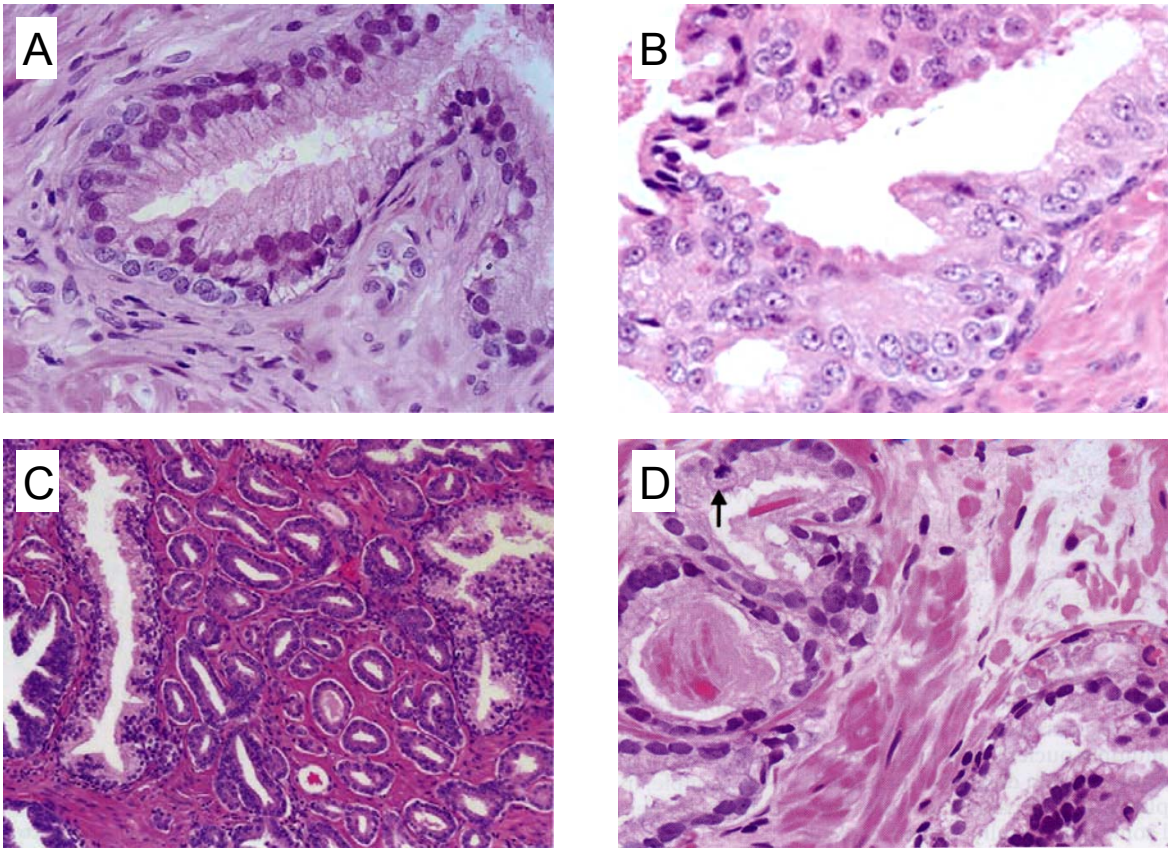


**Fig. 1 Prostate histology.**

Hematoxylin & eosin stainings of human prostatic tissues. **(A)** Benign prostate gland with secretory and basal cells surrounded by stroma. **(B)** High grade PIN (HGPIN), note the prominent nucleoli. **(C)** Prostate adenocarcinoma with small glands (center) infiltrating between benign glands. **(D)** Prostate adenocarcinoma showing enlarged nuclei with nucleoli. Note the mitotic figure (arrow). A benign gland is seen in the lower right. A, C and D from [5], B from [4].

The main characteristic of prostate adenocarcinoma is the absence of basal cells. Further, glands are small, tend to crowd and infiltrate between benign glands. Nuclei look similar to PIN, additionally, mitotic figures and apoptotic bodies are observed. Mucinous secretions can be found in the lumina of the glands [5] (**Fig. 1**).

### 1.1.2 Epidemiology, risk factors and general course of the disease

Prostate cancer is diagnosed 5500 to 6000 times a year in Switzerland and is therefore the most common malignancy in men. However, regarding mortality, with 1300 deaths per year prostate cancer stays behind lung cancer, which has a death rate of 2000 cases per year [6]. Similar incidence and mortality rates are observed in other western countries [7]. Yet, in Afroamericans incidence is up to 34 % higher and mortality is even two fold elevated compared to Caucasians [8]. This difference is probably genetically determined, as it is reflected in the American population [9]. In contrast, the clearly lower incidence of prostate cancer among Japanese is believed to be related to their low-fat diet with high concentrations of phytoestrogens [9].

Independent on the ethnic origin, age is the major risk factor for prostate cancer [9]. Autopsies revealed that actually 80 % of men above 80 have prostate cancer [10] (**Fig. 2**). The fact, that most of these tumors are never diagnosed, reflects the disease course. Prostate cancer is usually slowly growing and most of the tumors never affect the patient and are therefore called insignificant carcinomas. However, a significant fraction of the cases progresses and metastasizes or relapses after initial surgery or radiotherapy. These tumors are generally treated by hormonal therapy, which leads to tumor shrinkage in the beginning. Finally, basically all of these tumors start growing again within two years and are then called castration-resistant prostate carcinomas (CRPC) [9].

Further, family history influences the risk for prostate cancer. Men, whose brother or father suffers from the disease, have a double risk to develop prostate cancer theirselves [11].


**Fig. 2 Prevalence of prostate cancer.**

Relation between prevalence of prostate cancer at autopsy, clinically diagnosed cases and prostate cancer deaths. *Prostate cancer at autopsy implies examination of prostate in men dying from reasons other than prostate cancer and undergoing autopsy. From [9].

### 1.1.3 Diagnosis

#### 1.1.3.1 Diagnostic scheme at the University Hospital Zurich

The initial indication to conduct a more elaborate diagnostic procedure for prostate cancer is usually a positive digital rectal examination (DRE) or elevated levels of prostate-specific antigen (PSA) in serum. The threshold at the University Hospital Zurich ranges from 2.5 to 4 ng/ml, depending on the age of the patient and the difference compared to the previous measurement [11]. However, increased PSA secretion into the blood also occurs in benign prostatic hyperplasia (BPH) or prostatitis. Further, serum PSA levels depend on age, body mass index and race. Hence, most of the men with increased PSA levels actually do not have prostate cancer [8]. Therefore, for further discrimination, ten systematic needle biopsies are taken transrectal, analyzed histologically and the Gleason score is determined. For the final diagnosis of suspicious lesions, immunohistochemistry is applied. The presence of basal cells in normal prostate glands is proven by expression of the marker proteins p63 or cytokeratin 5/6, whereas tumor cells can be identified by strong staining with alpha-methylacyl-CoA racemase (AMACR), Golgi membrane protein (GOLM) 1 and fatty acid synthase (FASN) antibodies. In the case of a positive prostate cancer diagnosis, additional imaging techniques are employed to detect metastases. Since no unified diagnostic guidelines exist for prostate cancer, the scheme varies between hospitals and countries [9].

In 2004, the World Health Organization called to search for novel biomarkers with a higher specificity than serum PSA [9], which specifically detect prostate cancer but are not elevated in benign prostatic diseases. Until now, our and other groups examined myriad patient samples including blood, urine and tissue concerning changes in transcriptomics, miRNA expression, proteomics and metabolomics [12-19]. However, no marker has been identified so far, which has generally been accepted as being superior to PSA. The most promising novel candidate is the non-coding RNA prostate cancer antigen (PCA) 3, for which a diagnostic kit has been developed [20].

#### 1.1.3.2 PSA screening

The serine protease PSA is important to liquify seminal fluid. Increased PSA levels in the serum are a hallmark of prostate cancer. PSA is one of the few molecular markers that are routinely used in the diagnosis of common types of cancer. Also prognosis and monitoring of prostate cancer rely on serum PSA levels. Notably, this increase is not due to overpression of the enzyme by tumor cells, rather, increased secretion is the cause [8]. Since 1994 a screening for prostate cancer based on PSA detection in the serum was introduced in various countries [21, 22]. In Switzerland a regular check-up is recommended for men with a life expectancy of more than 10 years [11]. Thus, the increasing number of tests resulted in an increase of incidence during the past two decades [9, 23, 24]. Simultaneously, the percentage of patients below 70 as well as of low-grade tumors has increased, probably because these tumors do not show any symptoms and therefore remained undetected before [9, 11]. Because this group of tumors often does not affect the patient's health, benefit of the screening has been questioned. Two studies including 200.000 patients claim that the risk to die from prostate cancer is decreased by 50 and 20 %. However, 293 and 1410 men need to be screened of which 12 and 48 men, respectively, need to be treated to save one life [23, 24]. A third study did not reveal any benefit in the screening cohort [25]. These trials substantiate the need of novel non-invasive diagnostic tools to minimize the number of biopsies as well as of novel prognostic biomarkers to better distinguish insignificant carcinomas that do not need to be treated.

#### 1.1.3.3 Clinicopathological parameters

In general, staging of malignant tumors is done according to the TNM classification, which describes the circumference of the primary tumor (T) and the existence of regional lymph node metastases (N) and/or distant metastases (M). Tumors can be classified according to clinical (TNM classification) or pathological (pTNM classification) standards [26]. In **Tab. 2**, the criteria of each category for prostate carcinomas are listed.

**Tab. 2 TNM classification for prostate carcinomas.**

| stage | criteria |
|---|---|
| T1 | tumor not palbable and not detectable with imaging techniques |
| T1a | tumor ≤ 5 % of the resected tissue |
| T1b | tumor > 5 % of the resected tissue |
| T1c | tumor identified by needle biopsy |
| T2 | tumor confined to prostate |
| T2a | tumor ≤ 50 % of one lobe |
| T2b | tumor > 50 % of one lobe |
| T2c | tumor involves both lobes |
| T3 | tumor extends through the prostate capsule |
| T4 | tumor is fixed or invades adjacent structures other than seminal vesicles |
| N1 | regional lymph node metastases |
| M1 | distant metastases |

Grading of prostate cancer is done according to the Gleason score, which was established by Donald Gleason. He described five patterns of prostate gland organization and designated these patterns Gleason grade one to five. Gleason grade one corresponds to small, uniform glands, whereas Gleason grade five corresponds to poorly differentiated tumors with lack of any glandular structure and single tumor cells (**Fig. 3 a**). In radical prostatectomy (RPE) specimens, the Gleason score is built of the sum of the two most common patterns, resulting in possible values from two to ten (reviewed in [27], examples in **Fig. 3 b, c**). In needle biopsies, the highest value is always included, independent of the area [9]. A further clinicopathological parameter is the resection margin being either free of tumor cells (R0) or not (R1).

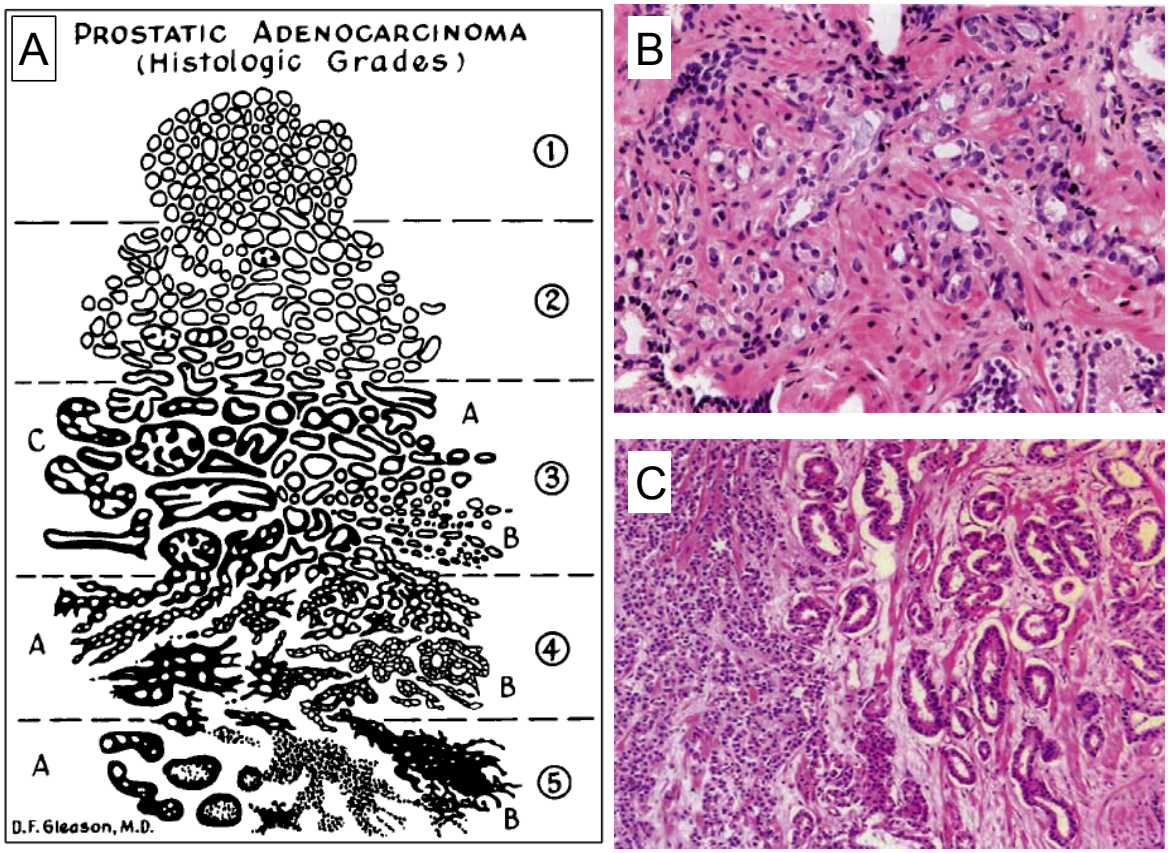


**Fig. 3 Gleason grading.**

**(A)** Gleason grades: standard drawing. **(B)** Hematoxylin & eosin staining of prostate adenocarcinoma Gleason score 3+4=7, gleason pattern 4 left. **(C)** Hematoxylin & eosin staining of prostate adenocarcinoma Gleason score 3+5=8, gleason pattern 5 left. A from [27], C and D from [5].

### 1.1.4 Prognosis

Prognosis for the patient mainly depends on the tumor stage at the time of diagnosis. Patients with so called localized carcinomas without metastases, generally have the highest chance not to die from their tumor. Based on the PSA level, Gleason score and T-stage, these patients are sub-divided into a low risk (PSA level < 10 ng/ml, Gleason score ≤ 6, T1c-2a, in Zurich maximal two of ten biopsies positive), intermediate risk (PSA level 10 to 20 ng/ml, Gleason score 7, T2b) and high risk group (PSA level > 20 ng/ml, Gleason score ≥ 8, T2c). The 5 year-survival rate for these three groups is 85 %, 60 % and 30 %, respectively [28, 29]. For patients with metastases to regional lymph nodes (stage N1) the median cancer-specific survival is eight years. In contrast, patients with distant metastases (stage M1) die within 24 to 48 months upon diagnosis [9]. Especially for the intermediate risk group with Gleason score 7, novel biomarkers that are able to predict the risk of recurrence, are

needed. In general, the main challenge concerning prognosis is to distinguish insignificant carcinomas from such cases that have a high probability to progress in order to decide for the optimal treatment.

### 1.1.5 Treatment

Generally, selection of the therapeutic strategy is very individual. Patient's age, disease stage, medical condition and will are the parameters that determine the treatment modality. Possible options are active surveillance, RPE, radiotherapy, hormonal therapy, chemotherapy, immunotherapy and various other approaches. Active surveillance is mainly applied for early-stage cancer patients (high probability to be insignificant) with a live expectancy of less than ten years [9] to avoid treatment side-effects [30]. RPE and radiotherapy are the major options for localized tumors, whereas radiotherapy is additionally administered to patients with locally advanced disease. Hormonal therapy is the treatment of choice for patients with distant metastases at the first diagnosis, after a PSA-relapse or adjuvant to radiotherapy in case of locally advanced tumors [9]. Chemotherapy and immunotherapy are the main options for treatment of CRPC. In 2004, clinicians succeeded for the first time to prolong overall survival of CRPC patients using chemotherapeutics [31, 32]. Recently, the first immunotherapeutic, Sipuleucel-T, was approved by the US Food and Drug Administration for patients with asymptomatic or minimally symptomatic CRPC. Peripheral blood mononuclear cells are harvested from the patient, incubated with a chimeric protein and reinfused into the patient's blood. The protein is composed of granulocyte-macrophage colony-stimulating-factor (GM-CSF) to activate antigen presentation and prostatic acid phosphatase (PAP) as tumorassociated antigen. Median survival was prolonged from 21.7 to 25.8 months [33].

#### 1.1.5.1 Hormonal therapy

Efficacy of androgen ablation by orchiectomy or estrogen injection was first proven 60 years ago [34]. Further approaches at the stage of pituitary hormone secretion, androgen synthesis in the testes and adrenal glands and androgen receptor (AR) action in the tumor cells were addressed in several studies. Gonadotropin-releasing hormone antagonists and agonists block the corresponding receptors in the pituitary gland and thus prevent release of follicle-stimulating hormone and luteinizing hormone which normally trigger testosterone production in the testes. The pregnenolone derivative arbiraterone acetate (currently phase III) blocks steroid synthesis in the adrenal glands and testes. Similarly the glucocorticoid prednisone inhibits androgen synthesis in the adrenal glands. Finally antiandrogens are widely used to block the AR function within the prostate cells. Bicalutamide and MDV3100 (currently phase III) belong to the group of competing androgen antagonists that interact with the ligand binding domain of AR. Such compounds prevent androgens from binding to AR and thus

inhibit AR-mediated transcriptional activation by disabling AR from either nuclear translocation, DNA binding or coactivator recruitment [35] (**Fig. 4**).

Usually a combination treatment of androgen depletion and antiandrogens is applied, called combined androgen blockade [35]. Overall, hormonal therapy initially reduces the disease symptoms in 70-80 % of the patients [9]. However, after a certain period of quiescence, PSA levels rise again indicating relapse of the tumor, which is then castration-resistant (CRPC) [35].

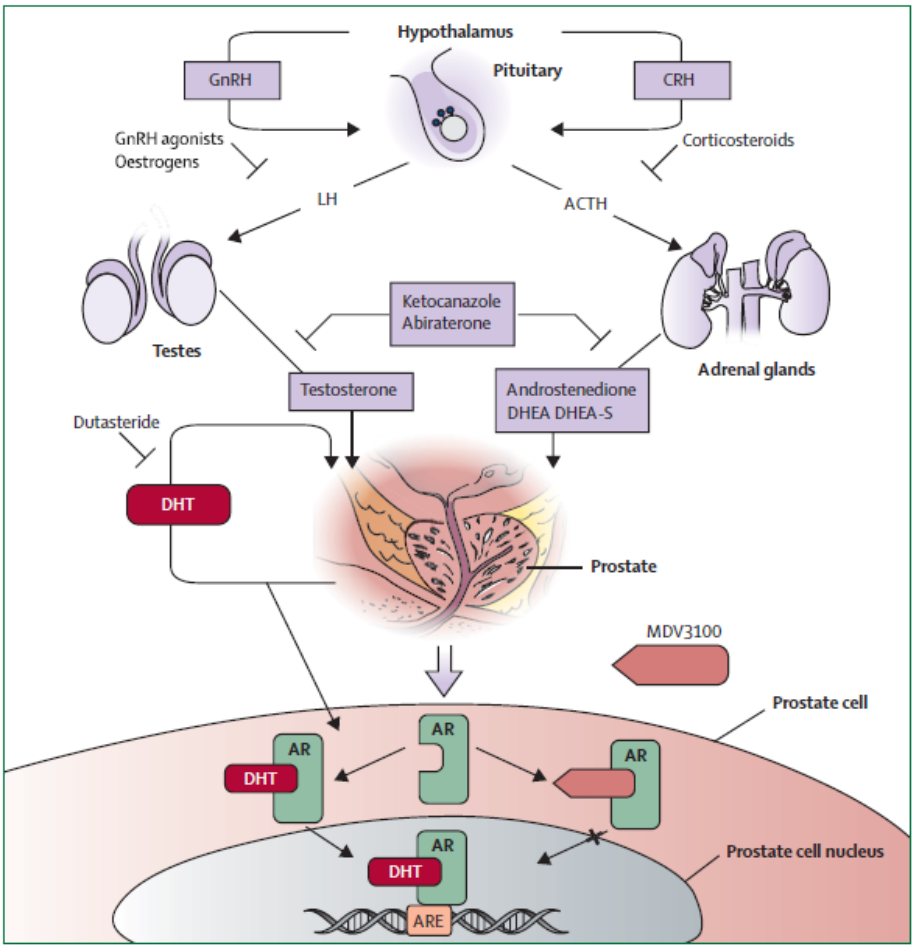


**Fig. 4 The androgen-signaling axis and its inhibitors.**

Androgen synthesis is regulated by the hypothalamus-pituitary axis and takes place in the testes and adrenal glands. Within the prostate dihydrotestosterone (DHT) is generated from testosterone and activates AR signaling. The mode of action of various agents to block androgen synthesis or signaling is illustrated. For further explanations concerning AR signaling see chapter 1.2.1. From [35]. CRH = corticotropin-releasing hormone, ACTH = adrenocorticotropic hormone, DHEA = dehydroepiandrosterone, DHEA-S = DHEA-sulphate, ARE = androgen responsive element.

## 1.2 *The molecular biology of prostate cancer*

### 1.2.1 Steroid hormones and their receptors

Prostate cell growth and survival generally depend on androgens, which are provided by the testes and the adrenal glands. Androgen signaling is induced by binding of dihydro-testosterone (DHT) to the ligand-binding domain of AR. DHT is the active derivative of testosterone and is generated by reduction of the hormone, this reaction is catalyzed by the 5α-reductase in the stromal cells of the prostate. Upon ligand binding, the active steroid hormone receptor dimerizes, translocates into the nucleus and binds to corresponding androgen responsive elements (ARE) in the promoter or enhancer regions of target genes via its DNA-binding domain. Following recruitment of coactivators via the N-terminal domain, transcription is initialized [36, 37] (**Fig. 5**). Also prostate cancer cells rely on androgen signaling, even in cancer cells of CRPC AR is detected in the nucleus and androgen responsive genes are expressed [38].

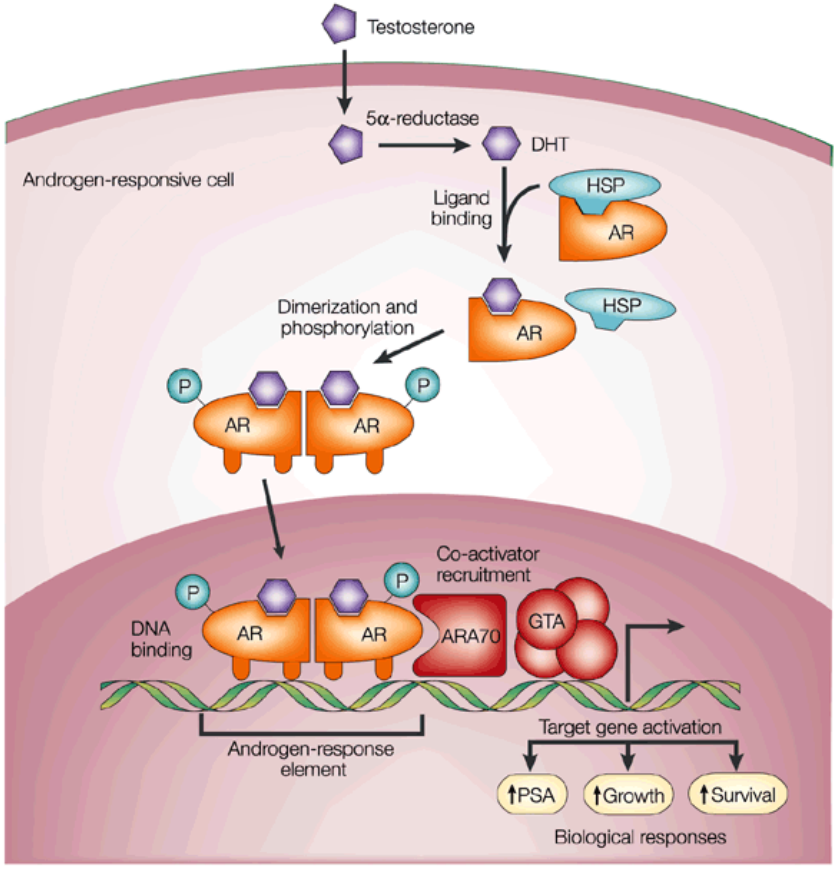


**Fig. 5 Androgen signaling in a prostatic cell.**

Modified from [36]. HSP = heat-shock protein, ARA70 = 70 kDa AR-activator, GTA = general transcription apparatus, P = phosphate.

Estrogens play a dual role during development of prostate cancer. On the one hand, estrogens have been shown to delay prostate cancer progression, which was related to their antiandrogenic effect by preventing luteinizing hormone release in the pituitary [34, 39]. On the other hand, several studies indicate a promoting role of estrogens in prostate carcinogenesis, which is probably mediated by ERα. Comparison of estrogen and testosterone levels during aging and between ethnicities substantiates the positive correlation between estrogen levels and prostate carcinogenesis. At the age when prostate cancer starts to develop, testosterone levels decline, however, estrogen levels remain unchanged or even increase. Further, testosterone levels are similar in men of different ethnic background, in contrast estrogen levels are higher in African Americans compared to Caucasian Americans and very low in Japanese, strikingly correlating with prostate cancer incidence rates (reviewed in [40, 41]).

ERβ has a high affinity to phytoestrogens. Soy products, which are staple food in Japan, contain high concentrations of these agents. Phytoestrogens were shown to reduce serum PSA levels, activity of 5α-reductase and expression of AR and thus to inhibit cell proliferation and angiogenesis. Probably these reactions are mediated by ERβ. Altogether, ERα is designated the “bad” and ERβ the “good” estrogen receptor concerning prostate cancer development (reviewed in [9, 41]). Both receptors have a similar, highly conserved DNA binding domain. However, ligand-specificity and N-terminal domains are different and important for signal processing [42].

### 1.2.2 Epithelial-stromal interactions

Interactions between epithelial and stromal cells are of great importance within the prostate. The stromal cells express 5α-reductase and AR and thus process androgen signals, which are forwarded to the epithelial cells via paracrine factors and their corresponding receptors. These factors include extracellular matrix proteins, transforming growth factor (TGF) β, platelet-derived growth factor (PDGF), vascular endothelial growth factor (VEGF), insulin-like growth factor (IGF), fibroblast growth factor (FGF), hepatocyte growth factor (HGF), epidermal growth factor (EGF) and chemokine (C-X-C motif) ligand (CXCL) 12. Although epithelial AR expression increases during prostate cancer development, these interactions still remain essential for tumor survival (reviewed in [43, 44]).

### 1.2.3 Genomic alterations

In general, prostate cancer is a very heterogenous and complex disease [45]. However, there are two specific genomic alterations that are frequently observed: phosphatase and tensin homolog (PTEN) deletion and gene fusion between a prostate-specific androgen-regulated gene and an avian erythroblastosis virus E26 (v-ets) oncogene homolog (ETS) gene. PTEN deletion was detected in 23 % of HGPIN and 68 % of primary carcinomas [46].

Gene fusions occur in 56 % of prostate carcinomas [47], the most frequent fusion transcript is the one between transmembrane protease, serine 2 and the ETS family member ERG (TMPRSS2:ERG) for which our group revealed a prevalence of 41 % [48]. In two cases, calcium-activated nucleotidase (CANT) 1 was identified as 5' androgen-regulated fusion partner [47, 49]. The promoters of these genes are used to induce expression of the oncogenic ETS transcription factors [50] in the prostate. Interestingly, serine peptidase inhibitor, Kazal type (SPINK) 1 was reported to be exclusively overexpressed in fusion negative carcinomas and to be related to poor prognosis. Cell culture and mouse studies revealed an association between SPINK1 expression and tumorigenic potential [51, 52].
Mutations or amplifications of the AR gene are barely found in primary prostate carcinomas. In contrast, 58 % of metastatic lesions display alterations regarding AR, which is either mutated, amplified or overexpressed [53].

### 1.2.4 Gene and protein expression in prostate cancer

The heterogeneity of prostate cancer becomes obvious also on the level of gene expression. Various gene expression studies have been conducted and identified many genes that are up- or downregulated in the cancer cells [54-57]. Our group performed a gene array study including matched normal and cancerous tissue, which was microdissected, from 42 patients and identified non-conding RNA PCA3, prostate-specific G-protein coupled receptor (PSGR), ATP-binding cassette sub-family C member (ABCC) 4, GOLM1, T-cell receptor gamma alternate reading frame protein (TARP), CANT1, FASN, anterior gradient homolog (AGR) 2, forkhead box (FOX) A1 and a disintegrin and metallopeptidase domain (ADAM) 9 amongst the top ugregulated genes in prostate cancer [15]. The overexpression on protein level was confirmed for GOLM1, TARP, FASN and ADAM9 [16, 17, 58, 59] so far. The detailed analysis of the protein expression pattern of CANT1 and FOXA1 in prostatic tissues is part of this thesis.

## *1.3 CANT1*

### 1.3.1 CANT1 gene and protein

The CANT1 gene is located on chromosome 17q25.3 [60], two alternative first exons (exon 1 and 1a) have been described [49].
The corresponding transcripts result in the same full-length protein, which consists of 401 amino acids and was detected at 37 to 42 kDa by Western Blot analysis [60, 61]. Analysis of the protein sequence predicted two internal start codons, one N-glycosylation site, one tyrosine sulfation site, two N-myristoylation sites, one cyclic AMP- and cyclic GMP-dependent protein kinase phosphorylation site, one cysteine residue, and six protein kinase (PK) C and casein kinase II phosphorylation sites [60, 62]. Further, a weak and a strong

hydrophobic stretch were identified, suggesting full-length CANT1 to be a transmembrane protein, most likely a single pass transmembrane protein of type II with the strong hydrophobic stretch crossing the membrane and the long C-terminus facing the extracellular space. However, also a model with both protein termini facing the extracellular space and two transmembrane domains is discussed [62, 63]. Treatment with peptide: N-glycosidase (PNGase) F confirmed glycosylation of the protein. Yet, also after deglycosylation, a double band was seen in Western Blots, indicating further modifications of the protein or use of an internal start codon [60, 62]. Post-translational modifications as well as the transmembrane domain appear not to have any functional relevance as the truncated soluble form of CANT1, which was expressed in bacteria, displayed similar nucleotidase activity compared to its full-length counterpart, which was expressed in mammalian cells [61].

### 1.3.2 CANT1 enzymatic activity

#### 1.3.2.1 CANT1 is an apyrase

CANT1 was discovered in the human expressed sequence tag GenBank database as a homologous clone of the apyrase cDNA clone from the blood-sucking insect *C.lectularius* (bed bug) and therefore its functionality as apyrase was examined [60]. Apyrases (Enzyme Commission number 3.6.1.5, ATP-diphosphohydrolases) hydrolyze ADP and ATP to AMP and inorganic phosphate. While also other di- and triphosphates can be substrates, monophosphates or nonnucleoside phosphates are not dephosphorylated. The activity of this enzyme class is dependent on divalent cations [64]. Indeed, calcium-dependent ADPase and ATPase activity was detected in CANT1-transfected cells [60, 61]. Analysis of further potential substrates revealed UDP as preferred target for CANT1, followed by IDP and GDP. Weak hydrolytic activities were also measured for UTP, GTP, ITP, CDP and CTP. In comparison to UDP, hydrolytic activities for ADP and ATP were weak as well. No monophosphates were hydrolyzed by CANT1 [60-62].

Enzymatic activity of CANT1 was shown to be dependent on homodimerization of the protein, which in turn is dependent on calcium [61, 63, 65, 66]. Dimerization has been demonstrated for the truncated soluble as well as for the full-length transmembrane form of CANT1 [63].

#### 1.3.2.2 Apyrase families

Two families of apyrases have been described so far, based on their primary amino acid similarity. The first family of so called NTPDases is characterized by five invariant apyrase-conserved regions that are essential for enzymatic function. Eight family members with different substrate-specificities have been identified so far. The ectoenzymes NTPDase 1, 2, 3 and 8 are highly glycosylated and are expressed on the surface of vessels, nerves and in

the liver. NTPDase 1 and 2 are critical regulators of blood vessel homeostasis. Less research has been carried out on NTPDases 4 to 7. NTPDase 5 and 6 are usually expressed intracellular, although they are secreted upon heterologous expression. NTPDase 4 and 7 are localized in intracellular organelles (reviewed in [67]).

The second family consists of apyrases from blood-feeding insects and their vertebrate homologs. CANT1 is a member of this latter family and besides the bed bug apyrase further homologs are known in *C.elegans* (APYrase [apy]-1), *X.laevis*, rat and mouse [62, 68, 69]. No traditional apyrase-conserved regions or nucleotide-binding domains were found in this class of enzymes, however, eight nucleotidase-conserved regions could be identified [65, 70, 71].

Both families show no amino acid homology and are evolutionarily unrelated to each other, however, their enzymatic function is highly analogous. For example, NTPDase 1 efficiently hydrolyzes ADP [72], which usually induces coagulation by activating purinergic receptors on platelets. Hence, this enzyme is an important regulator of blood fluidity [67]. Similarly, the bed bug apyrase is secreted into the host's wound to hydrolyze ADP [73] and thus to inhibit platelet clotting and enable the insect to blood-feed for extended times. This feature of apyrases could be useful in treating thrombosis. In fact, NTPDase 1 is tested as thrombosis drug [74]. However, the disadvantage of this enzyme is that it also hydrolyzes ATP to ADP which promotes thrombosis [75]. Therefore, approaches to modify CANT1 in a way that it effectively hydrolyzes ADP but not ATP are under investigation. Indeed, certain CANT1 mutants were generated that inhibited coagulation, dissolved existing platelet aggregates and inhibited thrombosis in a mouse model [76, 77].

### 1.3.3 CANT1 expression

CANT1 mRNA was detected in a variety of human organs. Strongest expression was revealed in testis, small intestine, placenta and prostate. Additionally, the transcript was detected in the lung, stomach, salivary glands, colon, spleen, ovary, thymus and trachea [49, 60]. Transcript-specific measurement revealed the transcript starting at exon 1a to be prostate-specific [49].

Yet, both transcripts were shown to be inducible by treatment of LNCaP cells with the synthetic androgen R1881 [49]. As demonstrated by chromatin immunoprecipitation analysis this was caused by direct binding of AR to the promoter of CANT1 [47].

### 1.3.4 CANT1 mutations in a chondrodysplasia

Desbuquois dysplasia is a rare autosomal recessive chondrodysplasia. It is a severe skeletal disorder characterized by short limbs, spondylometaphyseal abnormalities, osteopenia, advanced carpotarsal ossification, ligamentous joint laxity, flat midface, cleft palate and

progressive scoliosis [78]. Mutations in the CANT1 gene were revealed to be causative for most of the cases. Several nonsense or missense mutations in the nucleotidase-conserved regions were identified. All mutations resulted in CANT1 loss-of-function [70, 79-81].

## *1.4 FOXA1*

FOXA1 was first detected in nuclear extracts of rat liver and hepatoma cells (HepG2) and therefore named initially hepatocyte nuclear factor 3α (HNF3α). It was identified as the transcription factor that induces expression of transthyretin and α1-antitrypsin [82-84]. The gene is located on chromosome 14q12-q13.

### 1.4.1 The FOX family

Due to the similarity between the DNA binding domains of HNF3α and the *D.melanogaster* protein *fork head*, Weigel *et al.* suggested to designate this domain "forkhead box" and to found a corresponding family of transcription factors [85, 86]. HNF3α as the first member of the first subfamily was later renamed into FOXA1 [87, 88]. Meanwhile the forkhead transcription factor family comprises 19 subfamilies and 50 members [89]. These are characterized by a so called „winged helix" 3D-structure similar to that of linker histones [90-93] (**Fig. 6**). This enables FOX proteins to open highly compacted chromatin [94] and thus to facilitate the binding of other transcription factors, which prompted researchers to call this class of proteins "pioneer factors". Hence, with a few exceptions, these proteins activate target gene transcription [95].

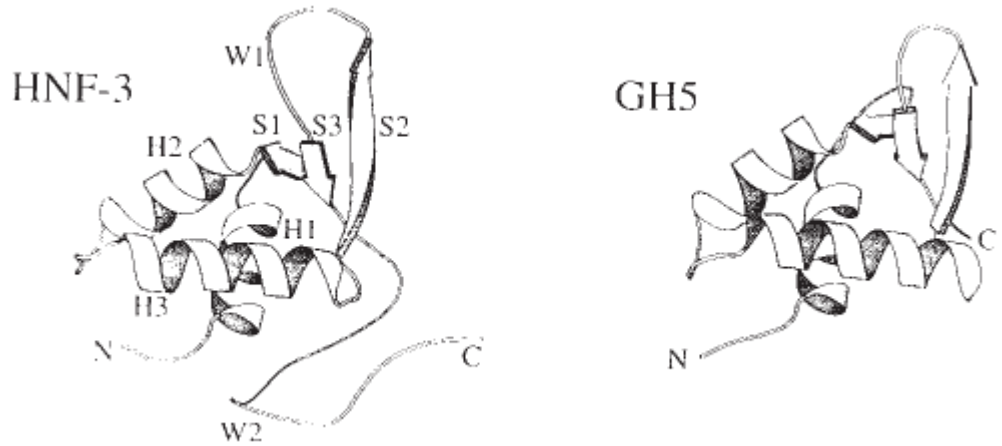


**Fig. 6 Comparison of the structure of HNF3 (= FOXA) proteins to that of linker histones.**

Schematics of the tertiary structure of the DNA binding domain of HNF3y (= FOXA3, amino acid 107-223), which is very similar to that of FOXA1 [84], and the globular domain of linker histone H5 (GH5). Both proteins are viewed looking towards the DNA-binding surface as if the target DNA was running vertically. Modified from [90]. N = N-terminus, C = C-terminus, H = α-helix, S = β-strand, W = loop region.

In general, FOX transcription factors are important during early vertebrate development and organogenesis. In the adult organisms, these proteins play a role in glucose and lipid metabolism and energy balance [95]. Several family members, amongst others also FOXA1, are involved in the development and progression of various carcinomas [96].

### 1.4.2 FOXA1 in development and metabolism

FOXA1 in particular is involved in the organogenesis of the prostate, lung, liver, pancreas and breast [97-102]. In adult rodents expression of FOXA1 was detected in the brain, gastrointestinal tract, respiratory tract, thyroid glands and urogenital tract including the prostate [95, 103, 104]. FOXA1 knockout mice die early after birth due to hypoglycaemia, which indicates that the major function of FOXA1 in the adult organism is glucose homeostasis. Accordingly, dramatically reduced glucagon levels in the blood and proglucagon levels in pancreatic islets were measured [105, 106].

### 1.4.3 FOXA1 in the prostate

FOXA1 is essential for prostate development and is still expressed in the adult prostate [98, 99, 103, 104]. The protein has been shown to be responsible for activating transcription of prostatic genes specifically in the prostate but not in other tissues, e.g. probasin [107], the transcription factor homeobox (HX) B13, which is important during prostate development [108] and NK3 homeobox (NKX3.) 1 [98].

A small study on whole mount RPE sections from 20 primary prostate carcinomas, which included benign and malignant tissue, revealed a strong expression of FOXA1 in normal tissue and no upregulation in PIN or carcinoma tissue [109]. Very recently, analysis of a cohort of 80 primary and 28 metastatic prostate carcinomas revealed a much higher prevalence of strongly stained cases in the metastatic group and positive correlation of FOXA1 with tumor size, extraprostatic extension, angiolymphatic invasion, lymph node metastases at diagnosis and AR staining [110].

### 1.4.4 FOXA1 regulation and signaling

The consensus DNA binding sequence for FOXA transcription factors is A(A/T)TRTT(G/T)RYTY (R = purine, Y = pyrimidine) [111]. Lupien *et al.* [112] suggested that the methylation status of histones H3 at lysine 4 is critical for binding of FOXA1 to chromatin, which was confirmed by Wang *et al.* [113]. Thus, histone methylation is critical for lineage-specific FOXA1 transcriptional regulation (**Fig. 7**).

Once bound to chromatin, FOXA1 recruits various other transcription factors to activate gene transcription, amongst others ERα [114], AR [98, 115, 116], breast cancer (BRCA) 1 [117] and CCCTC-binding Factor (CTFC) [118]. However, interaction with for example transducin-like enhancer of split (TLE) 3 represses expression of usually positively regulated target

genes and interaction with NKX2.1 can influence target gene transcription in both ways [117-122].

FOXA1 itself can be induced by GATA binding protein (GATA) 3, ERα, SRY (sex determining region Y)-box (SOX) 17, β-Catenin and SOX 4 [123-126].

### 1.4.5 The relationship between FOXA1 and steroid hormone receptors

The relationship between FOXA1 and ERα was best investigated in breast cells so far. A correlation between FOXA1 and ERα expression in breast cell lines and tissue was revealed [117]. In the same study, these two transcription factors were identified as downstream targets of GATA3. Together, these three proteins build a hormonal transcription factor network, which is specific for the luminal cell type in the breast [101, 123, 127]. The overlap between FOXA1 and ERα binding to chromatin was more than 50 % in three breast cancer cell lines [114].

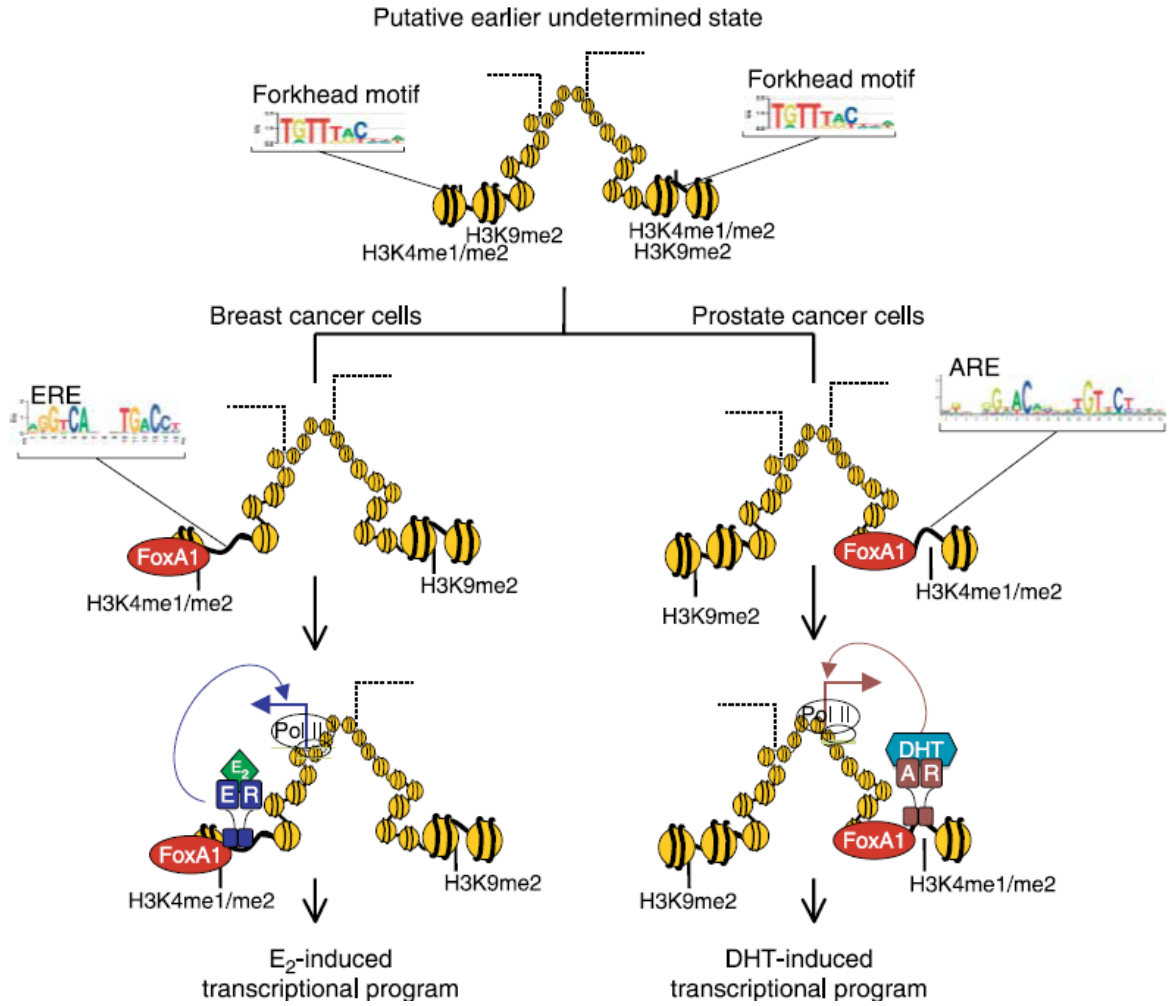


**Fig. 7 Lineage-specific transcriptional regulation by FOXA1 in breast and prostate cancer cells.**

FOXA1 binds to genomic regions harbouring the FOXA binding motif and carrying the activating histone methylation (histone 3 lysine 4). Subsequent chromatin remodelling opens the DNA and allows estrogen receptor and AR to bind and to induce estrogen and androgen-dependent target gene transcription, respectively. From [128]. H = histone, K = lysine, me =

methylated, $E_2$ = estradiol, ER = estrogen receptor, ERE = estrogen responsive element.

Accordingly, FOXA1 was shown to be needed for the recruitment of ERα to the promoters of 50 % of ERα target genes [114, 125, 129, 130] and for ERα transcriptional activity [114]. Thus, FOXA1 is essential for hormonal responsiveness of luminal breast cells during mammary development as well as in breast cancer [101, 123, 127] (**Fig. 7**). FOXA1 itself is also inducible by estrogens [125] and ERα expression in turn is regulated by FOXA1 [101].

The binding motif for FOXA1 is also enriched in the AR cistrome [131]. FOXA1 binding to ARE independent of androgen concentrations as well as a direct physical interaction between FOXA1 and AR was reported [115, 116, 132, 133]. Hence, various androgen-regulated genes are not expressed in the prostate of FOXA1 deficient mice [98] (**Fig. 7**).

## *1.5 GOLM1*

GOLM1 was first described in a patient suffering from acute adult giant-cell hepatitis as Golgi protein, which was detected at 73 kDa by Western Blot analysis, and therefore named GP73 [134]. Another designation is GOLPH2 (Golgi phosphoprotein 2). The function of the protein is still unknown.

### 1.5.1 GOLM1 gene and protein

The gene GOLM1 is located on chromosome 9q21.33. Two transcript variants exist that result in the same protein with a theoretical mass of 45 kDa. Due to glycosylation in combination with additional post-translational modifications or abnormal migration because of the high rate of acidic amino acids, the protein is detected at a molecular weight of 73 kDa in Western Blot analyses [134, 135]. Sequence analysis suggests a mainly hydrophilic protein with a hydrophobic N-terminus, a single transmembrane domain, a signal peptidase cleavage site, a N-myristoylation site, several coiled-coil domains after the transmembrane domain, five glycosylation sites and no enzymatic activity [134]. Indeed, GOLM1 was found to be a transmembrane protein of type II with a short cytoplasmic N-terminus and a long luminal C-terminus, which is structurally similar to p63, 130 kDa Golgi-localized phosphoprotein (GPP130) and Golgin-84 [134, 136, 137].

### 1.5.2 Expression of GOLM1

Several organs were shown to express GOLM1, amongst others stomach, colon, prostate and trachea, the expression is weaker in testes, spleen and liver [134].

A Golgi targeting sequence was identified within the coiled-coil domains [136, 137]. Consistently, in immunofluorescence studies the protein was detected in the cis- and medial-compartments of the Golgi apparatus [134]. Additionally, it was detected at the cell surface and in sorting endosomes, from where it is directly transported to the trans-Golgi network bypassing late endosomes [136]. Further, a truncated soluble form is detectable in serum. A

concordant consensus sequence for proprotein convertases was identified 20 amino acids away from the transmembrane domain on the luminal side of the protein and cleavage by furine was proven [138].

### 1.5.3 GOLM1 in the liver

In the healthy liver, GOLM1 is only expressed in epithelial cells, however, elevated levels were detected in diseased hepatocytes, either due to cirrhosis, hepatitis or hepatitis C virus-infection [137, 139]. In liver cell lines GOLM1 was shown to be induced by adenoviral infection [134, 140].

It is further upregulated in hepatocellular carcinoma (HCC) [141-143] and serves as serum marker for the diagnosis and disease surveillance of HCC that is superior to alpha-fetoprotein (AFP) in certain applications [138, 141, 142, 144]. Hyperfucosylation of GOLM1 in HCC was reported [141], followed by the discovery that GOLM1 expression in Hep3B cells can be induced by overexpression of the fucosyltransferase 8 [145].

### 1.5.4 GOLM1 in prostate cancer

GOLM1 mRNA was shown to be elevated in prostate cancer in several studies [15, 54, 146-148] and applicability of GOLM1 mRNA as urinary marker was proven [147, 149].

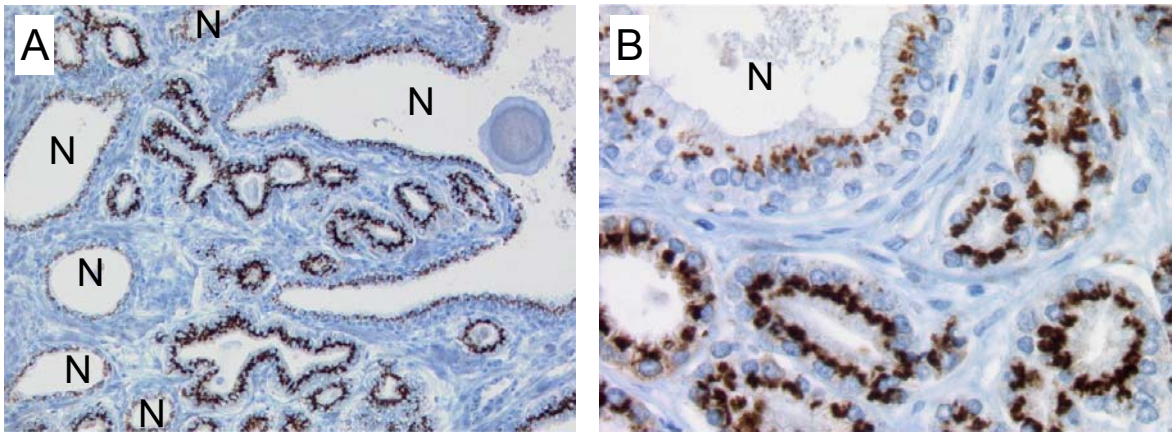


**Fig. 8 GOLM1 immunohistochemistry of human prostatic tissues.**

**(A)** Gleason 3+3=6 adenocarcinoma (center) infiltrating in between normal glands (N). Note the upregulation of GOLM1 in comparison to normal glands. **(B)** The same case at a higher magnification. Note the characteristic Golgi pattern. From [16].

Corresponding augmented GOLM1 protein levels in prostate cancer were revealed in a small cohort of 40 patients [146] and confirmed by our group in a study including 640 patients. Although a weak staining was detected in normal tissue, GOLM1 expression was increased in 92 % of the tumors. Thus, GOLM1 was suggested as novel histological biomarker for the diagnosis of prostate cancer and is already applied in the University Hospital Zurich. The

difference in the staining intensity being low in normal tissue, intermediate in PIN and high in carcinoma was highly significant. However, no correlation with pT stage, Gleason score, pre-operative (pre-OP) serum PSA level or PSA-relapse was found [16] (**Fig. 8**).

### 1.5.5 GOLM1 in other diseases

In lung cancer, a strong association between GOLM1 expression and adenocarcinomas in contrast to squamous carcinomas was revealed [150]. In seminomas, GOLM1 is overexpressed in comparison to normal tissue and was therefore suggested as novel diagnostic biomarker [151]. Further, GOLM1 expression is more frequent in the hepatic phenotype of Wilson disease compared to the neurologic phenotype [152]. Finally, a polymorphism in the GOLM1 gene is discussed as risk factor for Alzheimer disease [153-155].

## *1.6 Protein glycosylation*

Protein glycosylation, here defined as adding of sugar molecules to peptide chains, plays a role in three cellular processes: synthesis of glycoproteins and proteoglycans and protein folding. This chapter gives an overview of these processes and the associated unfolded protein response (UPR).

### 1.6.1 Glycoproteins

Glycoproteins are defined as proteins that are covalently linked to more or less branched oligosaccharides, which are composed of miscellaneous monosaccharides. Depending on the sugar-peptide bond, glycoproteins are subdivided into N- and O-glycosylated proteins. In N-glycosylated proteins the oligosaccharide is bound to the amido-group of asparagine, whereas in O-glycosylated proteins the oligosaccharide is bound to the hydroxy group of serine or threonine (reviewed in [156]).

#### 1.6.1.1 N-glycosylated proteins

N-glycosylation takes place in the endoplasmic reticulum (ER) and the Golgi apparatus. The consensus-sequence for N-glycosylation is asparagine-X-serine/threonine, whereas X can be any amino acid except proline. In all eukaryotes, the sugar-peptide bond is built between the asparagine and N-acetylglucosamine (GlcNAc), which is part of the core oligosaccharide $GlcNAc_2Man_9Glc_3$ (Glc = glucose, Man = mannose). This core oligosaccharide is synthesized by transferring the monosaccharides to dolicholphosphate (Dol-PP), which is integrated in the ER-membrane. This biosynthesis takes place in the cytoplasm and in the ER, whereby cytoplasmic sugar donors are UDP-GlcNAc, GDP-Man and UDP-Glc and ER-sugar donors are Dol-P-Man and Dol-P-Glc. The core oligosaccharide is added to the nascent peptide chain, which is translocated into the ER during protein synthesis. Next, the three Glc and one

Man are trimmed, the polypeptide chain is folded into its native 3D-structure and the protein is transported into the Golgi apparatus. There, diverse sugar molecules are removed and added in a protein- and tissue-specific manner. The used monosaccharides are GlcNAc, galactose (Gal), sialic acid and fucose that are donated by the nucleotides CMP, GDP and UDP (reviewed in [156], **Fig. 9**).

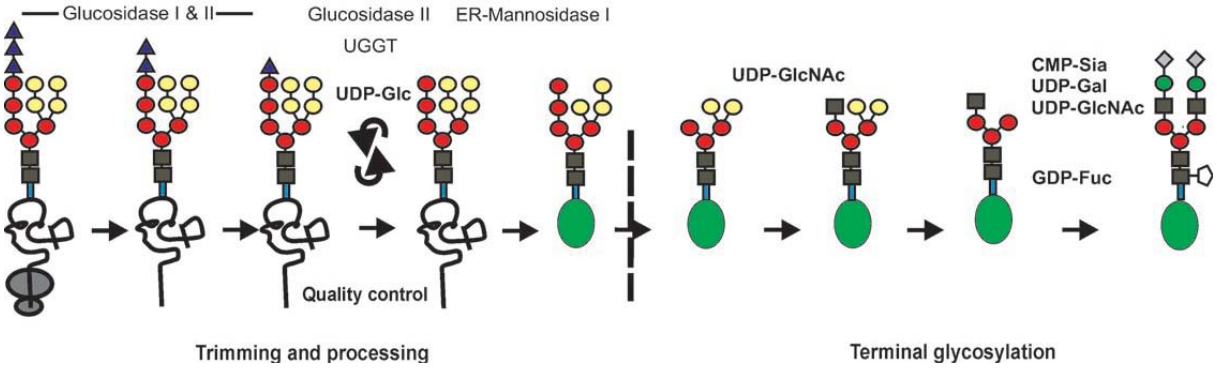


**Fig. 9 N-glycosylation of proteins.**

For explanations of the quality control step see chapter 1.6.2. Green ellipse symbolizes correctly folded glycoprotein. Modified from [156]. UGGT = UDP-Glc glycoprotein glucosyltransferase, Sia = sialic acid, Fuc = fucose.

#### 1.6.1.2 O-glycosylated proteins

O-glycosylation takes as well place in the ER and the Golgi apparatus. The first sugar can either be Man, which is derived from Dol-P-Man in the ER, or N-acetylgalactosamine, which is donated by UDP in the cis-Golgi apparatus. All the following sugar molecules are added in the Golgi apparatus and are transferred from nucleotides (reviewed in [156]).

### 1.6.2 Protein folding and quality control

As described in chapter 1.6.1.1, a core oligosaccharide is added to freshly translated proteins as soon as the consensus sequence enters the ER lumen. Subsequently all three Glc are hydrolyzed. The question is why does the core oligosaccharide contain Glc molecules that are removed shortly after transfer? These Glc have two important functions: Firstly, they are a signal for correct transfer of the core oligosaccharide. Secondly, glucosylation status is a marker of the protein's folding status [156].

Immediately after transfer of the core oligosaccharide, the outermost two Glc are removed and the polypeptide chain associates with calnexin or calreticulin. These two chaperones assist protein folding and most of the proteins leave the complex in their native 3D-structure. Subsequently, also the innermost Glc is cleaved and the protein can leave the ER towards the Golgi apparatus. However, if the protein is not folded correctly, which is sensed by the enzyme UDP-Glc glycoprotein glucosyltransferase (UGGT), the polypeptide chain is reglucosylated by this enzyme and enters another calnexin/calreticulin cycle. In this case,

UDP-Glc is the donor for the Glc molecule. Terminally misfolded proteins are unfolded, retrotranslocated into the cytoplasm and degraded in the proteasome, a pathway called ER-associated degradation (ERAD) (reviewed in [157], **Fig. 10**).

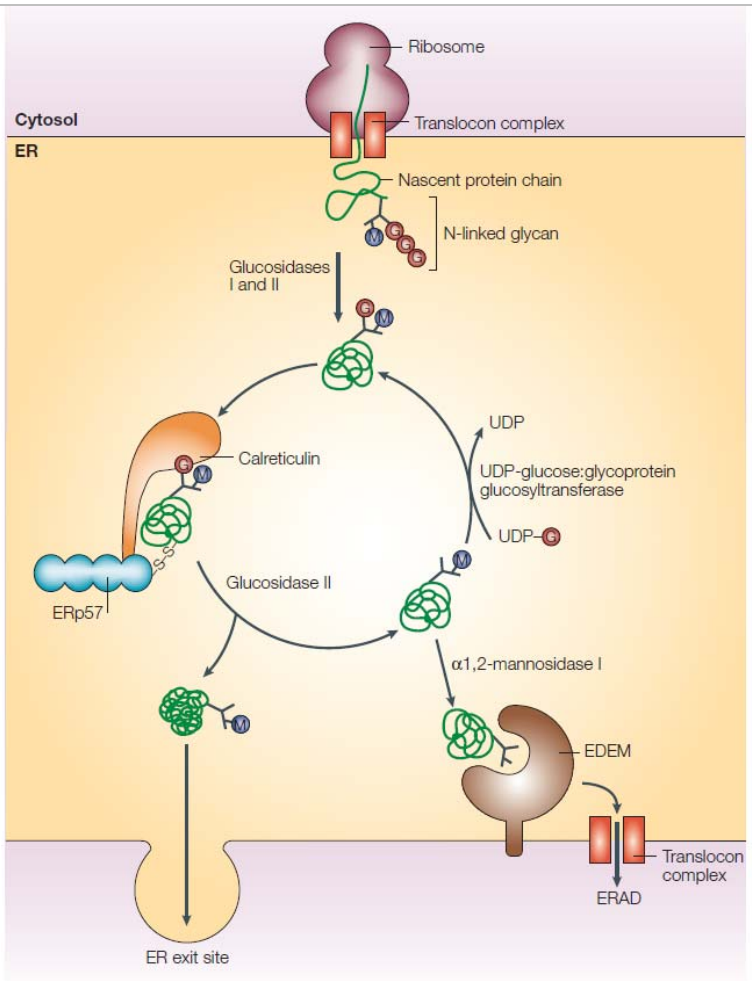


**Fig. 10 Protein folding and quality control.**
From [158]. EDEM = ER degradation enhancer, mannosidase alpha-like.

### 1.6.3 UPR

In case of overload of the ER with newly synthesized unfolded and/or misfolded proteins the capacity of the folding machinery is exceeded, which triggers a signaling pathway named UPR. Simultaneously, general protein synthesis is stopped to reduce the amount of unfolded proteins and expression of specific proteins, that handle unfolded proteins, is promoted. “Handle” means either folding of the proteins or degradation of misfolded proteins (ERAD). If the cell fails to re-establish the balance between unfolded and misfolded proteins on the one side and capacity of the folding machinery on the other side, cell death is initiated.

The three major mediators of this signaling pathway are inositol-requiring protein (IRE) 1, activating transcription factor (ATF) 6 and protein kinase RNA-like endoplasmic reticulum kinase (PERK). IRE1 mainly activates X-box binding protein (XBP) 1, which induces transcription of ERAD genes. A truncated form of ATF6 directly enters the nucleus and

induces transcription of UPR genes. PERK phosphorylates and thus inactivates eukaryotic translation initiation factor (eIF) 2, which leads to general translational inhibition. Yet, translation of the transcription factor ATF4 is specifically activated, which induces transcription of further UPR- as well as cell death-related genes. In its function as ER chaperone, heat-shock protein (HSP) A5 is the main sensor of overload with misfolded proteins and is in turn upregulated in the course of the UPR (reviewed in [159, 160], **Fig. 11**).

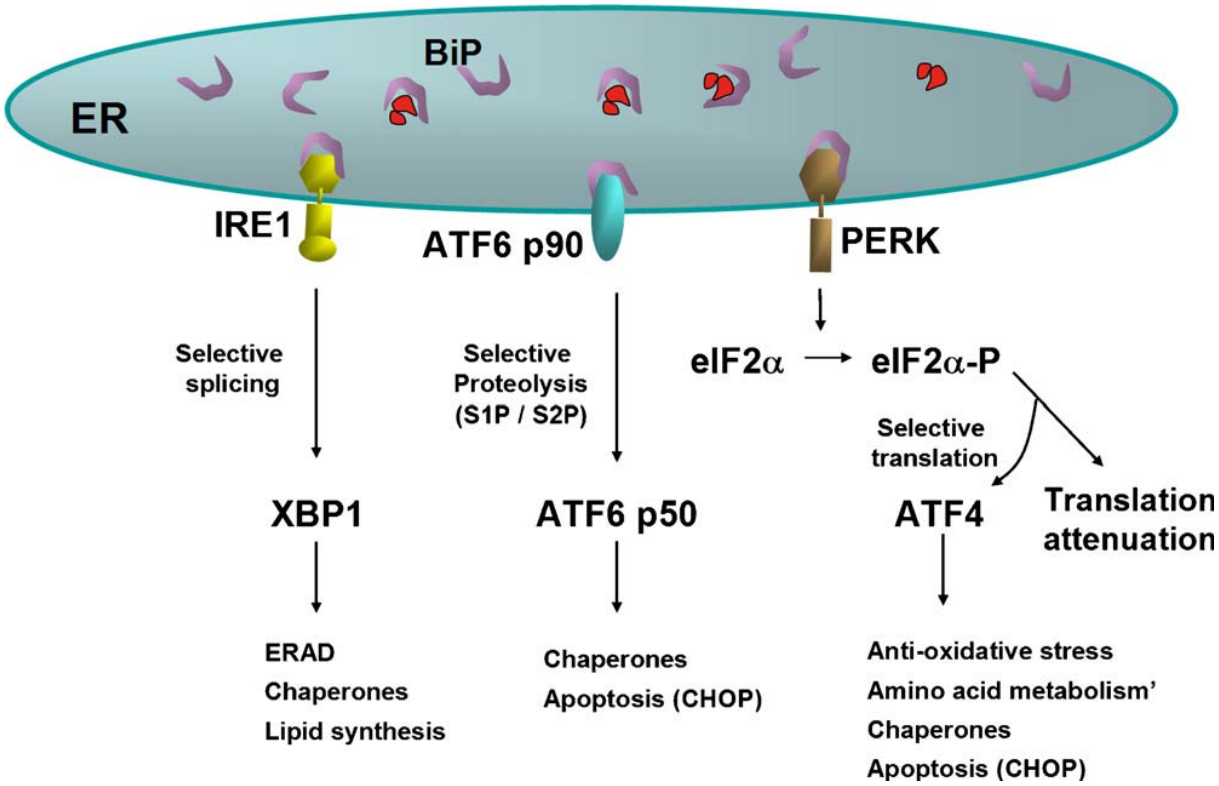


**Fig. 11 Signaling during the UPR.**
From [160]. Bip = HSPA5, CHOP = CCAAT/enhancer-binding protein homologous protein.

### 1.6.4 Proteoglycans

In contrast to glycoproteins, proteoglycans are defined as proteins that are covalently linked to long unbranched polysaccharides, which consist of repeating disaccharides. The polysaccharide chains are designated glycosaminoglycans because the disaccharide unit is composed of an amino sugar that alternates with an acidic sugar. Hence, these chains are highly negatively charged. Proteoglycan synthesis takes place in the Golgi apparatus and is initiated by adding the tetrasaccharide Xyl-Gal-Gal-GlcA (Xyl = xylose, GlcA = glucuronic acid) to the hydroxyl group of serine (compare chapter 1.6.1). Afterwards the respective monosaccharides are added alternating (reviewed in [161]). In all reactions donor molecules are again nucleotides.

### 1.6.5 Nucleotide sugar transporters

As explained above sugar molecules have to be activated by addition to nucleotides or dolicholphosphate before they can be transferred to proteins. Sugar donors for dolicholphosphate-sugar conjugates are again nucleotide sugars. These nucleotide sugar molecules are generally synthesized in the cytoplasm, except CMP-sialic acid, which is synthesized in the nucleus. In any case, they need to be imported into the lumen of the ER and Golgi apparatus, which is catalyzed by a family of nucleotide sugar transporters. These proteins are antiporters that exchange one nucleotide sugar molecule for the corresponding nucleotide monophosphate, e.g. UDP-Glc for UMP in the ER (reviewed in [162, 163], **Fig. 12**). Thus, for being exported, the nucleotide diphosphates need to be hydrolyzed after transfer of the sugar.

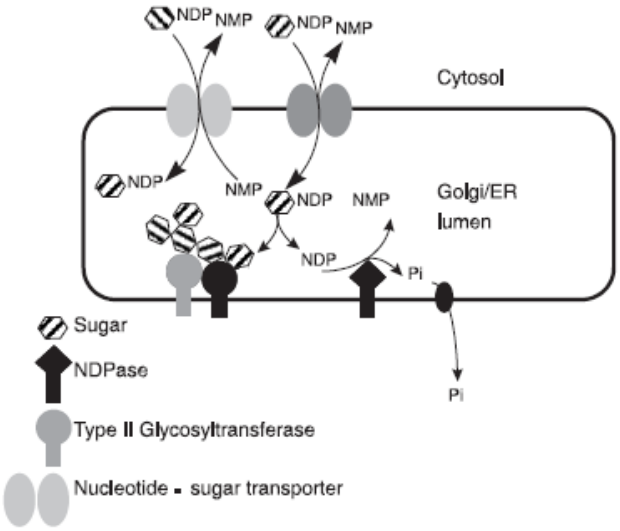


**Fig. 12 Import of nucleotide sugars into the ER or Golgi apparatus.**

After transfer of the sugar to the protein, the remaining NDP is hydrolyzed by an NDPase and the emerging NMP is exported into the cytosol in exchange for an incoming nucleotide sugar. From [164].

# 2 Aims of the study

This study addressed the challenges of prostate cancer diagnosis, prognosis and treatment by the description of novel diagnostic and/or prognostic biomarkers for prostate cancer and the functional characterization of these proteins. From a previous gene array study published by our group, CANT1, FOXA1 and GOLM1 were selected for further analyses due to overexpression of these genes in prostate cancer specimens.

Recently, overexpression of GOLM1 was confirmed on protein level. Immunohistochemical analysis of GOLM1 protein expression in tissue specimens as well as GOLM1 mRNA measurement in urine were suggested to be applied in prostate cancer diagnostics. In the first part of this study, similar analyses were conducted for CANT1 and FOXA1. The expression patterns of both proteins were analyzed immunohistochemichally in tissue specimens of different stages of prostate cancer development. For CANT1, protein secretion was evaluated in the supernatant of prostate cancer cells as well as serum samples. The diagnostic and prognostic potential of the candidate markers was evaluated by comparing CANT1 and FOXA1 protein expression levels between normal and cancer samples and by analysing the correlation between protein expression and clinicopathological and survival data, respectively.

For each protein, the tumorbiological relevance was investigated. Therefore, expression of the protein was analyzed in benign and malignant prostatic cell lines and specific knockdown and/or overexpression protocols were established in the corresponding cell lines with high or low endogenous protein levels. Of these cells, cell proliferation and migration rate and cell cycle distribution were studied in *in vitro* assays in comparison to control cells.

Finally, the underlying mechanism responsible for the involvement of CANT1 in tumor initiation was examined in more detail. This will help to better understand the molecular processes during prostate cancer development and thus contribute to the identification of novel therapeutic targets and finally to the design of more effective treatments.

# 3 Materials and Methods

## *3.1 Materials*

### 3.1.1 Reagent lists

#### 3.1.1.1 Primary antibodies

**Tab. 3 Primary antibodies.**

WB = Western Blot, IHC = immunohistochemistry, IF = immuofluorescence, ELISA = enzyme-linked immunosorbent assay, GFP = green fluorescent protein.

| protein | company, clone | species | clonality | application |
|---|---|---|---|---|
| Actin | Millipore (MAB1501, Billerica, MA, USA) | mouse | monoclonal | WB |
| CANT1 | Abnova (clone 2D3, Taipei, Taiwan) | mouse | monoclonal | WB, IHC, IF, ELISA |
| CANT1 | Sigma-Aldrich (HPA019639, St. Louis, MO, USA) | rabbit | polyclonal | ELISA |
| FOXA1/2 (HNF3α/β) | Santa Cruz Biotech-nologies (clone C-20, Santa Cruz, CA, USA) | goat | polyclonal | WB, IHC, IF |
| GOLM1 (GOLPH2) | Abnova (clone 3B10) | mouse | monoclonal | WB |
| GOLM1 (GOLPH2) | Abcam (Cambridge, UK) | rabbit | polyclonal | IF |
| tGFP | OriGene (Rockville, MD, USA) | mouse | monoclonal | WB |
| HSPA5 | Sigma-Aldrich (HPA038846) | rabbit | polyclonal | WB |
| NTPDase5 (ENTPD5) | Sigma-Aldrich (HPA002927) | rabbit | polyclonal | WB |
| AR | BioGenex (clone F39.4.1, San Ramon, CA, USA) | mouse | monoclonal | IHC, IF |
| ERα | Ventana Medical Systems (clone SP1, Tucson, AZ, USA) | rabbit | monoclonal | IHC |
| ERβ | AbD Serotec (clone 57/3, Oxford, UK) | mouse | monoclonal | IHC |

### 3.1.1.2 Secondary antibodies

**Tab. 4 Secondary antibodies.**

| antibody, conjugate | company | application |
|---|---|---|
| goat anti mouse – horseradish peroxidase | Pierce Biotechnology (Rockford, IL, USA) | WB |
| goat anti rabbit – horseradish peroxidase | Pierce Biotechnology | WB |
| donkey anti goat – horseradish peroxidase | Santa Cruz Biotechnologies | WB |
| goat anti mouse – Alexa 488 | Invitrogen (Carlsbad, CA, USA) | IF |
| goat anti rabbit – Alexa 546 | Invitrogen | IF |
| donkey anti goat – Alexa 546 | Invitrogen | IF |
| goat anti rabbit – horseradish peroxidase | Sigma-Aldrich | ELISA |

### 3.1.1.3 Primers

**Tab. 5 Primers.**

ALAS = aminolevulinate, delta-, synthase, HPRT = hypoxanthine phosphoribosyltransferase, TRIB = tribbles homolog, Herpud = homocysteine-inducible, endoplasmic reticulum stress-inducible, ubiquitin-like domain member,

| gene | forward primer | reverse primer | probe # |
|---|---|---|---|
| ALAS1 | 5’ TAA TGA CTA CCT AGG AAT GAG TCG 3’ | 5’ CCA TGT TGT TTC AAA GTG TCC A 3’ | 43 |
| HPRT1 | 5’ TGA CCT TGA TTT ATT TTG CAT ACC 3’ | 5’ CGA GCA AGA CGT TCA GTC CT 3’ | 73 |
| CANT1 | 5’ CTG GGT GTC CAA CTA CAA CG 3’ | 5’ ACT CCA GCA GGC AGA CTC AT 3’ | 42 |
| FOXA1 | 5’ AGG GCT GGA TGG TAT TG 3’ | 5’ ACC GGG ACG GAG GAG TAG 3’ | 1 |
| GOLM1 | 5’ AAC AAC GAC CAG AGA CAG CA 3’ | 5’ CCT TGT GGC ACC TCT GTG T 3’ | 64 |
| HSPA5 | 5’ CAG CCT GGC GAC AAG AGT 3’ | 5’ CCT TGG GCA GTA TTG GAT TC 3’ | 39 |
| TRIB3 | 5’ GTC TTC GCT GAC CGT GAG A 3’ | 5’ CAG TCA GCA CGC AGG AGT C 3’ | 67 |
| Herpud1 | 5’ CAA AAA TGC CAG AAA TCA ACG 3’ | 5’ CTG TCC CCG ATT AGA ACC AG 3’ | 82 |
| NTPDase5 | 5’ TTT GGA TTG AAA GCT GCA AG 3’ | 5’ GAA AGT GTG CCC ATC AGT CC 3’ | 80 |

All probes were labeled with a FAM reporter dye. Primers and probes were purchased from Microsynth (Balgach, Switzerland) and Roche Applied Science (Mannheim, Germany), respectively.

#### 3.1.1.4 SiRNAs

**Tab. 6 SiRNAs.**

| gene | # siRNA | target sequence |
|---|---|---|
| unspecific | | 5' AAT TCT CCG AAC GTG TCA CGT 3' |
| CANT1 | #1<br>#2 | 5' CCA GAT CAT TGT GGC CCT CAA 3'<br>5' ACC CGG AAT GGA ATG AGT CTA 3' |
| FOXA1 | #1<br>#2<br>#3 | 5' CCA GAC GGG TTT CAT TAT TAT 3'<br>5' CAA ACC GTC AAC AGC ATA ATA 3'<br>5' CTC CTC CGT CCC GGT CAG CAA 3' |
| GOLM1 | #1<br>#2<br>#3 | 5' AAG CGG AAT CAT ACA CTC TGA 3'<br>5' CAT GTT TAA TTT GTA CGC ATA 3'<br>5' TAG GCT CTT ACC ACT TGC AAA 3' |
| NTPDase5 | | 5' CTG CCT AAC CAC TCA AGA GTA 3' |

SiRNAs were purchased from Qiagen (Hilden, Germany) and were applied in a final concentration of 10 nM.

### 3.1.2 Patients material

#### 3.1.2.1 Tissue samples for the study on CANT1

Two patient cohorts were used to follow CANT1 expression during prostate cancer development and to evaluate the diagnostic and prognostic potential of CANT1 immunohistochemistry.

Cohort #1 consists of formalin-fixed paraffin-embedded prostate tissues from 529 patients, who were diagnosed at the Institute of Surgical Pathology, University Hospital Zurich, between 1993 and 2006 [18]. Clinical follow-up data were available for 201 patients following RPE. Seventy-nine patients (39 %) experienced a PSA-relapse, defined as a rising PSA level exceeding 0.1 ng/ml, having reached a nadir after surgery. The median follow-up time (of all patients) was 67 months. This study was approved by the Cantonal Ethics Committee of Zurich (approval number StV 25-2007). The clinicopathological data for evaluable (see chapter 3.2.1.1) primary carcinoma cases are given in **Tab. 7**.

**Tab. 7 Clinicopathological data of primary prostate carcinoma specimens (RPE) in cohort #1 (n=238).**

Only the cases are included that were evaluable for CANT1 staining.

| parameter | median (range) / cases (percentage) |
|---|---|
| age | 65 (50-77) |
| pre-OP PSA | 12.3 (0.2-209) |
| Gleason score | |
| 5-6 | 37 (15.5 %) |
| 7 | 138 (58 %) |
| 8-10 | 63 (26.5 %) |
| pT stage | |
| pT2 | 142 (59.7 %) |
| pT3/4 | 96 (40.3 %) |
| margin status | |
| R0 | 150 (63 %) |
| R1 | 85 (35.7 %) |

Formalin-fixed paraffin-embedded RPE specimens from 640 patients who underwent RPE between 1999 and 2005 at the Department of Urology, Charité–Universitätsmedizin Berlin, were included in cohort #2 (**Tab. 8**), which was approved by the Charité University Ethics Committee (approval number EA1/06/2004) on 20 September 2004. Eighty-five patients (14.6 %) experienced a PSA-relapse. The median follow-up time of all cases was 47.5 months.

**Tab. 8 Clinicopathological data of primary prostate carcinoma specimens (RPE) in cohort #2 (n=640).**

| parameter | median (range) / cases (percentage) |
|---|---|
| age | 62 (43-74) |
| pre-OP PSA | 7.2 (0.8-39) |
| Gleason score | |
| 5-6 | 234 (36.6 %) |
| 7 | 293 (45.8 %) |
| 8-10 | 112 (17.5 %) |
| pT stage | |
| pT2 | 442 (69.1 %) |
| pT3/4 | 197 (30.8 %) |
| margin status | |
| R0 | 463 (72.3 %) |
| R1 | 173 (27 %) |

#### 3.1.2.2 Tissue samples for the study on FOXA1 and steroid hormone receptors

For the analysis of FOXA1, AR, ERα and ERβ expression in prostatic tissue cohort #1 with updated patient data was applied. Ninety-two patients (44.4 %) experienced a biochemical (PSA) relapse after a median time of 24 months. The median follow-up time of all patients was 60 months. The clinicopathological data for evaluable (see chapter 3.2.1.1) primary carcinoma cases are given in **Tab. 9**.

**Tab. 9 Clinicopathological data of primary prostate carcinoma specimens (RPE) in cohort #1 (n=288).**

Only the cases are included that were evaluable for FOXA1 staining.

| parameter | median (range) / cases (percentage) |
|---|---|
| age | 65 (46-57) |
| pre-OP PSA | 11.1 (0.4-357) |
| Gleason score | |
| 5-6 | 35 (16.9 %) |
| 7 | 119 (57.5 %) |
| 8-10 | 53 (25.6 %) |
| pT stage | |
| pT2 | 129 (62.3 %) |
| pT3/4 | 78 (37.7 %) |
| margin status | |
| R0 | 131 (63.9 %) |
| R1 | 74 (35.7 %) |

Additionally, 23 cases of CRPC patients that were transurethrally resected for palliation and one bone trephine of a CRPC metastasis from the archives of the Institute of Surgical Pathology, University Hospital Zurich, were enclosed. This study was approved by the Cantonal Ethics Committee of Zurich (approval number StV 25-2007).

#### 3.1.2.3 Patients sera

Serum samples (n=38) were collected from 15 healthy individuals and 23 prostate cancer patients who were treated at the Clinic and Policlinic for Oncology, University Hospital Zurich, between 2008 and 2010 and gave informed consent.

## *3.2 Methods*

### 3.2.1 Studies on patients material

#### 3.2.1.1 Tissue microarray (TMA) construction

The TMA of cohort #1 was constructed as described [18], each case was represented by a single 0.6 mm core of tissue. Three-hundred-fourty-nine of 529 cores were evaluable for CANT1 staining. These cases represent 30 BPH, 269 primary prostate carcinomas, 29 lymph node and distant metastases and 21 CRPC.

FOXA1 staining was analyzable in 288 cores. The distribution was as follows: 15 cases of BPH, 207 primary prostate carcinomas, 39 lymph node and distant metastases and 27 CRPC. Because FOXA1 staining was much lower in the transitional zone (data not shown), where BPH is derived from, adjacent normal tissue around the tumor that was of peripheral zone origin was analyzed instead, enough evaluable normal tissue was present in 204 of the primary carcinomas.

The TMA of cohort #2 was constructed as described before [16, 17, 58]. Briefly, each case was represented by five cores of 2 mm in diameter each, encompassing BPH of the transitional zone, normal tissue from the peripheral zone, PIN if present (otherwise another core from the peripheral zone), and two cores of invasive carcinoma, ideally of primary and secondary Gleason score. CANT1 staining of normal and cancerous cores was evaluable for 618 patients, the PIN core was evaluable for 467 patients.

#### 3.2.1.2 Immunohistochemistry and immunofluorescence

Freshly cut sections (3 µm) from the TMAs or cell blocks were analyzed by immunohistochemistry using the Ventana Benchmark automated staining system and Ventana reagents (Ventana Medical Systems) according to the manufacturer's recommendations. Following antigen retrieval using the "CC1 protocol", primary antibodies (CANT1 mouse, FOXA1/2, AR, ERα, ERβ) were detected by the UltraVIEW DAB detection kit. Subsequently, the slides were counterstained with haematoxylin, dehydrated and mounted.

To prove specificity of the CANT1 antibody, two consecutive slides were stained as described above. The antibody solution for one slide was pre-incubated with CANT1 recombinant protein (Q1, Abnova) 100 times in excess overnight at 4 °C.

Double immunofluorescence stainings were performed as described previously [16] using the same CANT1, FOXA1/2 and AR antibody as for immunohistochemistry and the GOLM1 rabbit antibody.

#### 3.2.1.3 Evaluation of immunohistochemistry

On the slides of TMA #1 and additional CRPC cases, CANT1, FOXA1, AR, ERα and ERβ staining intensity was evaluated using a scoring system that differentiates between negative (0), weak (1), moderate (2) and strong (3) staining.

Since TMA #2 with its multiple cores and the larger diameter per core allowed a better estimation of intratumoral heterogeneity, a more differentiated evaluation scheme was applied to evaluate CANT1 staining intensity in addition to the simpler 0-3 rating. A *Histochemical score* (H-score) was set up to include the percentages of weak, moderate and strong expression and to sum these up in a weighted manner (H-score = (1 * percentage weak) + (2 * percentage moderate) + (3 * percentage strong)).

### 3.2.2 Cell biological methods

#### 3.2.2.1 Cell culture

Three prostate cancer cell lines derived from a lymph node metastasis (LNCaP), bone metastasis (PC-3) and brain metastasis (DU-145), one immortalized prostate epithelium cell line (RWPE-1) and one embryonic kidney cell line (HEK293) were used. All cell culture consumables were purchased from Invitrogen if not otherwise indicated. LNCaP cells (DSMZ, Braunschweig, Germany) were cultivated in RPMI-1640 Medium, PC-3 cells (ATCC, Manassas, VA, USA) were cultivated in Ham's F-12 Medium/Kaighn's Modification, DU-145 and HEK293 (ATCC) cells were cultivated in Eagle's Minimal Essential Medium, all of these media were supplemented with 10 % fetal bovine serum (FBS). RWPE-1 cells (ATCC) were grown in Keratinocyte Serum Free Medium mixed with bovine pituitary extract and human recombinant EGF. All cell lines were cultivated in cell culture flasks (TPP, Trasadingen, Switzerland) at 37 °C and 5 % $CO_2$. For experiments cell culture test plates of different sizes (all TPP) were applied.

To passage the cells, PC-3 and DU-145 cells were washed with phosphate buffered saline (PBS), trypsinized for 10 min at 37 °C, resuspended in medium and seeded in new flasks. LNCaP cells were trypsinized for 15 min and centrifuged for 3 min at 1.200 rpm and room temperature (RT) before seeding. RWPE-1 cells were washed with PBS, trypsinized for 10 min at 37 °C and centrifuged for 3 min at 1.200 rpm and RT before seeding. HEK293 cells were detached by tapping the flask and centrifuged for 3 min at 1.200 rpm and RT before seeding. All cell lines were passaged maximal 30 times upon receipt.

PC-3, DU-145, RWPE-1 and HEK293 cells were frozen in complete medium supplemented with additional 10 % FBS and 10 % DMSO (Dimethylsulfoxid, Merck, Darmstadt, Germany). LNCaP cells were frozen in complete medium supplemented with additional 20 % FBS and 5 % DMSO. Frozen cells were stored at -70 °C overnight and at -170 °C for long-time storage.

#### 3.2.2.2 Cell counting

Cell counting was performed using the Nucleocounter and the corresponding cassettes, which are filled with propidium iodide (PI). The signal was detected by a camera. Thus, if applied to untreated cell suspensions, dead cells were counted. The total cell number was measured by lysing the cells before with lysis buffer and treating them with stabilizing buffer (machine and consumables chemometec, Allerød, Denmark). The number of living cells was then calculated.

#### 3.2.2.3 Generation of cell blocks

A pellet of 1 x $10^7$ cells was mixed with four drops blood plasm (blood bank) and one drop thrombin (Diagnotec, Liestal, Switzerland) and fixed with 4 % formalin (Kantonsapotheke Zürich, Zurich, Switzerland). The coagulum was dehydrated overnight and embedded in paraffin (Paraplast, McCormick Scientific, Richmond, IL, USA).

#### 3.2.2.4 Transient gene knockdown and overexpression

For transient gene knockdown PC-3 cells were transfected using Lipofectamine 2000 (Invitrogen). The transfection mix was prepared according to the manufacturer's instructions and added to the cells immediately after seeding. Twenty-four hours later the transfection medium was removed and the cells were cultivated in complete medium. For transfection of CANT1 and FOXA1 siRNAs LNCaP cells were transfected using HiPerFect transfection reagent (Qiagen) following the FastForward Protocol provided by the manufacturer. For GOLM1 and NTPDASE5 siRNAs, the transfection efficiency in LNCaP cells was higher with Lipofectamine 2000. A similar protocol as for PC-3 cells was applied, due to weaker adhesion to the test plate surface, no medium was changed 24 h after transfection. Higher cell numbers were needed compared to transfection with HiPerFect, because Lipofectamine 2000 was more aggressive to the cells and decreased vitality. DU-145 cells were transfected with HiPerFect, twice as much transfection reagent was necessary for efficient knockdown. The variable parameters in the transfection protocol are listed in **Tab. 10**.

**Tab. 10 Parameters for siRNA transfection.**

| cell line | target gene | test plate | cell number | transfection reagent | |
|---|---|---|---|---|---|
| PC-3 | all | 6-well plate | 2 x $10^5$ | 5 µl | Lipofectamine 2000 |
| | | 6 cm-dish | 4 x $10^5$ | 10 µl | Lipofectamine 2000 |
| LNCaP | CANT1, FOXA1 | 6-well plate | 3 x $10^5$ | 6 µl | HiPerFect |
| | | 6 cm-dish | 6 x $10^5$ | 10 µl | HiPerFect |
| | GOLM1, NTPDase5, double knockdown of CANT1 and NTPDase5 | 6 cm-dish | 8 x $10^5$ | 10 µl | Lipofectamine 2000 |
| DU-145 | GOLM1 | 6 cm-dish | 2.5 x $10^5$ | 20 µl | HiPerFect |

For transient overexpression, cells were seeded in 6 cm-dishes and grown for the indicated time periods until a confluence of ~80 % was reached. Then, cells were transfected with pCMV6-AN-GFP (named GFP) or pCMV6-XL6-CANT1 (named CANT1, both OriGene) or a mixture of both in the ratio 2:1 using Lipofectamine 2000 or FuGENE 6 (Roche Applied Science, Mannheim, Germany) according to the manufacturers' protocols. Five hours after transfection of DU-145 medium was changed.

To rescue CANT1 expression, CANT1 knockdown PC-3 cells (PC-3 siRNA) were transfected with CANT1 vectors. Therefore, CANT1 was knocked down using siRNA as described above and 3 days later the cells were transfected with CANT1 DNA vector. Due to decreased vitality of siRNA treated cells, more cells were seeded in comparison to untreated PC-3 cells (PC-3 untr). The variable transfection parameters of the vector transfection protocol are given in **Tab. 11**.

**Tab. 11 Parameters for vector transfection.**

| cell line | days before transfection | cell number | amount of DNA | transfection reagent | |
|---|---|---|---|---|---|
| RWPE-1 | 3 | 1.2 x $10^6$ | 8 µg | 20 µl | FuGENE 6 |
| DU-145 | 2 | 5 x $10^5$ | 4 µg | 20 µl | Lipofectamine 2000 |
| HEK293 | 1 | 2 x $10^6$ | 8 µg | 24 µl | Lipofectamine 2000 |
| PC-3 untr | 3 | 2.5 x $10^5$ | 8 µg | 40 µl | FuGENE 6 |
| PC-3 siRNA | 3 | 5 x $10^5$ | 8 µg | 40 µl | FuGENE 6 |

All transfection mixes were prepared in Opti-MEM (Invitrogen).

#### 3.2.2.5 DNA synthesis rate

DNA synthesis rate measurement was conducted using the Cell Proliferation ELISA, bromodeoxyuridine (BrdU) kit (Roche Applied Science) according to the manufacturer's instructions. The kit is based on brome-labeled uridine (BrdU), which is incorporated into newly synthesized DNA strands instead of thymidine. Briefly, cells were seeded (**Tab. 12**) in 96-well plates, after 6 h, BrdU labeling reagent was added to the medium and cells were incubated at 37 °C overnight. Subsequently, cells were fixed and stained with an anti-BrdU antibody, which was detected with substrate solution. The color reaction was stopped by adding $H_2SO_4$ (Sigma-Aldrich) and the optical density (OD) was measured at 450 nm and at 595 nm as reference wavelength using the infinite F200 microplate reader (Tecan, Männedorf, Switzerland).

**Tab. 12 Cell number for proliferation assay.**

| cell line | cell number |
|---|---|
| LNCaP | 2 x $10^4$ |
| PC-3 knockdown cells | 5 x $10^3$ |
| PC-3 overexpression cells (untr) | 5 x $10^3$ |
| PC-3 overexpression cells (siRNA) | 1 x $10^4$ |
| RWPE-1 | 2 x $10^4$ |
| DU-145 | 5 x $10^3$ |
| HEK293 | 2 x $10^4$ |

3.2.2.6 Cell cycle analysis

Cells were cultivated in 6 cm-dishes and detached as described in chapter 3.2.2.1, washed twice with sample buffer (1 % glucose [Merck] in PBS) and fixed with 70 % ethanol (Merck) overnight at 4 °C. The next day, 1 x $10^6$ cells were incubated with 50 µg/ml PI (Sigma-Aldrich), 0.3 mg/ml RNaseA (Qiagen) and 0.05 % Triton X-100 (Sigma-Aldrich) in sample buffer for 30 min at RT and analyzed by flow cytometry using the FACSCalibur (BD, Franklin Lakes, NJ). Proportion of cells in gap (G) 1-, synthesis (S) - and G2/mitotic (M)-phase was determined applying the Dean/Jett/Fox-model provided by the FlowJo 6.3 software (Tree Star, Ashland, OR, USA).

For cell cycle analyses it is of special importance that the cells have not reached 100 % confluence at the time of analysis, else they would undergo G1-arrest. Thus, to circumvent this phenomenon, lower numbers of untransfected cells were seeded because these cells proliferated stronger than transfected cells (**Tab. 13**).

**Tab. 13 Cell number for cell cycle analyis.**

| cell line | cell number | |
|---|---|---|
| | untr | siRNA |
| LNCaP HiPerFect | 5 x $10^5$ | 6 x $10^5$ |
| LNCaP Lipofectamine 2000 | 6 x $10^5$ | 8 x $10^5$ |
| PC-3 | 2 x $10^5$ | 4 x $10^5$ |
| DU-145 | 1.5 x $10^5$ | 2.5 x $10^5$ |

3.2.2.7 Transmigration assay

Haptotactic cell migration was analyzed in a modified boyden chamber assay. Transwell chambers (Corning, Corning, NY, USA) were coated at the bottom side with 10 µg/ml fibronectin (Roche Applied Science) for 2 h at RT in a humid chamber. Then, the inserts were placed into 24-well plates, the lower chamber was filled with 600 µl serum free RPMI-

1640 Medium supplemented with 0.5 % bovine serum albumine (BSA, Sigma-Aldrich) and the cells were seeded (**Tab. 14**) in 200 µl of this migration medium in the upper chamber. In the case of RWPE-1 cells Keratinocyte Serum Free Medium without supplements with 0.5 % BSA was used. After 24 h incubation at 37 °C non-migrated cells were removed with a cotton swab and the remaining cells were fixed by placing the inserts in 600 µl of methanol/acidic acid (both Simga-Aldrich) in a 3:1 ratio. After the inserts had been air-dried, they were incubated in a DAPI (4′,6-Diamidino-2-phenylindole dihydrochloride) solution (2.5 µg/ml DAPI [Sigma-Aldrich] in PBS) for 15 min at RT on a shaker. Afterwards the wells were washed twice with PBS and the amount of migrated cells was analyzed under the microscope (magnification 25x). Pictures were taken at nine defined places of the membrane and analyzed with ImageJ 1.4 software (National Institutes of Health, Bethesda, MD, USA). The migration rate was quantified by determining the area of the membrane that was covered with stained nuclei. A negligible small number of cells, which was not quantified, had migrated through the membrane, detached from the membrane and attached to the bottom of the well.

**Tab. 14 Cell number for transmigration assay.**

| cell line | cell number |
|---|---|
| LNCaP | $5 \times 10^4$ |
| PC-3 knockdown cells | $5 \times 10^4$ |
| PC-3 overexpression cells (untr) | $3 \times 10^4$ |
| PC-3 overexpression cells (siRNA) | $5 \times 10^4$ |
| RWPE-1 | $1 \times 10^5$ |
| DU-145 | $5 \times 10^4$ |
| HEK293 | $7 \times 10^4$ |

#### 3.2.2.8 Scratch wound assay

DU-145 cells were seeded in 6 cm-dishes and transfected with siRNAs as described in chapter 3.2.2.4. A total of $4 \times 10^5$ cells were seeded to reach confluence after 72 h, transfection efficiency was similar as with $2.5 \times 10^5$ seeded cells (data not shown). Then, a wound was introduced into the cell monolayer using a yellow pipette tip and pictures were taken at the marked areas after 0 and 8 h. Because the full knockdown efficiency of PC-3 cells was reached already after 8 h (data not shown) and PC-3 cells close the wound slowlier than DU-145 cells do, the protocol was adapted accordingly. The cells were grown to ~95 % confluence before they were transfected with siRNAs as described in chapter 3.2.2.4 and pictures were taken after 0 and 24 h. In both cases, the area of the wound was measured using ImageJ 1.4 software.

3.2.2.9 Ultracentrifugation and precipitation of supernatants

Cells were cultivated in 75 cm² cell culture flasks in 10 ml complete medium to ~70 % confluence, then the medium was changed to serum-free medium. Therefore, PC-3 cells were washed three times with PBS, LNCaP cells were washed twice with prewarmed serum-free medium. To enrich secreted proteins only 7.5 ml serum-free medium were added. After 24 h cell supernatants were centrifuged for 20 min at 1.200 rpm and 4 °C, transferred to new tubes and centrifuged again for 20 min at 4.000 rpm and 4 °C to pellet detached cells and cell debris. Afterwards ~16 ml supernatant were transferred to Ultra-Clear centrifuge tubes and vesicles were separated by ultracentrifugation in a SW32.1 Ti rotor (both Beckman Coulter, Palo Alto, CA, USA) for 2.5 h at 24.000 rpm and 4 °C. The ultracentrifugation pellet was resuspended in 30 µl 1x Lämmli-buffer or NuPAGE LDS sample buffer (Invitrogen) and incubated for 5 min at 95 °C. Supernatants were then precipitated by adding trichloroacetic acid (Simga-Aldrich) to a final concentration of 10 % and centrifugation for 15 min at 14.000 rpm and 2 °C. Pellets were washed with icecold acetone (Simga-Aldrich) by centrifugation for 15 min at 14.000 rpm and 2 °C, air-dried, resuspended in 1x sample buffer and incubated for 5 min at 95 °C.

5x Lämmli-buffer:

| | | |
|---|---|---|
| 17.5 | ml | glycerine |
| 8 | mg | SDS |
| 16 | ml | 1M TrisHCL pH 6.8 |

All ingredients were purchased from Sigma-Aldrich. SDS = sodium dodecyl sulfate.

3.2.2.10 ER stress induction

To induce ER stress, cells were grown in 6 cm-dishes to ~50 % confluence (**Tab. 15**) and treated with 30 nM thapsigargin (AppliChem, Darmstadt, Germany) or 1 µM tunicamycin (Sigma-Aldrich) for 8 to 48 h as indicated. The stock solution (300 µM) of thapsigargin was dissolved in 70 % ethanol, this stock was further diluted 1:10 in cell culture medium freshly before usage. The stock solution (1.2 mM) of tunicamycin was dissolved in DMSO. This solution was directly added to the cells. As negative control, the cells were treated with 70 % ethanol freshly diluted 1:10 in cell culture medium or pure DMSO, respectively.

**Tab. 15 Cell seeding for ER stress induction.**

| cell line | cell number | days before treatment |
|---|---|---|
| RWPE-1 | 1.2 x $10^6$ | 2 |
| LNCaP | 1 x $10^6$ | 2 |
| DU-145 | 4 x $10^5$ | 1 |
| PC-3 | 6 x $10^5$ | 1 |

### 3.2.3 Molecular biological methods

#### 3.2.3.1 Cell lysis

Cells were detached as described in chapter 3.2.2.1 and washed with PBS before lysis in a buffer containing 60 mM n-Octyl-ß-D-glucopyranoside (Sigma-Aldrich) and protease inhibitors (complete, Mini, EDTA-free, Protease Inhibitor cocktail tablets; Roche Applied Science) for 30 min on ice. Lysates were centrifuged for 15 min at 14.000 rpm and 4 °C, supernatants were supplemented with 5x Lämmli-buffer or 4x NuPAGE LDS sample buffer and incubated for 5 min at 95 °C.

20x PBS:

| | | |
|---|---|---|
| 160 | g | NaCl |
| 6 | g | KCl |
| 28.8 | g | $Na_2HPO_4$ x 2 $H_2O$ |
| 4 | g | $KH_2PO_4$ |

add 1 l $H_2O$

The pH was adjusted to pH 7.4. NaCl was obtained from the Kantonsapotheke Zürich, the other ingredients were purchased from Merck. This self-made PBS was only used for non-cell culture experiments.

#### 3.2.3.2 Measurement of protein concentration

Cell lysates without sample buffer were diluted 1:200 in Quick-Start Bradford Dye Reagent (Bio-Rad, Hercules, CA, USA) and incubated for 5 min at RT. A standard curve with increasing concentrations of BSA was included in the same 96-well plate. The optical density at 595 nm was measured using the infinite F200 microplate reader (Tecan).

#### 3.2.3.3 Western Blot analysis

Before Western Blot analysis, β-Mercaptoethanol (Sigma-Aldrich) was added freshly to a final concentration of 5 % and lysates were incubated again for 5 min at 95 °C. Twenty microgram of lysates were separated by SDS-polyacrylamid gelelectrophoresis (Mini-PROTEAN Tetra Electrophoresis System, Bio-Rad). Depending on the size of the protein to be detected, gels containing 10 % or 12.5 % acrylamide were used. In parallel, a protein standard was loaded (Precision Plus Protein Kaleidoscope standard [Bio-Rad] or MagicMark XP Western Protein Standard mixed with SeeBlue Prestained Standard [Invitrogen]). Subsequently, proteins were transferred (Mini Trans-Blot Cell, Bio-Rad) onto a polyvinylidene fluoride-membrane (Bio-Rad). The membrane was blocked for 1-2 h at RT with 3 % skim milk (Rapilait, MIGROS, Zurich, Switzerland) or 1 % BSA in PBS-Tween (0.5 % Tween 20

[Sigma-Aldrich] in PBS) or in 1x Roti-Block (Carl Roth, Karlsruhe, Germany) and incubated overnight at 4 °C in primary antibody solution, which was diluted in the corresponding blocking buffer (in case of Roti-Block in 1:10 diluted Roti-Block in PBS-Tween). The next day, the membrane was washed four times in PBS-Tween, incubated in the secondary antibody solution, which was diluted as the primary antibody solution, and washed again four times in PBS-Tween. To detect the horseradish peroxidase signal, the membrane was either incubated for 1 min in Amersham ECL Western Blotting Detection Reagents (GE Healthcare, Fairlield, CT, USA; for Actin, tGFP) or for 5 min in SuperSignal West Dura Extended Duration Substrate (Pierce Biotechnology; all remaining primary antibodies). Subsequently, the membrane was either exposed to X-ray films (Amersham Hyperfilm ECL, GE Healthcare) or a camera system (ChemiDoc XRS+ System, Bio-Rad) was used to record the signal.
As loading control, membranes were reprobed with anti-Actin antibody.

| | resolving gel | | | | | |
|---|---|---|---|---|---|---|
| | 10 % | | 12.5 % | | stacking gel | |
| $H_2O$ | 4.6 | ml | 3.7 | ml | 1.8 | ml |
| Resolving buffer | 2.8 | ml | 2.8 | ml | | |
| Stacking buffer | | | | | 960 | µl |
| Protogel | 3.7 | ml | 4.6 | ml | 280 | µl |
| 10 % APS | 32 | µl | 32 | µl | 13 | µl |
| TEMED | 2.8 | µl | 2.8 | µl | 4 | µl |

Resolving buffer, Stacking buffer, Protogel, ammonium persulfate (APS) and tetramethyl-ethylenediamine (TEMED) were purchased from national diagnostics (Atlanta, GA, USA).

10x running buffer:

| | | |
|---|---|---|
| 60.6 | g | Tris |
| 288.3 | g | glycine |
| 10 | g | SDS |

add 2 l $H_2O$

The pH was adjusted to pH 8.3. All ingredients were purchased from Sigma-Aldrich.

10x blotting buffer:

| | | |
|---|---|---|
| 48.5 | g | Tris |
| 225.5 | g | glycine |

add 2 l $H_2O$

1x blotting buffer:

| | | |
|---|---|---|
| 100 | ml | 10x blotting buffer |
| 200 | ml | methanol |

add 1 l $H_2O$

The pH was adjusted to pH 8.3.

#### 3.2.3.4 RNA isolation and quantitative real-time polymerase chain reaction (qRT-PCR)

Cells were detached as described in chapter 3.2.2.1 and washed with PBS. RNA was isolated using the RNeasy kit (Qiagen), DNA was digested on-column with the RNase free DNase Set (Qiagen). For cDNA synthesis the High-Capacity cDNA Reverse Transcription Kit (Applied Biosystems, Foster City, CA, USA) was applied, 200 ng total RNA were transcribed per 20 µl-reaction. QRT-PCR was performed using TaqMan Universal PCR MasterMix (Applied Biosystems) and the Universal Probe Library (Roche Applied Science). Gene expression was normalized to aminolevulinate, delta-, synthase (ALAS) 1, if not otherwise indicated. In certain experiments hypoxanthine phosphoribosyltransferase (HPRT) 1 was used as second housekeeping gene to achieve increased robustness of the results. Both genes are stably expressed in prostate cancer cells [165]. All reactions were run in 96- or 384-well plates (Applied Biosystems) on the 7900HT Fast Real-Time PCR System or Viia7 Real-Time PCR System (both Applied Biosystems). Kits and reagents were used according to the manufacturer's instructions.

#### 3.2.3.5 ELISA

Patients sera and cell culture supernatants were submitted to an ELISA assay for detection of soluble CANT1. The ELISA was performed as a sandwich ELISA as follows: Maxisorb plates (NUNC, Langenselbold, Germany) were coated overnight at 4°C with monoclonal mouse CANT1 antibody. The following day, plates were washed with PBS and blocked using 10 % BSA and 0.5 % Tween 20 for 1 h at RT. Samples were diluted 1:10 and applied in triplicates to the plate for 1.5 h at RT. Recombinant CANT1 protein (P01, Abnova) was plated in increasing concentrations (0.05 µg/ml, 0.1 µg/ml, 0.2 µg/ml, 0.5 µg/ml, 1 µg/ml, 2 µg/ml, 10 µg/ml and 20 µg/ml). Then, plates were incubated with polyclonal rabbit CANT1 antibody for 1 h at RT that was detected by the horseradish peroxidase-linked secondary antibody for 45 min. Inbetween each incubation step, plates were extensively washed. Wells were replenished with 100 µl staining solution (TMBsolution, Pierce Biotechnology) per well and left at RT in the dark for 20 min. The colour reaction was stopped by adding 50 µl 2 N $H_2SO_4$. The absorbance at 450 nm was measured using an Emax microplate reader and analyzed with Softmax Pro V3.0 software (both Molecular devices, Sunnyvale, CA, USA).

#### 3.2.3.6 PNGase F treatment

PNGase F (New England BioLabs, Ipswich, MA, USA) treatment was performed according to the manufacturer's protocol, 20 µg of cell lysate (cell lysis described in chapter 3.2.3.1) without sample buffer were used per reaction. After treatment sample buffer and β-Mercaptoethanol were added and samples were incubated as described in chapters 3.2.3.1 and 3.2.3.3.

### 3.2.4 Statistical analyses

Mean immunohistochemical staining intensities were compared between different groups of tumor stage using the Mann-Whitney Test for TMA #1 and the Wilcoxon Matched-pairs Test for TMA #2. For analysis of the association of staining intensity with clinicopathological parameters cross tables were calculated (chi square test, 2-tailed Fisher's exact test). Univariate survival analyses were conducted according to Kaplan-Meier (log rank test). For correlation significance tests Spearman's rho test (2-tailed) has been used. These statistics were calculated with PASW18 (SPSS, Chicago, IL, USA). Mean optical density values from the ELISA assay were compared with help of the 2-tailed unpaired t-test.

The cell culture results are displayed as mean ± standard deviation, each experiment was repeated at least three times if not otherwise indicated. Significance was tested in a 2-tailed paired or unpaired t-test depending on the experiment. If necessary, Welch's correction was applied.

# 4 Results

## *4.1 The role of CANT1 in prostate cancer*

### 4.1.1 The expression of CANT1 in human prostatic tissue

Previously, our group has reported an overexpression of CANT1 mRNA in human prostate carcinoma tissue compared to adjacent normal tissue [15]. To confirm the results on protein level and to evaluate the diagnostic and prognostic potential of CANT1 expression, two TMAs representing a total of 989 patients were stained with the CANT1 mouse antibody. The specificity of this antibody was verified by preincubation with CANT1 recombinant protein, which led to the complete blocking of the immunohistochemical staining (**Fig. 13**).

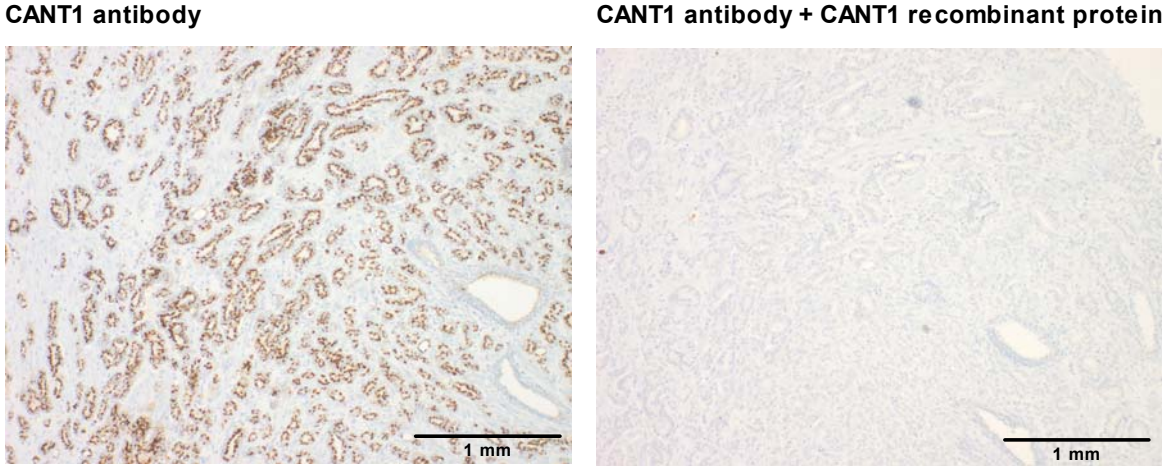


**Fig. 13 Blocking of CANT1 immunohistochemical staining by antigen preincubation.**
Consecutive slides from a prostate adenocarcinoma case were stained with CANT1 antibody or with CANT1 antibody, which was pre-incubated with CANT1 recombinant protein. Magnification 25x.

#### 4.1.1.1 CANT1 protein is overexpressed in human prostate cancer

To compare protein expression levels among different tumor stages and to evaluate the potential of CANT1 as diagnostic marker, the staining intensity of each core was analyzed. In general, CANT1 was only detected in epithelial cells, stroma cells did not express the protein. The pattern of CANT1 immunoreactivity appeared semigranular and was detected perinuclear at the apical side of the epithelium, resembling a typical Golgi apparatus staining pattern (**Fig. 14 a**). Additionally, a diffuse cytoplasmic staining was observed in some cases (**Fig. 14 c**), which was recorded separately on TMA #1. In normal tissue, CANT1 staining was only detected in secretory epithelial cells, whereas basal cells were generally negative for CANT1 (**Fig. 14 a**).

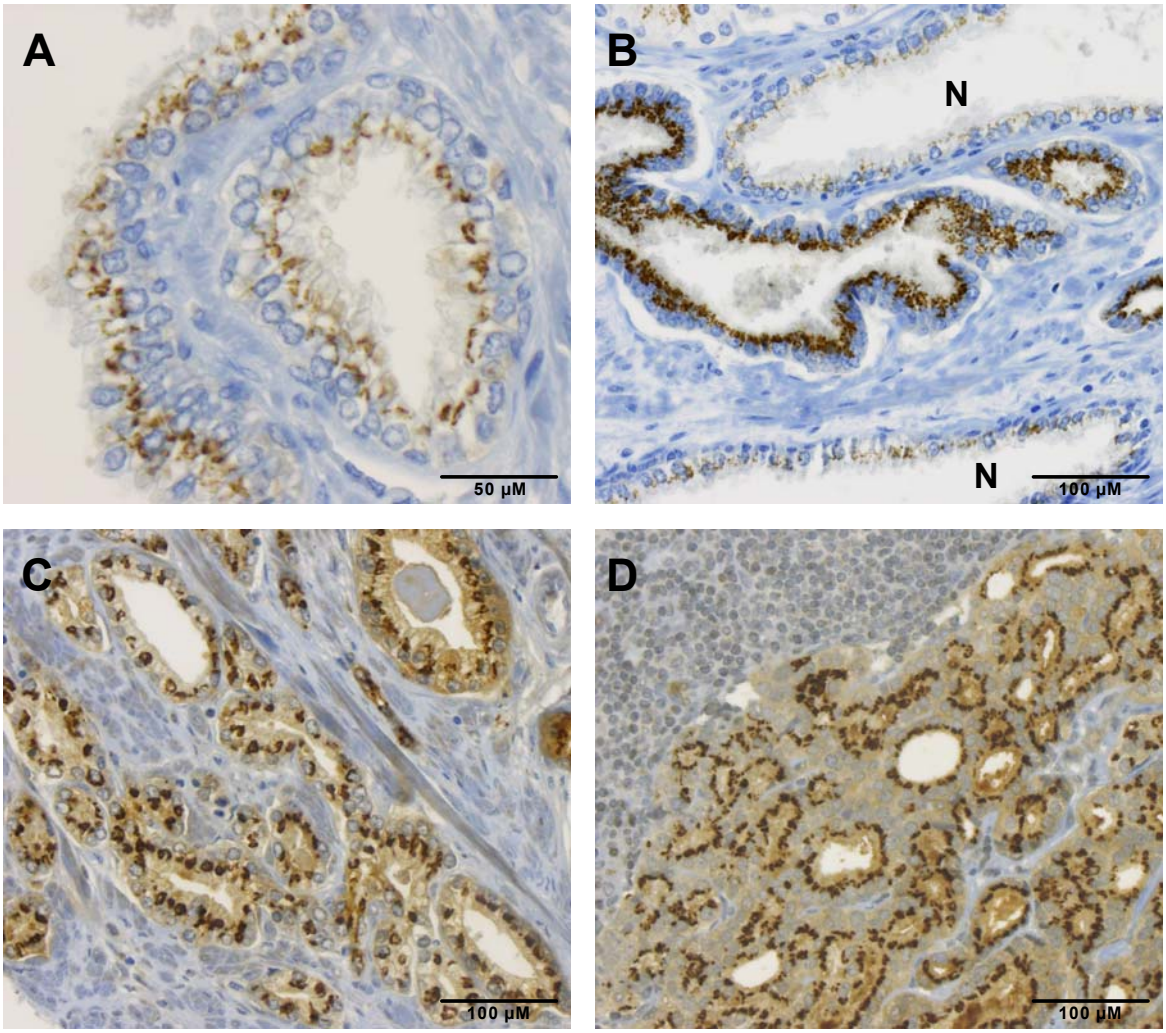


**Fig. 14 CANT1 immunohistochemistry of human prostatic tissues.**

Immunohistochemistry of human prostatic tissues, magnification 200x if not otherwise indicated. **(A)** Normal prostate glands, magnification 400x. **(B)** Prostate adenocarcinoma infiltrating inbetween normal glands (N). **(C)** Prostate adenocarcinoma; note the strong diffuse cytoplasmic staining. **(D)** Prostate cancer metastasis in a lymph node; note the lymphocytes in the upper left corner.

On TMA #1, which contained samples from 30 normal cases, 269 primary carcinomas, 29 metastases and 21 CRPC, CANT1 staining intensity was monitored throughout carcinoma progression. The mean intensity of Golgi and cytoplasmic staining was 1.4 and 0.4 in normal tissue, 2.3 and 1.2 in primary carcinomas, 2.3 and 1.3 in metastases (lymph node metastasis in **Fig. 14 d**) and 1.9 and 0.7 in CRPC, respectively. The difference in the mean staining intensity of CANT1 between normal tissues and primary carcinomas, metastases as well as all cancerous tissues was highly significant for Golgi staining as well as for cytoplasmic staining. However, only the Golgi staining intensity was significantly different between normal tissues and CRPC (**Fig. 15**).

On TMA #2 the mean intensity of CANT1 Golgi staining was 1.0 in normal cores, 1.7 in PIN cores and 1.8 in carcinoma cores (**Fig. 15**). In addition, the composition of TMA #2 allowed

the direct comparison of CANT1 staining intensity between cancerous and adjacent normal tissue from each patient. To detect also subtle differences between carcinoma and normal cores that would in some cases be assigned the same staining score, it was also reported if the cancer area was stained stronger than adjacent normal glands. This was found in 97.2 % of the cases (example in **Fig. 14 b**).

TMA #1

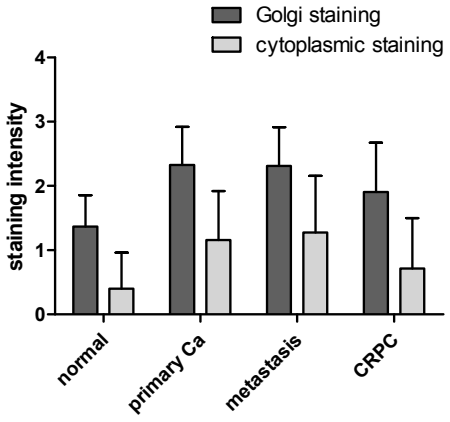


TMA #2

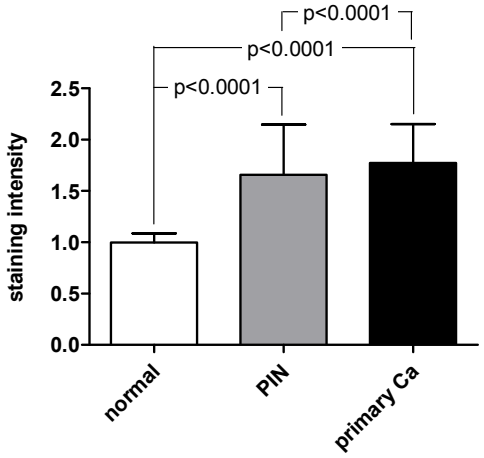


| Golgi staining | normal | primary Ca | metastasis | CRPC | tumor |
|---|---|---|---|---|---|
| normal | - | <0.0001* | <0.0001* | 0.009* | <0.0001* |
| primary Ca | | - | 0.889 | 0.008* | - |
| metastasis | | | - | 0.053 | - |

| cytoplasmic staining | normal | primary Ca | metastasis | CRPC | tumor |
|---|---|---|---|---|---|
| normal | - | <0.0001* | 0.001* | 0.152 | <0.0001* |
| primary Ca | | - | 0.489 | 0.012* | - |
| metastasis | | | - | 0.028* | - |

* statistically significant

**Fig. 15 CANT1 staining intensity in human prostatic tissue samples.**

Mean CANT1 staining intensity during neoplasia development and progression on TMA #1 and #2. P-values for TMA #1 are put together in the tables below. Ca = carcinoma.

Altogether, these data confirm the overexpression of CANT1 in human prostate carcinomas compared to normal prostate epithelium on protein level, which was reported on mRNA level before [15]. We additionally showed that this upregulation occurs already in PIN lesions. Further, CANT1 expression was slightly reduced in CRPC.

#### 4.1.1.2 Relationship of CANT1 staining to clinicopathological parameters and survival analysis

For analysis of the prognostic value of CANT1, the relationship between staining intensities and corresponding clinicopathological and survival data was examined. For these statistical analyses (crosstables and survival analyses) both staining qualities of TMA #1 were dichotomized by the median. No correlations of Golgi and cytoplasmic CANT1 staining with patient age, Gleason score, pT stage and margin status were found. However, cytoplasmic CANT1 staining correlated inversely with pre-OP serum PSA-levels (p=0.026) (**Tab. 16**).

**Tab. 16 Relationship between CANT1 expression and clinicopathological data of primary prostate carcinoma specimens (RPE) in cohort #1.**

* statistically significant

| | Golgi staining | | | cytoplasmic staining | | |
|---|---|---|---|---|---|---|
| parameter | CANT1 low | CANT1 high | p-value | CANT1 low | CANT1 high | p-value |
| age | | | 0.894 | | | 0.782 |
| ≤ 64 years | 68 | 46 | | 78 | 36 | |
| > 64 years | 76 | 48 | | 82 | 42 | |
| pre-OP PSA | | | 0.669 | | | 0.026* |
| ≤ 10 ng/ml | 55 | 35 | | 51 | 39 | |
| > 10 ng/ml | 67 | 49 | | 84 | 32 | |
| Gleason score | | | 0.764 | | | 0.823 |
| 5-6 | 21 | 16 | | 24 | 13 | |
| 7 | 86 | 52 | | 95 | 43 | |
| 8-10 | 37 | 26 | | 41 | 22 | |
| pT stage | | | 0.893 | | | 0.069 |
| pT2 | 85 | 57 | | 102 | 40 | |
| pT3/4 | 59 | 37 | | 58 | 38 | |
| margin status | | | 0.583 | | | 0.563 |
| R0 | 92 | 58 | | 100 | 50 | |
| R1 | 49 | 36 | | 60 | 25 | |

On TMA #2 CANT1 staining intensity values were dichotomized by H-score 1.9, they did not correlate with patient age, serum PSA-levels and margin status. A trend between high Gleason grade and low H-score was noted as well as a significant correlation between high pT stage and low H-score (**Tab. 17**).

**Tab. 17 Relationship between CANT1 expression and clinicopathological data of primary prostate carcinoma specimens (RPE) in cohort #2.**

* statistically significant

| parameter | CANT1 low | CANT1 high | p-value |
|---|---|---|---|
| age | | | 0.273 |
| ≤ 62 years | 196 | 116 | |
| > 62 years | 205 | 100 | |
| pre-OP PSA | | | 0.701 |
| ≤ 10 ng/ml | 293 | 153 | |
| > 10 ng/ml | 104 | 59 | |
| Gleason score | | | 0.054 |
| 5-6 | 136 | 84 | |
| 7 | 185 | 103 | |
| 8-10 | 80 | 29 | |
| pT stage | | | 0.014* |
| pT2 | 262 | 162 | |
| pT3/4 | 139 | 54 | |
| margin status | | | 0.569 |
| R0 | 287 | 159 | |
| R1 | 113 | 55 | |

On univariate analysis of PSA-relapse free survival times no association of CANT1 tissue levels with disease relapse was found on TMA #1, neither for the Golgi nor the cytoplasmic staining (**Fig. 16**). However, due to the larger cores of TMA #2 it was possible to also consider heterogeneity of CANT1 staining and to derive a more differentiated H-score. A careful analysis of these data revealed a good prognosis of patients with the highest CANT1 expression (the upper quartile), whereas the majority of the patients experienced a PSA-relapse much earlier (**Fig. 16**). This prognostic value is maintained in a multivariate analysis including pT stage, Gleason score, margin status and pre-OP serum PSA levels (p-value CANT1 = 0.034). However, this survival difference was not detectable, when only the simpler overall intensity score (0-3) was analyzed (data not shown).

In summary, a prognostic value of CANT1 staining intensity and a corresponding association with pT stage was revealed on TMA #2 using the H-score.

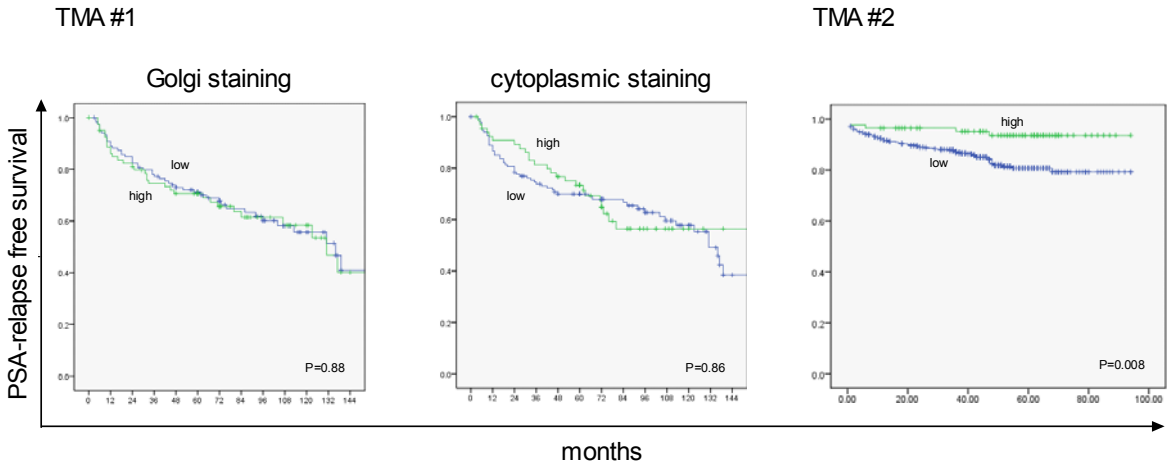


**Fig. 16 Univariate survival analysis dependent on CANT1 staining intensity.**

Kaplan-Meier curves of CANT1 Golgi and cytoplasmic expression on TMA #1 (dichotomized by the median in low [blue] and high [green] levels) and of CANT1 Golgi expression on TMA #2 (green: upper quartile, blue: lower three quartiles of H-score).

### 4.1.2 The influence of CANT1 knockdown and overexpression on *in vitro* tumorigenicity

#### 4.1.2.1 Characterization of CANT1 expression in prostatic cell lines

To test if CANT1 overexpression has a functional relevance in prostate cancer, prostatic cell lines were evaluated for endogenous CANT1 expression levels and selected for subsequent functional studies. The expression on gene and protein level was determined in the immortalized epithelial cell-line, RWPE-1, and in three metastasis-derived cancer cell lines, LNCaP, DU-145 and PC-3. As observed by Western Blot analysis CANT1 protein was strongly expressed in LNCaP and PC-3 cells whereas the band was much weaker in the lysates of DU-145 and RWPE-1 cells. In all four cell lysates a clear double band was visible. Similarly, mRNA expression was strongest in LNCaP and PC-3 cells. High levels of CANT1 mRNA were also detected in DU-145 and RWPE-1 cells (**Fig. 17**).

Thus, two prostate cancer cell lines with high CANT1 levels and a third prostate cancer cell line with low endogenous levels of the protein were identified. Weak expression of CANT1 was detected in the selected benign prostatic cell line.

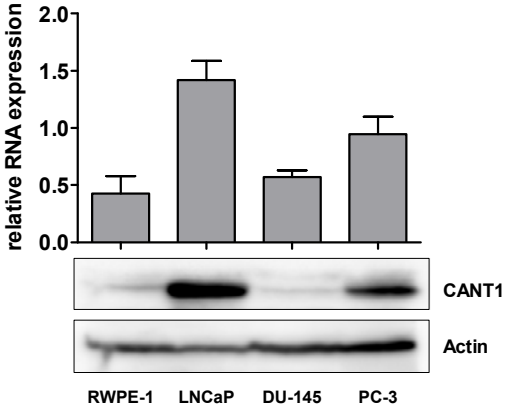


**Fig. 17 Expression of CANT1 in prostatic cell lines.**

RWPE-1, LNCaP, DU-145 and PC-3 cells were cultivated in 75 cm² cell culture flasks to 70-80 % confluence. CANT1 mRNA and protein expression was determined by qRT-PCR (top) and Western Blot analysis (bottom), respectively.

#### 4.1.2.2 Transient knockdown of CANT1 in prostate cancer cell lines with high endogenous CANT1 levels

The goal of this part of the study was to investigate if endogenous CANT1 overexpression contributes to tumorigenicity of prostate cancer cells. According to the strong CANT1 expression on mRNA and protein level (see chapter 4.1.2.1), LNCaP and PC-3 cells were selected for these studies. A knockdown protocol based on RNA interference was established for both cell lines using two CANT1-specific siRNAs. QRT-PCR and Western Blot analysis revealed a potent CANT1 knockdown on mRNA and protein level 72 h after siRNA transfection. The mRNA levels were reduced to 28 % and 49 % in LNCaP cells and to 2 % and 13 % in PC-3 cells, using CANT1 siRNA #1 and #2, respectively. No differences in knockdown efficiency were visible on protein level (**Fig. 18**).

Thus, CANT1 expression was efficiently downregulated using two specific siRNAs in LNCaP and PC-3 cells.

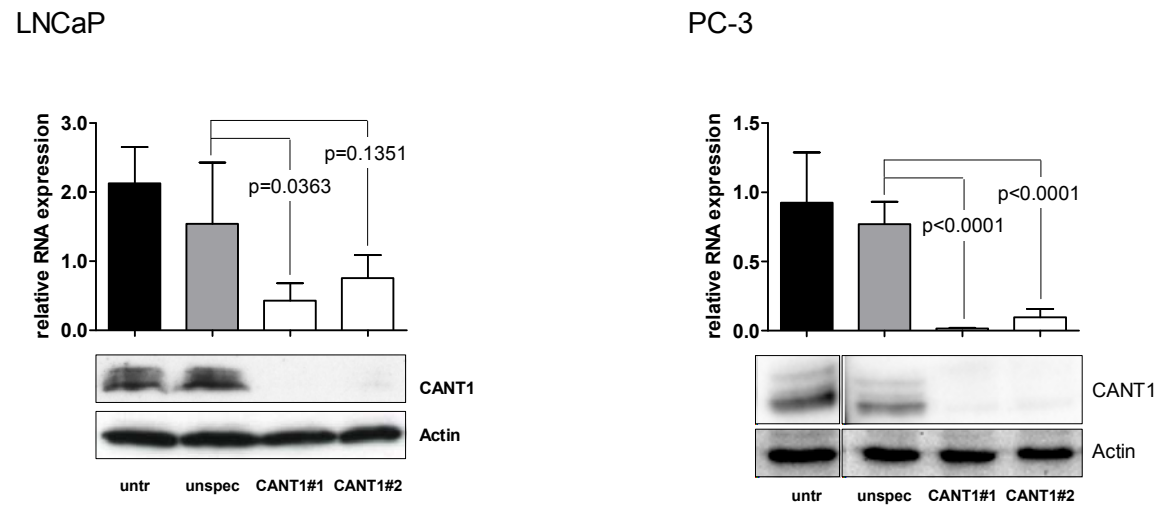


**Fig. 18 Knockdown of CANT1 in LNCaP and PC-3 cells.**

LNCaP and PC-3 cells were cultivated in 6-well plates and left untreated or transfected with unspecific or CANT1-specific siRNAs as indicated. After 72 h CANT1 mRNA and protein expression was determined by qRT-PCR (top) and Western Blot analysis (bottom). untr = untreated, unspec = unspecific.

The strong reduction of the Western Blot band upon transfection with both CANT1-specific siRNAs further substantiated the specificity of the CANT1 antibody, which was used as well for immunohistochemistry and in the ELISA assay, and confirmed that there is no cross-reactivity with other molecules.

#### 4.1.2.3 CANT1 knockdown reduces cell proliferation

One of the main hallmarks of cancer cells is uncontrolled proliferation [166]. To determine if CANT1 expression has an influence on prostate cancer cell proliferation, LNCaP and PC-3 cells were transfected with CANT1-specific or control siRNAs. Compared to unspecific siRNA transfected cells, the cell number of CANT1 siRNA #1 and #2 transfected LNCaP cells was reduced significantly by 17 % and 21 %. Although siRNA treatment itself strongly affected the propagation of PC-3 cells, the number of CANT1 siRNA #1 and #2 transfected cells was further decreased by 38 % and 26 % compared to control cells (**Fig. 19**).

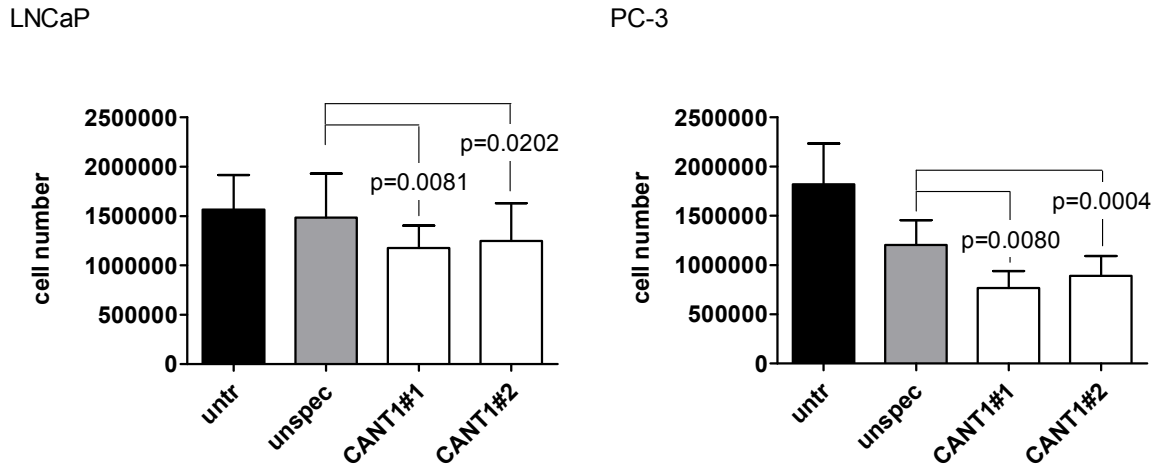


**Fig. 19 Cell number of LNCaP and PC-3 cells upon CANT1 knockdown.**

LNCaP and PC-3 cells were seeded in 6-well plates, left untreated or transfected with siRNAs as indicated, and counted after 72 h.

To test whether the reduction of cell number upon CANT1 knockdown was caused by a reduction of cell proliferation rate, DNA synthesis rate was determined by measuring BrdU incorporation. As shown in **Fig. 20**, 32 % and 36 % less BrdU was detected after transfection of LNCaP cells with CANT1 siRNA #1 and #2, respectively. The DNA synthesis rate of PC-3 cells was decreased highly significantly by 67 % and 30 % in CANT1 siRNA #1 and #2 transfected cells compared to unspecific siRNA transfected cells (**Fig. 20**).

Taken together, these results show a potent reduction of proliferation of LNCaP and PC-3 cells after CANT1 knockdown.

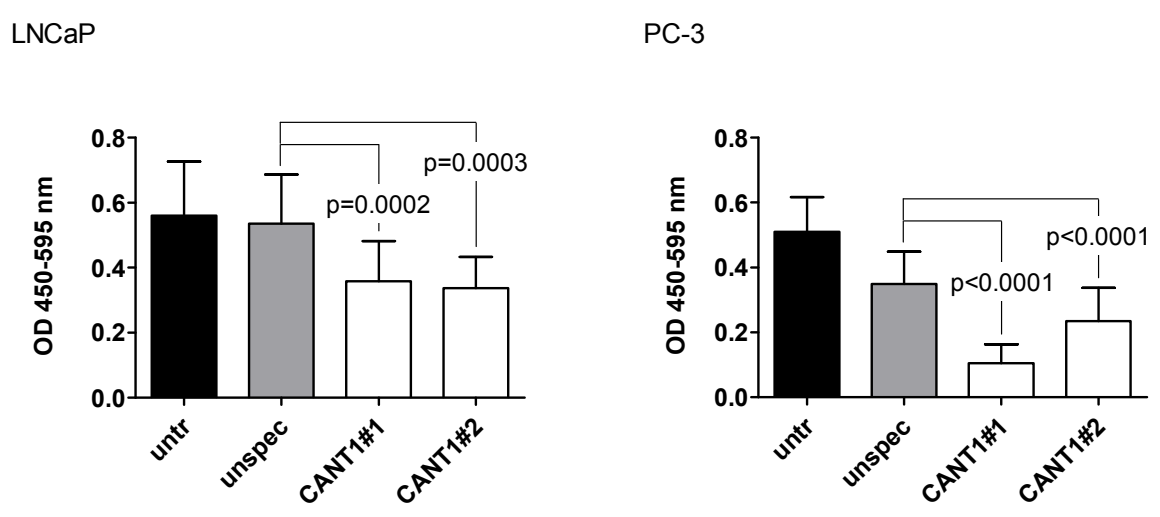


**Fig. 20 DNA synthesis rate of LNCaP and PC-3 cells upon CANT1 knockdown.**

LNCaP and PC-3 cells were seeded in 6 cm-dishes and left untreated or transfected with siRNAs as indicated. After 72 h DNA synthesis rate measurement was performed.

### 4.1.2.4 Recuded cell proliferation is associated with G1-arrest

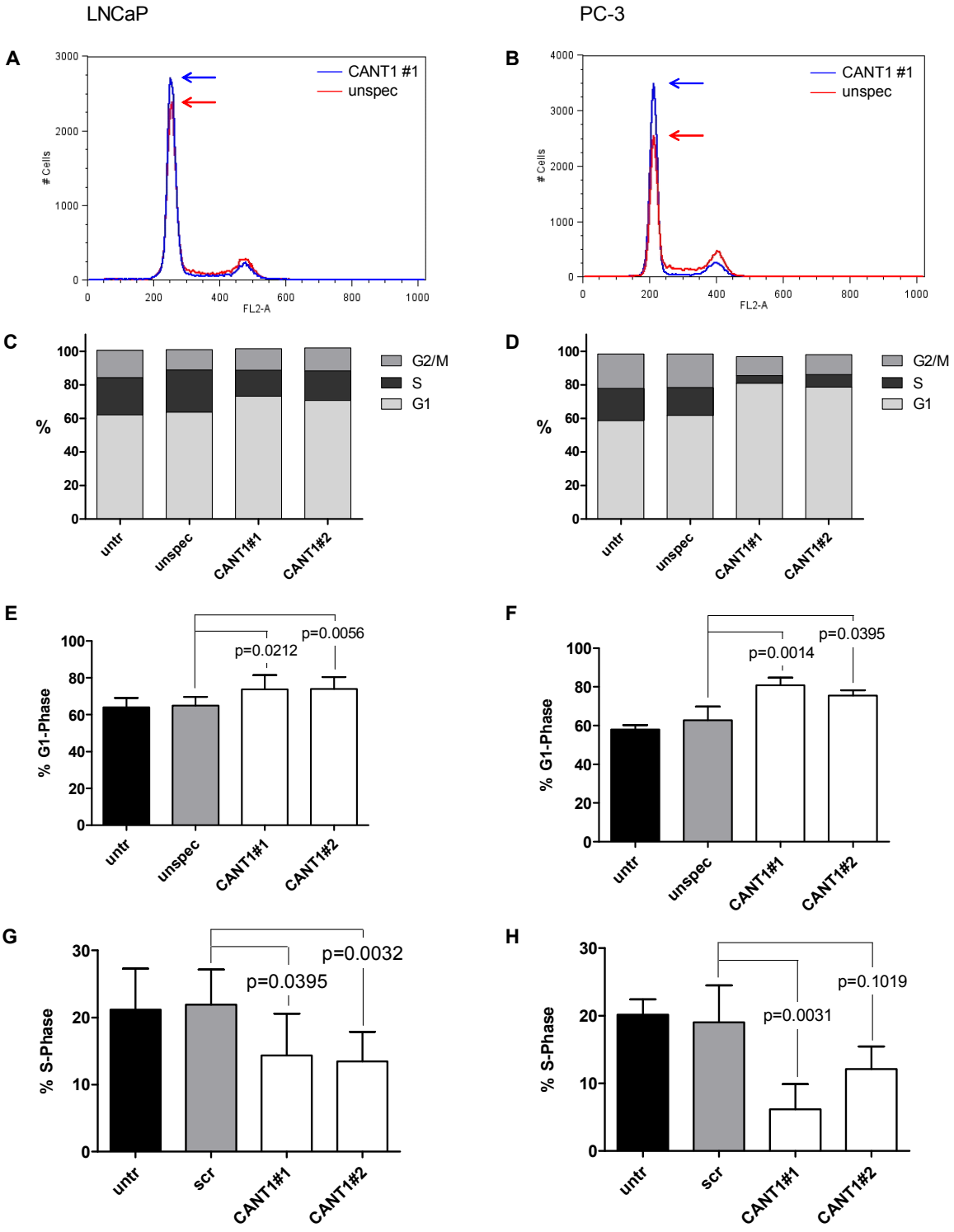


**Fig. 21 Cell cycle distribution of LNCaP and PC-3 cells upon CANT1 knockdown.**

LNCaP cells (A, C, E, G) and PC-3 cells (B, D, F, H) were left untreated or transfected with siRNAs as indicated. After 72 h, cell cycle analysis was performed. **(A, B)** Representative histogram of cells that were treated either with unspecific siRNA (red) or CANT1 siRNA #1 (blue); note the higher G1-phase peak and lower S-phase plateau and G2-phase peak in the CANT1 siRNA histogram compared to the unspecific siRNA histogram. **(C, D)** Representative distribution of G1-, S-, and G2/M-phase cells. **(E, F)** Proportion of cells in G1-phase from all replicates. **(G, H)** Proportion of cells in S-phase from all replicates.

The observed reduction of cell proliferation upon CANT1 knockdown provoked the question, if this was reflected in a change of cell cycle distribution. Hence, the proportion of cells in G1-, S- and G2/M-phase was determined by flow cytometry of PI-stained cells. The proportion of LNCaP cells in G1-phase rose from 68 % in control cells to 76 % in CANT1 knockdown cells, whereas the proportion of cells in S-phase declined from 20 % to 13 % in the respective groups. The mean proportion of cells in G2/M-phase remained unchanged (**Fig. 21 a, c, e, g**). These differences were even more pronounced in PC-3 cells: Sixty-three percent of the cells treated with unspecific siRNA were in G1-phase in contrast to 81 % and 76 % of the cells treated with CANT1-specific siRNA #1 and #2, respectively. Different from the LNCaP cells, the proportion of cells in S- as well as G2/M-phase was altered in PC-3 knockdown cells. S-phase cells decreased from 19 % in the control cells to 6 % and 12 % in the knockdown cells, in parallel G2/M-phase cells decreased from 17 % to 11 % in the corresponding groups (**Fig. 21 b, d, f, h**).
In summary, these data clearly demonstrate G1-arrest upon CANT1 knockdown in LNCaP and PC-3 cells.

#### 4.1.2.5 Cell migration is inhibited upon CANT1 knockdown

With regard to the concept suggested by Hanahan and Weinberg, elevated migratory potential is another feature that cells adapt during transformation to malignant cancer cells [166]. The relevance of CANT1 expression during cell migration was therefore elucidated in a transmigration assay. In particular, haptotactic migration towards the extracellular matrix component fibronectin was investigated. Downregulation of CANT1 reduced highly significantly migration of LNCaP cells through the porous membrane by 55 % and 20 % using siRNA #1 and #2 compared to control cells. The reduction of PC-3 cell migration accounted for 61 % and 13 % with the respective siRNAs (**Fig. 22**).

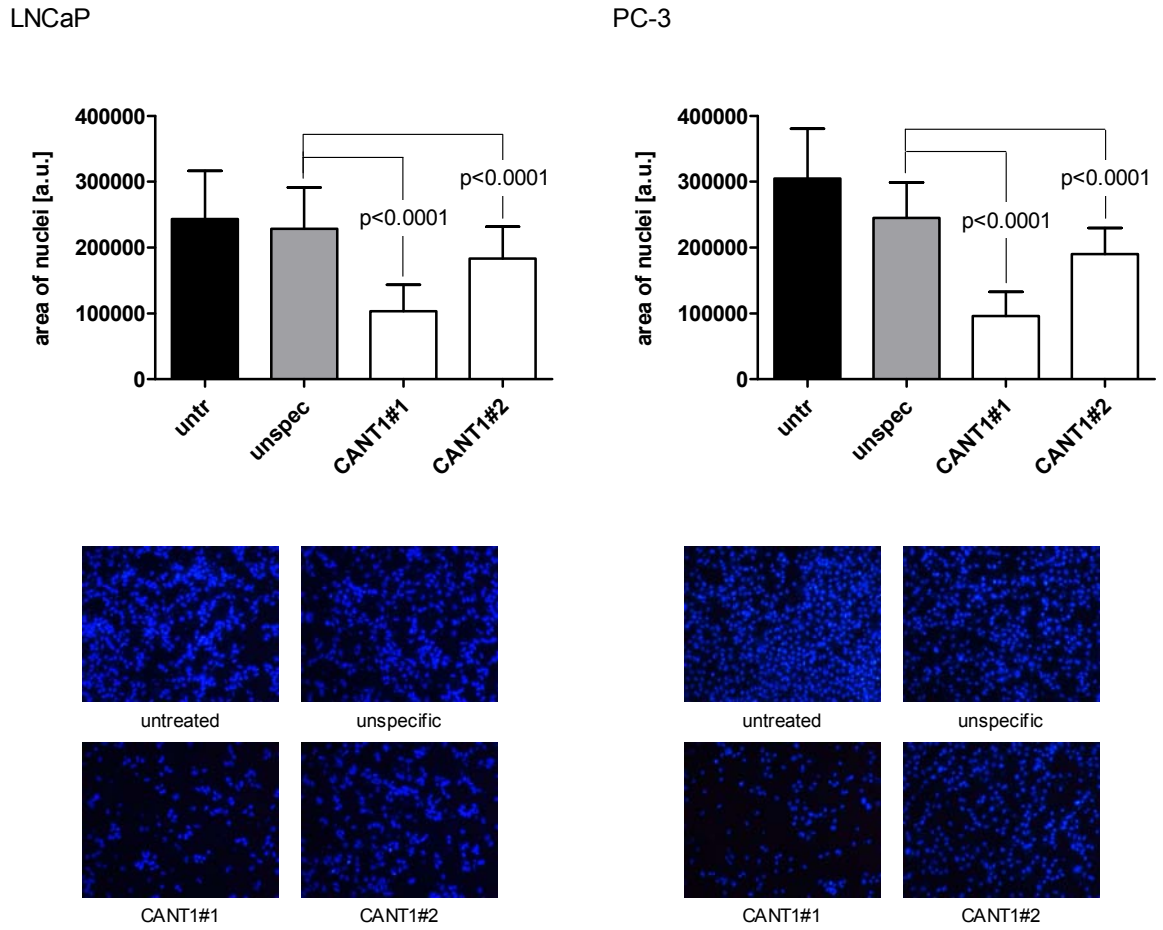


**Fig. 22 Haptotactic transmigration of LNCaP and PC-3 cells upon CANT1 knockdown.**

LNCaP and PC-3 cells were seeded in 6 cm-dishes and left untreated or transfected with siRNAs as indicated. After 72 h, the transmigration assay was performed. Below, representative pictures of the DAPI-stained membranes are displayed (magnification 100x).

Additionally, migration of PC-3 cells on a plain, non-coated surface was assessed in a scratch wound assay. This assay is less reliably applicable to LNCaP cells as these do not build a confluent monolayer.

The area, which was not recovered with migrated cells within 24 h after introducing the wound, was 1.4 and 1.6 times larger following CANT1 downregulation with specific siRNA #1 and #2, respectively, compared to unspecific siRNA treatment (**Fig. 23**), further confirming a diminished cell motility after loss of CANT1 expression.

Altogether, these data show that the reduction of CANT1 expression induces strong inhibition of LNCaP and PC-3 cell migration.

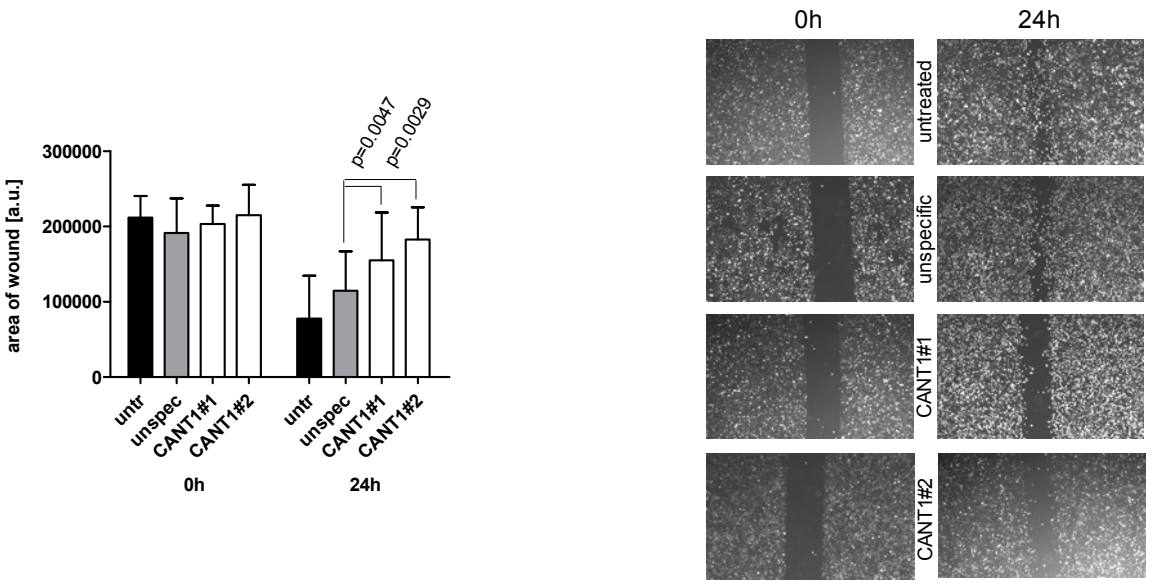


**Fig. 23 Wound healing of PC-3 cells upon CANT1 knockdown.**

PC-3 cells were seeded in 6 cm-dishes and the scratch wound assay was conducted. On the right, representative pictures of the wounds are shown (magnification 25x).

#### 4.1.2.6 Transient overexpression of CANT1

Having shown that loss of endogenous CANT1 expression results in reduced proliferation and migration of prostate cancer cells, we next examined if enforced expression of CANT1 is sufficient to induce or enhance *in vitro* tumorigenicity. Therefore, the benign prostatic cell line RWPE-1 and the prostate cancer cell line DU-145, which both express little endogenous CANT1 protein (see chapter 4.1.2.1), were transfected with a CANT1-encoding vector. Further, it was evaluated, whether similar CANT1-related effects could be observed in the HEK293 cell line, which is a benign cell line of non-prostatic origin and expresses similar CANT1 protein amounts as RWPE-1 cells (**Fig. 24**). Additionally, it was examined if a further increase of CANT1 expression in PC-3 cells, which showed a clear response to CANT1 knockdown (see chapters 4.1.2.3 to 4.1.2.5), would induce the contrary effects. Finally, CANT1 downregulation by RNA interference and the resulting effects were attempted to be rescued by subsequent transfection with a CANT1-encoding vector. In all cases, increasing amounts of CANT1 DNA were introduced into the cells by transfecting the cells with a GFP vector alone as negative control, with a mixture of GFP and CANT1 vector, which consisted of 33 % CANT1 vector and 67 % GFP vector to keep the DNA content constant, and with pure CANT1 vector.

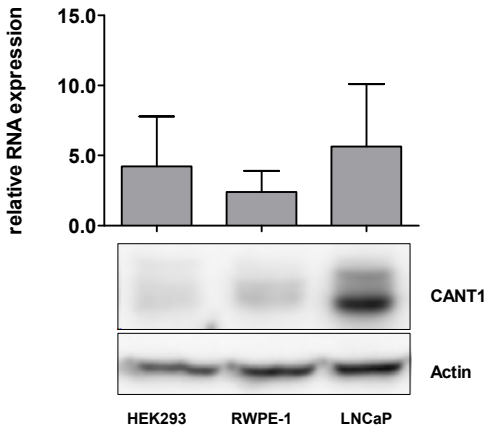


**Fig. 24 Expression of CANT1 in HEK293 cells.**

HEK293, RWPE-1 and LNCaP cells were cultivated in 75 cm² cell culture flasks to 70-80 % confluence. CANT1 mRNA and protein expression was determined by qRT-PCR (top, n=2) and Western Blot analysis (bottom, n=1).

A dose-dependent increase of CANT1 expression on mRNA and protein level was achieved in RWPE-1, DU-145 and HEK293 cells. On mRNA level, the fold change upon transfection of pure CANT1 vector was 186, 16 and 562 times in these cell lines, respectively (**Fig. 25**).

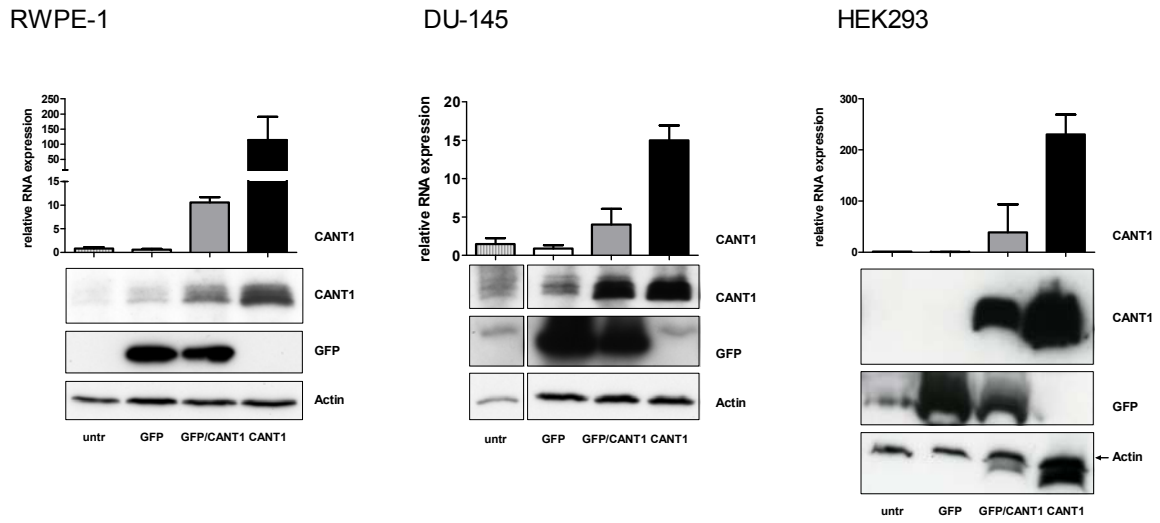


**Fig. 25 Overexpression of CANT1 in RWPE-1, DU-145 and HEK293 cells.**

RWPE-1 (n=3), DU-145 (n=4) and HEK293 (n=2) cells were left untreated or transfected with GFP vector, CANT1 vector or a mixture of both in a 2:1 ratio as indicated. After 24 h CANT1 mRNA and protein expression was determined by qRT-PCR (top) and Western Blot analysis (bottom), respectively. The mRNA levels for HEK293 cells were normalized to that of untreated cells.

Transfection of wildtype PC-3 cells with CANT1 vector resulted as well in elevated expression levels of CANT1 compared to endogenous levels (fold change 6.8). In CANT1 knockdown PC-3 cells endogenous mRNA levels were restored upon transfection with CANT1 vector, fold change compared to GFP transfected knockdown cells was 12.5. However, the protein was not reexpressed (**Fig. 26**).

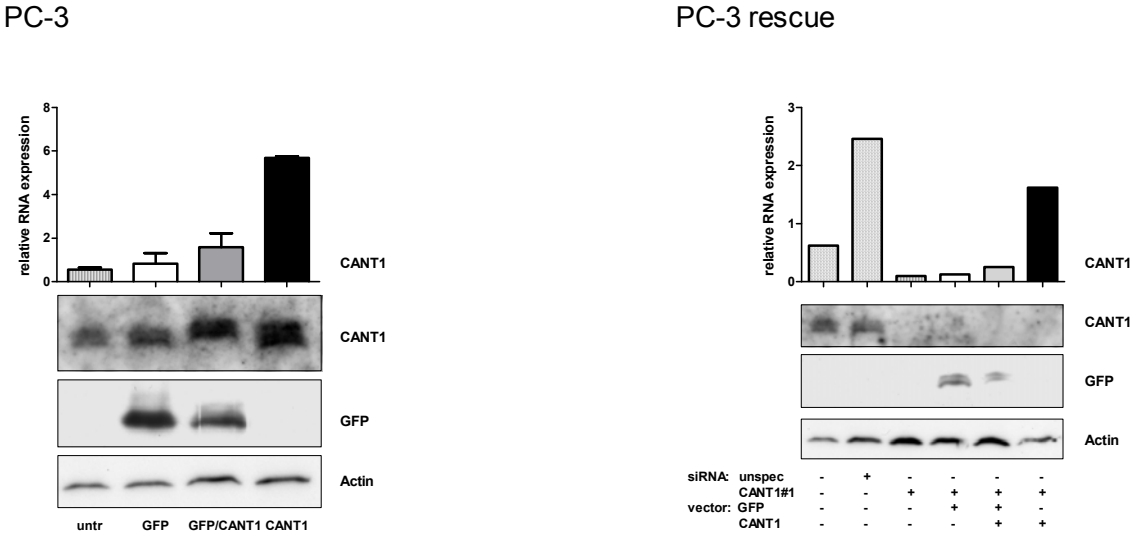


**Fig. 26 Overexpression of CANT1 in wildtype and CANT1 knockdown PC-3 cells.**

PC-3 cells were left untreated or transfected with unspecific or CANT1-specific siRNA #1 and/or GFP vector, CANT1 vector or a mixture of both in a 2:1 ratio as indicated. In the case of combination siRNAs were transfected 3 days before DNA vectors. Twenty-four hours after transfection of DNA vectors CANT1 mRNA and protein expression was determined by qRT-PCR (top) and Western Blot analysis (bottom), respectively. MRNA expression was measured twice for transfection of wildtype PC-3 cells and once for CANT1 knockdown PC-3 cells.

Summarized, strongly augmented expression of CANT1 was achieved in RWPE-1, DU-145, HEK293 and wildtype PC-3 cells. Rescue of CANT1 expression following RNA interference was successful on mRNA level. However, protein levels could not be restored.

#### 4.1.2.7 CANT1 overexpression does not change cell proliferation rate

Cell proliferation upon CANT1 overexpression was assessed by measuring the DNA synthesis rate. RWPE-1, DU-145 and HEK293 cells were slightly affected by the treatment (compare bars of untreated and GFP transfected cells), however, the DNA synthesis rate was independent of CANT1 levels (**Fig. 27**).

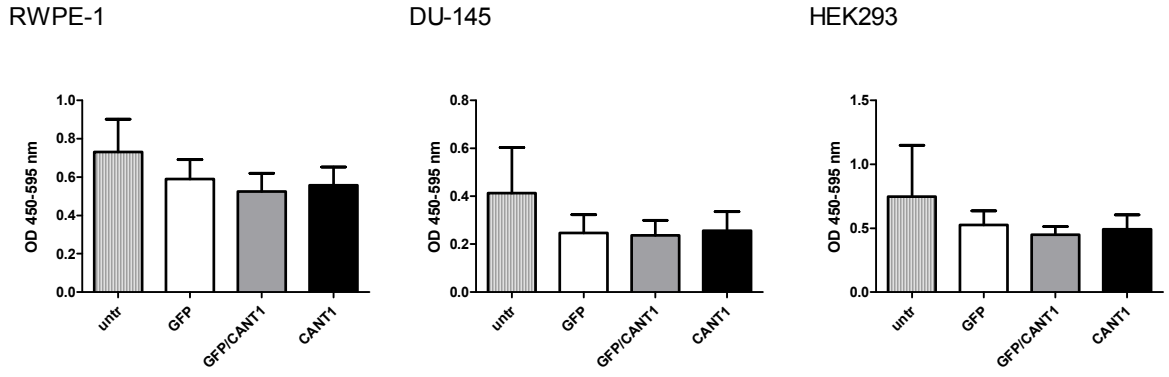


**Fig. 27 DNA synthesis rate of RWPE-1, DU-145 and HEK293 cells upon CANT1 overexpression.**

RWPE-1, DU-145 and HEK293 cells were left untreated or transfected with DNA vectors as indicated. After 24 h DNA synthesis rate measurement was performed.

Similar results were obtained in PC-3 cells. Neither in wildtype cells nor in CANT1 knockdown cells, forced expression of CANT1 changed the DNA synthesis rate (**Fig. 28**). Yet, reduced DNA synthesis activity upon CANT1 knockdown was confirmed (compare chapter 4.1.2.3).

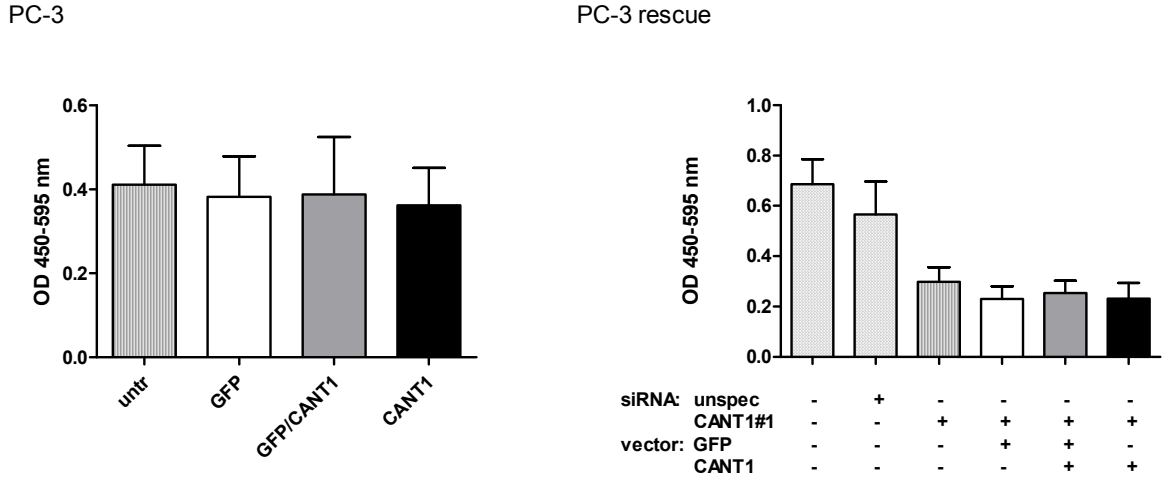


**Fig. 28 DNA synthesis rate of wildtype and CANT1 knockdown PC-3 cells upon CANT1 overexpression.**

PC-3 cells were left untreated or transfected with siRNAs and/or DNA vectors as indicated. In the case of combination siRNAs were transfected 3 days before DNA vectors. Twenty-four hours after transfection of DNA vectors, DNA synthesis rate measurement was performed.

4.1.2.8 CANT1 overexpression does not influence cell migration

Next, the influence of increased CANT1 expression on transwell migration was examined. Similar to DNA synthesis rate, also transwell migration was decreased upon vector transfection in RWPE-1, DU-145 and particularly in HEK293 cells. In all of these cell lines, the effect on the migration rate was independent of CANT1 overexpression (**Fig. 29**).

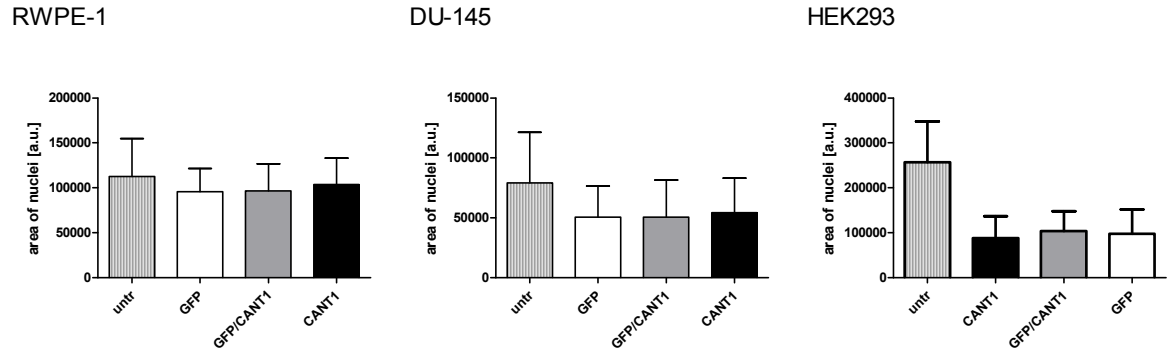


**Fig. 29 Haptotactic transmigration of RWPE-1, DU-145 and HEK293 cells upon CANT1 overexpression.**

RWPE-1, DU-145 and HEK293 cells were left untreated or transfected with DNA vectors as indicated. After 24 h, the transmigration assay was performed.

In wildtype PC-3 cells, neither the transfection process nor exogenous CANT1 expression affected the migration rate (**Fig. 30**). Upon CANT1 knockdown, transwell migration was reduced as observed before (compare chapter 4.1.2.5). However, transfection with CANT1 vector had no influence on cell motility (**Fig. 30**).

Summarized, these results show that increased expression of CANT1 does not increase the tumorigenic potential of prostatic and non-prostatic, cancerous and non-cancerous cell lines.

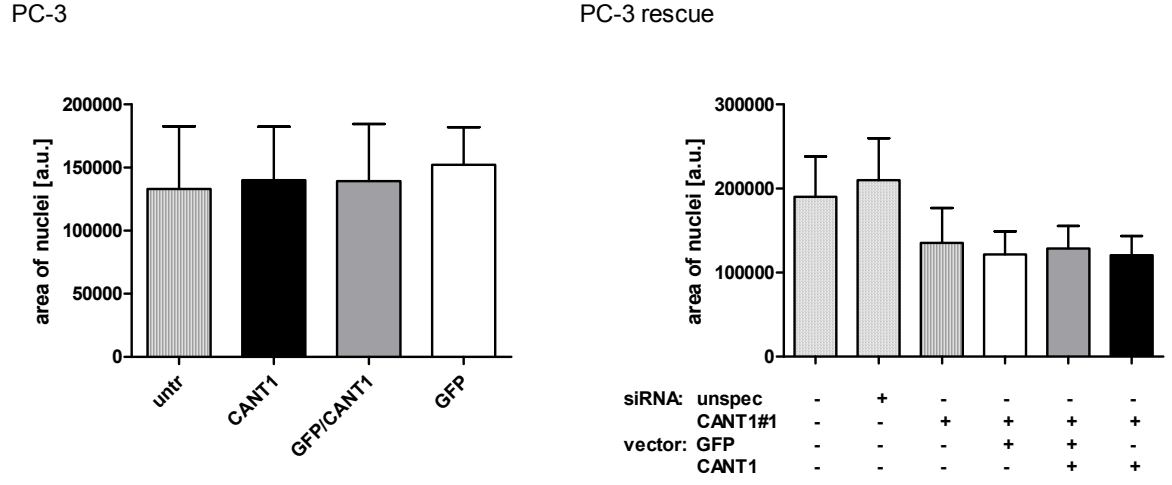


**Fig. 30 Haptotactic transmigration of wildtype and CANT1 knockdown PC-3 cells upon CANT1 overexpression.**

PC-3 cells were left untreated or transfected with siRNAs and/or DNA vectors as indicated. In the case of combination siRNAs were transfected 3 days before DNA vectors. Twenty-four hours after transfection of DNA vectors, the transmigration assay was performed.

### 4.1.3 Characterization of CANT1

#### 4.1.3.1 Endogenous CANT1 is glycosylated

Smith *et al.* demonstrated that human CANT1, which was transfected into COS-1 cells, was glycosylated. Upon PNGase F treatment the band was shifted by 2 kDa, showing that the protein is N-glycosylated [60]. To test, if this is also the case for endogenous CANT1, lysates of LNCaP and PC-3 cells were incubated with PNGase F and analyzed by Western Blot analysis. In both cell lines a shift of the double band by ~2 kDa was observed (**Fig. 31**), indicating that, similar to artificially expressed CANT1, endogenous CANT1 is N-glycosylated.

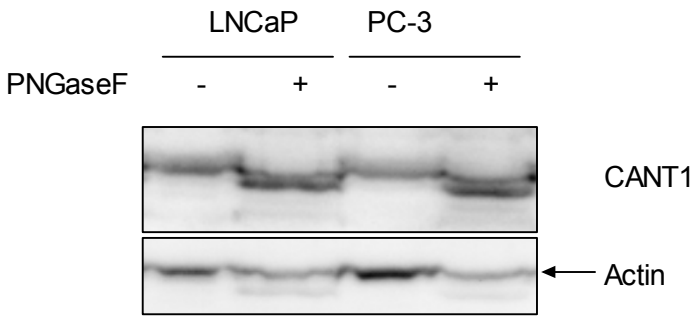


**Fig. 31 N-glycosylation of CANT1.**

A total of 6 x $10^5$ LNCaP and 4 x $10^5$ PC-3 cells were seeded in 6 cm-dishes. After 3 days cells were lysed, parts of the lysates were treated with PNGase F and treated and untreated lysates were analyzed by Western Blot analysis.

#### 4.1.3.2 Intracellular localization of CANT1

In transfected CHO cells the full-length rat homolog of CANT1 localizes to the membranes of the ER and pre-Golgi intermediates [62], whereas a truncated form of human CANT1 was detected in the supernatant of transfected COS-1 cells, indicating cleavage and secretion [60]. As shown in chapter 4.1.1.1, the main immunohistochemical staining pattern resembled a Golgi apparatus staining pattern. Therefore, double immunofluorescence stainings of normal and cancerous prostate tissue with GOLM1, which is known as Golgi resident protein [134], were performed. An extensive overlap of both staining patterns was seen, illustrating that CANT1 is predominantly localized in the Golgi apparatus. Similar to immunohistochemistry, also an additional diffuse CANT1 staining was observed in the cytoplasm in some cases (**Fig. 32**).

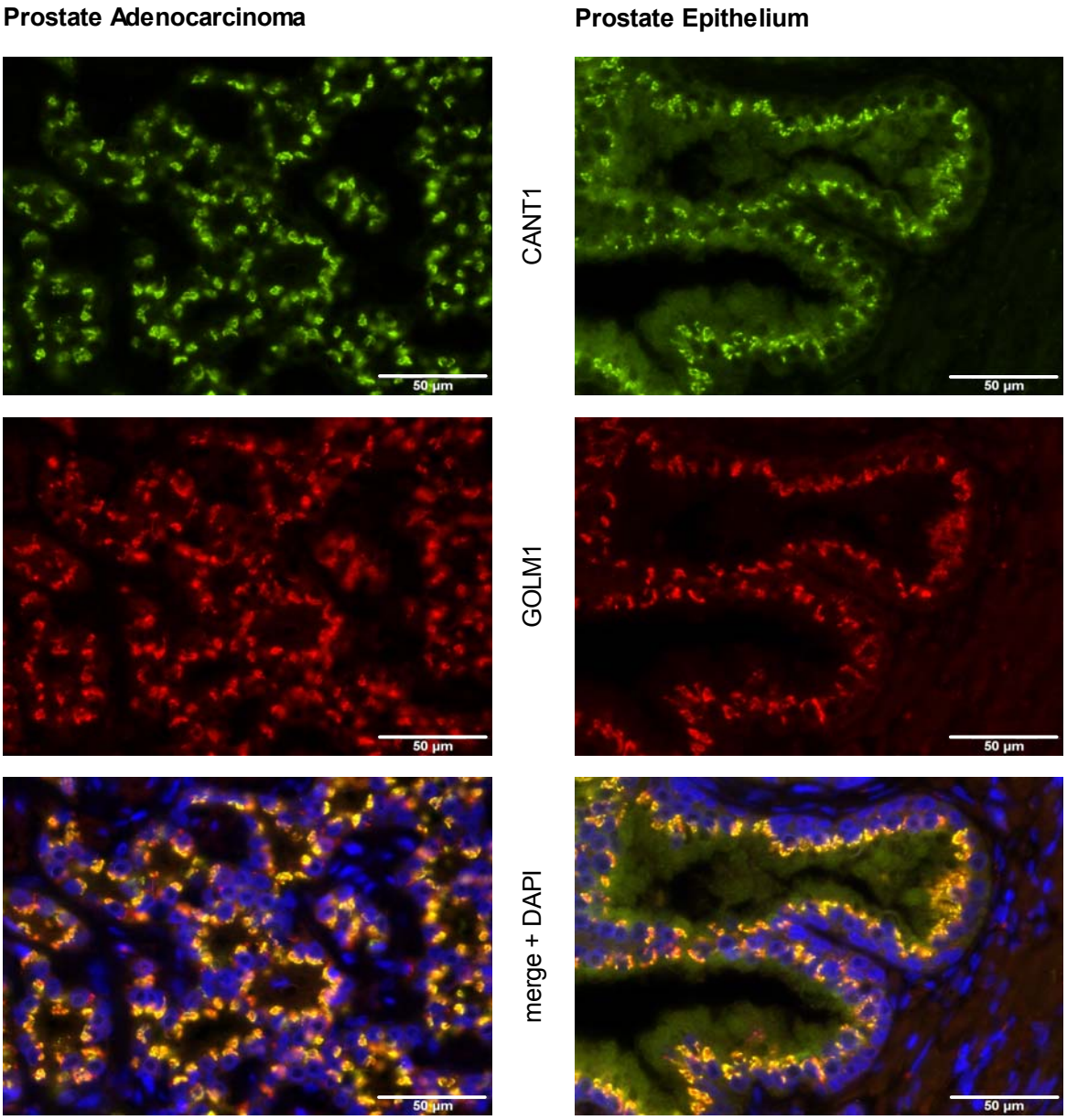


**Fig. 32 Intracellular localization of endogenous CANT1 in prostatic tissue.**

Double immunofluorescence of CANT1 (green) and GOLM1 (red) in human prostate adenocarcinoma and normal prostate epithelium, magnification 400x.

Similar analyses were performed in LNCaP and PC-3 cells. Cellblock slides were stained immunohistochemically. The granular staining on one side of the nucleus suggested localization in the Golgi apparatus. This was confirmed by double immunofluorescence staining with GOLM1 (**Fig. 33**).

Hence, it was demonstrated that CANT1 is mainly localized in the Golgi apparatus in human prostatic tissue as well as in prostate cancer cell lines.

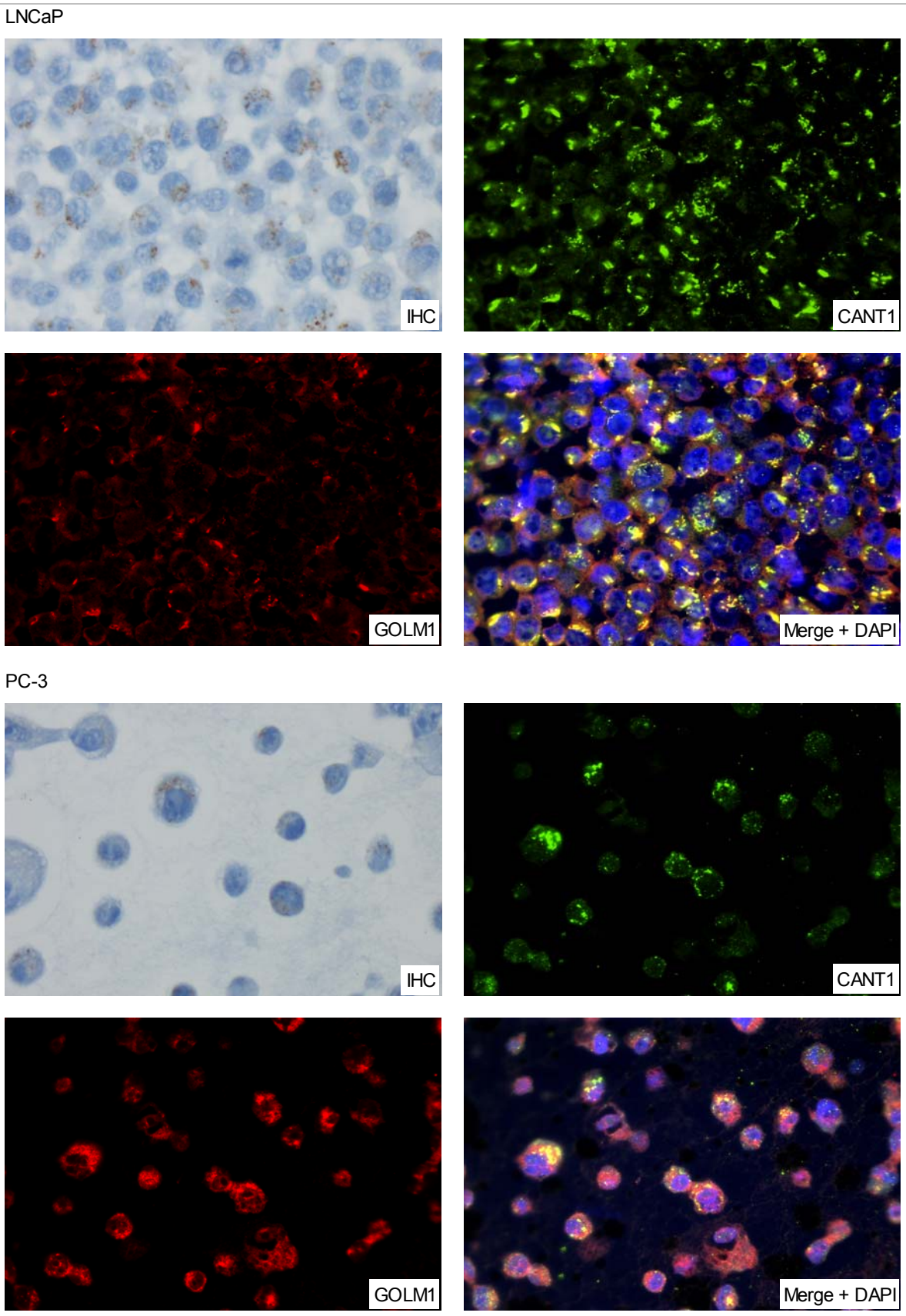


**Fig. 33 Intracellular localization of endogenous CANT1 in LNCaP and PC-3 cells.**

LNCaP and PC-3 cell blocks were immunohistochemically stained with CANT1 (IHC) and a double immunofluorescence staining with CANT1 (green) and GOLM1 (red) was performed.

#### 4.1.3.3 Secretion of CANT1

To examine if CANT1 is also secreted by cells that express the protein endogenously, the supernatants of LNCaP and PC-3 cells were analyzed. Therefore, the cells were cultivated in serum-free medium for 24 h and soluble proteins in the supernatants were separated from vesicles by ultracentrifugation. Supernatants before and after ultracentrifugation were precipitated and analyzed by Western Blot analysis in comparison to lysates from the corresponding cells and the vesicle pellet derived from ultracentrifugation.

The Western Blot analysis showed that a truncated form of CANT1, which was approximately 2 kDa smaller compared to the lowest band from the cell lysate, was detectable in the supernatants of both cell lines before as well as after ultracentrifugation. This band was clearly singular, in contrast to the triple band in the lysates. In the lysate of LNCaP cells an additional weak band of the same molecular weight as the band observed in the supernatant was detected. In the ultracentrifugation pellet of LNCaP supernatant no CANT1 was detected. A weak double band was visible in the ultracentrifugation pellet of PC-3 cell supernatant at the same size as in the cell lysate (**Fig. 34 a**).

To further evaluate the secretion and quantify the amount of CANT1 in serum-free cell culture supernatants, an ELISA assay was established. When testing commercially available antibodies, the combination of mouse monoclonal CANT1 antibody for capturing the antigen and rabbit polyclonal CANT1 antibody for detection was found to be the most reproducible design. In two independent experiments, 0.4 and 0.15 µg/ml CANT1 protein were measured in the supernatant of PC-3 cells. The CANT1 concentrations in LNCaP supernatant were 0.08 and 0.1 µg/ml (**Fig. 34 b**).

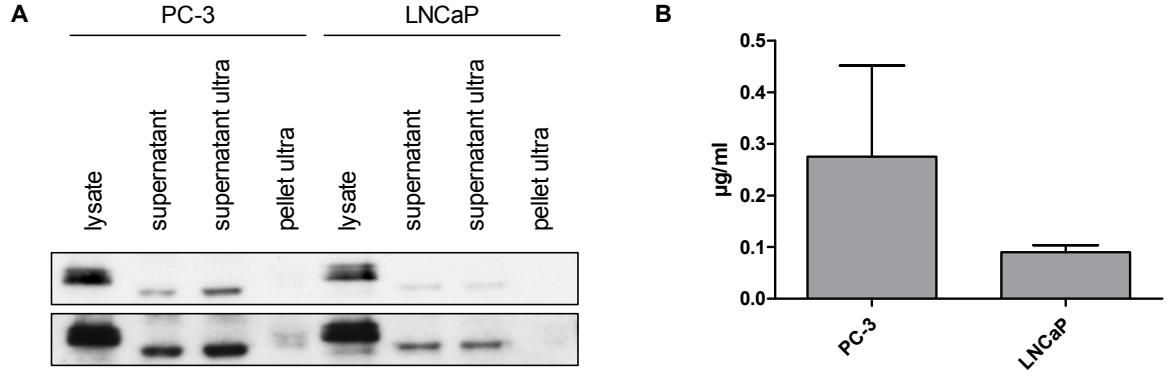


**Fig. 34 Secretion of endogenous CANT1.**

PC-3 and LNCaP cells were cultivated in 75 cm² cell culture flasks to ~70 % confluence before incubation in serum-free medium for 24 h. **(A)** Supernatants from 3 flasks each were pooled and 16 ml were ultracentrifuged. In parallel, cells were lysed. Supernatants before (supernatant) and after ultracentrifugation (supernatant ultra) were precipitated. Cell lysate, supernatants and the ultracentrifugation pellet were analyzed by Western Blot analysis. Pictures from a short (top) and long (bottom) exposed film are depicted. **(B)** CANT1 levels in the supernatants were measured in an ELISA-assay (n=2). ultra = ultracentrifugation.

Thus, secreted endogenous CANT1 was detected using two different approaches. The soluble form of the protein is ~2 kDa smaller than the full-length form.

#### 4.1.3.4 CANT1 is detectable in blood serum

The confirmation of the secretion of CANT1 prompted us to clarify if CANT1 is detectable in human blood serum and if the levels are different in prostate cancer patients compared to healthy individuals. Thus, the same ELISA assay as for CANT1 detection in cell culture supernatans was applied to human sera. Serum CANT1 levels appeared to be too low for quantification with this ELISA assay, which had a detection range from 0.1 to 20 µg/ml. Therefore results are shown as measurement of absorbance at 450 nm. Serum CANT1 levels in 23 tested prostate carcinoma patients were slightly higher than in 15 healthy test persons, however, this difference failed statistical significance (median patients: 0.096, median controls: 0.061; **Fig. 35**). No correlation was noted between serum PSA and serum CANT1 levels (data not shown).

In conclusion, CANT1 protein was detectable in human blood samples, however, the amounts were not quantifiable with the current method.

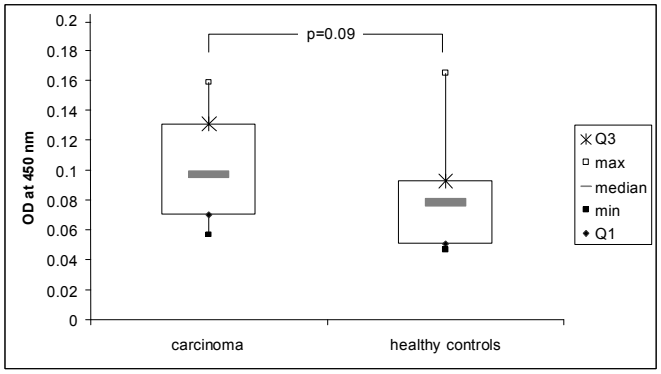


**Fig. 35 CANT1-ELISA of human blood serum.**

Serum CANT1 levels of 23 prostate carcinoma patients and 15 healthy individuals were measured in an ELISA assay.

### 4.1.4 The involvement of CANT1 in the UPR

CANT1, being an apyrase with preference for UDP and GDP and being located in the ER or Golgi apparatus, is believed to hydrolyze these nucleotide disphosphates, which are sugar carriers in these organelles, and thus to indirectly drive nucleotide sugar antiporters. By thereby ensuring sugar supply, CANT1 is speculated to be an important player in protein glycosylation [62, 68, 80]. An involvement in glycoprotein or proteoglycan synthesis would be reflected in a reduced amount of these molecules upon CANT1 knockdown. Presuming that CANT1 plays a role in protein folding, CANT1 knockdown would induce an increased ratio of misfolded to correctly folded proteins, which would trigger the UPR, while CANT1 would in turn be a target gene of the UPR.

Experimental results, which support the latter scenario, were published previously. Uccelletti *et al.* demonstrated constitutive activation of the UPR upon knockdown of the *C.elegans* CANT1 homolog apy-1, whereas apy-1 expression was upregulated upon tunicamycin treatment, which is a chemical inducer of the UPR [68]. Similarly, in LNCaP cells Fang *et al.* observed activation of the UPR upon knockdown of NTPDase5, a UDPase that is located in the ER [167]. To test if also human CANT1 is involved in protein folding, the expression of UPR target genes following CANT1 knockdown as well as the expression of CANT1 following ER stress induction was measured.

#### 4.1.4.1 UPR activation upon CANT1 and NTPDase5 single or double knockdown

To analyze UPR activation, three established UPR target genes were selected. The expression of HSPA5, tribbles homolog (TRIB) 3 and homocysteine-inducible, endoplasmic reticulum stress-inducible, ubiquitin-like domain member (Herpud) 1 was measured on RNA level, HSPA5 expression was additionally evaluated on protein level. This was not only done for CANT1 knockdown but also for double knockdown with the before mentioned ER-UDPase NTPDase5 to evaluate a putative redundancy of these two proteins. As positive control of UPR activation, LNCaP and PC-3 cells were treated with thapsigargin or tunicamycin. Thapsigargin prevents calcium pumping into the ER and thus induces calcium depletion in the organelle [168]. The resulting ER stress leads to UPR induction. Differently, tunicamycin inhibits transfer of the core oligosaccharide to newly synthesized peptide chains [169]. Thus, protein folding and quality control are disturbed, which leads to accumulation of misfolded proteins and finally to UPR induction.

As shown in **Fig. 36**, expression of all three genes was strongly increased in both cell lines upon ER stress induction by both agents, also HSPA5 protein amounts were clearly higher after treatment. Thus, UPR activation can be detected via measurement of HSPA5, TRIB3 and Herpud1 expression.

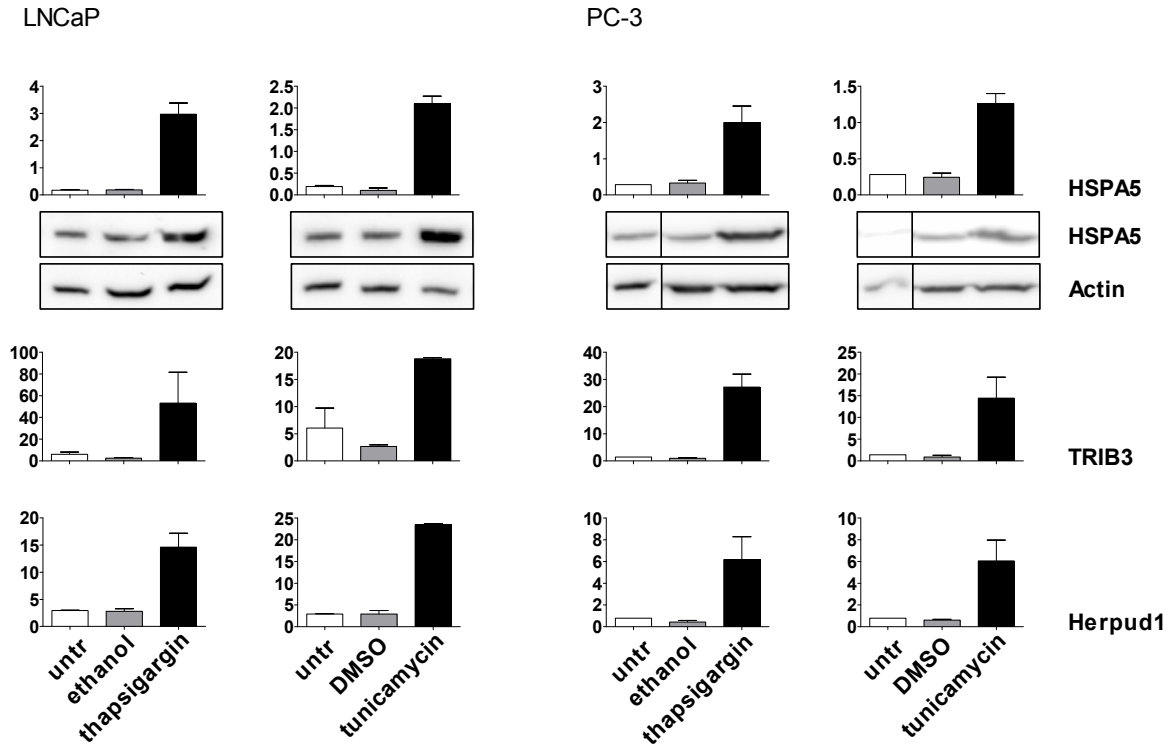


**Fig. 36 UPR activation upon induction of ER stress in LNCaP and PC-3 cells.**

LNCaP and PC-3 cells were treated with thapsigargin (n=3) and tunicamycin (n=2) or ethanol and DMSO as corresponding negative controls for 24 h. MRNA expression of HSPA5, TRIB3 and Herpud1 and protein expression of HSPA5 were determined by qRT-PCR and Western Blot analysis. MRNA expression levels were normalized to ALAS1 and HPRT1.

Next, single knockdown of NTPDase5 and double knockdown of CANT1 and NTPDase5 were established in the same cell lines. CANT1 mRNA levels were reduced to approximately 30 % in LNCaP cells and 5 % in PC-3 cells, while NTPDase5 mRNA levels were reduced to approximately 30 % in both cell lines. Knockdown on protein level was very efficient for both proteins in both cell lines.

Further, in PC-3 cells NTPDase5 mRNA was increased 1.8 fold following knockdown of CANT1 and also a weak tendency towards increased CANT1 expression was seen in NTPDase5 knockdown cells on mRNA level. However, protein levels were unaffected by mutual knockdown of both apyrases (**Fig. 37**).

Hence, an efficient knockdown of CANT1 and NTPDase5 alone and together was established in LNCaP and PC-3 cells. Additionally, a redundancy of these two genes was indicated in PC-3 cells.

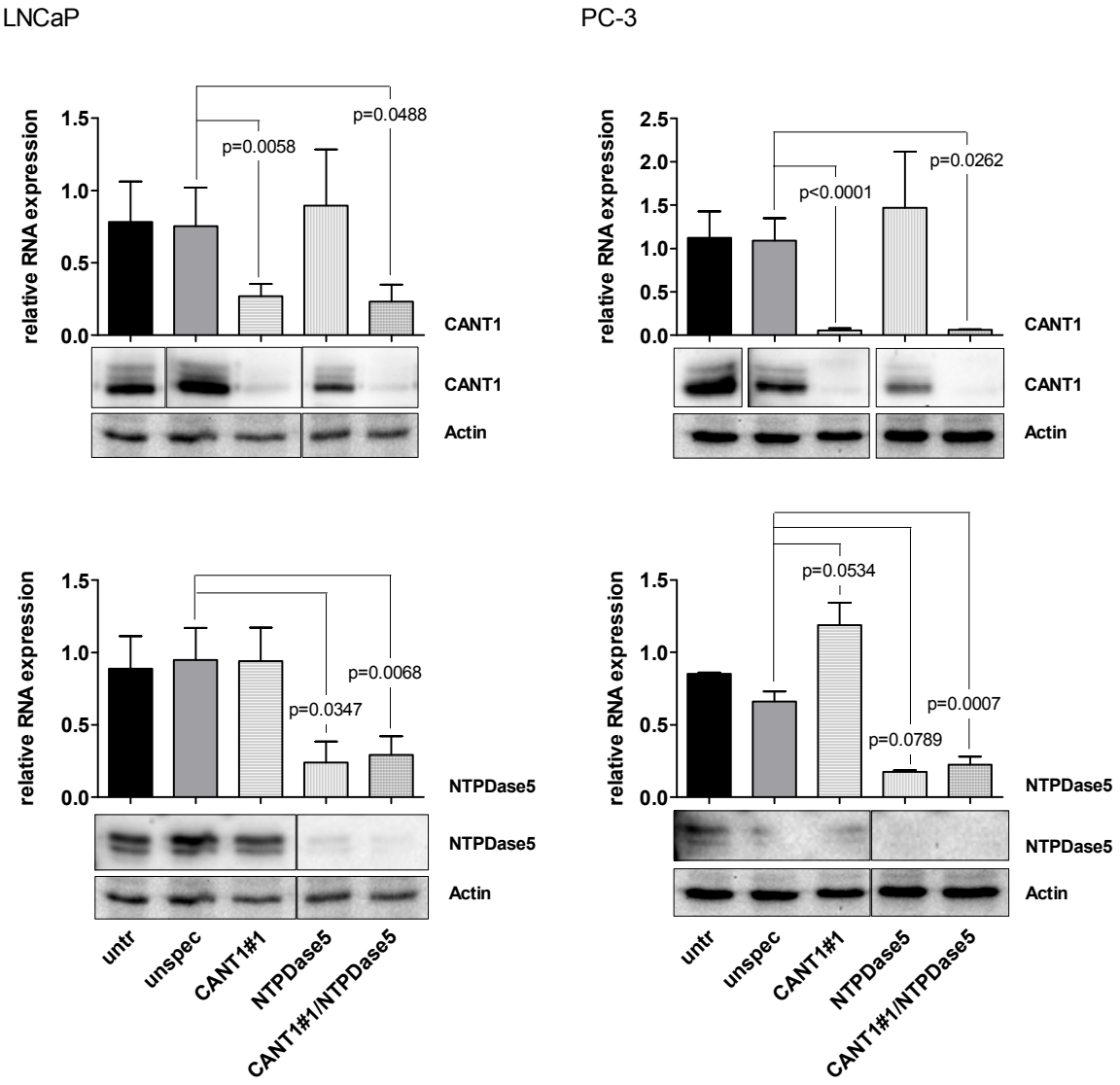


**Fig. 37 Single and double knockdown of CANT1 and NTPDase5 in LNCaP and PC-3 cells.**

LNCaP and PC-3 cells were cultivated in 6 cm-dishes and left untreated or transfected with unspecific or CANT1 and/or NTPDase5-specific siRNA as indicated. After 72 h CANT1 and NTPDase5 mRNA and protein expression was determined by qRT-PCR (top) and Western Blot analysis (bottom). MRNA levels were normalized to that of untreated cells 48 h after seeding, house-keeping genes were ALAS1 and HPRT1. To measure CANT1 and Actin protein expression, the same samples were loaded on different gels in a different order.

The measurement of UPR target gene and protein expression upon CANT1 and NTPDase5 knockdown revealed no changes in LNCaP cells. However, in PC-3 cells HSPA5 expression was increased on RNA level following NTPDase5 knockdown, which was significant for the single knockdown. The amount of protein was clearly augmented upon CANT1/NTPDase5 double knockdown. MRNA expression of TRIB3 was significantly enhanced in CANT1 single knockdown PC-3 cells. Further, higher mRNA levels of Herpud1 were detected in all three knockdown samples, a statistical trend was observed for CANT1 single knockdown (**Fig. 38**).

Summarized, while UPR is not activated in LNCaP cells upon knockdown of CANT1 and/or NTPDase5, evidence for UPR activation reflected in the upregulation of corresponding marker genes was observed in PC-3 cells following downregulation of CANT1 and NTPDase5.

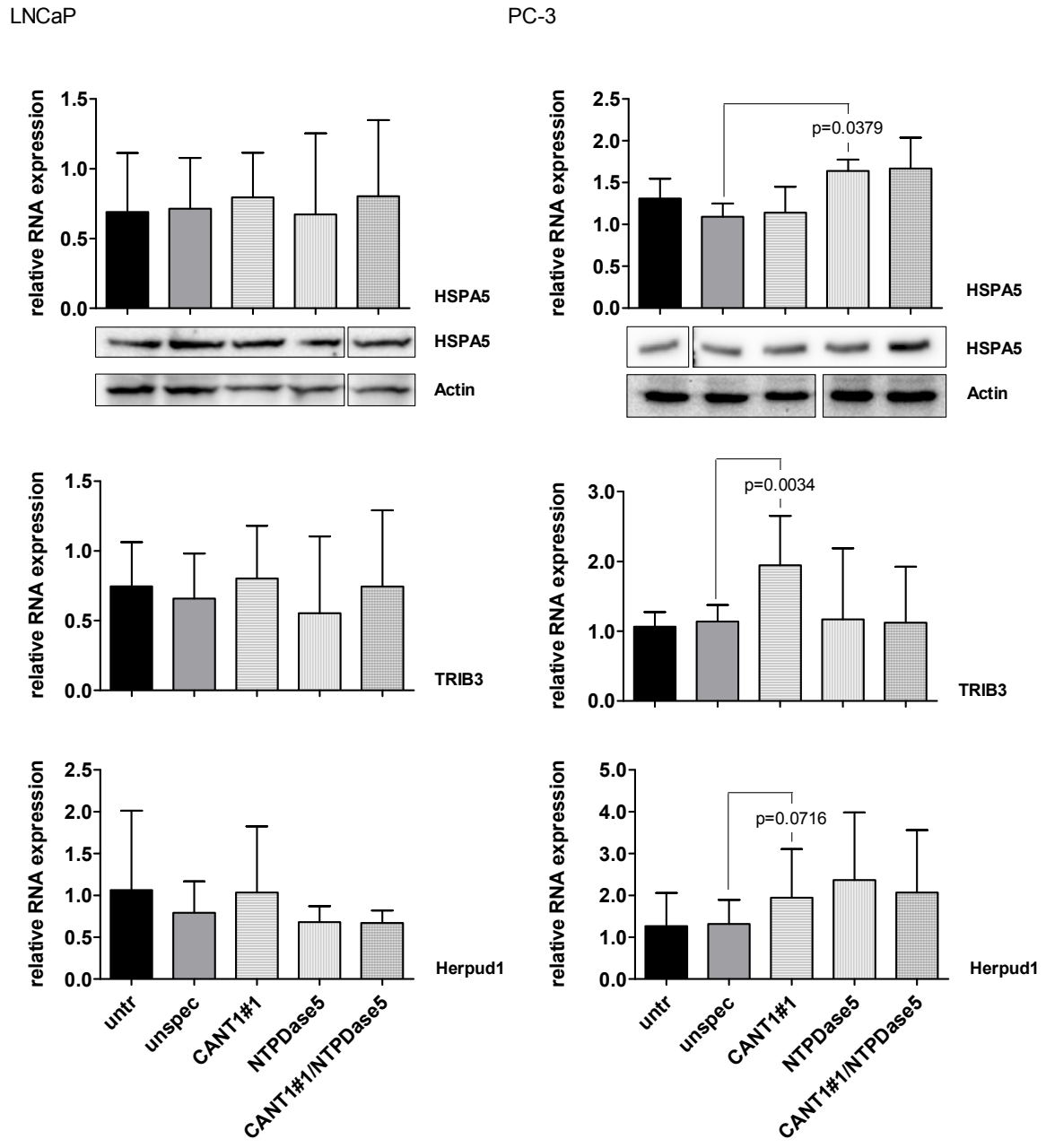


**Fig. 38 UPR activation upon CANT1 and NTPDase5 single and double knockdown in LNCaP and PC-3 cells.**

LNCaP and PC-3 cells were seeded in 6 cm-dishes and left untreated or transfected with siRNAs as indicated. After 72 h mRNA expression of HSPA5, TRIB3 and Herpud1 and protein expression of HSPA5 were determined by qRT-PCR and Western Blot analysis. MRNA levels were normalized to that of untreated cells 48 h after seeding, house-keeping genes were ALAS1 and HPRT1. To measure HSPA5 and Actin protein expression in PC-3 cells, the same samples were loaded on different gels in a different order.

#### 4.1.4.2 CANT1 expression upon ER stress induction

To clarify if CANT1 is a UPR target gene, i.e. if CANT1 expression is upregulated upon UPR induction, a kinetic analysis of CANT1 expression upon ER stress induction by thapsigargin or tunicamycin in comparison to known UPR target genes was performed in three cell lines differing in endogenous CANT1 expression and malignancy status. In the benign cell line RWPE-1 with low CANT1 levels, expression of HSPA5 was strongly augmented on RNA level during the whole experiment, whereas the corresponding protein was only increased after 24 h and 48 h of treatment with tunicamycin. This clearly showed that the UPR was activated upon thapsigargin and tunicamycin treatment. However, TRIB3 expression was unaffected indicating that this gene is not involved in UPR signaling in this cell line. Herpud1 mRNA was strongly upregulated 8 h after treatment, within the following 40 h the levels decreased, yet, the expression was still much higher compared to ethanol or DMSO treated control cells. Similarly, CANT1 mRNA was slightly increased 8 h after thapsigargin as well as tunicamycin treatment. At later timepoints, the mRNA levels were similar to untreated cells and protein expression decreased in comparison to ethanol or DMSO treated cells (**Fig. 39**).
In the malignant cell line DU-145 with low CANT1 levels, expression of all three UPR target genes and HSPA5 protein was strongly increased over the whole treatment period. After 48 h, treatment with ethanol also induced expression of HSPA5, TRIB3 and Herpud1. A similar but weaker effect was observed upon DMSO treatment. CANT1 mRNA expression was unaffected by ER stress induction via thapsigargin as well as tunicamycin. However, after 14 h of treatment, CANT1 protein level was reduced which was also observed at later time points (**Fig. 40**).
UPR activation proceeded very similar in the malignant cell line PC-3 with high CANT1 levels. HSPA5 mRNA and protein expression as well as TRIB3 and Herpud1 mRNA expression were strongly enhanced during the whole period of thapsigargin and tunicamycin treatment. After 48 h of treatment with DMSO, the mRNA levels of these UPR target genes were increased as well. This effect was less pronounced for the treatment with ethanol. CANT1 mRNA levels increased continuously from 14 h to 48 h after thapsigargin and tunicamycin treatment compared to control treatment. Similar to the UPR target genes, expression was also elevated 48 h after ethanol and DMSO treatment. However, CANT1 protein expression is lower in thapsigargin and tunicamycin treated samples compared to ethanol and DMSO treated samples during the whole experiment (**Fig. 41**).
In summary, CANT1 protein expression was decreased in all three cell lines upon ER stress induction. On mRNA level, CANT1 changed in a similar but less pronounced manner as the established UPR target gene Herpud1 in the case of RWPE-1 cells and as all three analyzed UPR target genes in the case of PC-3 cells. Thus, some evidence for CANT1 being a novel UPR target gene was seen in these two cell lines.

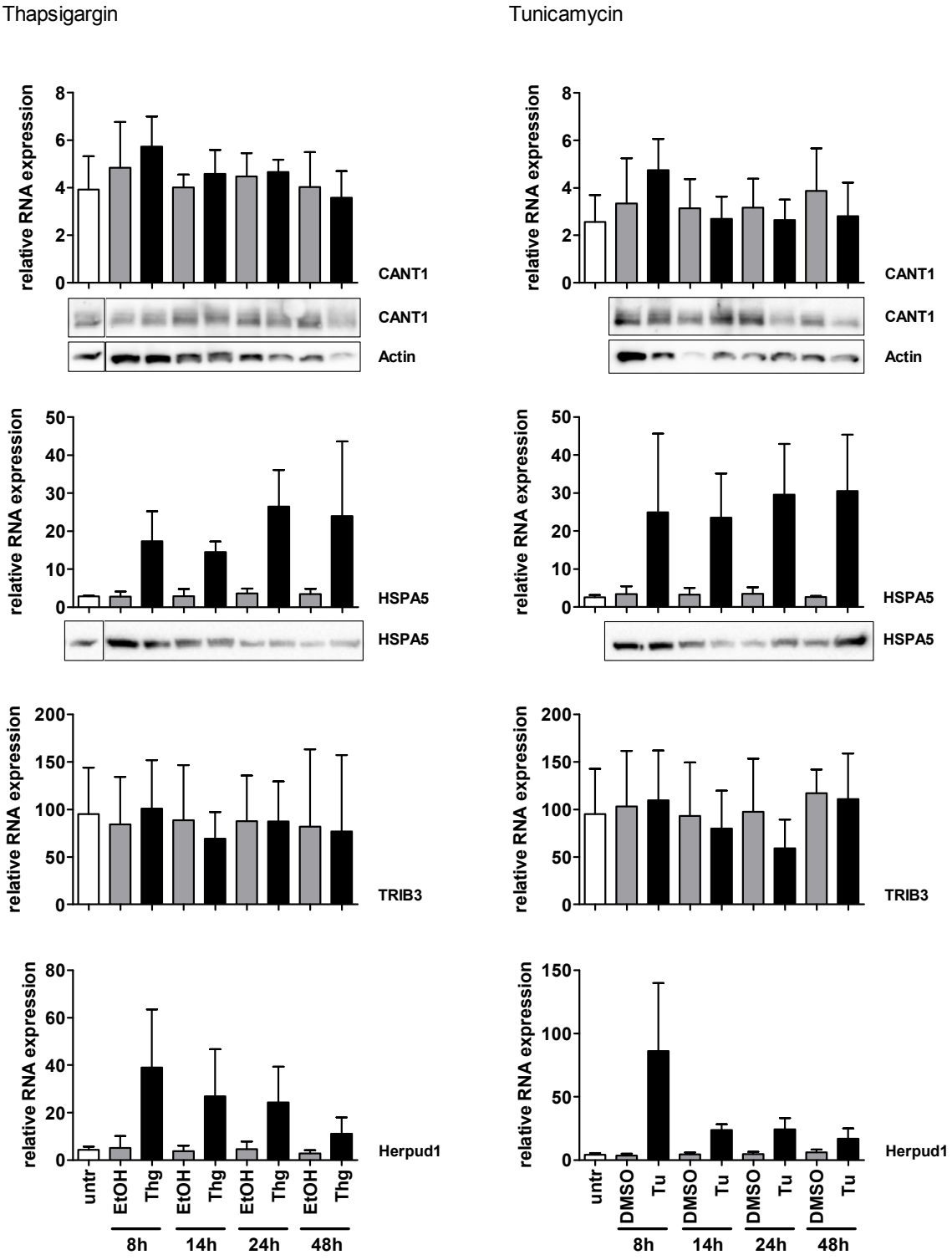


**Fig. 39 CANT1 expression upon ER stress induction in RWPE-1 cells.**

RWPE-1 cells were treated with thapsigargin and tunicamycin or ethanol and DMSO as corresponding negative controls for the indicated time periods. MRNA expression of CANT1, HSPA5, TRIB3 and Herpud1 and protein expression of CANT1 and HSPA5 were determined by qRT-PCR and Western Blot analysis. EtOH = ethanol, Thg = thapsigargin, Tu = tunicamycin.

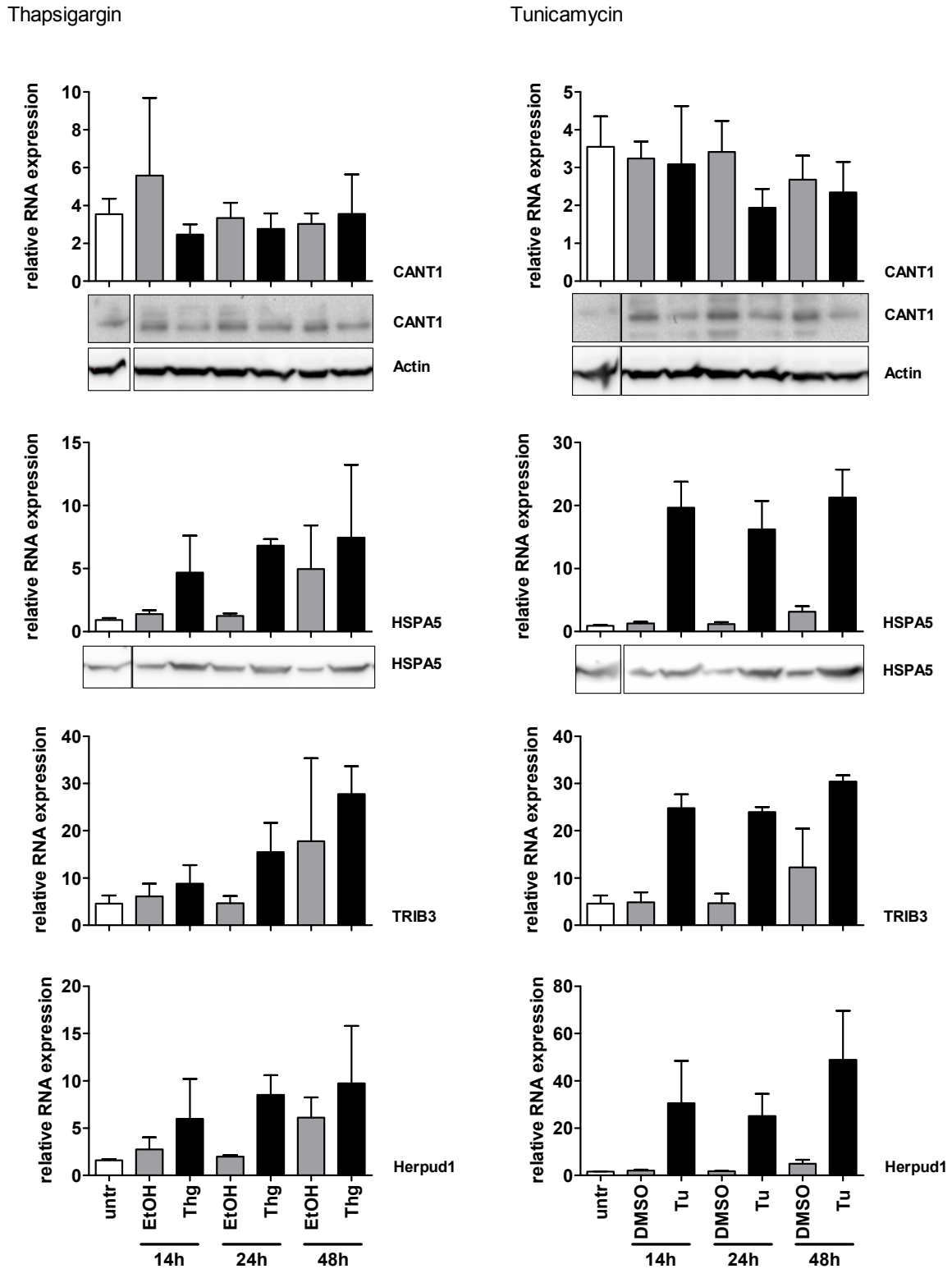


**Fig. 40 CANT1 expression upon ER stress induction in DU-145 cells.**

DU-145 cells were treated with thapsigargin and tunicamycin or ethanol and DMSO as negative control, respectively, for the indicated time periods. MRNA expression of CANT1, HSPA5, TRIB3 and Herpud1 and protein expression of CANT1 and HSPA5 was determined by qRT-PCR and Western Blot analysis. EtOH = ethanol, Thg = thapsigargin, Tu = tunicamycin.

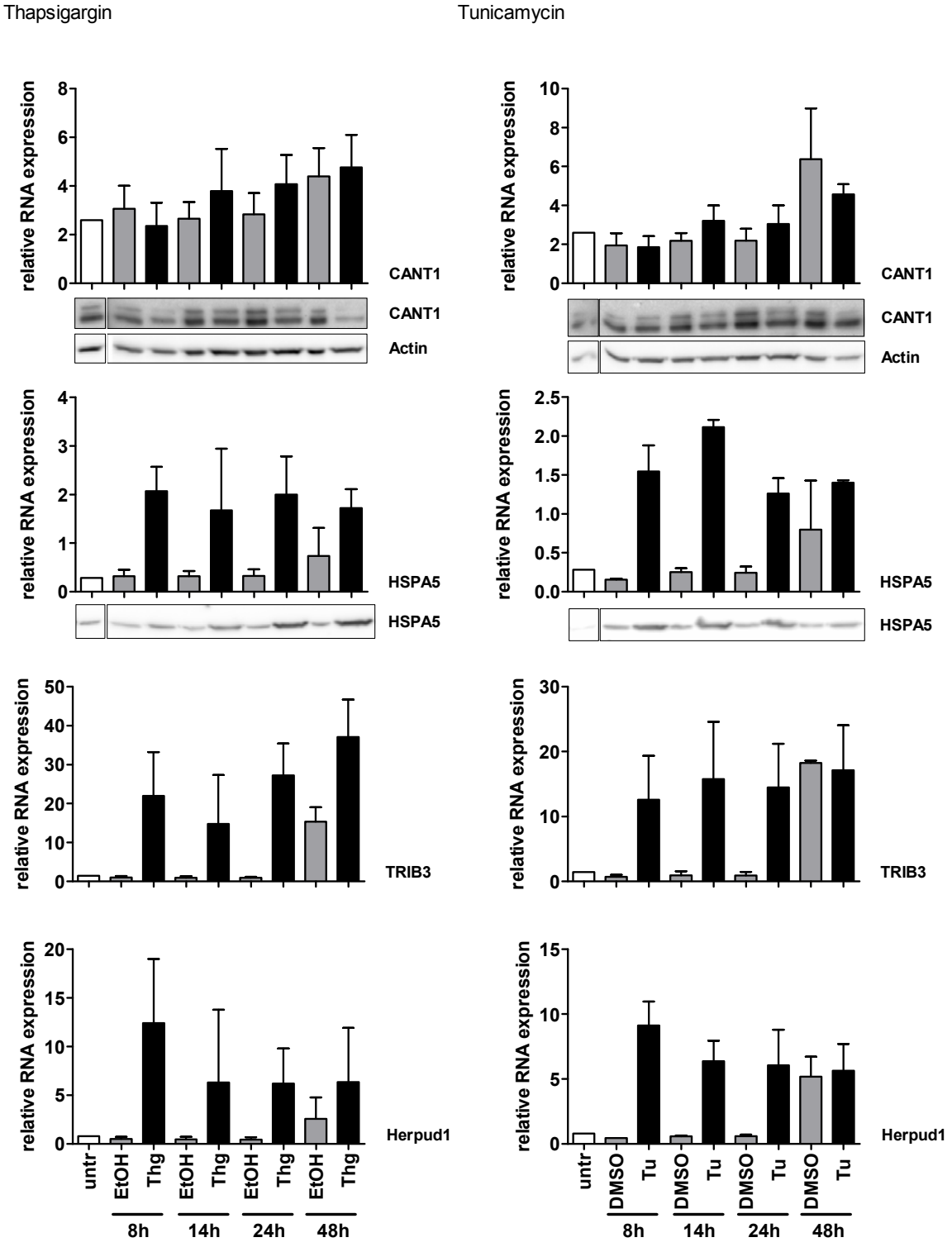


**Fig. 41 CANT1 expression upon ER stress induction in PC-3 cells.**

PC-3 cells were treated with thapsigargin (n=3) and tunicamycin (n=2) or ethanol and DMSO as negative control, respectively, for the indicated time periods. MRNA expression of CANT1, HSPA5, TRIB3 and Herpud1 and protein expression of CANT1 and HSPA5 was determined by qRT-PCR and Western Blot analysis. MRNA expression levels were normalized to ALAS1 and HPRT1. EtOH = ethanol, Thg = thapsigargin, Tu = tunicamycin.

## *4.2 The role of FOXA1 in prostate cancer*

### 4.2.1 The expression of FOXA1 in human prostatic tissue

In the before mentioned comparative study of normal and cancerous prostatic tissue, FOXA1 was a second gene to be identified as upregulated in prostate cancer [15]. Thus, protein expression and diagnostic and prognostic value of FOXA1 were analyzed in a TMA format in cohort #1.

#### 4.2.1.1 FOXA1 expression increases with prostate carcinoma progression

FOXA1 protein levels and the corresponding diagnostic value of FOXA1 were assessed by analyzing the staining intensities of FOXA1. FOXA1 was found almost exclusively in nuclei of epithelial cells, no stromal immunoreactivity was observed (**Fig. 42 a**), neither in normal nor in tumor tissues. In cases with strong FOXA1 expression, a mild degree of additional cytoplasmic staining was noted (**Fig. 42 b**) but not recorded. In normal prostatic tissues, FOXA1 was found in secretory cells, while basal cells were either negative or only weakly and inconsistently positive (**Fig. 42 a**).

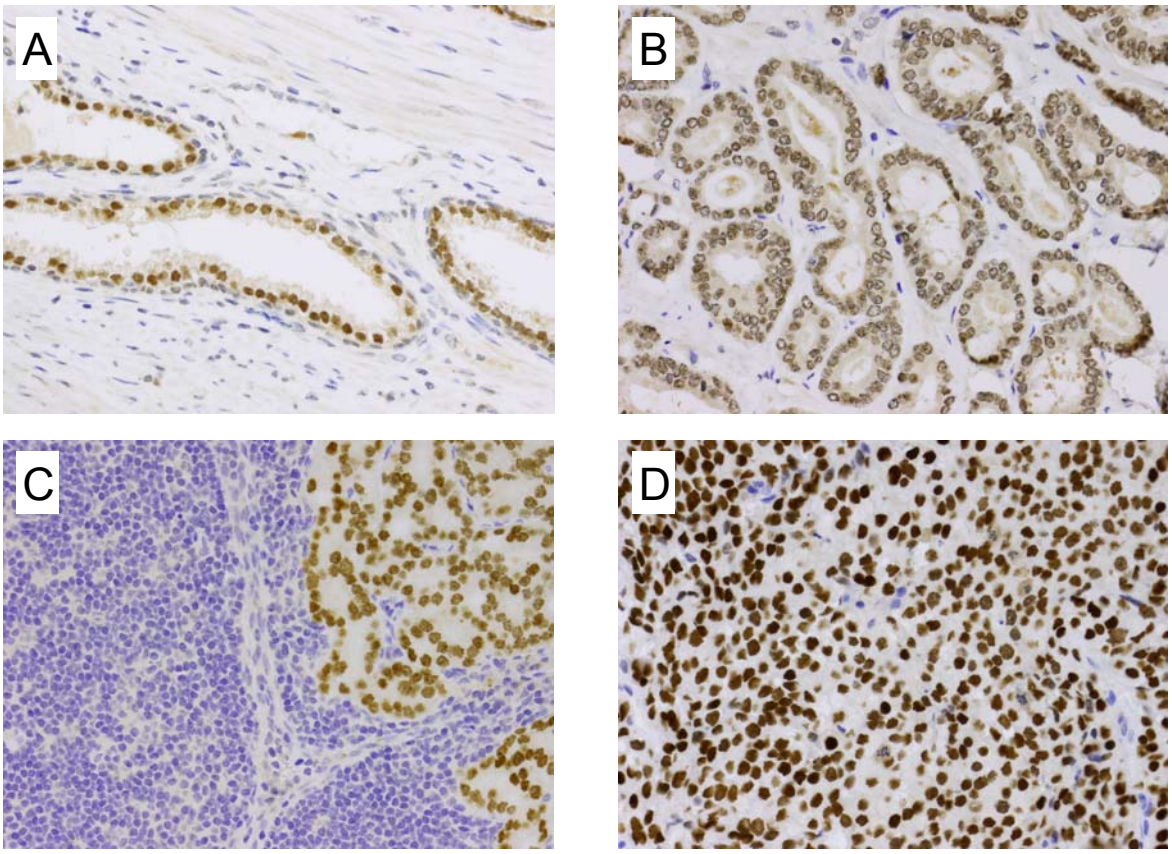


**Fig. 42 FOXA1 immunohistochemistry of human prostatic tissues.**

Immunohistochemistry of human prostatic tissues, magnification 200x. **(A)** Normal prostate glands. Note the FOXA1 negative stromal cells. **(B)** Prostate adenocarcinoma. Note the cytoplasmic signal. **(C)** Prostate cancer metastasis in a lymph node. Note the lymphocytes (smaller nuclei) on the left. **(D)** CRPC.

Close to the tumor (adjacent normal, n=204), the distribution of FOXA1 expression was as follows: three cases (1.5 %) negative, 42 (20.6 %) staining score 1, 146 (71.6 %) staining score 2 and 13 (6.4 %) staining score 3. The mean expression score was 1.83 (**Fig. 42 a, Fig. 43**). In primary carcinomas, FOXA1 was expressed as follows: 22 cases (10.6 %) negative, 56 (27.1 %) staining score 1, 114 (55.1 %) staining score 2 and 15 (7.2 %) staining score 3. The mean expression score was 1.59 (**Fig. 42 b, Fig. 43**). In metastases, FOXA1 was expressed as follows: seven cases (17.9 %) negative, four (10.3 %) staining score 1, ten (25.6 %) staining score 2 and 18 (46.2 %) staining score 3. The mean expression score was 2.0 (lymph node metastasis in **Fig. 42 c, Fig. 43**). In CRPC, FOXA1 was expressed as follows: two cases (3.9 %) negative, two (3.9 %) staining score 1, 23 (45.1 %) staining score 2 and 24 (47.1 %) staining score 3. The mean expression score was 2.35 (**Fig. 42 d, Fig. 43**).

In summary, little differences were seen between normal tissue and primary carcinomas, although a tendency to slightly decreased FOXA1 levels in primary carcinomas was observed. Significant upregulation of FOXA1 was seen in metastases and even more pronounced in CRPC.

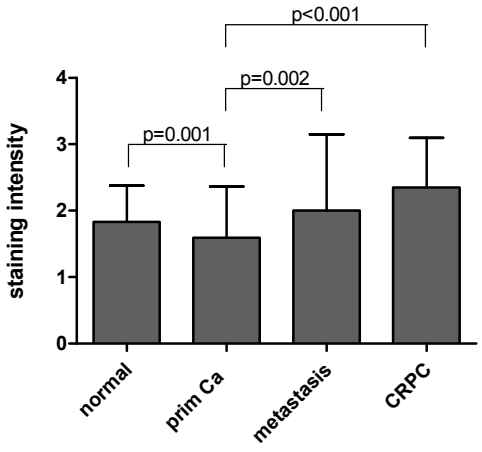


**Fig. 43 FOXA1 staining intensity in human prostatic tissue samples.**
Mean FOXA1 staining intensity during neoplasia progression. Ca = carcinoma.

#### 4.2.1.2 Relationship of FOXA1 staining to clinicopathological parameters and survival analysis

The prognostic value of FOXA1 was determined by analyzing the relationship between FOXA1 staining intensities and clinicopathological and survival data. In primary carcinomas, FOXA1 expression was significantly associated with pT stage and Gleason score. No correlation to age, pre-OP PSA levels and surgical margins were revealed (**Tab. 18**).

**Tab. 18 Relationship between FOXA1 expression and clinicopathological data of primary prostate carcinoma specimens (RPE) in cohort #1 (n=207).**

* statistically significant

| parameter | FOXA1 low | FOXA1 high | p-value |
|---|---|---|---|
| age | | | 0.774 |
| ≤ 64 years | 37 | 65 | |
| > 64 years | 41 | 64 | |
| pre-OP PSA | | | 0.779 |
| ≤ 10 ng/ml | 35 | 54 | |
| > 10 ng/ml | 40 | 69 | |
| Gleason score | | | 0.017* |
| 5-6 | 20 | 15 | |
| 7 | 42 | 77 | |
| 8-10 | 16 | 37 | |
| pT stage | | | 0.018* |
| pT2 | 57 | 72 | |
| pT3/4 | 21 | 57 | |
| margin status | | | 0.294 |
| R0 | 53 | 78 | |
| R1 | 24 | 50 | |

The analysis of patient follow-up data concerning serum PSA levels revealed a significant association between high FOXA1 expression levels and shorter relapse free survival times in Kaplan Meier analysis (mean 87 *vs.* 70 months, p=0.018, **Fig. 44**). However, FOXA1 expression failed to represent an independent prognostic marker (Cox regression analysis including pre-OP PSA level, pT stage, Gleason score, margin status; data not shown).
Together, a clear prognostic value of FOXA1 was revealed.

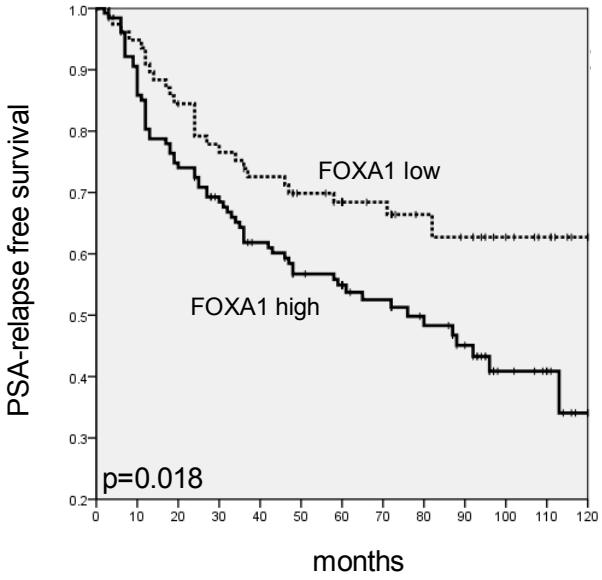


**Fig. 44 Univariate survival analysis dependent on FOXA1 staining intensity.**
Kaplan-Meier curves of FOXA1 expression (dichotomized by the median).

4.2.1.3 Relationship between FOXA1 and steroid hormone receptors.

Because FOXA1 was shown to cooperate amongst others with ERα and AR to induce gene expression [98, 115, 116, 125, 129], the relationship between FOXA1 and steroid hormone receptors in prostate cancer was analyzed. Therefore, the TMA slides were additionally stained with antibodies against AR, ERα and ERβ. Staining intensities were evaluated separately in the nuclei of the stroma and the epithelium. Within the group of primary carcinomas, FOXA1 staining intensity was significantly correlated to epithelial and stromal AR, stromal ERα and epithelial and stromal ERβ (**Tab. 19**).

**Tab. 19 Bivariate correlations between FOXA1 and steroid hormone receptor staining intensities.**

* statistically significant

| | | AR epithelium | AR stroma | ERα epithelium | ERα stroma | ERβ epithelium | ERβ stroma |
|---|---|---|---|---|---|---|---|
| FOXA1 | correlation coefficient | 0.534 | 0.213 | 0.105 | 0.444 | 0.410 | 0.354 |
| | p-value | <0.001* | 0.002* | 0.145 | <0.001* | <0.001* | <0.001* |
| | n | 200 | 201 | 196 | 196 | 189 | 189 |

Due to the strong correlation of FOXA1 to epithelial AR a double immunofluorescence staining of both proteins was conducted in a small subset of cases. This demonstrated a strong concordance of immunoreactivity of both markers (**Fig. 45**).

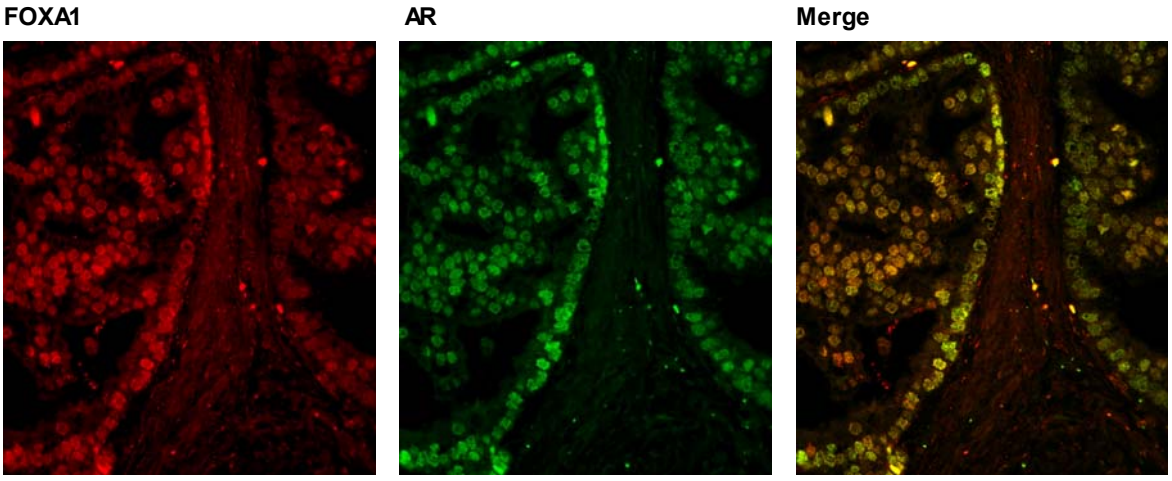


**Fig. 45 Colocalization of FOXA1 and AR in prostate cancer.**

Double immunofluorescence of FOXA1 (red) and AR (green) in a human prostate adenocarcinoma, magnification 400x.

Further, a stratified Kaplan Meier analysis according to low (staining score 0 to 2) and high (staining score 3) AR levels was performed. This demonstrated an even increased prognostic significance of FOXA1 in cases with low AR levels (mean 86 *vs*. 56 months, p<0.001), whereas in cases with high AR levels, no prognostic significance at all was discerned (**Fig. 46**). Cox regression analysis including pre-OP PSA level, pT stage, Gleason score and margin status revealed FOXA1 not to be independent also in this patient subgroup (data not shown).

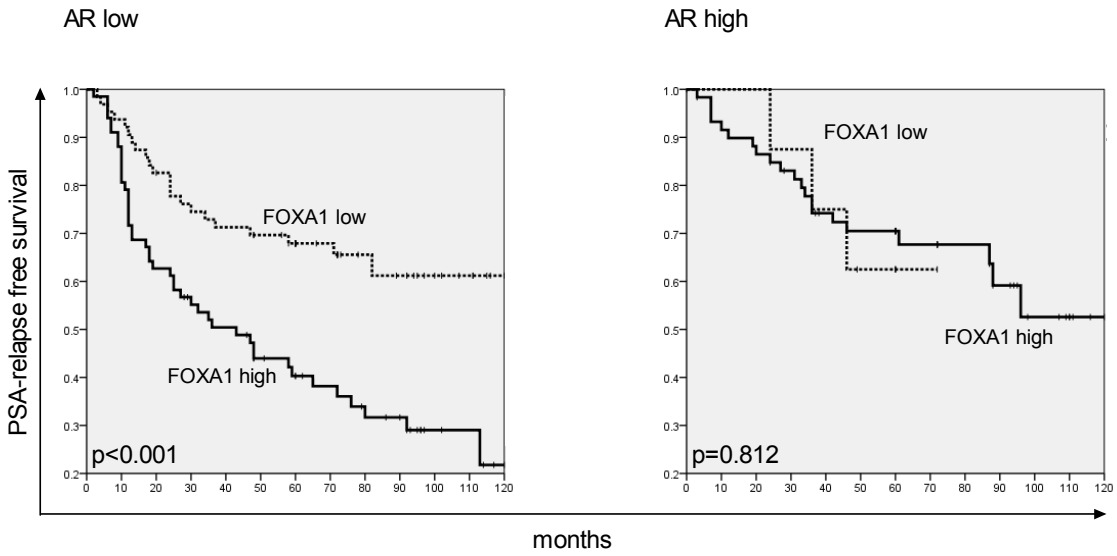


**Fig. 46 Univariate survival analysis dependent on AR and FOXA1 staining intensity.**

Kaplan-Meier curves of FOXA1 expression in patients with low (staining score 0 to 2) and high (staining score 3) AR levels.

In summary, a strong correlation between FOXA1 and steroid horomone receptor expression in primary prostate carcinomas was demonstrated, which is reflected in a coexpression of FOXA1 and AR. The prognostic value for FOXA1 staining that was revealed before (see chapter 4.2.1.2), was even more pronounced in the patient subgroup with prostate carcinomas that express low AR protein.

### 4.2.2 The influence of FOXA1 knockdown on *in vitro* tumorigenicity

#### 4.2.2.1 Characterization of FOXA1 expression in prostatic cell lines

To test if FOXA1 overexpression has a functional relevance in prostate cancer cell lines the expression on transcript and protein level was determined in the four prostatic cell lines using an antibody that detects FOXA1 as well as FOXA2. As observed by Western Blot analysis, FOXA1 protein was strongly expressed in LNCaP and PC-3 cells, whereas it was undetectable in DU-145 and RWPE-1 cells. FOXA2 was strongly expressed in PC-3 and DU-145 cells, less amounts were detected in RWPE-1 and LNCaP cells. FOXA1 mRNA expression was strongest in LNCaP cells. Medium levels of FOXA1 mRNA were detected in PC-3 and DU-145 cells, whereas mRNA levels in RWPE-1 cells were very low (**Fig. 47**).
In summary, a similar expression pattern as for CANT1 was revealed. FOXA1 protein is strongly expressed in the prostate cancer cell lines LNCaP and PC-3. In contrast, the expression is very low in the third prostate cancer cell line DU-145 and the benign prostatic cell line RWPE-1.

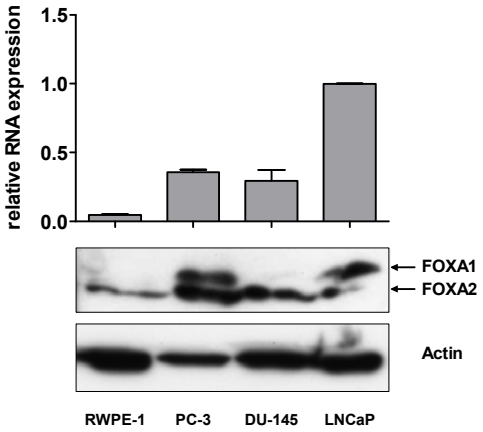


**Fig. 47 Expression of FOXA1 in prostatic cell lines.**

RWPE-1, PC-3, DU-145 and LNCaP cells were cultivated in 75 cm² cell culture flasks to 70-80 % confluence. FOXA1 mRNA and protein expression was determined by qRT-PCR (top) and Western Blot analysis (bottom), respectively. MRNA levels were normalized to that of LNCaP cells.

#### 4.2.2.2 Transient knockdown of FOXA1 in prostate cancer cell lines with high endogenous FOXA1 levels

According to the strong protein expression of FOXA1 LNCaP and PC-3 cells were chosen for tumorigenicity studies. A knockdown protocol based on RNA interference was established for both cell lines using three FOXA1-specific siRNAs. QRT-PCR and Western Blot analysis revealed a potent FOXA1 knockdown on mRNA and protein level, respectively, 72 h after siRNA transfection. The mRNA levels were reduced to 39 %, 57 % and 37 % in LNCaP cells and to 22 %, 42 % and 16 % in PC-3 cells using FOXA1 siRNA #1, #2 and #3, respectively. Except for siRNA #1 in PC-3 cells, knockdown efficiencies on protein level were similar strong. In all samples, only the levels of FOXA1 protein were reduced, while the expression levels of FOXA2 remained unchanged, indicating the specificity of the siRNAs used (**Fig. 48**). Summarized, efficient downregulation of FOXA1 expression was achieved in LNCaP and PC-3 cells using three specific siRNAs.

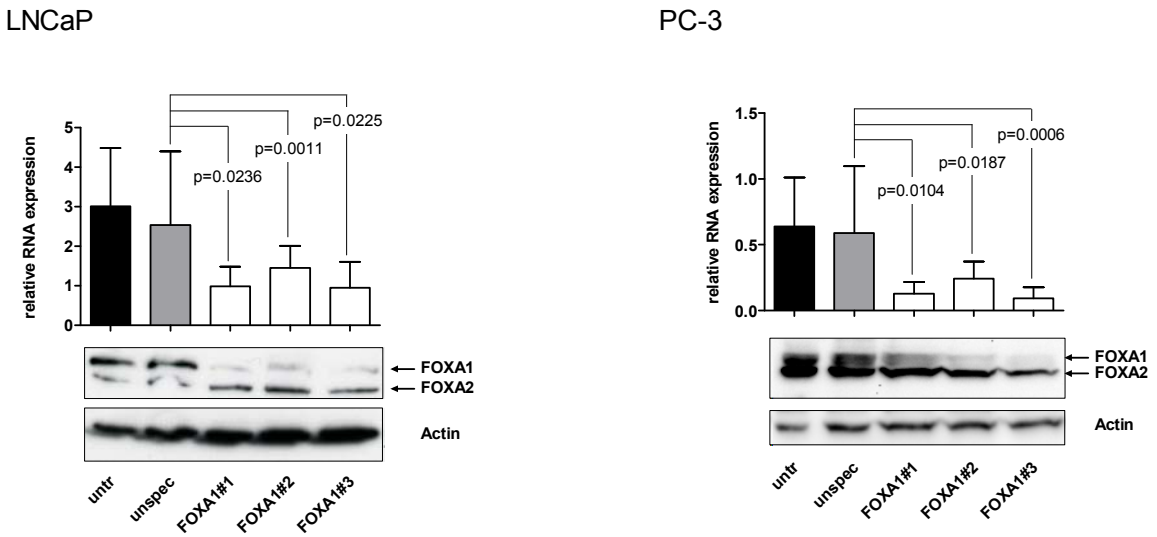


**Fig. 48 Knockdown of FOXA1 in LNCaP and PC-3 cells.**

LNCaP and PC-3 cells were cultivated in 6-well plates and left untreated or transfected with unspecific or FOXA1-specific siRNAs as indicated. After 72 h FOXA1 mRNA and protein expression was determined by qRT-PCR (top) and Western Blot analysis (bottom), respectively.

4.2.2.3 FOXA1 knockdown reduces cell proliferation

To determine if FOXA1 expression has an influence on prostate cancer cell proliferation, LNCaP and PC-3 cells were transfected with FOXA1-specific siRNAs and cells were counted. Compared to corresponding unspecific siRNA transfected cells, the cell number of FOXA1 siRNA #1, #2 and #3 transfected LNCaP cells was reduced significantly by 24 %, 18 % and 20 %. Although siRNA treatment itself strongly affected the propagation of PC-3 cells, the number of FOXA1 siRNA #1, #2 and #3 transfected cells was further decreased by 32 %, 44 % and 36 % compared to cells transfected with control siRNA and untreated cells (**Fig. 49**).

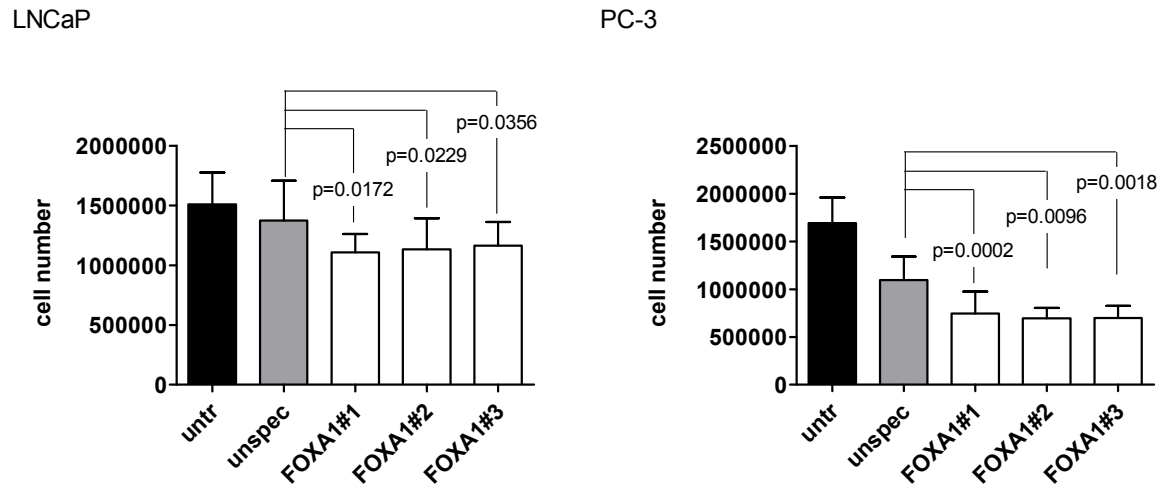


**Fig. 49 Cell number of LNCaP and PC-3 cells upon FOXA1 knockdown.**

LNCaP and PC-3 cells were seeded in 6-well plates, left untreated or transfected with siRNAs as indicated, and counted after 72 h.

To test whether the reduction of cell number after FOXA1 knockdown was caused by a reduction of cell proliferation rate, DNA synthesis rate was determined by measuring BrdU incorporation. As shown in **Fig. 50**, 44 %, 47 % and 29 % less BrdU was detected after transfection of LNCaP cells with FOXA1 siRNA #1, #2 and #3, respectively. The DNA synthesis rate of PC-3 cells was decreased in a highly significant manner by 18 %, 48 % and 28 % in FOXA1 siRNA #1, #2 and #3 transfected cells compared to unspecific siRNA transfected cells.

Taken together, these results show a significant reduction of LNCaP and PC-3 cell proliferation after FOXA1 knockdown.

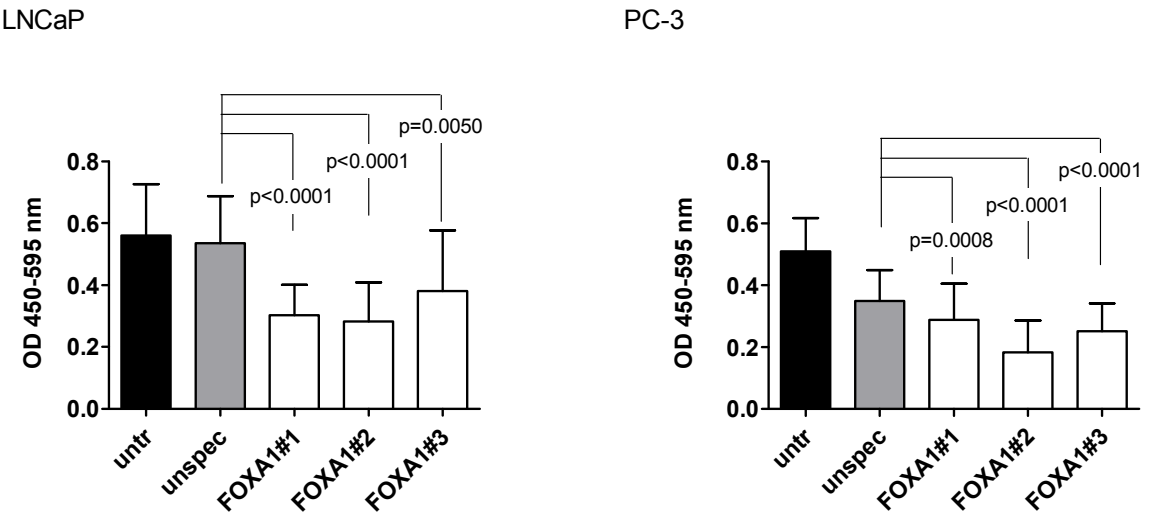


**Fig. 50 DNA synthesis rate of LNCaP and PC-3 cells upon FOXA1 knockdown.**

LNCaP and PC-3 cells were seeded in 6 cm-dishes and left untreated or transfected with siRNAs as indicated. After 72 h DNA synthesis rate measurement was performed.

#### 4.2.2.4 Reduced cell proliferation is associated with G1-arrest

To examine whether the observed reduction of proliferation was reflected in a change of cell cycle distribution, the proportion of cells in G1-, S-, and G2/M-phase was determined by flow cytometry of PI-stained cells. The proportion of LNCaP cells in G1-phase increased from 65 % in control cells to 70–75 % in FOXA1 knockdown cells, whereas the proportion of cells in S-phase declined from 22 % to 15–20 % in the respective groups; the proportion of cells in G2/M-phase also decreased slightly from 13 % to 10 % (**Fig. 51 a, c, e, g**). The differences were more pronounced in PC-3 cells. Sixty-three percent of the cells treated with unspecific siRNA were in G1-phase in contrast to 72–81 % of the cells treated with FOXA1-specific siRNAs. According to this up to 18 % increase of cells in G1-phase, the proportions of S- and G2/M-phase cells decreased in FOXA1 knockdown PC-3 cells from 19 % to 6–14 %, and from 17 to 10–13 %, respectively (**Fig. 51 b, d, f, h**). In summary, these data clearly indicate G1-arrest upon FOXA1 knockdown, which is very prominent in PC-3 cells.

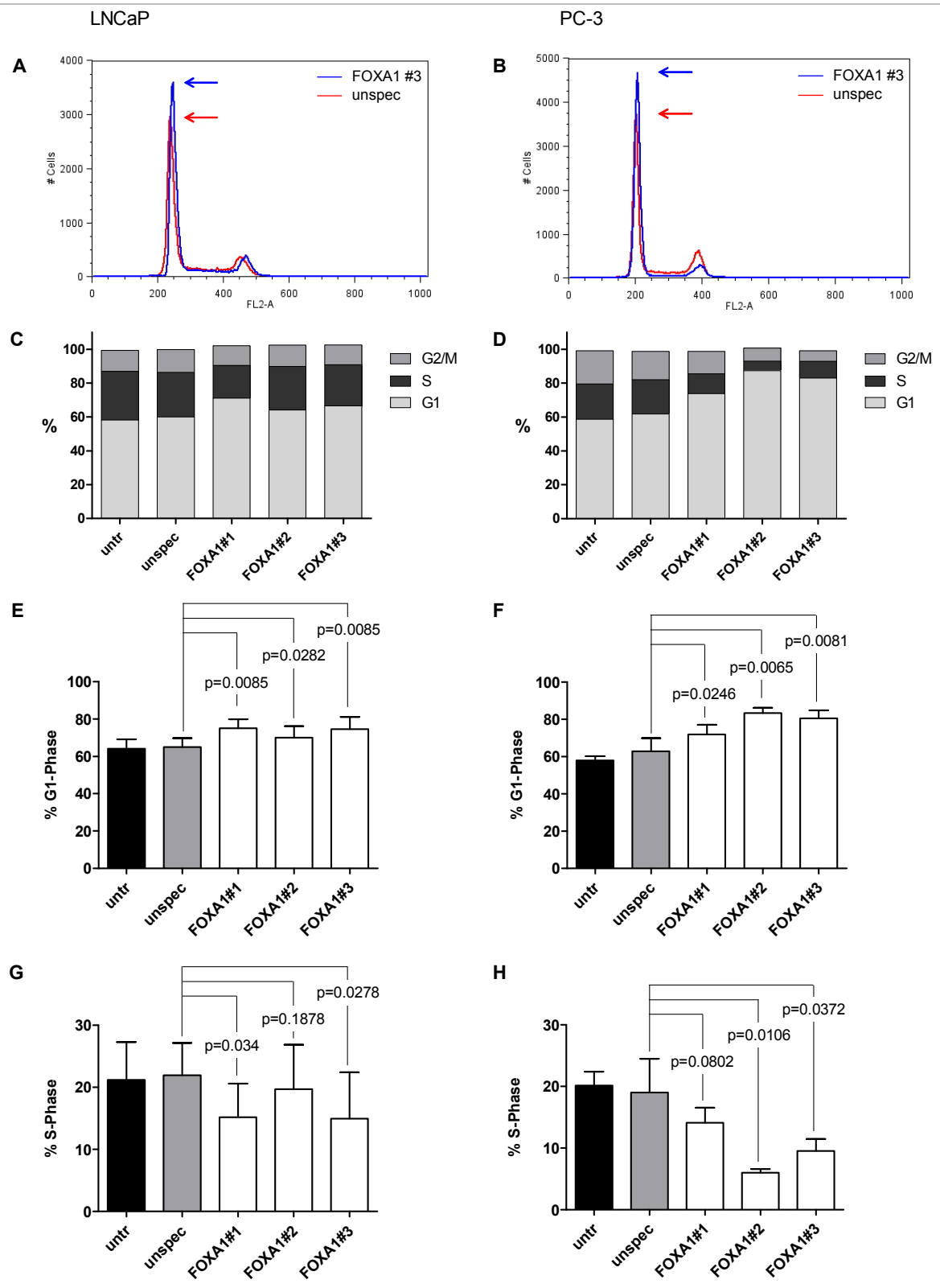


**Fig. 51 Cell cycle distribution of LNCaP and PC-3 cells upon FOXA1 knockdown.**

LNCaP (A, C, E, G) and PC-3 (B, D, F, H) cells were left untreated or transfected with siRNAs as indicated. After 72 h, cell cycle analysis was performed. **(A, B)** Representative histogram of cells that were treated either with unspecific siRNA (red) or FOXA1 siRNA #3 (blue); note the higher G1-phase peak and lower S-phase plateau and G2-phase peak in the FOXA1 siRNA histogram compared to the unspecific siRNA histogram. **(C, D)** Representative distribution of G1-, S-, and G2/M-phase phase. **(E, F)** Proportion of cells in G1-phase from all replicates. **(G, H)** Proportion of cells in S-phase from all replicates.

4.2.2.5 Cell migration is inhibited upon FOXA1 knockdown

The relevance of FOXA1 expression during cell migration was elucidated in a transmigration assay using fibronectin coated wells. Downregulation of FOXA1 reduced migration of LNCaP cells through the porous membrane highly significantly by 18 %, 12 % and 25 % using siRNA #1, #2 and #3 compared to control cells. The reduction of PC-3 cell migration accounted for 12 %, 20 % and 29 % with the respective siRNAs in comparison to corresponding control cells (**Fig. 52**).

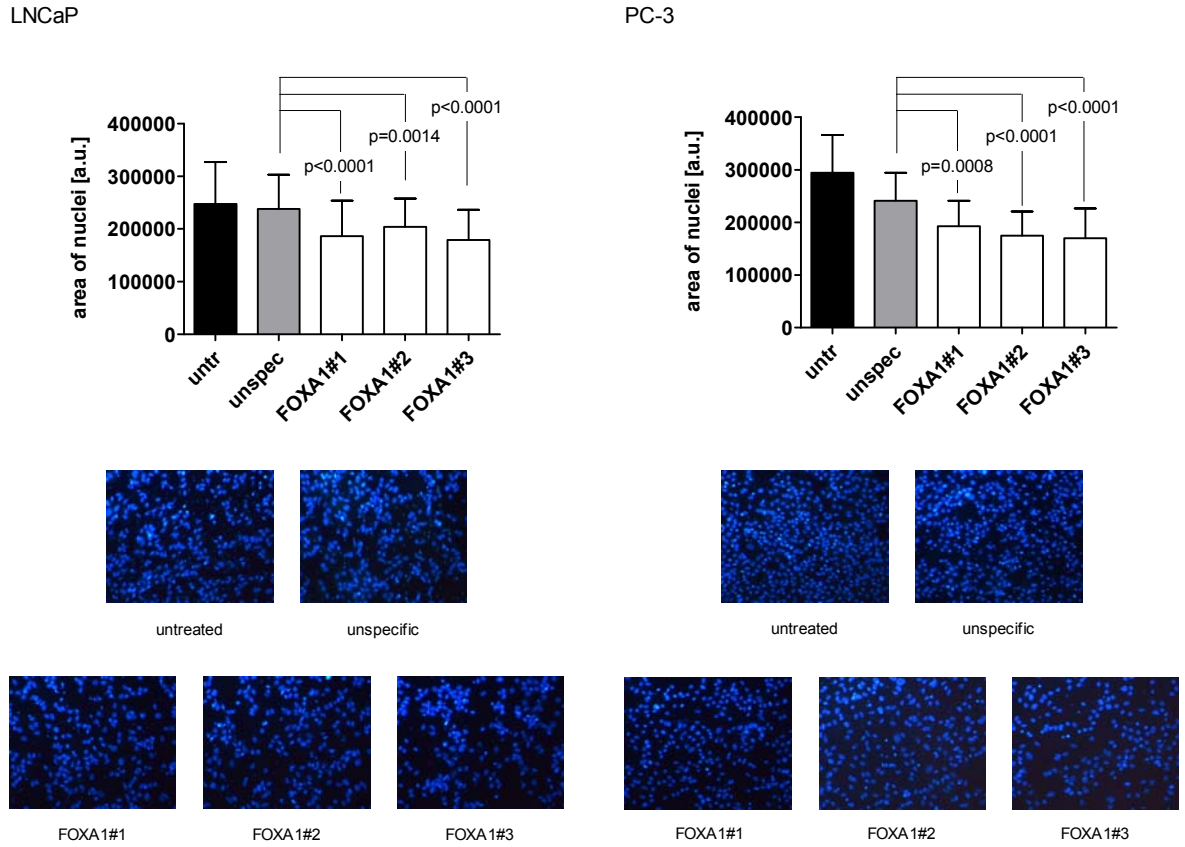


**Fig. 52 Haptotactic transmigration of LNCaP and PC-3 cells upon FOXA1 knockdown.**

LNCaP and PC-3 cells were seeded in 6 cm-dishes and left untreated or transfected with siRNAs as indicated. After 72 h, the transmigration assay was performed. Below, representative pictures of the DAPI-stained membranes are displayed (magnification 100x).

Migration of PC-3 cells on an uncoated surface was assessed in a scratch wound assay. The area, which was not recovered with migrated PC-3 cells within 24 h after introducing the wound, was 1.9, 2.1 and 1.6 times larger following FOXA1 downregulation with siRNA #1, #2 and #3, respectively, compared to unspecific siRNA treatment (**Fig. 53**), indicating a diminished cell motility.

Altogether, these data show that the reduction of FOXA1 expression induces considerable inhibition of LNCaP and PC-3 cell migration.

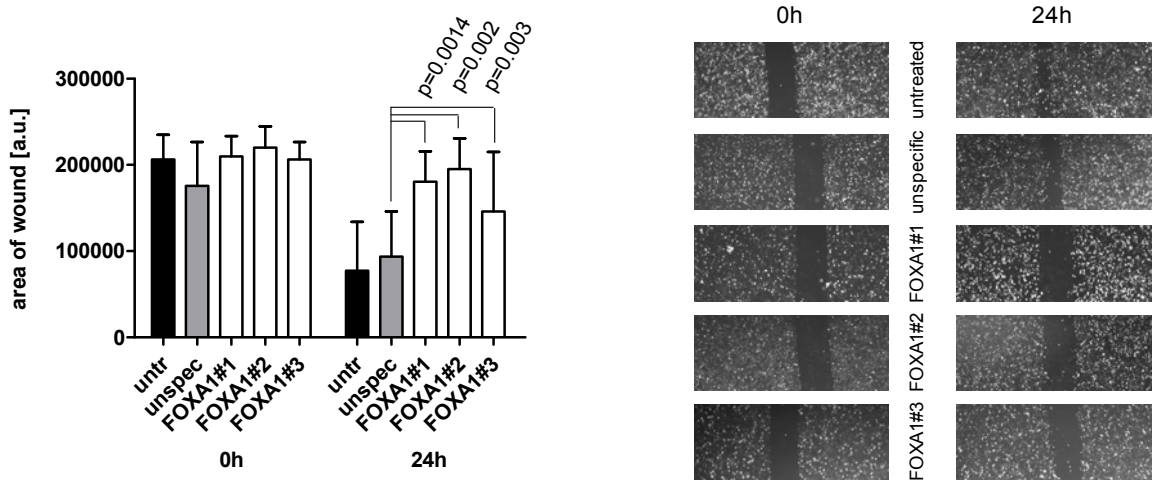


**Fig. 53 Wound healing of PC-3 cells upon FOXA1 knockdown.**

PC-3 cells were seeded in 6 cm-dishes and the scratch wound assay was conducted. On the right, representative pictures of the wounds are shown (magnification 25x).

## *4.3 Functional characterization of GOLM1* in vitro

The third candidate protein for functional analyses is GOLM1, which was also identified from our gene array study of matched normal and prostate cancer tissue [15]. Recently, our group confirmed overexpression of GOLM1 protein in prostate carcinomas in 92.3 % of the patients [16].

### 4.3.1 Characterization of GOLM1 expression in prostatic cell lines

To test if GOLM1 overexpression has a functional relevance in prostate cancer, the four prostatic cell lines were evaluated for endogenous GOLM1 expression levels and selected for subsequent functional studies. As observed by Western Blot analysis, GOLM1 protein was strongly expressed in LNCaP and DU-145 cells, whereas it was undetectable in PC-3 cells. A weak band was detected in the lysate of the epithelium derived cell line RWPE-1. Similarly, mRNA expression was strongest in DU-145 cells followed by LNCaP and RWPE-1 cells. In contrast to the protein, GOLM1 mRNA was also detected in PC-3 cells (**Fig. 54**). Thus, the GOLM1 expression pattern in the four analyzed cell lines differs from that of CANT1 and FOXA1. Similar to these before analyzed proteins, high expression in LNCaP cells and weak expression in RWPE-1 cells was detected. Contrary, DU-145 expressed very high levels of GOLM1, whereas the protein was undetectable in PC-3 cells.

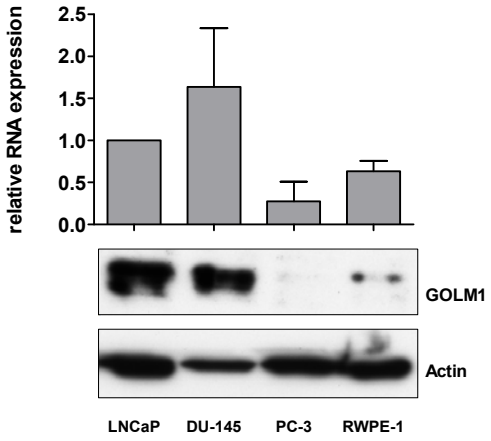


**Fig. 54 Expression of GOLM1 in prostatic cell lines.**

LNCaP, DU-145, PC-3, and RWPE-1 cells were cultivated in 75 cm² cell culture flasks to 70-80 % confluence. GOLM1 mRNA and protein expression was determined by qRT-PCR (top) and Western Blot analysis (bottom). MRNA levels were normalized to LNCaP cells.

### 4.3.2 Transient knockdown of GOLM1 in prostate cancer cell lines with high endogenous GOLM1 levels

According to the strong GOLM1 expression on mRNA and protein level, LNCaP and DU-145 cells were chosen for knockdown studies. A knockdown protocol based on RNA interference was established for both cell lines. QRT-PCR and Western Blot analysis revealed a potent GOLM1 knockdown on mRNA and protein level, respectively, 72 h after siRNA transfection (**Fig. 55**). A reduction of mRNA amounts to ~33 % in LNCaP cells and to 15-26 % in DU-145 cells was achieved. Protein expression was hardly detectable in any of the GOLM1-specific siRNA treated samples. Thus, GOLM1 expression was efficiently downregulated in LNCaP and DU-145 cells using three specific siRNAs.

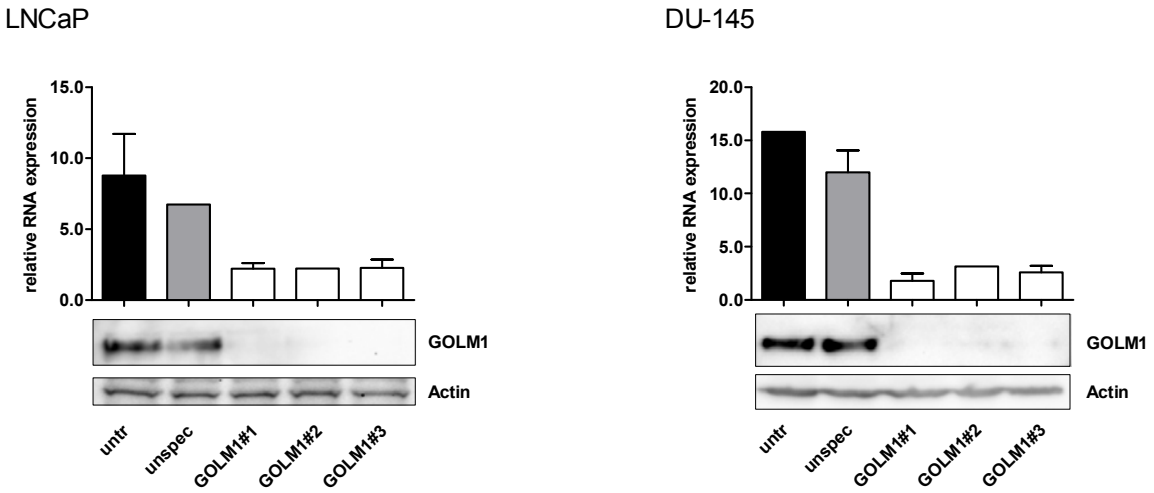


**Fig. 55 Knockdown of GOLM1 in LNCaP and DU-145 cells.**

LNCaP and DU-145 cells were cultured in 6 cm-dishes and left untreated or transfected with unspecific or GOLM1-specific siRNAs as indicated. After 72 h GOLM1 mRNA and protein expression was determined by qRT-PCR (top, n=2) and Western Blot analysis (bottom, n=5).

### 4.3.3 GOLM1 knockdown does not change cell proliferation rate

To determine if GOLM1 expression has an influence on prostate cancer cell proliferation, LNCaP and DU-145 cells were transfected with GOLM1-specific siRNAs and cells were counted. Transfection of GOLM1 siRNA #2 in DU-145 cells slightly increased the cell number, however no significant changes were observed in either of the cell lines using any siRNA (**Fig. 56**).

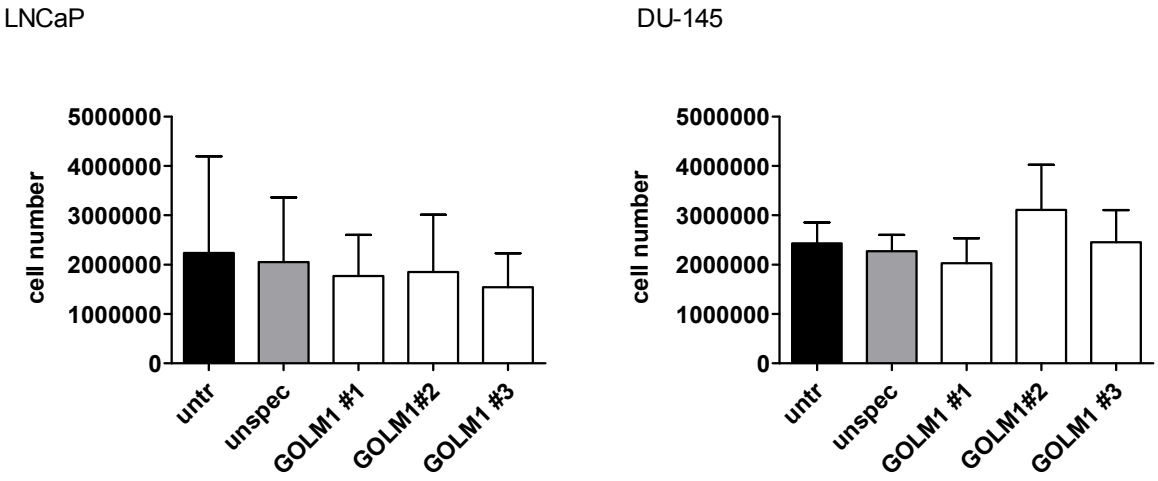


**Fig. 56 Cell number of LNCaP and DU-145 cells upon GOLM1 knockdown.**

LNCaP and DU-145 cells were seeded in 6 cm-dishes, left untreated or transfected with siRNAs as indicated, and counted after 72 h.

Further, DNA synthesis rate was determined by measuring BrdU incorporation. As shown in **Fig. 57**, similar amounts of BrdU as in control cells were detected after transfection of LNCaP and DU-145 cells with GOLM1 siRNAs.

Taken together, these results show that proliferation of prostate cancer cell lines is independent of GOLM1 expression.

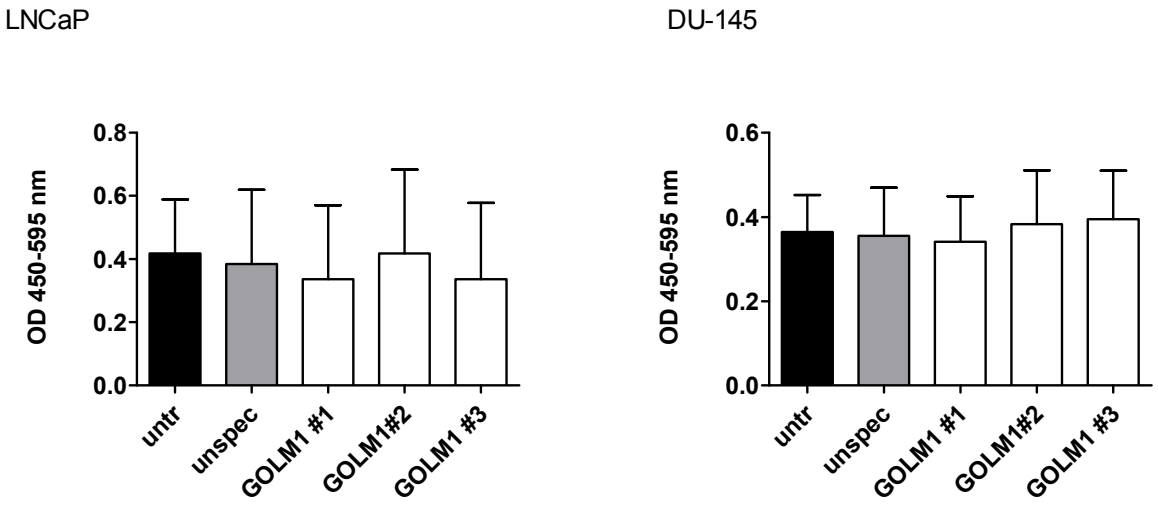


**Fig. 57 DNA synthesis rate of LNCaP and DU-145 cells upon GOLM1 knockdown.**

LNCaP and DU-145 cells were seeded in 6 cm-dishes and left untreated or transfected with siRNAs as indicated. After 72 h DNA synthesis rate measurement was performed.

### 4.3.4 GOLM1 knockdown has no influence on cell cycle distribution

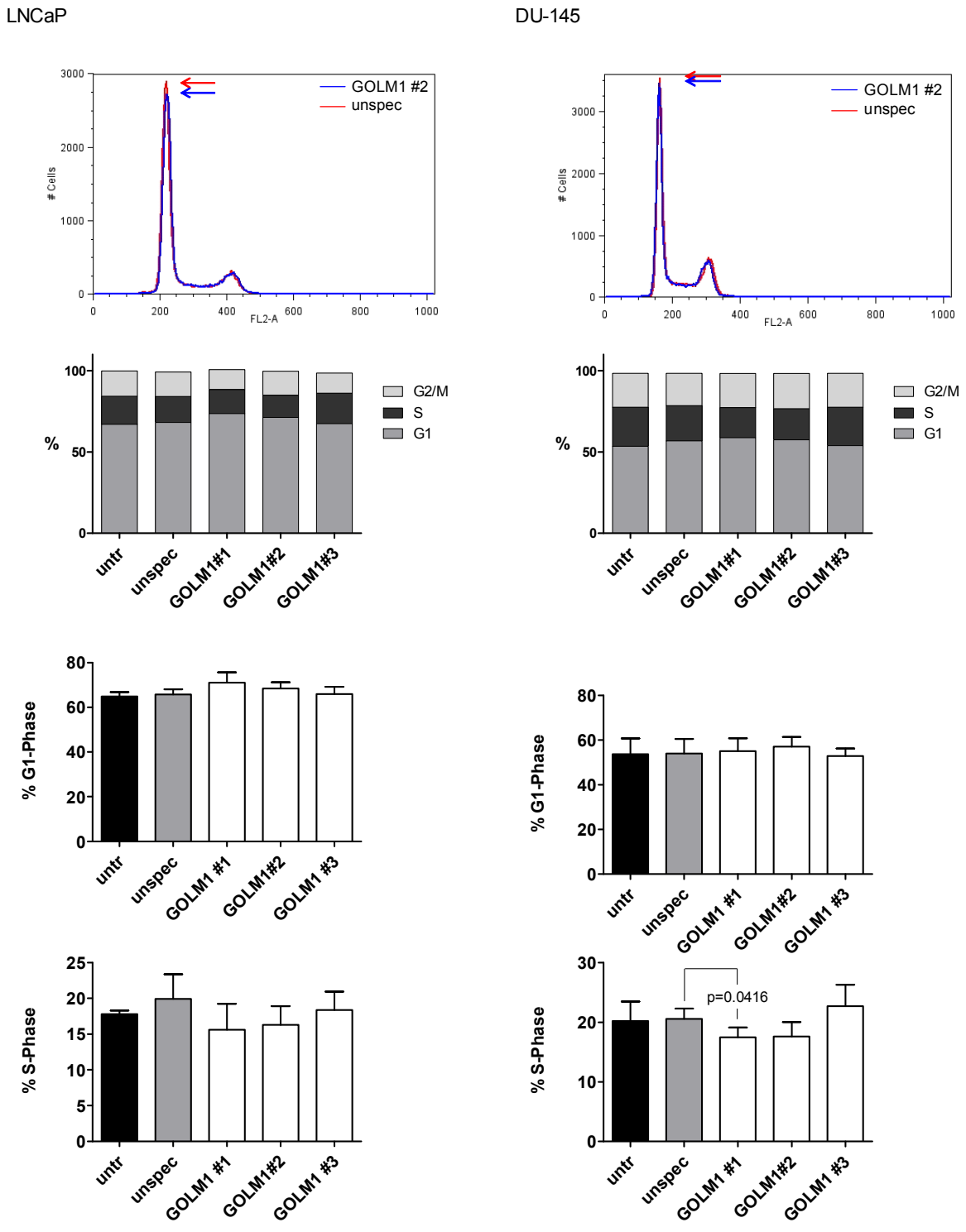


**Fig. 58 Cell cycle distribution of LNCaP and DU-145 cells upon GOLM1 knockdown.**

LNCaP (A, C, E, G) and DU-145 cells (B, D, F, H) were left untreated or transfected with siRNAs as indicated. After 72 h, cell cycle analysis was performed. **(A, B)** Representative histogram of cells that were treated either with unspecific siRNA (red) or GOLM1 siRNA #2 (blue). **(C, D)** Representative distribution of G1-, S-, and G2/M-phase cells. **(E, F)** Proportion of cells in G1-phase from all replicates. **(G, H)** Proportion of cells in S-phase from all replicates.

To analyze cell cycle distribution upon GOLM1 knockdown the proportion of cells in G1-, S- and G2/M-phase was determined by flow cytometry of PI-stained cells. The proportion of LNCaP cells in G1-phase ranged from 65 % to 71 % in all groups, the proportion of cells in S-phase ranged from 15 % to 20 %. No significant changes were observed. In DU-145 cells 53 % to 57 % of the cells were in G1-phase and 17 % to 23 % of the cells were in S-phase. Only the reduction of S-phase cells between cells that were transfected with unspecific siRNA and GOLM1 siRNA #1 from 20.6 % to 17.5 % was significant (**Fig. 58**). Yet altogether, these data show that GOLM1 knockdown has no reproducible effect on cell cycle regulation in LNCaP as well as in DU-145 cells.

### 4.3.5 Cell migration is not influenced by GOLM1 knockdown

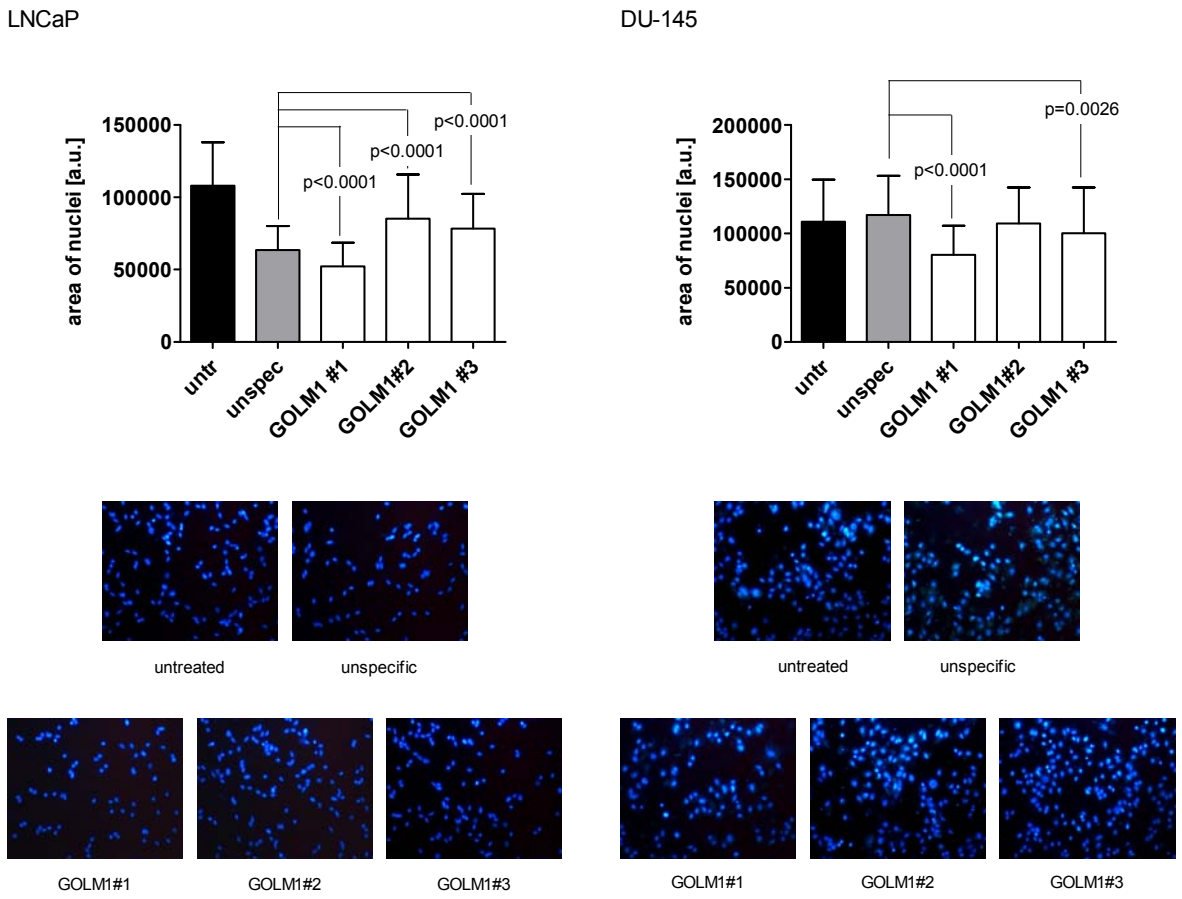


**Fig. 59 Haptotactic transmigration of LNCaP and DU-145 cells upon GOLM1 knockdown.**

LNCaP and DU-145 cells were seeded in 6 cm-dishes and left untreated or transfected with siRNAs as indicated. After 72 h, the transmigration assay was performed. Below, representative pictures of the DAPI-stained membranes are displayed (magnification 100x).

The relevance of GOLM1 expression during cell migration was elucidated in a transmigration assay using fibronectin coated wells. Transmigration of LNCaP cells was strongly affected by transfection with Lipofectamine 2000 (compared with the effect of transfection using

HiPerFect in chapters 4.1.2.5 and 4.2.2.5). The effect of downregulation of GOLM1 differed between the siRNAs. The proportion of migrated LNCaP cells was reduced by 18 % upon transfection with GOLM1 siRNA #1, whereas transfection with siRNA #2 and #3 increased the proportion significantly by 34 % and 23 %. In DU-145 cells, transfection with siRNA #1 led to a highly significant reduction of migrated cells by 31 %. Upon transfection with siRNA #2 migration rate was also reduced by 14 %. The change upon transfection with siRNA #3 was not significant (**Fig. 59**).

Migration of DU-145 cells on an uncoated surface was assessed in a scratch wound assay. The area, which was not recovered with migrated cells within 8 h after introducing the wound, remained unchanged following GOLM1 downregulation with specific siRNAs (**Fig. 60**).

Altogether, these data show that the reduction of GOLM1 expression does not mediate a change of cell migration.

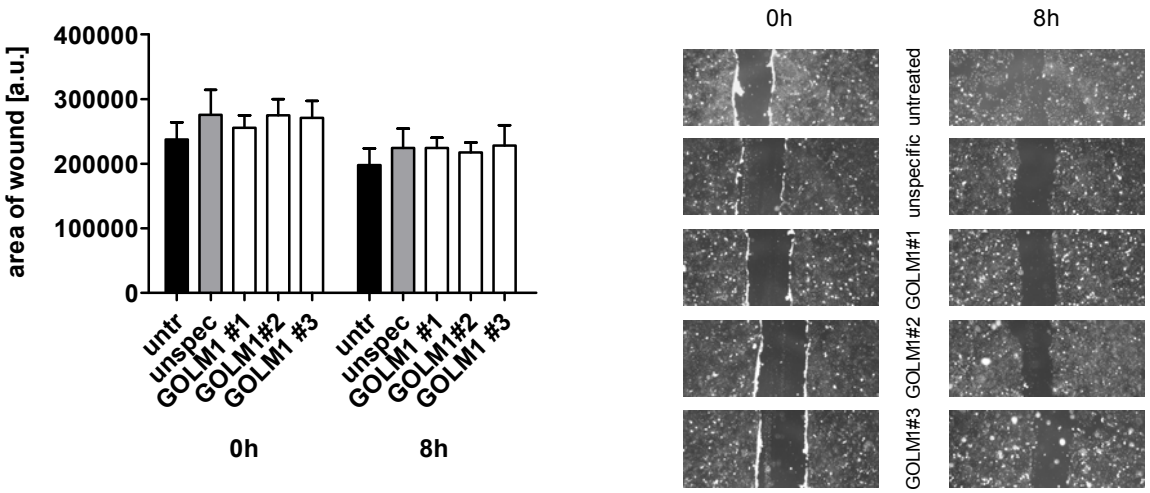


**Fig. 60 Wound healing of DU-145 cells upon GOLM1 knockdown.**

DU-145 cells were seeded in 6 cm-dishes and the scratch wound assay was conducted. On the right, representative pictures of the wounds are shown (magnification 25x).

# 5 Discussion

## *5.1 The role of CANT1 in prostate cancer*

### 5.1.1 Expression, relationship to clinicopathological parameters and survival analysis of CANT1 in human prostatic tissue

Previously, our group identified CANT1 as a highly upregulated gene in human prostate cancer [15]. Further, CANT1 gene expression has been shown to be significantly higher in tumors of the prostate compared to 28 other tumor entities [47]. However, the clinical significance of CANT1 expression in prostate cancer tissues has not been investigated yet. To study CANT1 protein expression during prostate carcinoma initiation (normal, PIN, primary carcinoma) as well as during prostate carcinoma progression (primary carcinoma, metastasis, CRPC), two TMAs were constructed including nearly 1.000 prostate tissue samples from two different hospitals and a valid immunohistochemistry protocol was developed. CANT1 immunoreactivity was detected in secretory epithelial cells in the Golgi apparatus region as well as in the cytoplasm. Evaluation of TMA #1 showed ubiquitous CANT1 expression in normal prostate epithelial tissue, however, the overall staining intensities of the Golgi apparatus and the cytoplasm were generally stronger in cancer, thus suggesting CANT1 as a candidate diagnostic marker for prostate carcinomas. Slightly but significantly lower levels of CANT1 were noted in CRPC in comparison to primary carcinomas and metastases. With regard to normal tissue, the CANT1 levels of CRPC were only significantly different for the Golgi immunoreactivity. Similarly, in eleven prostate cancer xenografts in mice highest expression rates of CANT1 transcripts including exon 1a were detected in more differentiated, androgen-dependent tumors. In contrast, transcripts including exon 1 were expressed at variable levels in all xenografts independent of differentiation and androgen-dependency [49]. Assuming equal translation efficiency of both transcripts, the total amount of CANT1 protein was lower in androgen-independent tumors, which resemble CRPC, than in androgen-dependent tumors, which is consistent with our data.

This raises the question how CANT1 expression is regulated. First, it would be interesting to analyze if CANT1 transcripts including exon 1 or 1a contribute equally to changes in CANT1 expression. In any case, both transcripts were shown before to be androgen-regulated [49] and AR expression increases and decreases similarly from normal epithelium to primary carcinomas and from metastases to CRPC, respectively (data not shown), strongly indicating that CANT1 levels depend on AR levels.

CANT1 intensity levels of Golgi and cytoplasm staining show synchronous changes during prostate carcinoma development indicating that localization of the protein does not change.

The unique design of TMA #2 with matching normal and cancer tissues allowed to individually evaluate the diagnostic value of CANT1. The upregulation of CANT1 in carcinomas could be convincingly confirmed in this second independent cohort. Moreover, the direct case wise comparison of cancerous and adjacent normal glands revealed a gain of CANT1 expression in 97.2 % of the cases, clearly substantiating the applicability of CANT1 as potentially helpful ancillary marker to ascertain a cancer diagnosis in a suspicious lesion. Additionally, elevated expression levels of the protein were already detected in the precursor lesion PIN. Statistically, the mean staining intensity of PIN cores was significantly lower compared to primary carcinomas, however the absolute difference is too little to distinguish these stages in practice.

The initial survival analysis of CANT1 expression categorized into negative, weak, moderate or strong expression did not show significant differences in Kaplan-Meier analysis. However, a significant impact towards better prognosis in cases with strong CANT1 overexpression was noted in univariate and multivariate analyses in the larger study cohort (TMA #2) using a sophisticated semiquantitative evaluation scheme, which included area and intensity to compensate for expression heterogeneity. This more differentiated analysis allowed the separation of the upper quartile in the range of expression values, which was not feasible with the simpler three tiered scoring system applied to TMA #1. This finding was further substantiated by the association of lower H-scores with higher Gleason scores and pT stages, respectively. These results nicely fit to the observation that CANT1 expression is lower in the aggressive group of CRPC compared to primary carcinomas.

In summary, CANT1 is weakly expressed in normal prostatic epithelium, upregulation starts early in prostate carcinoma initiation (PIN), expression remains high in primary carcinomas and metastases before CANT1 levels decline again slightly during development of castration-resistance. Thus, despite ubiquitous overexpression in primary tumors, which was demonstrated in two independent patient cohorts, the diagnostic applicability of CANT1 as a prostate cancer marker is hampered by its basal expression in normal glands and its inability to discriminate PIN glands from invasive carcinoma glands.
The prognostic value of CANT1 appears to be limited, since it only became evident upon careful consideration of staining heterogeneity. However, if this more elaborate analysis is conducted, CANT1 expression is an independent prognostic biomarker for prostate cancer following RPE.

### 5.1.2 Functional characterization of CANT1 *in vitro*

Since CANT1 upregulation is apparently an early event during prostate carcinoma development, it was encouraging to investigate if CANT1 has tumor promoting functions. For this, we analyzed CANT1 expression in different prostatic cell lines and set up an *in vitro* system to test cell proliferation and migration behaviour in cells with high and low CANT1 levels.

In concordance with the TMA data, CANT1 protein levels were low in the benign cell line RWPE-1 and high in the metastasis-derived hormone-dependent cell line LNCaP. In the hormone-independent metastasis-derived cell lines PC-3 and DU-145, which are a model system for the castration-resistant stage of prostate carcinomas, CANT1 expression was strong and weak, respectively. Hence, the DU-145 cell line possibly represents a CRPC case that already repressed CANT1 expression after the protein had been upregulated during the stage of hormone-dependency. The expression differences were not that prominent on RNA level indicating post-transcriptional regulation of CANT1 protein expression. In all four prostatic cell lines as well as in HEK-293 kidney cells, Western Blot analysis detected one major band at ~38 kDa and one or two bands of higher molecular weight, confirming the results of Smith *et al.* [60].

We then investigated, if downregulation of CANT1 influences the tumorigenic potential of prostate cancer cells. Indeed, CANT1 knockdown heavily impaired the function of PC-3 and LNCaP cells, both being characterized by high endogenous CANT1 protein levels. It was shown that suppression of CANT1 expression slowed down propagation of LNCaP and PC-3 cells, which was caused by a decreased cell proliferation as demonstrated by DNA synthesis rate measurement. The reduction of DNA synthesis rate was strikingly stronger than the reduction of cell number, which probably was a consequence of the experimental setup. Cell counting is an endpoint measurement, which includes the establishment phase of the knockdown. In contrast, determination of DNA synthesis rate is a snap-shot measurement at the time point when knockdown is most efficient. Cell cycle distribution analysis revealed that lower proliferation rate in turn was caused by an arrest in G1-phase. Since DNA synthesis takes place during the S-phase [170], changes in BrdU incorporation should be reflected in changes in the amounts of cells that are in S-phase according to cell cycle analysis. Actually, upon CANT1 knockdown the decrease of S-phase cells was only minimally stronger than the decrease of BrdU incorporation in both cell lines. Additionally, a decreased motility of both cell lines upon CANT1 downregulation was observed in the transmigration assay, which could be verified for PC-3 cells in the scratch wound assay. Thus, in prostate cancer cells,

haptotactic cell migration towards fibronectin, which is part of the extracellular matrix [171], as well as migration on a non-coated surface is influenced by CANT1 expression.
In most of the assays, the effect of CANT1 knockdown was stronger in PC-3 cells than in LNCaP cells and in both cell lines the effect of transfection with siRNA #1 was stronger than the effect using siRNA #2, which was consistent with the efficiency of CANT1 downregulation in the respective samples. This dose-dependency underlines the specificity of the observed inhibition of cell proliferation and migration being actually related to a decrease of CANT1 expression.

To analyze, if CANT1 has any transforming capacities, the prostate epithelial cell line RWPE-1, which expresses low CANT1 protein levels, was transfected with a CANT1 vector. The analysis of cell proliferation rate via DNA synthesis rate measurement as well as the analysis of cell migration rate in a transmigration assay revealed no changes upon CANT1 overexpression. Despite an extremely high expression of CANT1 protein, similar results were obtained in transfected HEK-293 cells that as well are benign and endogenously express low CANT1 protein but that are derived from embryonic kidney instead of prostate. We next tested, if upregulation of CANT1 leads to enhanced *in vitro* tumorigenicity of prostate cancer cell lines. This was not the case for DU-145 cells that are characterized by very low CANT1 protein levels. Similarly, proliferation and migration rates of PC-3 cells that endogenously express abundant CANT1 protein remained constant upon further enhancement of CANT1 expression although *in vitro* tumorigenicity was strongly reduced upon CANT1 knockdown. To elucidate if the effects of CANT1 knockdown could be rescued by restoration of CANT1 expression, PC-3 cells were consecutively transfected with CANT1 siRNA and a CANT1-encoding vector. While endogenous mRNA levels of CANT1 were successfully restored, rescue on protein level failed. This was probably due to the potent effect of the siRNA which not only induces mRNA degradation but also translation inhibition. Because of the failed protein re-expression the effects of siRNA transfection were not reversed.

Altogether, these cell culture studies show that CANT1 downregulation strongly impairs cell proliferation and migration. However, CANT1 overexpression alone is not sufficient to induce or enhance *in vitro* tumorigenicity independent of the endogenous levels of CANT1 protein, the malignancy status and the prostatic origin of the cells. Accordingly, CANT1 appears not to be a driver of prostate cancer initiation, rather, CANT1 upregulation might be a consequence. Still, presence of CANT1 is essential to sustain cancer cell proliferation and migration. Especially in PC-3 cells, which were employed in CANT1 knockdown as well as in overexpression studies, it became clear that this effect of CANT1 expression is saturable. In conclusion, CANT1 appears to be relevant for the maintenance of prostate carcinomas.

### 5.1.3 Characterization of CANT1

The questions arise, what leads to CANT1 upregulation during carcinogenesis and what is the reason for CANT1 decline in CRPC? Which mechanisms underly the diminished tumorigenic potential of prostate cancer cell lines upon CANT1 knockdown? Why does the overexpression of CANT1 not induce an increase of *in vitro* tumorigenicity of prostatic cell lines? To answer these questions, knowledge about CANT1 protein and its cellular function would be helpful. Therefore, we characterized CANT1 protein, its glycosylation status and its localization within the cell and beyond (secretion).

We and others detected multiple bands in Western Blot analyses using CANT1 antibody [60, 62]. Possible explanations for this observation are glycosylation, usage of different start codons, splicing or other post-translational modifications. Smith *et al.* demonstrated that human CANT1, which is transfected into COS-1 cells, is N-glycosylated. However, since after PNGase F treatment two bands still remained visible, they concluded that other modifications are also involved [60]. To investigate if endogenously expressed CANT1 is also N-glycosylated, lysates of LNCaP and PC-3 cells were treated with PNGase F. Confirming the data of Smith *et al.* a double band was detected before and after treatment with a molecular weight difference of ~2 kDa.

Smith *et al.* further reported that nucleotidase activity was detected in the supernatant of COS-1 cells, indicating secretion of CANT1. Correspondingly, a cleavable signal peptide was identified (**Fig. 61**), whose truncation would result in a secreted protein of 333 amino acids. Confirming this prediction, Western Blot analysis detected a band in cell supernatants that was shifted by 2 kDa compared to cell lysates [60]. In contrast, upon transfection of the rat homolog of CANT1 into CHO cells, no CANT1 protein was detected in the supernatants. Rather, colocalization of the full-length protein including the predicted transmembrane domain with the ER resident protein calnexin was observed. In concordance, an RXR (amino acid 38-42 RFRPR, **Fig. 61**) ER-retention motif was identified in all vertebrate CANT1 homologs [62]. These amino acids are situated between both hydrophobic stretches. Thus, independent of the membrane topology this motif is located in the cytoplasmic domain of CANT1 as it was described also for other proteins with RXR ER-retention motif [172-174]. However, it was observed that these amino acids are only recognized in a certain distance to the membrane [175, 176]. In CANT1, this motif is only two and three amino acids away from the strong and weak hydrophobic stretch, respectively (**Fig. 61**), and is thus unlikely to be functional.

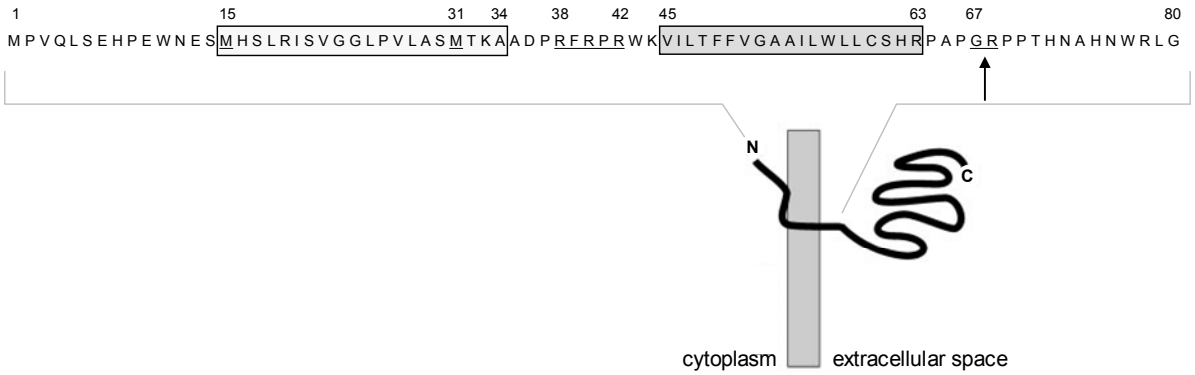


**Fig. 61 CANT1 membrane topology and the sequence of the N-terminus.**

The preferred model of CANT1 membrane topology (type II) is displayed together with the N-terminal amino acids 1 to 80. The weak and the strong hydrophobic stretch are framed and the strong hydrophobic stretch, which corresponds to the transmembrane domain in this model, is highlighted in grey. The alternative start codons (M), the RXR ER-retention motif (RFRPR) and the signal peptidase sequence (GR) are underlined, the cleavage site is further marked with an arrow. The numbers of the important amino acids are given above the sequence. Modified from [62]. N = N-terminus, C = C-terminus.

Here, both options were examined by analysing cell culture supernatants via precipitation and ELISA and by immunofluorescence of human tissue and cell lines.

The double immunofluorescence stainings clearly indicate a Golgi localization of CANT1 in normal prostate epithelium and prostate cancer as well as in LNCaP and PC-3 cells. Moreover, the diffuse cytoplasmic CANT1 staining, which was observed in the immunofluorescence and immunohistochemical stainings of prostatic tissue, might indicate additional ER localization.

In confirmation of Smith *et al.* [60] we further demonstrated secretion of a truncated form of CANT1 in wildtype CANT1 positive cells applying Western Blot analysis to precipitates. Secretion was further confirmed in an ELISA-assay. Analysis of ultracentrifuged supernatants that are devoid of vesicles demonstrated that this secreted form of CANT1 is soluble. Interestingly, the CANT1 band in supernatants was clearly singular. This indicates that the part of the protein, which is responsible for the modification that results in multiple Western Blot bands, is located N-terminal to the truncation side. This “responsible part” could either be the alternative start codons (amino acids 15 and 31) or amino acids that get glycosylated or otherwise modified post-translationally. According to computational analyses, the only predicted modification site N-terminal to the signal peptidase sequence is a phosphorylation site [60]. Following long exposition of the X-ray film, this truncated band was also detectable in the cell lysate of LNCaP cells. This argues that truncation of CANT1 takes already place in the ER or Golgi apparatus and export from the cell occurs via vesicles, which might be the source of this lower molecular weight band. Further, CANT1 containing vesicles represent another explanation for the diffuse cytoplasmic immunoreactivity that was observed in the

tissue stainings. Additionally, a full-length CANT1 band was detected in the ultracentrifugation pellet of PC-3 cells. As the strong shorter band in the precipitate of ultracentrifuged supernatant shows that secreted CANT1 is soluble, this signal in the pellet is probably derived from cell debris. Together, these observations support the signal peptidase model suggested by Smith *et al.* [60].

Irrespective of the function of secreted CANT1, we analyzed the applicability of this observation to construct a novel diagnostic serum test. In contrast to one predecessor, who failed to detect CANT1 in human sera by Western Blot analysis [61], we were able to do so using a newly constructed sandwich ELISA assay. In accordance with the overexpression of CANT1 in prostate carcinomas, higher CANT1-levels were measured in patient sera compared to age matched healthy individuals, although, statistical significance was not reached. Unfortunately, serum levels of CANT1 were in the range of the lower detection threshold of the assay (detection range from 0.1 to 20 µg/ml), which precluded exact quantification. Therfore, further assay optimization is needed before the value of serum CANT1 as routine diagnostic biomarker can be determined.

Summarizing the experiments for further characterization of CANT1, it was shown that endogenous CANT1 is glycosylated, is mainly localized in the Golgi apparatus and gets secreted in a truncated, soluble form. Although the clarification of post-translational modifications and the possible ER localization could not be completed, these findings add important information to the elucidation of the cellular function of CANT1.
Further, serum CANT1 is suggested as novel non-invasive biomarker candidate for prostate cancer diagnosis, which ought to be considered in future research.

### 5.1.4 The cellular function of CANT1

Having further characterized CANT1 protein, we aimed at determining its cellular function. So far, CANT1 was suggested to induce expression of nuclear factor kappa-light-chain-enhancer of activated B cells (NFκB) and mitogen-activated protein kinase (MAPK) and to be involved in protein glycosylation [62, 68, 80]. However, little experimental evidence to support these hypotheses exists.

#### 5.1.4.1 The involvement of CANT1 in protein glycosylation

As mentioned before in chapter 4.1.4, CANT1 is speculated to be an important player in protein glycosylation [62, 68, 80]. In more detail, in its function as NDP-hydrolase, CANT1 is suggested to be required for a continuous import of NDP-sugars into the ER or Golgi apparatus. The proposed mechanism is that CANT1 hydrolyzes NDP, which is a cleavage by-product after transfer of the sugar to the glycosylated protein, and thus promotes protein

glycosylation in two ways: Firstly, the NDP, which inhibits glycosyltransferases, is removed. Secondly, the corresponding NMP drives antiporters that exchange one NMP for one NDP-sugar molecule. Hence, product inhibition of the transferases is prevented and sugar supply is assured [62, 68, 177].

In this function, CANT1 may play a role either in glycoprotein or proteoglycan synthesis or protein folding, depending on its intracellular localization. Glycoprotein synthesis takes place in the ER and in the Golgi apparatus, but only in the Golgi apparatus nucleotides serve as sugar donors [156]. Nucleotides are also the sugar donors during proteoglycan synthesis which takes solely place in the Golgi apparatus [161]. These donor nucleotides are UDP, GDP and CMP, whereof UDP and GDP are the major potential targets of CANT1 according to nucleotidase activity measurements [60-62]. The crucial step during the protein folding process, where nucleotides (UDP) play a role, is the reglucosylation of misfolded proteins in the ER [159].

Thus, if CANT1 is located in the ER, it might be important for protein folding, whereas Golgi apparatus localization would imply involvement in glycoprotein or proteoglycan synthesis. The same holds true for NTPDase5, which was shown to hydrolyze UDP and to be located in the ER [177]. However, since Fang *et al.* demonstrated an involvement of NTPDase5 in protein folding as well as in glycoprotein synthesis [167], one has to assume that this enzyme is also expressed in the Golgi apparatus.

#### *5.1.4.1.1 The involvement of CANT1 in glycoprotein synthesis*

Immunohistochemistry as well as immunofluorescence of human tissue and cell blocks revealed CANT1 to be mainly localized in the Golgi apparatus. Therefore, it was planned to analyze the glycoprotein pattern of CANT1 knockdown cells by Western Blot analysis using the lectin Phaseolus vulgaris Erythoragglutinin (PHA-E), which specifically binds to complex-type N-glycans [178]. As positive control, LNCaP and PC-3 cells were treated with tunicamycin, which inhibits synthesis of the core oligosaccharide [169]. Thus, no N-glycosylation can take place and the bands that are stained by PHA-E are expected to be weaker. As this was not clearly the case, these experiments had to be cancelled and the question if CANT1 is involved in glycoprotein synthesis cannot be unambiguously answered in this experimental setup. Disturbance of glycoprotein synthesis would have broad-ranging effects that would probably include inhibition of cell proliferation and migration.

#### *5.1.4.1.2 The involvement of CANT1 in proteoglycan synthesis*

Two observations from the analysis of the *C.elegans* homolog of CANT1, apy-1, and patients that suffer from Desbuquois dysplasia, which was shown to be caused by CANT1 mutations, support an involvement of CANT1 in proteoglycan synthesis. Apy-1 loss-of-function worm mutants display pharyngeal alterations resembling mutants defective in proteoglycan

synthesis [68] and bone specimens of Desbuquois dysplasia patients are characterized by a decreased amount of proteoglycans [79]. An impaired proteoglycan synthesis upon CANT1 downregulation could imply a miscomposed extracellular matrix and thus affect cell motility.

#### *5.1.4.1.3 The involvement of CANT1 in the UPR*

Since we speculate that the origin of the additional cytoplasmic immunoreactivity in immunohistochemical and immunofluorescent stainings of prostatic tissue samples may be derived from ER-located CANT1, the involvement of CANT1 in the UPR was addressed.

Before, a possible redundancy between CANT1 and the known ER-UDPase NTPDase5 was examined by expression analyses in mutual knockdown cells. In LNCaP cells, no changes of CANT1 or NTPDase5 expression levels were seen. However, in PC-3 cells a strong statistical trend for increased NTPDase5 transcription was revealed in CANT1 knockdown cells. Vice versa, average CANT1 mRNA levels were slightly augmented in NTPDase5 knockdown cells compared to control cells. In both cases no changes in protein levels were observed. Steady-state CANT1 as well as NTPDase5 [167] levels are very high in LNCaP cells. Reduction of this basic protein amount by 2/3 is apparently not enough to induce expression of the second apyrase. In contrast, basic expression of NTPDase5 is very low in PC-3 cells [167]. Hence, CANT1 knockdown, which was nearly complete, strongly decreased the total amounts of UDPases in the ER. The consequently strong upregulation of NTPDase5 mRNA indicates redundant function of these two apyrases and supports an involvement of CANT1 in the UPR as it was shown for NTPDase5 [167]. Besides ADP-hydrolysis in the blood by human NTPDase1 and bed bug apyrase [72, 73], this would be another example of analogous function of the two apyrase families.

Next, the role of CANT1 in the UPR was investigated. We pursued a similar approach as Uccelletti *et al.* applied to analyze apy-1 function in *C.elegans* [68]. First, activation of the UPR following CANT1 and NTPDase5 knockdown was analyzed by expression analyses of established UPR target genes. As positive control for the readout, LNCaP and PC-3 cells were treated with chemical inducers of the UPR, which resulted in strong increase of HSPA5 mRNA and protein levels as well as TRIB3 and Herpud1 mRNA levels. Application of this sensitive readout to CANT1 and/or NTPDase5 knockdown LNCaP cells revealed no activation of the UPR contrasting the observations of Fang *et al.* [167]. Similar to the observations concerning redundancy of CANT1 and NTPDase5, the knockdown might not have been strong enough to activate the UPR. However, in PC-3 cells specific changes were detected. Upon CANT1 knockdown, TRIB3 mRNA was significantly upregulated, a trend was seen for Herpud1 induction. NTPDase5 single knockdown resulted in significantly augmented HSPA5 mRNA levels and tended to increase Herpud1 mRNA. Augmented mRNA levels of HSPA5 and Herpud1 were also observed following double knockdown of both proteins, accompanied by enhanced expression of HSPA5 protein. These data indicate

involvement of both proteins in the UPR, thus partly confirming the results of Fang *et al.* [167]. However, concerning redundancy of CANT1 and NTPDase5 our data are not entirely conclusive. Knockdown of CANT1 and NTPDase5 was needed to induce elevated expression of HSPA5 protein supporting a redundancy. Yet, TRIB3 expression was unaffected in the double knockdown cells and no additive effect was seen on Herpud1 upregulation upon downregulation of both apyrases. Further, in comparison to the positive control, the observed upregulation of UPR target genes upon CANT1 and NTPDase5 knockdown were minimal. Thus, these two proteins do not seem to be essential for protein folding. Possibly, the sequence on chromosome 6, which is as well homologous to the bed bug apyrase [60], codes for a third hitherto unknown ER-UDPase that cooperates with CANT1 and NTPDase5 to regulate protein folding.

In a second approach, CANT1 expression was measured during chemically induced UPR. In the benign RWPE-1 cells with low endogenous CANT1 levels, the total amount of the protein further decreased after 24 h of treatment consistent with a general translation inhibition during UPR. In contrast, increased mRNA levels were detected at the beginning similar to Herpud1. In the malignant DU-145 cells with similarly low endogenous CANT1 levels, the total amount of the protein was as well decreased during the whole kinetics, while mRNA expression was not affected by any treatment. Finally, CANT1 protein expression was also reduced upon ER stress induction in the malignant cell line PC-3 with high endogenous CANT1 levels. In contrast, CANT1 mRNA expression increased over time during thapsigargin and tunicamycin treatment and was also elevated 48 h after ethanol and especially DMSO treatment, similar to the selected known UPR target genes. In conclusion, DU-145 cells generally do not depend on CANT1 expression, regardless of the treatment. However, the striking similarity of CANT1 mRNA expression pattern with that of established UPR target genes in RWPE-1 and PC-3 cells suggests CANT1 to be a novel cell-type-specific UPR target gene. In RWPE-1 cells the changes on protein level were either too little to be detectable by Western Blot analysis or the time point was missed. In PC-3 cells, CANT1 mRNA levels were increasing towards the end of the experiment, maybe this would have been reflected on protein levels at later time points. Indeed, in one experiment upregulation of the CANT1 protein was observed after 48 h.

Together, these results indicate that CANT1 plays a role in protein folding, which is supported by further published observations. As already mentioned in chapter 4.1.4, apy-1 is induced upon ER stress triggered by tunicamycin or high temperature and knockdown of apy-1 leads to constitutive activation of the UPR only in the presence of functional ER stress sensors [68]. Furthermore, in patients suffering from Desbuquois dysplasia [179], inclusion bodies were detected in distended rough ER [70], which might be a hint for impaired protein folding and subsequent accumulation of misfolded proteins. A similar skeletal dysplasia was

shown to be caused by a functional defect in a nucleotide sugar transporter [180, 181], which is also involved in sugar supply of the ER and Golgi apparatus, as explained in the chapters 1.6.5 and 4.1.4. Hence, by interfering with protein folding, CANT1 knockdown possibly causes the disruption of various cellular processes, amongst others cell proliferation and migration. It is tempting to speculate that this explains the significantly reduced rate of proliferation and migration, which we observed in prostate cancer cell lines upon knockdown of CANT1. Since ATP is needed to rephosphorylate the UMP in the cytoplasm to UDP before a sugar molecule can be added and imported into the ER, NTPDase5 was shown to promote ATP consumption, lower the ATP/AMP ratio and thus to increase glucose uptake, glycolysis and provision of intermediates for biomass production and thereby to finally support cell proliferation [167, 182]. This might be the mechanism underlying the prostate cancer promoting function, which was already assigned repeatedly to NTPDase5. In 2007, it was shown that NTPDase5 is upregulated in PIN lesions and prostate carcinomas similar to CANT1. Knockdown in LNCaP cells decreased collagen I expression and invasiveness, contrary reactions were detected in PC-3 cells upon overexpression of the protein [183]. Later, NTPDase5 knockdown was shown to increase the sensitivity to cisplatin, which was caused by decreased B-cell leukemia/lymphoma 2 (Bcl2) phosphorylation. [184]. Finally, Fang *et al.* were able to stop progression of LNCaP-derived carcinomas by NTPDase5 knockdown in mice [167]. These signaling pathways should also be analyzed in CANT1 knockdown cells in the future.

Having shown that CANT1 mRNA is upregulated following ER stress induction, the promoter region of CANT1 was analyzed. However, no corresponding ER-stress response element (ERSE) or ERSE II [185, 186] were identified.

Besides general translation inhibition and upregulation of proteins that assist protein folding or degradation, cell cycle arrest in the G1-phase is another feature of the UPR [187]. Thus, G1-arrest, which was observed upon CANT1 knockdown in LNCaP and especially in PC-3 cells, adds further evidence to the putative involvement of CANT1 in protein folding and the UPR.

An impaired protein folding following CANT1 knockdown together with general translation inhibition in the context of consequently activated UPR could be another reason for the failed rescue of CANT1 protein expression by CANT1 vector transfection in knockdown PC-3 cells although mRNA was successfully re-expressed.

#### *5.1.4.1.4 The role of the UPR in solid tumors*

Solid tumors commonly encounter stressful conditions as hypoxia, nutrient starvation, acidosis, disturbance of calcium homeostasis and misfolded mutated proteins. Consequently, UPR activation has been detected in various tumor entities. Amongst others, increased

expression levels of HSPA5, XBP1 or ATF6 were observed in HCC, breast, colon, gastric and esophagal carcinomas. Consisting with these human expression data, overexpression of HSPA5 and XBP1 has been shown to act tumor-promoting in mouse models. In contrary, suppression of XBP1 and PERK expression inhibited tumor development in animals. However, besides cell-protective effects, UPR elicits also cell-destructive pathways. Especially long-term activation of the UPR results in apoptosis. Thus, different mechanisms are conceivable for the tumor to avoid UPR-induced apoptosis. Either simultaneous disruption of the apoptotic machinery is sufficient to inhibit cell death induction, or the tumor cells activate specifically the cell-protective pathways of the UPR, or the tumor cell inhibits UPR instead of activating the stress response. Activation of single UPR branches has so far only been demonstrated in B-cells (reviewed in [188-191]). Evidence for UPR inhibition was claimed in mouse prostate cancer models. Indeed, ATF4, ATF6, HSPA5 and Herpud1 were downregulated in HGPIN, but the expression levels of PERK, XBP1, IRE1 and HSPA5 were either unchanged or increased in HGPIN or prostate cancer. In human prostate carcinomas, HSPA5 was reported to be upregulated several times, especially in CRPC [192-194]. Thus, the role of the UPR branches in prostate cancer needs to be elucidated in detail. Our data about CANT1 suggest at least activation of certain UPR target genes.

#### 5.1.4.2 The function of secreted CANT1

The function of truncated CANT1, which was detected in cell culture supernatant by Western Blot analysis and ELISA, is currently unknown. Since soluble CANT1 is still enzymatically functional [60, 61, 77], it is conceivable that it is involved in the regulation of pyrimidinergic signaling of UDP and UTP. These extracellular nucleotides activate the cell-surface G-protein coupled receptors $P2Y_2$, $P2Y_4$ and $P2Y_6$, which stimulate Phospholipase (PL) Cβ. PLCβ-induced cleavage of phosphatidylinositol bisphosphate ($PIP_2$) into diacylglycerol (DAG) and inositol tri-phosphate ($IP_3$) finally triggers intracellular calcium release mainly from the ER (reviewed in [195]). Via calcium/calmodulin and calcium/calmodulin dependent kinases, a complex, cell-type-specific signaling involving phosphorylation cascades and gene transcription is then initiated [196], which would be prevented by the degradation of UDP and UTP by CANT1. Moreover, it has been reported recently that $IP_3$-mediated calcium release is increased during ER stress [197]. Hence, by hydrolyzing extracellular UDP and UTP and thus preventing calcium release from the ER, soluble CANT1 may support intracellular CANT1 in coping with ER stress. It is tempting to speculate that upon ER stress induction CANT1 expression is increased and newly synthesized CANT1 is secreted to inhibit calcium release from the ER. Consequently, CANT1 mRNA would be increased while simultaneously intracellular CANT1 protein levels would not change or even decrease because of enhanced

secretion of the protein. Increased CANT1 mRNA but decreased CANT1 protein levels were indeed observed upon thapsigargin and tunicamycin treatment of RWPE-1 and PC-3 cells, decreased protein levels were additionally detected in DU-145 cells.

#### 5.1.4.3 CANT1 as NFκB and MAPK inducing gene

A study looking for novel genes that activate MAPK and NFκB signaling offers another approach to explain the missing link between CANT1 knockdown and decreased cell proliferation and migration. A cDNA library was transfected into HEK293 cells and luciferase-activity of two reporter constructs, either containing a promoter with an NFκB- binding site or a promoter of a MAPK target gene, was measured. Upon transfection with a cDNA clone that contained parts of the CANT1 sequence, expression of the reporter constructs increased 19- or 15-fold, respectively, indicating that CANT1 activates both pathways, which are frequently deregulated in tumorigenesis, including prostate cancer [198-202]. In the NFκB-inducing clone, the first 100 amino acids of the CANT1 sequence including the putative ER-retention signal and the transmembrane domain were missing. However, to prove biological relevance of the NFκB-induction, the cells were simultaneously transfected with dominant-negative mutant of IκB kinase β. This kinase phosphorylates inhibitor of kappa B (IκB), which subsequently gets ubiquitinated and thus releases NFκB, which can then enter the nucleus [196]. The luciferase signal remained stable in this case, which demonstrated that CANT1 acts upstream of IκB kinase β. Since NFκB is activated in the course of the UPR, a link to CANT1 is reasonable. The MAPK activating clone encoded the first 219 amino acids of CANT1, however nearly half of the protein was missing, giving rise to doubts if full-length CANT1 is also able to activate MAPK [203].

#### 5.1.4.4 A model of CANT1's cellular function

Collectively, involvement of CANT1 in glycoprotein and proteoglycan synthesis, protein folding or NFκB, MAPK or pyrimidinergic signaling was proposed. Activation of NFκB and MAPK signaling was only detected in a screen with sequence fragments of CANT1 [203], a confirmation with full-length protein is lacking. Participation of CANT1 in pyrimidinergic signaling or glycoprotein synthesis was considered because of its enzymatic function in combination with the ascertained secretion or Golgi localization, respectively, but was not substantiated experimentally so far. Concerning proteoglycan synthesis, supportive observations were reported from *C.elegans* and Desbuquois dysplasia patients [68, 79]. Yet, experimental evidence was only demonstrated for protein folding. Additionally to previous analyses in *C.elegans* [68], we showed partially significant upregulation of established UPR target genes upon CANT1 knockdown accompanied by G1-arrest in PC-3 cells and an increase of CANT1 mRNA in a similar pattern as UPR target genes upon ER stress induction in RWPE-1 and PC-3 cells. These data are substantiated by matching cellular changes in the

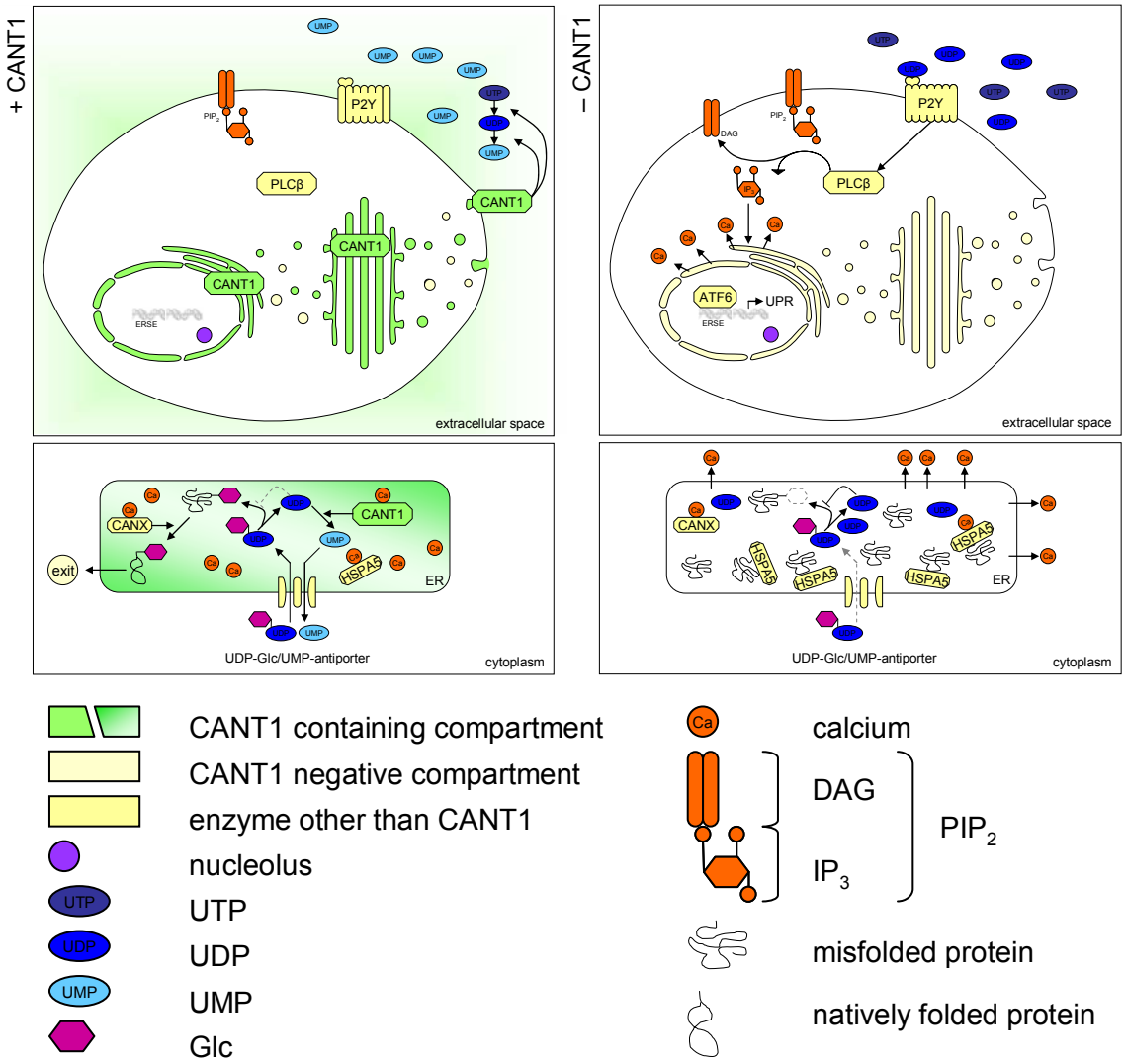


**Fig. 62 A hypothetical model of CANT1's cellular function.**

In a CANT1 positive cell (upper left), CANT1 is localized in the ER and is secreted via the Golgi apparatus and vesicles. Soluble CANT1 hydrolyzes UTP and UDP to UMP and inorganic phosphate [60, 61, 77]. Through degradation of extracellular UTP and UDP, pyrimidinergic signaling is interrupted [195]. In the ER (lower left) CANT1, whose enzymatic activity is calcium dependent [60, 61] similar to other ER proteins, hydrolyzes UDP, which is a by-product of reglucosylation of misfolded proteins, to UMP and inorganic phosphate [157]. By degradation of UDP, product inhibition of UGGT is prevented [62, 68, 177]. The resulting UMP is exchanged for another UDP-Glc via the corresponding antiporter [163]. The reglucosylated protein is recognized by calnexin or calreticulin, which assist folding. After successful folding, the native protein can exit the ER [157].

In a CANT1 negative cell (upper right) no soluble CANT1 exists in the extracellular space to degrade UTP and UDP. Thus, pyrimidinergic signaling is active. The P2Y receptor activates PLCβ, which cleaves $PIP_2$ into DAG and $IP_3$. The latter intracellular signaling molecule triggers calcium release from the ER [195], which impairs the function of several ER proteins. Addtionally, UDP accumulates in the ER (lower right) because it is not hydrolyzed by CANT1. This inhibits UGGT, so that no Glc can be transferred to misfolded proteins [62, 68, 177]. Hence, these are not recognized by calnexin or calreticulin [157]. Further, no UDP-Glc molecules can be imported into the ER due to missing UMP, which drives the antiporter [163]. The consequent accumulation of misfolded proteins induces the UPR. The transcription factors ATF4, ATF6 and XBP1 are activated and promote transcription of UPR target genes, whose promoters contain special sequences, for example ERSE elements. Amongst others HSPA5 expression is increased [160]. CANX = calnexin.

bones of Desbuquois dysplasia patients [70]. A prerequisite for a nucleotidase to be involved in protein folding however is localization in the ER [159], which could neither be convincingly demonstrated nor excluded for CANT1. The fact that CANT1 overexpression in contrast to knockdown does not influence cell proliferation or migration indicates that the amount of CANT1 protein is tightly regulated and its function is saturable. Combining all observations from the current study with previous results, we propose a hypothetical model for CANT1's cellular function, which suggests an interplay between intracellular and secreted CANT1 (**Fig. 62**).

To completely elucidate CANT1's cellular function, the mode of secretion and the relevance of CANT1 in pyrimidinergic, NFκB and MAPK signaling as well as in glycoprotein and proteoglycan synthesis ought to be clarified in future studies.

### 5.1.5 Conclusion about the role of CANT1 in prostate cancer

This study is the first to depict a functional relevance of the apyrase CANT1 in a human neoplasia. CANT1 expression is ubiquitously increased not only in primary prostate carcinomas, but also in the precursor lesion PIN. Further, CANT1 is essential for maintaining tumorigenic potential. Thus, although CANT1 overexpression does not actively induce or increase *in vitro* tumorigenicity, CANT1 upregulation seems to be an important event during prostate cancer initiation and primary prostate carcinomas rely on CANT1 expression. We added further evidence to the putative involvement of CANT1 in protein folding and thus propose that increased expression of CANT1 is a consequence of increased protein turnover within a cancer cell, which warrants higher folding capacity to avoid accumulation of misfolded proteins (**Fig. 62**). Augmented CANT1 mRNA levels following chemical ER stress induction suggests active induction of CANT1 expression rather than passive upregulation by selection for cells with high CANT1 levels.

Given the proposed importance of CANT1 expression in prostate cancer cells for the reduction of ER stress, it appears illogical that progression to castration-resistance is accompanied by a loss of CANT1. Thus, the mechanisms behind this as well as the consequences for the CRPC need to be clarified in future studies.

Clinically, the good prognosis for patients with very high CANT1 protein levels, who barely experience disease progression, is maintained in multivariate analysis. Thus, CANT1 is a novel independent prognostic factor for prostate cancer. Yet, on account of the virtually equally intensive upregulation in PIN, CANT1 is not recommended as a diagnostic tool for the surgical pathologist.

## *5.2 The role of FOXA1 in prostate cancer*

### 5.2.1 Expression, relationship to clinicopathological parameters and survival analysis of FOXA1 in human prostatic tissue

To my knowledge, this study is the largest yet to analyze the role of FOXA1 in prostate tissues including benign tissue, a large set of clinically characterized primary prostate cancer cases, metastases and for the first time advanced CRPC. In general, FOXA1 immunoreactivity was mainly detected in nuclei, which was expected as FOXA1 is a transcription factor that was not described to cycle in and out of the nucleus as it is for example the case for AR [36]. Only in strongly stained cases, additional weak cytoplasmic staining was observed, which is either unspecific immunoreactivity or derived from newly synthesized FOXA1 molecules that have not yet been imported into the nucleus.

Paradoxically, the overexpression of FOXA1 in tumor tissue in comparison to normal tissue, which was found on RNA level before [15], could not be confirmed. Rather, we report similar expression levels of FOXA1 in normal epithelium and primary carcinomas. Actually, at first analysis of the TMA, lower FOXA1 expression in benign tissue (mean staining intensity: 1.48) compared to prostate cancer tissue was found. Further, a high variability of FOXA1 expression levels in benign tissue was noted. During the consequently performed re-analysis of the cases, it turned out that the zonal origin of the benign tissue determines FOXA1 expression levels. Tissue cores from the transitional zone, where BPH occurs, showed very low levels of FOXA1 whereas tissue cores from the peripheral zones, where primary carcinomas mostly arise, showed levels comparable to those of primary carcinomas. Many of the benign cases that were included on this TMA as well as in the previous gene array study [15], which was the basis of this work, were derived from BPH, which resolves the apparent discrepancy between our results of FOXA1 mRNA and protein expression in normal and prostate cancer. Hence, we decided to evaluate the staining intensity of adjacent normal tissue, which was present in nearly every core of primary carcinomas, instead of the BPH cores. To support the zonal model of FOXA1 expression, twelve additional RPE specimens with transitional zone carcinomas were included and indeed very low FOXA1 expression was noticed, comparable to the expression levels of the adjacent transitional zone glands. Thus, it was confirmed that FOXA1 expression does not increase during tumor initiation, which was already reported before by Mirosevich *et al.*, who probably used normal and cancerous tissue from the peripheral zone to compare FOXA1 expression levels [109]. Similar results were obtained in mouse models of prostate cancer [204, 205]. However, one study analyzing FOXA1 expression in mouse models reported a consistent upregulation of FOXA1 in PIN and prostate adenocarcinoma [109].

In concordance with the first study that dealt with FOXA1 expression in prostate cancer tissues so far [110], we found an upregulation of the protein between primary carcinomas and metastases. As this upregulation of FOXA1 was also indicated in the 27 CRPC cases that were included in the TMA (mean staining intensity 2.19), additional 24 cases were included from the archives to substantiate this interesting finding. Thus, in a cohort of together 51 cases, strong FOXA1 expression in the group of CRPC, which have not been looked at so far, was demonstrated.
A growing stock of literature underscores the importance of FOXA1 in human neoplasia. Gene amplification and protein overexpression were observed in Barrett's and lung adenocarcinomas [206, 207].

Higher levels of FOXA1 in prostate cancer metastases and CRPC than in primary carcinomas indicate a role of the protein in prostate cancer progression. Accordingly, FOXA1 correlates positively to conventional parameters of tumor progression, in particular higher Gleason scores and higher pT stages within the group of primary carcinomas. Although Jain *et al.* did not reveal correlations with these two parameters, they detected correlations with other progression parameters [110]. These results are reflected in a prognostic relevance, which we assigned to FOXA1 expression. High expression of the transcription factor in primary prostate carcinomas was associated with short times to PSA-relapse. This is in contrast to the prognostic value of FOXA1 in breast cancer, where a favourable prognosis has been related to high FOXA1 levels, particularly in estrogen receptor positive cases [208-211].

Main findings of the TMA-based analysis of FOXA1 staining intensity in different stages of prostate carcinoma development are a zonal dependence of FOXA1 expression in normal and tumor tissues, increasing FOXA1 levels with tumor progression with highest rates in CRPC and a prognostic value in primary tumors. The different expression levels of FOXA1 in the transitional and peripheral zone of the prostate underscore the importance to more accurately define the origins of normal tissue for comparative analyses. The more appropriate normal tissue to compare to peripheral zone prostate carcinomas ought to be normal tissue of the very same zone. This observation should be considered for future assembly of patient cohorts as well as for evaluation of existing studies.

### 5.2.2 Relationship between FOXA1 and steroid hormone receptors

Functional interactions between FOXA1 and ERα as well as AR have been reported before in breast and prostate cell lines and tissues [114-116, 125, 129, 130, 132, 133]. Therefore, AR and ERα and additionally ERβ were analyzed in parallel in this study. Close and significant correlation with FOXA1 was found for all three steroid hormone receptors, which

was strongest for AR. The coexpression of FOXA1 and AR could further be verified on single cell level by double immunofluorescence. A correlation with AR expression in prostate tissue was also found by Jain *et al.* [110], correlation with ERα expression was reported manifold in breast tissues, whereas a correlation between FOXA1 and ERβ is novel.

Coexpression of FOXA1 and AR was also reported in a subset of ERα negative breast carcinomas. In these cases FOXA1 expression was probably induced via heregulin and v-erb-b2 erythroblastic leukemia viral oncogene homolog (ERBB) 2. [212-214]. The consequences of FOXA1-AR-interaction on androgen-dependent gene transcription have been studied in detail for PSA: Gao *et al.* showed that mutations in the FOXA1 binding sites inhibit maximal androgen induction of PSA [115]. In contrast, Lee *et al.* observed that overexpression of FOXA1 reduced androgen induced PSA expression, probably by competition of FOXA1 and other transcriptional coactivators [133]. Further analyses including more androgen-regulated genes are required to unravel the relationship between FOXA1 and AR.
Further, this is the first study that demonstrated a prognostic value of FOXA1 in prostate cancer. Interestingly, the association between strong FOXA1 expression and shorter relapse free survival was particularly significant in the subgroup of primary prostate carcinomas with low (staining score 1) and moderate (staining score 2) AR expression levels. In contrast, relapse free survival did not depend on FOXA1 expression levels in the subgroup of carcinomas with high AR levels (staining score 3).
These findings might indicate that high AR expression promotes prostate cancer progression in a FOXA1 independent way, whereas in carcinomas with low AR expression, FOXA1 is needed to maintain AR signaling and thus to promote prostate cancer progression.

As mentioned in the introduction, estrogens were shown to be important for complete prostate cancer development. Treatment of rats with testosterone alone resulted in HGPIN in 40 % of the animals. Additional administration of estradiol led to the development of prostate carcinomas in nearly all treated animals. However, no HGPIN or neoplasias were detected in ERα knockout rats. Similarly, less carcinomas were detected in rats lacking aromatase, the enzyme that converts testosterone to estradiol. In line with these animal studies, expression of aromatase is augmented in human prostate carcinomas. Also, ERα expression rises from low-grade tumors via high-grade tumors to metastases and CRPC and high expression of ERα in prostate carcinomas is associated with progression. Consequently, treatment of HGPIN patients with the ERα antagonist toremifene led to a 50 % reduction of carcinoma development (reviewed in [40, 41]). By virtue of the strong correlation between FOXA1 and ERα in primary prostate carcinomas, FOXA1 is probably involved in the transcription of ERα

target genes, which mediate the above described effects of estrogen treatment. One potential target is the fusion gene TMPRSS2:ERG, which is frequently detected in prostate cancer, and was shown to be inducible by ERα agonists [41]. Although a transcription promoting interaction between FOXA1 and ERα was not yet examined in prostatic cells, it was convincingly demonstrated several times in breast cells [114, 125, 129, 130].

Since we identified FOXA1 as an unfavourable prognostic factor, the correlation between FOXA1 and ERβ expression contradicts the current assumption that ERβ is the “good” estrogen receptor in prostate cancer development. However, also other recent studies question this hypothesis. So far, four studies investigated expression of ERβ and association with aggressiveness in human prostate carcinomas. Three reported a general loss of ERβ mRNA and/or protein expression in prostate carcinomas [215-217], one of these revealed upregulation of ERβ in metastases [216]. The fourth study showed a decreased expression of ERβ in 40 % of HGPIN compared to normal tissue, high expression in hormone-dependent carcinomas and their metastases and again a loss of ERβ expression in CRPC [218]. Poor prognosis was associated with low [215] as well as with high [219, 220] ERβ expression.
Two cell culture studies dealing with the role of ERβ in prostate cancer cells, however support the theory of ERβ being the “good guy” as seen from the perspective of the patient. Induction of apoptosis and downregulation of the fusion protein TMPRSS2:ERG upon treatment with ERβ agonists were reported [221]. Further, it was shown that ERβ together with its ligand 3β-adiol maintains the epithelial phenotype and represses epithelial-mesenchymal transition. Conversely, ERβ expression was reduced upon epithelial-mesenchymal transition induction by TGFβ or hypoxia [222].
Analysis of ERβ expression in various independent patient cohorts is needed to clarify the role of this steroid hormone receptor in prostate cancer development.

In summary, FOXA1 expression strongly correlates with expression of AR, ERα and ERβ indicating that opening of the chromatin by FOXA1 might be important for transcription of steroid hormone receptor target genes in prostate carcinomas. The impact of FOXA1 interaction with steroid hormone receptors needs to be further elucidated. Survival analyses performed here added already one piece to that puzzle: FOXA1’s influence on progression free survival interestingly depends on the expression level of AR suggesting that the presence of FOXA1 is especially important for the survival of prostate cancer cells with lower amounts of AR.

### 5.2.3 Functional characterization of FOXA1 *in vitro*

The apparent connection between FOXA1 expression and prostate cancer progression prompted the question if FOXA1 can directly enhance tumorigenicity of prostate cancer cells. For this, expression of FOXA1 in prostatic cell lines was analyzed and *in vitro* experiments were set up in the same way as for CANT1 to study the influence of FOXA1 knockdown on cell migration and proliferation.

As for immunohistochemistry, an antibody that reacts with FOXA1 as well as FOXA2 was used for Western Blot analyses. Although RWPE-1 cells originate from the peripheral zone according to the information of the distributor, very little FOXA1 mRNA and no protein was detected, which contradicts TMA expression data. In accordance with the TMA data that were obtained from analysis of human tissue, strong expression was noticed in the metastatic cell line LNCaP and in the hormone-independent cell line PC-3. In addition, FOXA1 protein level is unexpectedly undetectable in the second hormone-independent cell line DU-145. The expression levels of FOXA1 mRNA clearly differed from these of FOXA1 protein, suggesting post-transcriptional regulation. Especially the comparison between these levels in PC-3 and DU-145 cells indicates suppression of FOXA1 protein expression in the latter cell line.
High levels of FOXA2 were detected in PC-3 and DU-145 cells, whereas expression of this transcription factor was low in RWPE-1 and LNCaP cells. Strong expression of both, FOXA1 and FOXA2, in PC-3 cells was already described before, as well as strong expression of FOXA1 in LNCaP. However, the previous expression analyses of these two proteins revealed absence of FOXA2 in DU-145 cells, contrasting our observation [109].

To further investigate FOXA1's role in prostate cancer, *in vitro* tumorigenicity assays were performed using wildtype and FOXA1 knockdown cells. These studies demonstrated that, similar to CANT1 knockdown, also FOXA1 knockdown slowed down propagation of LNCaP and PC-3 cells, which was caused by a reduced cell proliferation rate, which was in turn caused by an arrest in G1-phase as demonstrated by DNA synthesis rate measurement and cell cycle analysis. Also, a reduction of the S-phase cell population was observed in the cell cycle study. FOXA1 was shown before to promote expression of the negative cell cycle regulator p27 as well as of the cell cycle promoter cyclin D1 and thus suggested to balance cell proliferation and maintenance of differentiation [96]. Upon FOXA1 knockdown this balance is probably disrupted and other cell cycle arresting pathways are predominant.
Similar to our observations, strong expression of FOXA1 was also detected in ERBB2 positive breast cancer cell lines, which are a model of aggressive (ERBB2 positive) breast cancer. In these cells, knockdown of FOXA1 inhibited cell proliferation and promoted

response to trastuzumab (Herceptin) by induction of apoptosis [214]. In contrast, forced expression of FOXA1 in estrogen receptor-positive breast cancer cell lines inhibited clonal growth and FOXA1 expression levels correlated negatively with growth stimuli [208]. These results indicate different roles of FOXA1 in ERBB2- and estrogen receptor-positive breast cancer cells. Considering the proliferation promoting effect of FOXA1 expression, prostate cancer cells resemble more the ERBB2-positive breast cancer cells although a strong correlation between FOXA1 and estrogen receptor expression was demonstrated in parallel. Additionally, a decreased motility of both cell lines upon FOXA1 downregulation was observed in a haptotactic transmigration assay, which could be verified for PC-3 cells in the scratch wound assay.

Together, these data show an enhanced mitotic activity and augmented migration rates of prostate cancer cells with high FOXA1 levels and hence endorse a functional relevance of FOXA1 expression during progression of prostate carcinomas.

### 5.2.4 Is it FOXA1 or FOXA2, which is involved in prostate cancer progression?

One drawback of this study is the FOXA1-antibody, which was used for immunohistochemistry and Western Blot analyses, due to its crossreactivity with FOXA2. The cell culture studies were performed using FOXA1-specific siRNAs as confirmed by Western Blots analyses with this antibody. Therefore all effects that were observed upon FOXA1 knockdown were actually related to differences in FOXA1 expression levels. However, in immunohistochemistry, a distinction between immunoreactivity with FOXA1 or FOXA2 was not possible. Other groups that investigated FOXA2 expression in prostate cells, reported that FOXA2 is expressed in the prostate only during development [99], whereas in the urogenital tract of adult mice, FOXA2 was only detected in the epididymis [116]. One group detected FOXA2 in early PIN lesions [223], whereas expression of FOXA2 mostly in neuroendocrine carcinomas was shown repeatedly [109, 223, 224]. On our TMA, FOXA1/2 staining does not correlate with chromogranin, which is a strong marker of neuroendocrine differentiation, indicating that the FOXA2 signal is not predominant.
Mirosevich *et al.* speculated that FOXA2 is involved in the progression of prostate cancer to castration-resistance, because FOXA2 induced expression of androgen-dependent prostate-specific genes independent of AR and hormone [109]. Accordingly, an association between FOXA2 expression and the invasive type of prostate cancer was revealed [225] and FOXA2 expression was detected in some prostate carcinomas with high Gleason score [109]. Further supporting a relation between FOXA2 expression and castration-resistance, both hormone-independent cell lines that were analyzed in the here described work displayed strong FOXA2 expression.

Unfortunately, Jain *et al.*, who as well revealed a strong increase of FOXA1 expression in advanced prostate carcinomas, did not explicitly state if they used the FOXA1-specific antibody, which is meanwhile offered by Santa Cruz Biotechnologies, or the antibody that we were using. In any case, taking into account our definitely FOXA1-specific cell culture data and the absence of a correlation between FOXA1/2 staining and neuroendocrine differentiation, we are convinced that the upregulation of FOXA1/2 in metastases and CRPC, the prognostic value of FOXA1/2 expression and the resultant importance for prostate cancer progression is at least in part, if not mainly, caused by FOXA1 expression.

### 5.2.5 Conclusion about the role of FOXA1 in prostate cancer

Collectively, it emerges that the pioneer transcription factor FOXA1 is functionally relevant during the progression of prostate carcinomas from primary, hormone-dependent carcinomas to end-stage hormone-independent CRPC. This is probably mediated by the steroid hormone receptors ERα, ERβ and especially AR. Since carcinomas from the transitional zone showed invariably low FOXA1 expression, a FOXA1 independent development of this subtype of cancer can be assumed. Clinically, this study added another prognostic biomarker, although this was not maintained in multivariate analysis.

## 5.3 *The role of GOLM1 in prostate cancer*

### 5.3.1 Functional characterization of GOLM1 *in vitro*

Previously, our group showed that GOLM1 expression is stronger in primary prostate carcinomas compared to normal prostate epithelium, both on RNA and on protein level. In PIN lesions intermediate levels were detected [15, 16]. The analysis of GOLM1 expression in advanced carcinomas of the prostate is a matter of future research.

Another hitherto not pursued question is the functional relevance of GOLM1 overexpression in prostate cancer cells. To address this question, an expression analysis of GOLM1 in prostatic cell lines was conducted. Fitting to the expression data in human tissue, protein expression was detectable but low in the benign cell line RWPE-1. As no data for advanced carcinoma exist, the expression levels of GOLM1 in the metastatic cell lines, being high in the hormone-dependent cell line LNCaP as well as the hormone-independent cell line DU-145 and low in the second hormone-independent cell line PC-3, cannot be evaluated in comparison to tissue expression levels.

Next, a protocol to efficiently downregulate GOLM1 expression in LNCaP and DU-145 cells was established. In certain knockdown cells, cell proliferation or migration changed significantly in comparison to control cells. However, no consistent tendency for all three different GOLM1-specific siRNAs was observed in any of the conducted experiments.

Hence, despite of high expression differences on RNA and especially on protein level that were achieved between control and GOLM1 knockdown cells, *in vitro* tumorigenicity was not affected.

### 5.3.2 Conclusion about the role of GOLM1 in prostate cancer

Clinically, GOLM1 is a valuable diagnostic marker, which can be applied immuno-histochemically to tissue samples [16] as well as for non-invasive diagnosis of prostate cancer in the patients' urine [147, 149]. However, tumorbiologically it is unlikely that GOLM1 is functionally implicated in prostate cancer development, because neither an association with prognosis was found in the previous TMA-study of our group [16] nor a reduction of tumorigenicity was observed in *in vitro* assays. Thus, GOLM1 upregulation in primary prostate carcinomas is most probably a side-effect of tumor initiation without any functional relevance for the cancer cells. Still analyses of GOLM1 protein expression in advanced prostate carcinomas and of GOLM1 regulation in prostatic tissues are required.

## *5.4 The molecular biology of prostate cancer*

A major goal in the field of molecular biology of prostate cancer is to unravel the mechanisms of castration-resistance. A better knowledge of the underlying mechanisms is crucial for the development of more efficient therapies for end-stage carcinomas.

### 5.4.1 Gene and protein expression in prostate cancer

This study revealed the expression course of two proteins during prostate cancer initiation and progression. CANT1, whose expression had not been analyzed in any human neoplasia so far, was detected weakly in normal prostate epithelium. Its expression increased during tumor initiation and decreased again during progression to castration-resistance. The case-wise comparison of CANT1 expression in tumor glands with adjacent normal glands revealed an upregulation of the protein in the vast majority (97.2 %) of the cases.

FOXA1 expression was studied for the first time in a large cohort of prostate carcinomas including 51 CRPC cases. Being not affected during initiation of prostate cancer development, FOXA1 expression clearly increased in metastases and even more pronounced in CRPC.

Thus, in primary prostate carcinomas, the overexpression of the first candidate CANT1, which was identified within the initial gene array study [15], was confirmed, whereas

overexpression of the second candidate FOXA1 was contradicted. This discrepancy could be traced back to usage of tissue from different prostatic zones as benign control tissue. While the former study used samples from different zones of normal epithelium and primary carcinomas, samples from the same zonal origin were used in the current study. Thus, the finding that FOXA1 expression levels are similar in normal epithelium and primary carcinomas is correct.

### 5.4.2 Different ways to overcome castration

Following hormonal therapy most of the tumors regress initially, accompanied by a decline of serum PSA levels. However, after a certain period of quiescence, PSA levels rise again indicating relapse of the tumor, which is then castration-resistant. Various mechanisms have been described that enable the tumor to overcome androgen blockage. Frequently, the AR gene is amplified or mutated, which leads to overexpression or functional changes of the receptor. Overexpression allows the tumor cells to survive despite minimal extracellular androgen levels. Further, it was reported that overexpression of AR turns therapeutic antagonists into agonists. Treatment of cells with high AR levels with bicalutamide induces DNA binding of the AR, recruitment of coactivators and expression of target genes, while bicalutamide treatment of cells with low AR levels inhibits expression of androgen dependent genes. Various mutation variants of AR are known. These either can be activated by other endogenous steroids and antiandrogens, or have different binding characteristics to coactivators and corepressors, or lack the ligand binding domain and are constitutively active. The latter mutants cannot be targeted by any antiandrogens that interact with the ligand binding domain [226]. Further, AR can be activated independent of androgens via growth factor receptor signaling pathway, PKA pathway, interleukin (IL) 6 or bone-derived factors, for which the N-terminal domain of AR is important. Alternatively, ubiquitination of AR by RNF6 was reported, which results in modulation of the activity and specificity of the steroid hormone receptor. RNF6 was shown to be overexpressed selectively in CRPC and to promote prostate cancer cell growth especially under androgen depletion conditions [227]. Other resistence mechanisms involve upregulation of transcriptional AR coactivators or of androgen synthesis enzymes. Indeed, intratumoral testosterone concentrations were shown to be equal in primary tumors and CRPC (reviewed in [35, 38, 41], summarized in **Fig. 63**).
The novel agent EPI-001 that interacts with the N-terminal domain of AR is currently under investigation [226]. Great expectations are connected with this molecule, because it prevents transactivation of gene transcription independent of AR activation.
Given that FOXA1 is upregulated during establishment of castration-resistance and that FOXA1 epxression is needed for the progression of carcinomas with low and moderate AR expression levels in contrast to carcinomas with high AR expression levels, this thesis suggests expression of this transcription factor as a novel mechanism of castration-

resistance in the category of upregulation of coactivators (**Fig. 63**). This enables the cancer cells to sustain androgen signaling despite shortage of androgens. In the case of high AR expression, the additive support on transcription of androgen-regulated genes by FOXA1 is not needed.

One potential target gene is anterior gradient homolog (AGR) 2, whose regulation by androgens as well as by FOXA1 was demonstrated and which was shown to promote motility and invasiveness of prostate cancer cells [228, 229].

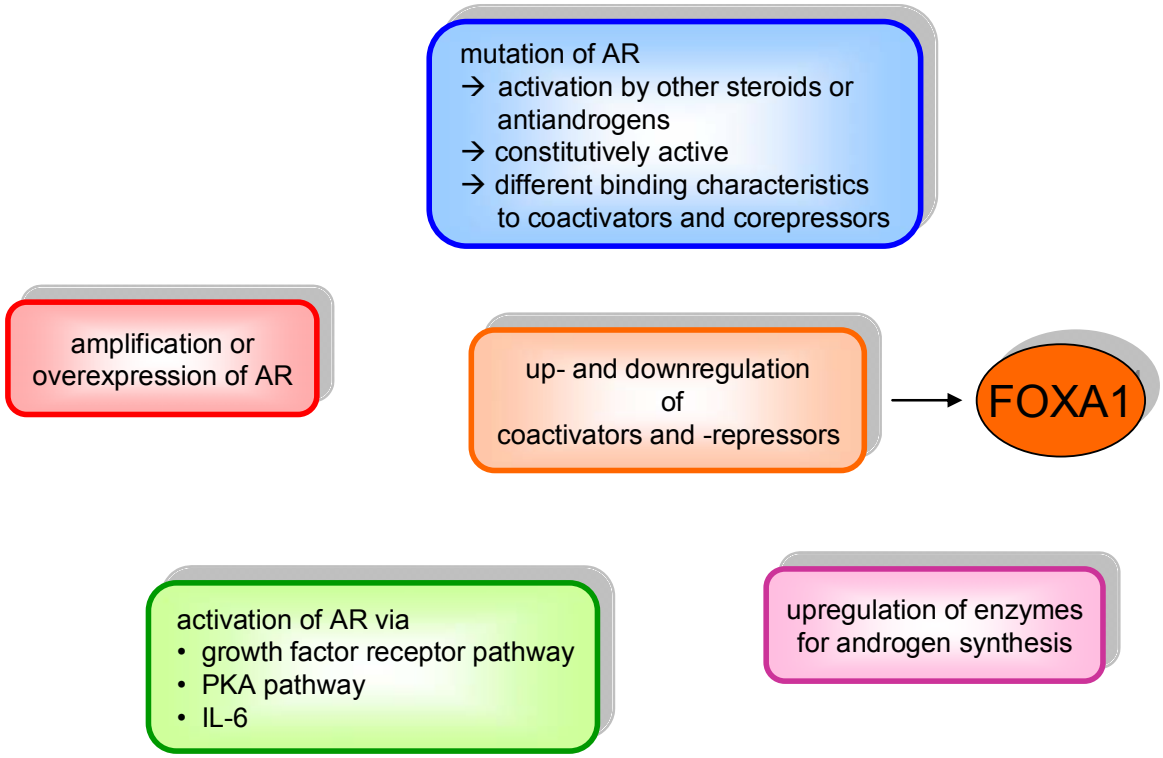


**Fig. 63 Mechanisms of castration-resistance in prostate cancer.**

## *5.5 The clinical aspects of prostate cancer*

As outlined in detail in the introduction, three major clinical aims are connected to prostate cancer: specific and sensitive non-invasive diagnosis, prognosis of disease course and life-prolonging treatment of CRPC.

### 5.5.1 Diagnosis

In most cases, prostate cancer can be diagnosed correctly using the current methods of DRE, serum PSA measurement, and most important, histology. However, some unclear cases remain, where immunohistochemical markers help to ascertain the diagnosis. Since FOXA1 expression levels are similar in normal prostate epithelium and in primary prostate carcinomas, it is ineligible for this application. Also, analysis of tissue CANT1 levels does not help in diagnosing prostate cancer, because this marker cannot discriminate between PIN

and cancer lesions, which would be important to determine the treatment modality for the patient.

In any case, currently needle biopsies are needed to make a definite diagnosis following initial suspicion of prostate cancer due to positive DRE or elevated serum PSA levels. Since increased secretion of PSA into the blood occurs also in other benign prostate diseases [8], many healthy individuals undergo invasive diagnostics (biopsies). To reduce the number of unnecessary biopsies, a more specific non-invasive diagnostic tool is desirable. Hence, biomarkers that are evaluable in patient serum or urine would represent an ideal alternative. Hitherto, the non-coding RNA PCA3 has been identified with an increased specificity in comparison to PSA. Further, PCA3 seems to be independent of the prostate volume in contrary to PSA [230]. Consequently, urine-detection of this gene was approved for the diagnosis of prostate cancer in Europe in 2006 [20, 231]. However, the test is expensive and is therefore not widely applied in the clinic.

Further improved statistical values that characterize specificity of biomarkers were revealed for a multiplex analysis of PCA3, TMPRSS2:ERG, GOLM1 and SPINK1 gene expression in post-DRE urine [149] as well as for a multiplex analysis of glutathione S-transferase pi (GSTP) 1, Ras association (RalGDS/AF-6) domain family member (RASSF) 1A, retinoic acid receptor (RAR) β2, and adenomatous polyposis coli (APC) methylation [232].

In this study, CANT1 was proven to be detectable in serum samples in contrary to a previous statement [61]. With the newly designed sandwich ELISA assay higher serum CANT1 levels were measured in prostate cancer patients in comparison to healthy individuals. Although this difference was not significant and CANT1 amounts were just below the detection threshold of the assay, CANT1 is a potential novel candidate as serum biomarker for the diagnosis of prostate cancer. Beneficial to PCA3, conduction of a serum ELISA assay is more economic than RNA-based diagnostic. However, since CANT1 upregulation in tissue was already detectable in the precursor lesion PIN, CANT1 serum levels need to be analyzed in PIN patients, before the optimization of CANT1 measurement in serum can proceed.

### 5.5.2 Prognosis

An early prognosis of the disease course is highly relevant for the prevention of overtreatment. Two major disease courses exist for prostate cancer. Either the (insignificant) carcinoma grows slowly, does not extend through the prostate capsule and never threatens the patients' life or the (aggressive) carcinoma relapses after primary treatment, gets inevitably castration-resistant within two years after hormonal therapy and finally involves death of the patient. To avoid treatment-associated side-effects [30] for patients with insignificant carcinomas, prognosis of the disease course ought to be carried out ideally with

help of blood serum, urine or needle biopsies. Classical analysis of histology is a strong prognostic factor in prostate cancer (**Fig. 64**).

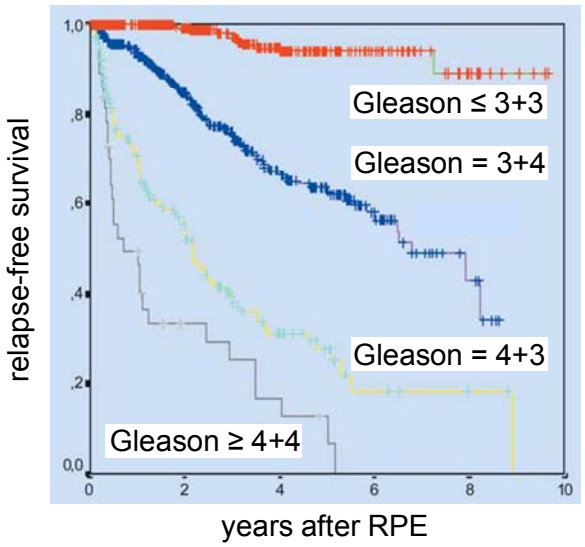


**Fig. 64 Univariate survival analysis dependent on Gleason scoring.**

Note the different survival curves of patients with Gleason score 7 dependent on the dominant Gleason pattern. Modified from [233].

However, as already mentioned in the introduction, especially for the intermediate risk group with Gleason score 7, novel biomarkers that are able to predict the risk of recurrence, are needed. Potential candidates with some superiority to Gleason score have been identified, amongst others increased detection of U-plasminogen activator (uPA) or uPA-receptor (uPAR), TGFβ, ILg-R and Endoglin in serum and increased immunohistomchemical staining of prostate-specific membrane antigen (PSMA), Ki67, AR, p53, HSP60, TATI (the protein of the SPINK1 gene), PTEN, SMAD4, cyclin D1 and secreted phosphoprotein (SPP)1 [234]. Furthermore, hypermethylation of CD44 and cyclin D2 that can be detected in tissue or serum, the overall number of DNA copy number alterations [53] or an increased number of circulating tumor cells have been suggested. In general, combinations of these candidates amongst themselves or with classical clinicopathological parameters increase the performance of the markers (reviewed in [232, 235-237]).

This study adds two further biomarker candidates for the prognosis of prostate cancer. Patients with very high expression levels of CANT1, which can only be identified using the more differentiated H-score, have a very good prognosis (5-year survival rate 93 %) compared to patients with lower CANT1 expression levels (5-year survival rate 81 %). In contrast, patients with high FOXA1 expression levels have a poor prognosis (5-year survival rate 55 %) compared to patients with low FOXA1 expression levels (5-year survival rate 68 %). This difference is even more pronounced in the subgroup of patients with low or moderate AR expression levels (5-year survival rate 68 % and 40 % for patients with high and low FOXA1 expression levels, respectively). The prognostic value of CANT1 is also

maintained in a multivariate analysis, which means that CANT1 is independent of Gleason score and other clinicopathological parameters. Thus, CANT1 expression adds further information to the prognosis of the disease course. Since these analyses were conducted on RPE specimens, these markers can only be applied in the clinic if the prognostic relevance is maintained in a large cohort of needle biopsies.

### 5.5.3 Treatment

Whereas the majority of prostate cancer patients can be cured by either surgery or radiotherapy [238] and hormonal therapy reduces disease symptoms successfully in the beginning, a significant fraction of patients experiences disease progression to CRPC. For these, treatment options are limited and survival rates are low [31, 32, 239, 240]. Thus, novel therapies urgently need to be developed to at least prolong the life-expectancy of CRPC patients. However, the final goal must be to keep the carcinoma in its hormone-dependent state to achieve a persistent control of the disease.

Concerning prolongation of the life-expectancy of CRPC patients, CANT1 is a potential target. Although CANT1 protein levels decline from primary prostate carcinomas to CRPC, proliferation of the hormone-independent cell line PC-3 was markedly reduced by transfection of CANT1-specific siRNA #1. Hence, CANT1 downregulation by RNA interference represents a promising approach to prevent growth of castration-resistant prostate cancer cells. A technically easier approach would be a small molecular inhibitor of CANT1 enzymatic activity. In the context of UPR, inhibition of CANT1 would be equal to induction of UPR, which was suggested as possible therapeutic approach for solid tumors, possibly in combination with overload of the protein folding machinery so that cells cannot handle the bulk of misfolded proteins, leading to death of the cancer cell [188].

In patients with low to moderate expression levels of AR, FOXA1 might be the target of choice to prevent the carcinoma from growing independent of androgens. Especially in this group, patients' prognosis was highly dependent on FOXA1 expression levels. However, further experimental evidence is needed to directly show that FOXA1 is required for the progression of primary carcinomas with low AR levels before a treatment based on FOXA1 inhibition is developed.

## *5.6 Final Conclusion*

Within this study, the expression patterns of two proteins were analyzed in detail in large patient cohorts. CANT1 is upregulated during prostate cancer initiation, whereas FOXA1 is upregulated during cancer progression. Due to the importance of FOXA1 for the progression of carcinomas with low AR levels, we suggest overexpression of FOXA1 in its function as AR coactivator as novel mechanism of castration-resistance for prostate cancer.

Both proteins are not suitable as immunohistochemical diagnostic biomarkers. However, under certain conditions both proteins have a prognostic value. Very strong CANT1 levels in RPE specimens identified the upper quartile of patients with a good prognosis. In contrast, the prognosis for patients with high FOXA1 expression is poor, especially in combination with low or moderate AR levels. Thus, FOXA1 might be a target for a treatment to prevent castration-resistance. Downregulation of CANT1 potentially impairs proliferation of prostate cancer cells during the whole tumor development.

# 6 References


1. *Gerhardt, J., et al.,* The Androgen-Regulated Calcium-Activated Nucleotidase 1 (*CANT1*) Is Commonly Overexpressed in Prostate Cancer and Is Tumor-Biologically Relevant in Vitro. *Am J Pathol, 2011. 178(4): p. 1847-60.*
2. *Montani, M., et al.,* FOXA1 promotes Tumor Progression in Prostate Cancer and represents a novel Hallmark of Castrate Resistant Prostate Cancer. *in revision.*
3. *Sakr, W.A. and A.W. Partin,* Histological markers of risk and the role of high-grade prostatic intraepithelial neoplasia. *Urology, 2001. 57(4 Suppl 1): p. 115-20.*
4. *Bostwick, D.G. and J. Qian,* High-grade prostatic intraepithelial neoplasia. *Mod Pathol, 2004. 17(3): p. 360-79.*
5. *Epstein, J.I. and G.J. Netto,* Biopsy interpretation of the prostate*. 4th ed. Biopsy interpretation series, ed. J.I. Epstein. 2008, Philadelphia, PA, USA: Lippincott Williams & Wilkins.*
6. *Krebsliga_Schweiz,* Krebs in der Schweiz: wichtige Zahlen*, in* Informationsblatt*. 2009.*
7. *Boyle, P. and B.E. Levin,* WHO World Cancer Report. Lyon, France, IARC, 2008. Available online at http://www.iarc.fr/en/publications/pdfs-online/wcr/. .
8. *Lilja, H., D. Ulmert, and A.J. Vickers,* Prostate-specific antigen and prostate cancer: prediction, detection and monitoring. *Nat Rev Cancer, 2008. 8(4): p. 268-78.*
9. *Damber, J.E. and G. Aus,* Prostate cancer. *Lancet, 2008. 371(9625): p. 1710-21.*
10. *Sakr, W.A., et al.,* The frequency of carcinoma and intraepithelial neoplasia of the prostate in young male patients. *J Urol, 1993. 150(2 Pt 1): p. 379-85.*
11. *Schweizerische_Gesellschaft_für_Urologie,* Prostata: Kleine Drüse - grosse Bedeutung*, in* Informationsschrift*. 2009.*
12. *Ambs, S., et al.,* Genomic profiling of microRNA and messenger RNA reveals deregulated microRNA expression in prostate cancer. *Cancer Res, 2008. 68(15): p. 6162-70.*
13. *Schaefer, A., et al.,* Diagnostic and prognostic implications of microRNA profiling in prostate carcinoma. *Int J Cancer, 2010. 126(5): p. 1166-76.*
14. *Sreekumar, A., et al.,* Metabolomic profiles delineate potential role for sarcosine in prostate cancer progression. *Nature, 2009. 457(7231): p. 910-4.*
15. *Kristiansen, G., et al.,* Expression profiling of microdissected matched prostate cancer samples reveals CD166/MEMD and CD24 as new prognostic markers for patient survival. *J Pathol, 2005. 205(3): p. 359-76.*

16. *Kristiansen, G., et al.,* GOLPH2 protein expression as a novel tissue biomarker for prostate cancer: implications for tissue-based diagnostics. *Br J Cancer, 2008. 99(6): p. 939-48.*
17. *Tischler, V., et al.,* Comparison of the diagnostic value of fatty acid synthase (FASN) with alpha-methylacyl-CoA racemase (AMACR) as prostatic cancer tissue marker. *Histopathology, 2010. 56(6): p. 811-5.*
18. *Tischler, V., et al.,* Periostin is up-regulated in high grade and high stage prostate cancer. *BMC Cancer, 2010. 10: p. 273.*
19. *Reed, A.B. and D.J. Parekh,* Biomarkers for prostate cancer detection. *Expert Rev Anticancer Ther, 2010. 10(1): p. 103-14.*
20. *Day, J.R., et al.,* PCA3: from basic molecular science to the clinical lab. *Cancer Lett, 2011. 301(1): p. 1-6.*
21. *Catalona, W.J., et al.,* Detection of organ-confined prostate cancer is increased through prostate-specific antigen-based screening. *Jama, 1993. 270(8): p. 948-54.*
22. *Karr, J.F., et al.,* The presence of prostate-specific antigen-related genes in primates and the expression of recombinant human prostate-specific antigen in a transfected murine cell line. *Cancer Res, 1995. 55(11): p. 2455-62.*
23. *Hugosson, J., et al.,* Mortality results from the Goteborg randomised population-based prostate-cancer screening trial. *Lancet Oncol, 2010. 11(8): p. 725-32.*
24. *Schroder, F.H., et al.,* Screening and prostate-cancer mortality in a randomized European study. *N Engl J Med, 2009. 360(13): p. 1320-8.*
25. *Andriole, G.L., et al.,* Mortality results from a randomized prostate-cancer screening trial. *N Engl J Med, 2009. 360(13): p. 1310-9.*
26. *Wittekind, C. and H.J. Meyer,* TNM Klassifikation maligner Tumoren*. 7th ed. 2010, Leipzig, Germany: WILEY-VCH Verlag GmbH&Co.KGaA.*
27. *Humphrey, P.A.,* Gleason grading and prognostic factors in carcinoma of the prostate. *Mod Pathol, 2004. 17(3): p. 292-306.*
28. *D'Amico, A.V., et al.,* Biochemical outcome after radical prostatectomy, external beam radiation therapy, or interstitial radiation therapy for clinically localized prostate cancer. *Jama, 1998. 280(11): p. 969-74.*
29. *Lughezzani, G., et al.,* Head-to-head comparison of the three most commonly used preoperative models for prediction of biochemical recurrence after radical prostatectomy. *Eur Urol, 2010. 57(4): p. 562-8.*
30. *Sanda, M.G., et al.,* Quality of life and satisfaction with outcome among prostate-cancer survivors. *N Engl J Med, 2008. 358(12): p. 1250-61.*
31. *Tannock, I.F., et al.,* Docetaxel plus prednisone or mitoxantrone plus prednisone for advanced prostate cancer. *N Engl J Med, 2004. 351(15): p. 1502-12.*

32. *Petrylak, D.P., et al.,* Docetaxel and estramustine compared with mitoxantrone and prednisone for advanced refractory prostate cancer. *N Engl J Med, 2004. 351(15): p. 1513-20.*
33. *Kantoff, P.W., et al.,* Sipuleucel-T immunotherapy for castration-resistant prostate cancer. *N Engl J Med, 2010. 363(5): p. 411-22.*
34. *Huggins, C. and C.V. Hodges,* Studies on prostatic cancer. I. The effect of castration, of estrogen and androgen injection on serum phosphatases in metastatic carcinoma of the prostate. *Cancer Res, 1941. 1: p. 293-297.*
35. *Chen, Y., N.J. Clegg, and H.I. Scher,* Anti-androgens and androgen-depleting therapies in prostate cancer: new agents for an established target. *Lancet Oncol, 2009. 10(10): p. 981-91.*
36. *Feldman, B.J. and D. Feldman,* The development of androgen-independent prostate cancer. *Nat Rev Cancer, 2001. 1(1): p. 34-45.*
37. *Galani, A., et al.,* Androgen insensitivity syndrome: clinical features and molecular defects. *Hormones (Athens), 2008. 7(3): p. 217-29.*
38. *Attard, G., C.S. Cooper, and J.S. de Bono,* Steroid hormone receptors in prostate cancer: a hard habit to break? *Cancer Cell, 2009. 16(6): p. 458-62.*
39. *Bosland, M.C.,* The role of estrogens in prostate carcinogenesis: a rationale for chemoprevention. *Rev Urol, 2005. 7 Suppl 3: p. S4-S10.*
40. *Ellem, S.J. and G.P. Risbridger,* Treating prostate cancer: a rationale for targeting local oestrogens. *Nat Rev Cancer, 2007. 7(8): p. 621-7.*
41. *Bonkhoff, H. and R. Berges,* The evolving role of oestrogens and their receptors in the development and progression of prostate cancer. *Eur Urol, 2009. 55(3): p. 533-42.*
42. *Ruff, M., et al.,* Estrogen receptor transcription and transactivation: Structure-function relationship in DNA- and ligand-binding domains of estrogen receptors. *Breast Cancer Res, 2000. 2(5): p. 353-9.*
43. *Cunha, G.R., P.S. Cooke, and T. Kurita,* Role of stromal-epithelial interactions in hormonal responses. *Arch Histol Cytol, 2004. 67(5): p. 417-34.*
44. *Niu, Y.N. and S.J. Xia,* Stroma-epithelium crosstalk in prostate cancer. *Asian J Androl, 2009. 11(1): p. 28-35.*
45. *Liu, W., et al.,* Homozygous deletions and recurrent amplifications implicate new genes involved in prostate cancer. *Neoplasia, 2008. 10(8): p. 897-907.*
46. *Yoshimoto, M., et al.,* Interphase FISH analysis of PTEN in histologic sections shows genomic deletions in 68% of primary prostate cancer and 23% of high-grade prostatic intra-epithelial neoplasias. *Cancer Genet Cytogenet, 2006. 169(2): p. 128-37.*

47. *Han, B., et al.,* A fluorescence in situ hybridization screen for E26 transformation-specific aberrations: identification of DDX5-ETV4 fusion protein in prostate cancer. *Cancer Res, 2008. 68(18): p. 7629-37.*
48. *Esgueva, R., et al.,* Prevalence of TMPRSS2-ERG and SLC45A3-ERG gene fusions in a large prostatectomy cohort *Mod Pathol, 2010. 23(4): p. 539-46.*
49. *Hermans, K.G., et al.,* Two unique novel prostate-specific and androgen-regulated fusion partners of ETV4 in prostate cancer. *Cancer Res, 2008. 68(9): p. 3094-8.*
50. *Feldman, R.J., V.I. Sementchenko, and D.K. Watson,* The epithelial-specific Ets factors occupy a unique position in defining epithelial proliferation, differentiation and carcinogenesis. *Anticancer Res, 2003. 23(3A): p. 2125-31.*
51. *Ateeq, B., et al.,* Therapeutic targeting of SPINK1-positive prostate cancer. *Sci Transl Med, 2011. 3(72): p. 72ra17.*
52. *Tomlins, S.A., et al.,* The role of SPINK1 in ETS rearrangement-negative prostate cancers. *Cancer Cell, 2008. 13(6): p. 519-28.*
53. *Taylor, B.S., et al.,* Integrative genomic profiling of human prostate cancer. *Cancer Cell, 2010. 18(1): p. 11-22.*
54. *Luo, J.H., et al.,* Gene expression analysis of prostate cancers. *Mol Carcinog, 2002. 33(1): p. 25-35.*
55. *Ross, A.E., et al.,* Gene expression pathways of high grade localized prostate cancer. *Prostate, 2011.*
56. *Heemers, H.V., et al.,* Identification of a clinically relevant androgen-dependent gene signature in prostate cancer. *Cancer Res, 2011. 71(5): p. 1978-88.*
57. *Xu, K., et al.,* A comparative analysis of gene-expression data of multiple cancer types. *PLoS One, 2010. 5(10): p. e13696.*
58. *Fritzsche, F.R., et al.,* Diagnostic and prognostic value of T-cell receptor gamma alternative reading frame protein (TARP) expression in prostate cancer. *Histol Histopathol, 2010. 25(6): p. 733-9.*
59. *Fritzsche, F.R., et al.,* ADAM9 expression is a significant and independent prognostic marker of PSA relapse in prostate cancer. *Eur Urol, 2008. 54(5): p. 1097-106.*
60. *Smith, T.M., et al.,* Cloning, expression, and characterization of a soluble calcium-activated nucleotidase, a human enzyme belonging to a new family of extracellular nucleotidases. *Arch Biochem Biophys, 2002. 406(1): p. 105-15.*
61. *Murphy, D.M., V.V. Ivanenkov, and T.L. Kirley,* Bacterial expression and characterization of a novel, soluble, calcium-binding, and calcium-activated human nucleotidase. *Biochemistry, 2003. 42(8): p. 2412-21.*

62. *Failer, B.U., N. Braun, and H. Zimmermann,* Cloning, expression, and functional characterization of a Ca(2+)-dependent endoplasmic reticulum nucleoside diphosphatase. *J Biol Chem, 2002. 277(40): p. 36978-86.*

63. *Yang, M., et al.,* Calcium-dependent dimerization of human soluble calcium activated nucleotidase: characterization of the dimer interface. *J Biol Chem, 2006. 281(38): p. 28307-17.*

64. *Meyerhof, O.,* THE ORIGIN OF THE REACTION OF HARDEN AND YOUNG IN CELL-FREE ALCOHOLIC FERMENTATION*. *J Biol Chem, 1945. 157: p. 105-120.*

65. *Yang, M. and T.L. Kirley,* Site-directed mutagenesis of human soluble calcium-activated nucleotidase 1 (hSCAN-1): identification of residues essential for enzyme activity and the Ca(2+)-induced conformational change. *Biochemistry, 2004. 43(28): p. 9185-94.*

66. *Yang, M., et al.,* Characterization and importance of the dimer interface of human calcium-activated nucleotidase. *Biochemistry, 2008. 47(2): p. 771-8.*

67. *Yegutkin, G.G.,* Nucleotide- and nucleoside-converting ectoenzymes: Important modulators of purinergic signalling cascade. *Biochim Biophys Acta, 2008. 1783(5): p. 673-94.*

68. *Uccelletti, D., et al.,* APY-1, a novel Caenorhabditis elegans apyrase involved in unfolded protein response signalling and stress responses. *Mol Biol Cell, 2008. 19(4): p. 1337-45.*

69. *Devader, C., et al.,* Xenopus apyrase (xapy), a secreted nucleotidase that is expressed during early development. *Gene, 2006. 367: p. 135-41.*

70. *Huber, C., et al.,* Identification of CANT1 mutations in Desbuquois dysplasia. *Am J Hum Genet, 2009. 85(5): p. 706-10.*

71. *Smith, T.M. and T.L. Kirley,* The calcium activated nucleotidases: A diverse family of soluble and membrane associated nucleotide hydrolyzing enzymes. *Purinergic Signal, 2006. 2(2): p. 327-33.*

72. *Kaczmarek, E., et al.,* Identification and characterization of CD39/vascular ATP diphosphohydrolase. *J Biol Chem, 1996. 271(51): p. 33116-22.*

73. *Valenzuela, J.G., et al.,* Purification, cloning, and expression of an apyrase from the bed bug Cimex lectularius. A new type of nucleotide-binding enzyme. *J Biol Chem, 1998. 273(46): p. 30583-90.*

74. *Fung, C.Y., et al.,* P2X(1) receptor inhibition and soluble CD39 administration as novel approaches to widen the cardiovascular therapeutic window. *Trends Cardiovasc Med, 2009. 19(1): p. 1-5.*

75. *Sevigny, J., et al.,* Differential catalytic properties and vascular topography of murine nucleoside triphosphate diphosphohydrolase 1 (NTPDase1) and NTPDase2 have implications for thromboregulation. *Blood, 2002. 99(8): p. 2801-9.*
76. *Yang, M. and T.L. Kirley,* Engineered human soluble calcium-activated nucleotidase inhibits coagulation in vitro and thrombosis in vivo. *Thromb Res, 2008. 122(4): p. 541-8.*
77. *Dai, J., et al.,* Structure and protein design of a human platelet function inhibitor. *Cell, 2004. 116(5): p. 649-59.*
78. *Desbuquois, G., et al.,* Nanisme chondrodystrophique avec ossification anarchique et polymalformations chez deux soeurs. *Arch Fr Pediatr 1966. 23: p. 573-87.*
79. *Faivre, L., et al.,* Homozygosity mapping of a Desbuquois dysplasia locus to chromosome 17q25.3. *J Med Genet, 2003. 40(4): p. 282-4.*
80. *Furuichi, T., et al.,* CANT1 mutation is also responsible for Desbuquois dysplasia, type 2 and Kim variant. *J Med Genet, 2010. 48(1): p. 32-7.*
81. *Laccone, F., et al.,* Desbuquois dysplasia type I and fetal hydrops due to novel mutations in the CANT1 gene. *Eur J Hum Genet, 2011.*
82. *Costa, R.H., D.R. Grayson, and J.E. Darnell, Jr.,* Multiple hepatocyte-enriched nuclear factors function in the regulation of transthyretin and alpha 1-antitrypsin genes. *Mol Cell Biol, 1989. 9(4): p. 1415-25.*
83. *Lai, E., et al.,* HNF-3A, a hepatocyte-enriched transcription factor of novel structure is regulated transcriptionally. *Genes Dev, 1990. 4(8): p. 1427-36.*
84. *Lai, E., et al.,* Hepatocyte nuclear factor 3 alpha belongs to a gene family in mammals that is homologous to the Drosophila homeotic gene fork head. *Genes Dev, 1991. 5(3): p. 416-27.*
85. *Weigel, D., et al.,* The homeotic gene fork head encodes a nuclear protein and is expressed in the terminal regions of the Drosophila embryo. *Cell, 1989. 57(4): p. 645-58.*
86. *Weigel, D. and H. Jackle,* The fork head domain: a novel DNA binding motif of eukaryotic transcription factors? *Cell, 1990. 63(3): p. 455-6.*
87. *Kaestner, K.H.,* The hepatocyte nuclear factor 3 (HNF3 or FOXA) family in metabolism. *Trends Endocrinol Metab, 2000. 11(7): p. 281-5.*
88. *Kaestner, K.H., W. Knochel, and D.E. Martinez,* Unified nomenclature for the winged helix/forkhead transcription factors. *Genes Dev, 2000. 14(2): p. 142-6.*
89. *Jackson, B.C., et al.,* Update of human and mouse forkhead box (FOX) gene families. *Hum Genomics, 2010. 4(5): p. 345-52.*
90. *Clark, K.L., et al.,* Co-crystal structure of the HNF-3/fork head DNA-recognition motif resembles histone H5. *Nature, 1993. 364(6436): p. 412-20.*

91. *Brennan, R.G.,* The winged-helix DNA-binding motif: another helix-turn-helix takeoff. *Cell, 1993. 74(5): p. 773-6.*

92. *Cerf, C., et al.,* Homo- and heteronuclear two-dimensional NMR studies of the globular domain of histone H1: full assignment, tertiary structure, and comparison with the globular domain of histone H5. *Biochemistry, 1994. 33(37): p. 11079-86.*

93. *Ramakrishnan, V., et al.,* Crystal structure of globular domain of histone H5 and its implications for nucleosome binding. *Nature, 1993. 362(6417): p. 219-23.*

94. *Cirillo, L.A., et al.,* Opening of compacted chromatin by early developmental transcription factors HNF3 (FoxA) and GATA-4. *Mol Cell, 2002. 9(2): p. 279-89.*

95. *Carlsson, P. and M. Mahlapuu,* Forkhead transcription factors: key players in development and metabolism. *Dev Biol, 2002. 250(1): p. 1-23.*

96. *Myatt, S.S. and E.W. Lam,* The emerging roles of forkhead box (Fox) proteins in cancer. *Nat Rev Cancer, 2007. 7(11): p. 847-59.*

97. *Lee, C.S., et al.,* The initiation of liver development is dependent on Foxa transcription factors. *Nature, 2005. 435(7044): p. 944-7.*

98. *Gao, N., et al.,* Forkhead box A1 regulates prostate ductal morphogenesis and promotes epithelial cell maturation. *Development, 2005. 132(15): p. 3431-43.*

99. *Mirosevich, J., N. Gao, and R.J. Matusik,* Expression of Foxa transcription factors in the developing and adult murine prostate. *Prostate, 2005. 62(4): p. 339-52.*

100. *Wan, H., et al.,* Compensatory roles of Foxa1 and Foxa2 during lung morphogenesis. *J Biol Chem, 2005. 280(14): p. 13809-16.*

101. *Bernardo, G.M., et al.,* FOXA1 is an essential determinant of ERalpha expression and mammary ductal morphogenesis. *Development, 2010. 137(12): p. 2045-54.*

102. *Gao, N., et al.,* Dynamic regulation of Pdx1 enhancers by Foxa1 and Foxa2 is essential for pancreas development. *Genes Dev, 2008. 22(24): p. 3435-48.*

103. *Besnard, V., et al.,* Immunohistochemical localization of Foxa1 and Foxa2 in mouse embryos and adult tissues. *Gene Expr Patterns, 2004. 5(2): p. 193-208.*

104. *Kopachik, W., S.W. Hayward, and G.R. Cunha,* Expression of hepatocyte nuclear factor-3alpha in rat prostate, seminal vesicle, and bladder. *Dev Dyn, 1998. 211(2): p. 131-40.*

105. *Kaestner, K.H., et al.,* Inactivation of the winged helix transcription factor HNF3alpha affects glucose homeostasis and islet glucagon gene expression in vivo. *Genes Dev, 1999. 13(4): p. 495-504.*

106. *Shih, D.Q., et al.,* Impaired glucose homeostasis and neonatal mortality in hepatocyte nuclear factor 3alpha-deficient mice. *Proc Natl Acad Sci U S A, 1999. 96(18): p. 10152-7.*

107. *Zhang, J., et al.,* Characterization of cis elements of the probasin promoter necessary for prostate-specific gene expression. *Prostate, 2010. 70(9): p. 934-51.*

108. *McMullin, R.P., et al.,* A FOXA1-binding enhancer regulates Hoxb13 expression in the prostate gland. *Proc Natl Acad Sci U S A, 2010. 107(1): p. 98-103.*

109. *Mirosevich, J., et al.,* Expression and role of Foxa proteins in prostate cancer. *Prostate, 2006. 66(10): p. 1013-28.*

110. *Jain, R.K., et al.,* High-level expression of forkhead-box protein A1 in metastatic prostate cancer. *Histopathology, 2011.*

111. *Cirillo, L.A. and K.S. Zaret,* Specific interactions of the wing domains of FOXA1 transcription factor with DNA. *J Mol Biol, 2007. 366(3): p. 720-4.*

112. *Lupien, M., et al.,* FoxA1 translates epigenetic signatures into enhancer-driven lineage-specific transcription. *Cell, 2008. 132(6): p. 958-70.*

113. *Wang, Q., et al.,* Androgen receptor regulates a distinct transcription program in androgen-independent prostate cancer. *Cell, 2009. 138(2): p. 245-56.*

114. *Hurtado, A., et al.,* FOXA1 is a key determinant of estrogen receptor function and endocrine response. *Nat Genet, 2011. 43(1): p. 27-33.*

115. *Gao, N., et al.,* The role of hepatocyte nuclear factor-3 alpha (Forkhead Box A1) and androgen receptor in transcriptional regulation of prostatic genes. *Mol Endocrinol, 2003. 17(8): p. 1484-507.*

116. *Yu, X., et al.,* Foxa1 and Foxa2 interact with the androgen receptor to regulate prostate and epididymal genes differentially. *Ann N Y Acad Sci, 2005. 1061: p. 77-93.*

117. *Williamson, E.A., et al.,* BRCA1 and FOXA1 proteins coregulate the expression of the cell cycle-dependent kinase inhibitor p27(Kip1). *Oncogene, 2006. 25(9): p. 1391-9.*

118. *Zhang, Y., et al.,* CTCF acts upstream of FOXA1 and demarcates the genomic response to estrogen. *J Biol Chem, 2010.*

119. *Achatz, G., et al.,* Functional domains of the human orphan receptor ARP-1/COUP-TFII involved in active repression and transrepression. *Mol Cell Biol, 1997. 17(9): p. 4914-32.*

120. *Kim, J.Y., et al.,* Orphan nuclear receptor small heterodimer partner represses hepatocyte nuclear factor 3/Foxa transactivation via inhibition of its DNA binding. *Mol Endocrinol, 2004. 18(12): p. 2880-94.*

121. *Minoo, P., et al.,* Physical and functional interactions between homeodomain NKX2.1 and winged helix/forkhead FOXA1 in lung epithelial cells. *Mol Cell Biol, 2007. 27(6): p. 2155-65.*

122. *Sekiya, T. and K.S. Zaret,* Repression by Groucho/TLE/Grg proteins: genomic site recruitment generates compacted chromatin in vitro and impairs activator binding in vivo. *Mol Cell, 2007. 28(2): p. 291-303.*

123. *Kouros-Mehr, H., et al.,* GATA-3 maintains the differentiation of the luminal cell fate in the mammary gland. *Cell, 2006. 127(5): p. 1041-55.*

124. *Sinner, D., et al.,* Sox17 and beta-catenin cooperate to regulate the transcription of endodermal genes. *Development, 2004. 131(13): p. 3069-80.*

125. *Laganiere, J., et al.,* From the Cover: Location analysis of estrogen receptor alpha target promoters reveals that FOXA1 defines a domain of the estrogen response. *Proc Natl Acad Sci U S A, 2005. 102(33): p. 11651-6.*

126. *Scharer, C.D., et al.,* Genome-wide promoter analysis of the SOX4 transcriptional network in prostate cancer cells. *Cancer Res, 2009. 69(2): p. 709-17.*

127. *Eeckhoute, J., et al.,* Positive cross-regulatory loop ties GATA-3 to estrogen receptor alpha expression in breast cancer. *Cancer Res, 2007. 67(13): p. 6477-83.*

128. *Lupien, M. and M. Brown,* Cistromics of hormone-dependent cancer. *Endocr Relat Cancer, 2009. 16(2): p. 381-9.*

129. *Carroll, J.S., et al.,* Chromosome-wide mapping of estrogen receptor binding reveals long-range regulation requiring the forkhead protein FoxA1. *Cell, 2005. 122(1): p. 33-43.*

130. *Carroll, J.S., et al.,* Genome-wide analysis of estrogen receptor binding sites. *Nat Genet, 2006. 38(11): p. 1289-97.*

131. *Wang, Q., et al.,* A hierarchical network of transcription factors governs androgen receptor-dependent prostate cancer growth. *Mol Cell, 2007. 27(3): p. 380-92.*

132. *Jia, L., et al.,* Genomic androgen receptor-occupied regions with different functions, defined by histone acetylation, coregulators and transcriptional capacity. *PLoS ONE, 2008. 3(11): p. e3645.*

133. *Lee, H.J., et al.,* Hepatocyte nuclear factor-3 alpha (HNF-3alpha) negatively regulates androgen receptor transactivation in prostate cancer cells. *Biochem Biophys Res Commun, 2008. 367(2): p. 481-6.*

134. *Kladney, R.D., et al.,* GP73, a novel Golgi-localized protein upregulated by viral infection. *Gene, 2000. 249(1-2): p. 53-65.*

135. *Norton, P.A., et al.,* N-linked glycosylation of the liver cancer biomarker GP73. *J Cell Biochem, 2008. 104(1): p. 136-49.*

136. *Puri, S., et al.,* Cycling of early Golgi proteins via the cell surface and endosomes upon lumenal pH disruption. *Traffic, 2002. 3(9): p. 641-53.*

137. *Kladney, R.D., et al.,* Expression of GP73, a resident Golgi membrane protein, in viral and nonviral liver disease. *Hepatology, 2002. 35(6): p. 1431-40.*

138. *Bachert, C., C. Fimmel, and A.D. Linstedt,* Endosomal trafficking and proprotein convertase cleavage of cis Golgi protein GP73 produces marker for hepatocellular carcinoma. *Traffic, 2007. 8(10): p. 1415-23.*

139. *Iftikhar, R., et al.,* Disease- and cell-specific expression of GP73 in human liver disease. *Am J Gastroenterol, 2004. 99(6): p. 1087-95.*

140. *Kladney, R.D., et al.,* Upregulation of the Golgi protein GP73 by adenovirus infection requires the E1A CtBP interaction domain. *Virology, 2002. 301(2): p. 236-46.*

141. *Block, T.M., et al.,* Use of targeted glycoproteomics to identify serum glycoproteins that correlate with liver cancer in woodchucks and humans. *Proc Natl Acad Sci U S A, 2005. 102(3): p. 779-84.*

142. *Giannelli, G. and S. Antonaci,* New frontiers in biomarkers for hepatocellular carcinoma. *Dig Liver Dis, 2006. 38(11): p. 854-9.*

143. *Riener, M.O., et al.,* Golgi phosphoprotein 2 (GOLPH2) expression in liver tumors and its value as a serum marker in hepatocellular carcinomas. *Hepatology, 2009. 49(5): p. 1602-9.*

144. *Marrero, J.A., et al.,* GP73, a resident Golgi glycoprotein, is a novel serum marker for hepatocellular carcinoma. *J Hepatol, 2005. 43(6): p. 1007-12.*

145. *Kawamoto, S., et al.,* Overexpression of alpha1,6-fucosyltransferase in hepatoma enhances expression of Golgi phosphoprotein 2 in a fucosylation-independent manner. *Int J Oncol, 2011. 39(1): p. 203-8.*

146. *Wei, S., et al.,* GOLPH2 and MYO6: putative prostate cancer markers localized to the Golgi apparatus. *Prostate, 2008. 68(13): p. 1387-95.*

147. *Varambally, S., et al.,* Golgi protein GOLM1 is a tissue and urine biomarker of prostate cancer. *Neoplasia, 2008. 10(11): p. 1285-94.*

148. *Lapointe, J., et al.,* Gene expression profiling identifies clinically relevant subtypes of prostate cancer. *Proc Natl Acad Sci U S A, 2004. 101(3): p. 811-6.*

149. *Laxman, B., et al.,* A first-generation multiplex biomarker analysis of urine for the early detection of prostate cancer. *Cancer Res, 2008. 68(3): p. 645-9.*

150. *Zhang, F., et al.,* Up-regulated Golgi phosphoprotein 2 (GOLPH2) expression in lung adenocarcinoma tissue. *Clin Biochem, 2010. 43(12): p. 983-91.*

151. *Fritzsche, F.R., et al.,* GOLPH2 expression may serve as diagnostic marker in seminomas. *BMC Urol, 2010. 10: p. 4.*

152. *Wright, L.M., et al.,* Hepatocyte GP73 expression in Wilson disease. *J Hepatol, 2009.*

153. *Li, H., et al.,* Candidate single-nucleotide polymorphisms from a genomewide association study of Alzheimer disease. *Arch Neurol, 2008. 65(1): p. 45-53.*

154. *Antunez, C., et al.,* GOLPH2 gene markers are not associated with Alzheimer's disease in a sample of the Spanish population. *J Alzheimers Dis, 2009. 18(4): p. 751-4.*

155. *Inkster, B., et al.,* Genetic variation in GOLM1 and prefrontal cortical volume in Alzheimer's disease. *Neurobiol Aging, 2010.*

156. *Lehle, L., S. Strahl, and W. Tanner,* Protein glycosylation, conserved from yeast to man: a model organism helps elucidate congenital human diseases. *Angew Chem Int Ed Engl, 2006. 45(41): p. 6802-18.*

157. *Ruddock, L.W. and M. Molinari,* N-glycan processing in ER quality control. *J Cell Sci, 2006. 119(Pt 21): p. 4373-80.*

158. *Ellgaard, L. and A. Helenius,* Quality control in the endoplasmic reticulum. *Nat Rev Mol Cell Biol, 2003. 4(3): p. 181-91.*

159. *Ron, D. and P. Walter,* Signal integration in the endoplasmic reticulum unfolded protein response. *Nat Rev Mol Cell Biol, 2007. 8(7): p. 519-29.*

160. *Malhotra, J.D. and R.J. Kaufman,* The endoplasmic reticulum and the unfolded protein response. *Semin Cell Dev Biol, 2007. 18(6): p. 716-31.*

161. *Prydz, K. and K.T. Dalen,* Synthesis and sorting of proteoglycans. *J Cell Sci, 2000. 113 Pt 2: p. 193-205.*

162. *Liu, L., Y.X. Xu, and C.B. Hirschberg,* The role of nucleotide sugar transporters in development of eukaryotes. *Semin Cell Dev Biol, 2010. 21(6): p. 600-8.*

163. *Csala, M., et al.,* Transport and transporters in the endoplasmic reticulum. *Biochim Biophys Acta, 2007. 1768(6): p. 1325-41.*

164. *Handford, M., C. Rodriguez-Furlan, and A. Orellana,* Nucleotide-sugar transporters: structure, function and roles in vivo. *Braz J Med Biol Res, 2006. 39(9): p. 1149-58.*

165. *Ohl, F., et al.,* Gene expression studies in prostate cancer tissue: which reference gene should be selected for normalization? *J Mol Med, 2005. 83(12): p. 1014-24.*

166. *Hanahan, D. and R.A. Weinberg,* The hallmarks of cancer. *Cell, 2000. 100(1): p. 57-70.*

167. *Fang, M., et al.,* The ER UDPase ENTPD5 Promotes Protein N-Glycosylation, the Warburg Effect, and Proliferation in the PTEN Pathway. *Cell, 2010. 143(5): p. 711-24.*

168. *Thastrup, O., et al.,* The inflammatory and tumor-promoting sesquiterpene lactone, thapsigargin, activates platelets by selective mobilization of calcium as shown by protein phosphorylations. *Biochim Biophys Acta, 1987. 927(1): p. 65-73.*

169. *Takatsuki, A., K. Arima, and G. Tamura,* Tunicamycin, a new antibiotic. I. Isolation and characterization of tunicamycin. *J Antibiot (Tokyo), 1971. 24(4): p. 215-23.*

170. *Lodish, H., et al.,* Molecular Cell Biology*. 4th ed. 2000, New York: W. H. Freeman and Company.*

171. *Hedman, K., A. Vaheri, and J. Wartiovaara,* External fibronectin of cultured human fibroblasts is predominantly a matrix protein. *J Cell Biol, 1978. 76(3): p. 748-60.*

172. *Scott, D.B., et al.,* An NMDA receptor ER retention signal regulated by phosphorylation and alternative splicing. *J Neurosci, 2001. 21(9): p. 3063-72.*

173. *Zerangue, N., et al.,* A new ER trafficking signal regulates the subunit stoichiometry of plasma membrane K(ATP) channels. *Neuron, 1999. 22(3): p. 537-48.*

174. *Schutze, M.P., P.A. Peterson, and M.R. Jackson,* An N-terminal double-arginine motif maintains type II membrane proteins in the endoplasmic reticulum. *Embo J, 1994. 13(7): p. 1696-705.*

175. *Gassmann, M., et al.,* The RXR-type endoplasmic reticulum-retention/retrieval signal of GABAB1 requires distant spacing from the membrane to function. *Mol Pharmacol, 2005. 68(1): p. 137-44.*

176. *Shikano, S. and M. Li,* Membrane receptor trafficking: evidence of proximal and distal zones conferred by two independent endoplasmic reticulum localization signals. *Proc Natl Acad Sci U S A, 2003. 100(10): p. 5783-8.*

177. *Trombetta, E.S. and A. Helenius,* Glycoprotein reglucosylation and nucleotide sugar utilization in the secretory pathway: identification of a nucleoside diphosphatase in the endoplasmic reticulum. *Embo J, 1999. 18(12): p. 3282-92.*

178. *Cummings, R.D. and S. Kornfeld,* Characterization of the structural determinants required for the high affinity interaction of asparagine-linked oligosaccharides with immobilized Phaseolus vulgaris leukoagglutinating and erythroagglutinating lectins. *J Biol Chem, 1982. 257(19): p. 11230-4.*

179. *Faden, M., et al.,* Mutation of CANT1 causes Desbuquois dysplasia. *Am J Med Genet A, 2010. 152A(5): p. 1157-60.*

180. *Hiraoka, S., et al.,* Nucleotide-sugar transporter SLC35D1 is critical to chondroitin sulfate synthesis in cartilage and skeletal development in mouse and human. *Nat Med, 2007. 13(11): p. 1363-7.*

181. *Furuichi, T., et al.,* Identification of loss-of-function mutations of SLC35D1 in patients with Schneckenbecken dysplasia, but not with other severe spondylodysplastic dysplasias group diseases. *J Med Genet, 2009. 46(8): p. 562-8.*

182. *Israelsen, W.J. and M.G. Vander Heiden,* ATP consumption promotes cancer metabolism. *Cell. 143(5): p. 669-71.*

183. *Villar, J., et al.,* PCPH/ENTPD5 expression enhances the invasiveness of human prostate cancer cells by a protein kinase C delta-dependent mechanism. *Cancer Res, 2007. 67(22): p. 10859-68.*

184. *Villar, J., et al.,* PCPH/ENTPD5 expression confers to prostate cancer cells resistance against cisplatin-induced apoptosis through protein kinase Calpha-mediated Bcl-2 stabilization. *Cancer Res, 2009. 69(1): p. 102-10.*

185. *Yoshida, H., et al.,* Identification of the cis-acting endoplasmic reticulum stress response element responsible for transcriptional induction of mammalian glucose-

regulated proteins. Involvement of basic leucine zipper transcription factors. *J Biol Chem, 1998. 273(50): p. 33741-9.*

186. *Kokame, K., H. Kato, and T. Miyata,* Identification of ERSE-II, a new cis-acting element responsible for the ATF6-dependent mammalian unfolded protein response. *J Biol Chem, 2001. 276(12): p. 9199-205.*
187. *Brewer, J.W., et al.,* Mammalian unfolded protein response inhibits cyclin D1 translation and cell-cycle progression. *Proc Natl Acad Sci U S A, 1999. 96(15): p. 8505-10.*
188. *Healy, S.J., et al.,* Targeting the endoplasmic reticulum-stress response as an anticancer strategy. *Eur J Pharmacol, 2009. 625(1-3): p. 234-46.*
189. *Moenner, M., et al.,* Integrated endoplasmic reticulum stress responses in cancer. *Cancer Res, 2007. 67(22): p. 10631-4.*
190. *Scriven, P., et al.,* The unfolded protein response and cancer: a brighter future unfolding? *J Mol Med (Berl), 2007. 85(4): p. 331-41.*
191. *Ma, Y. and L.M. Hendershot,* The role of the unfolded protein response in tumour development: friend or foe? *Nat Rev Cancer, 2004. 4(12): p. 966-77.*
192. *So, A.Y., et al.,* The unfolded protein response during prostate cancer development. *Cancer Metastasis Rev, 2009. 28(1-2): p. 219-23.*
193. *Tan, S.S., et al.,* GRP78 up-regulation is associated with androgen receptor status, Hsp70-Hsp90 client proteins and castrate-resistant prostate cancer. *J Pathol. 223(1): p. 81-7.*
194. *Pootrakul, L., et al.,* Expression of stress response protein Grp78 is associated with the development of castration-resistant prostate cancer. *Clin Cancer Res, 2006. 12(20 Pt 1): p. 5987-93.*
195. *Brunschweiger, A. and C.E. Muller,* P2 receptors activated by uracil nucleotides--an update. *Curr Med Chem, 2006. 13(3): p. 289-312.*
196. *Alberts, B., et al.,* Molecular Biology of the Cell*. 4th ed. 2002, New York: Garland Science.*
197. *Li, G., et al.,* Role of ERO1-alpha-mediated stimulation of inositol 1,4,5-triphosphate receptor activity in endoplasmic reticulum stress-induced apoptosis. *J Cell Biol, 2009. 186(6): p. 783-92.*
198. *Domingo-Domenech, J., et al.,* Activation of nuclear factor-kappaB in human prostate carcinogenesis and association to biochemical relapse. *Br J Cancer, 2005. 93(11): p. 1285-94.*
199. *Boutros, T., E. Chevet, and P. Metrakos,* Mitogen-activated protein (MAP) kinase/MAP kinase phosphatase regulation: roles in cell growth, death, and cancer. *Pharmacol Rev, 2008. 60(3): p. 261-310.*

200. *Andela, V.B., et al.,* NFkappaB: a pivotal transcription factor in prostate cancer metastasis to bone. *Clin Orthop Relat Res, 2003(415 Suppl): p. S75-85.*

201. *Uchino, R., et al.,* NFkappaB-dependent regulation of urokinase plasminogen activator by proanthocyanidin-rich grape seed extract: effect on invasion by prostate cancer cells. *Blood Coagul Fibrinolysis, 2010.*

202. *Shen, H.M. and V. Tergaonkar,* NFkappaB signaling in carcinogenesis and as a potential molecular target for cancer therapy. *Apoptosis, 2009. 14(4): p. 348-63.*

203. *Matsuda, A., et al.,* Large-scale identification and characterization of human genes that activate NF-kappaB and MAPK signaling pathways. *Oncogene, 2003. 22(21): p. 3307-18.*

204. *Gipp, J., et al.,* Hedgehog pathway activity in the LADY prostate tumor model. *Mol Cancer, 2007. 6: p. 19.*

205. *Chiaverotti, T., et al.,* Dissociation of epithelial and neuroendocrine carcinoma lineages in the transgenic adenocarcinoma of mouse prostate model of prostate cancer. *Am J Pathol, 2008. 172(1): p. 236-46.*

206. *Miller, C.T., et al.,* Gene amplification in esophageal adenocarcinomas and Barrett's with high-grade dysplasia. *Clin Cancer Res, 2003. 9(13): p. 4819-25.*

207. *Lin, L., et al.,* The hepatocyte nuclear factor 3 alpha gene, HNF3alpha (FOXA1), on chromosome band 14q13 is amplified and overexpressed in esophageal and lung adenocarcinomas. *Cancer Res, 2002. 62(18): p. 5273-9.*

208. *Wolf, I., et al.,* FOXA1: Growth inhibitor and a favorable prognostic factor in human breast cancer. *Int J Cancer, 2007. 120(5): p. 1013-22.*

209. *Thorat, M.A., et al.,* Forkhead box A1 expression in breast cancer is associated with luminal subtype and good prognosis. *J Clin Pathol, 2008. 61(3): p. 327-32.*

210. *Habashy, H.O., et al.,* Forkhead-box A1 (FOXA1) expression in breast cancer and its prognostic significance. *Eur J Cancer, 2008. 44(11): p. 1541-51.*

211. *Badve, S., et al.,* FOXA1 expression in breast cancer--correlation with luminal subtype A and survival. *Clin Cancer Res, 2007. 13(15 Pt 1): p. 4415-21.*

212. *Doane, A.S., et al.,* An estrogen receptor-negative breast cancer subset characterized by a hormonally regulated transcriptional program and response to androgen. *Oncogene, 2006. 25(28): p. 3994-4008.*

213. *Naderi, A. and L. Hughes-Davies,* A functionally significant cross-talk between androgen receptor and ErbB2 pathways in estrogen receptor negative breast cancer. *Neoplasia, 2008. 10(6): p. 542-8.*

214. *Yamaguchi, N., et al.,* FoxA1 as a lineage-specific oncogene in luminal type breast cancer. *Biochem Biophys Res Commun, 2008. 365(4): p. 711-7.*

215. *Horvath, L.G., et al.,* Frequent loss of estrogen receptor-beta expression in prostate cancer. *Cancer Res, 2001. 61(14): p. 5331-5.*

216. *Leav, I., et al.,* Comparative studies of the estrogen receptors beta and alpha and the androgen receptor in normal human prostate glands, dysplasia, and in primary and metastatic carcinoma. *Am J Pathol, 2001. 159(1): p. 79-92.*

217. *Latil, A., et al.,* Evaluation of androgen, estrogen (ER alpha and ER beta), and progesterone receptor expression in human prostate cancer by real-time quantitative reverse transcription-polymerase chain reaction assays. *Cancer Res, 2001. 61(5): p. 1919-26.*

218. *Fixemer, T., K. Remberger, and H. Bonkhoff,* Differential expression of the estrogen receptor beta (ERbeta) in human prostate tissue, premalignant changes, and in primary, metastatic, and recurrent prostatic adenocarcinoma. *Prostate, 2003. 54(2): p. 79-87.*

219. *Nanni, S., et al.,* Endothelial NOS, estrogen receptor beta, and HIFs cooperate in the activation of a prognostic transcriptional pattern in aggressive human prostate cancer. *J Clin Invest, 2009. 119(5): p. 1093-108.*

220. *Leung, Y.K., et al.,* Estrogen receptor beta2 and beta5 are associated with poor prognosis in prostate cancer, and promote cancer cell migration and invasion. *Endocr Relat Cancer, 2010. 17(3): p. 675-89.*

221. *Setlur, S.R., et al.,* Estrogen-dependent signaling in a molecularly distinct subclass of aggressive prostate cancer. *J Natl Cancer Inst, 2008. 100(11): p. 815-25.*

222. *Mak, P., et al.,* ERbeta impedes prostate cancer EMT by destabilizing HIF-1alpha and inhibiting VEGF-mediated snail nuclear localization: implications for Gleason grading. *Cancer Cell, 2010. 17(4): p. 319-32.*

223. *Gupta, A., et al.,* Neuroendocrine differentiation in the 12T-10 transgenic prostate mouse model mimics endocrine differentiation of pancreatic beta cells. *Prostate, 2008. 68(1): p. 50-60.*

224. *Qi, J., M. Pellecchia, and Z.A. Ronai,* The Siah2-HIF-FoxA2 axis in prostate cancer - new markers and therapeutic opportunities. *Oncotarget, 2010. 1(5): p. 379-85.*

225. *Yu, X., et al.,* Wnt/beta-catenin activation promotes prostate tumor progression in a mouse model. *Oncogene, 2011. 30(16): p. 1868-79.*

226. *Andersen, R.J., et al.,* Regression of castrate-recurrent prostate cancer by a small-molecule inhibitor of the amino-terminus domain of the androgen receptor. *Cancer Cell, 2010. 17(6): p. 535-46.*

227. *Xu, K., et al.,* Regulation of androgen receptor transcriptional activity and specificity by RNF6-induced ubiquitination. *Cancer Cell, 2009. 15(4): p. 270-82.*

228. *Bu, H., et al.,* The anterior gradient 2 (AGR2) gene is overexpressed in prostate cancer and may be useful as a urine sediment marker for prostate cancer detection. *Prostate, 2010. 71(6): p. 575-87.*

229. *Zhang, Y., et al.,* ErbB3 binding protein 1 represses metastasis-promoting gene anterior gradient protein 2 in prostate cancer. *Cancer Res, 2010. 70(1): p. 240-8.*

230. *Marks, L.S. in* AUA Meeting*. 2006. Atlanta, GA.*

231. *Vlaeminck-Guillem, V., et al.,* Urinary prostate cancer 3 test: toward the age of reason? *Urology, 2010. 75(2): p. 447-53.*

232. *Ahmed, H.,* Promoter Methylation in Prostate Cancer and its Application for the Early Detection of Prostate Cancer Using Serum and Urine Samples. *Biomark Cancer, 2010. 2010(2): p. 17-33.*

233. *Graefen, M., et al.,* [Indications for and results of radical prostatectomy]. *Urologe A, 2003. 42(9): p. 1203-11.*

234. *Ding, Z., et al.,* SMAD4-dependent barrier constrains prostate cancer growth and metastatic progression. *Nature, 2011. 470(7333): p. 269-73.*

235. *Shariat, S.F., et al.,* Tumor markers in prostate cancer I: blood-based markers. *Acta Oncol. 50 Suppl 1: p. 61-75.*

236. *Bjartell, A., et al.,* Tumour markers in prostate cancer II: diagnostic and prognostic cellular biomarkers. *Acta Oncol. 50 Suppl 1: p. 76-84.*

237. *Danila, D.C., M. Fleisher, and H.I. Scher,* Circulating tumor cells as biomarkers in prostate cancer. *Clin Cancer Res. 17(12): p. 3903-12.*

238. *Schulz, W.A., M. Burchardt, and M.V. Cronauer,* Molecular biology of prostate cancer. *Mol Hum Reprod, 2003. 9(8): p. 437-48.*

239. *Di Lorenzo, G., et al.,* Hormone-refractory prostate cancer: where are we going? *Drugs, 2007. 67(8): p. 1109-24.*

240. *Uzzo, R.G., et al.,* Mechanisms of apoptosis resistance and treatment strategies to overcome them in hormone-refractory prostate cancer. *Cancer, 2008. 112(8): p. 1660-71.*

# 7 Attachment

## *7.1 Abbreviations*

| | |
|---|---|
| a.u. | arbitrary unit |
| ABCC | ATP-binding cassette sub-family C member |
| ACTH | adrenocorticotropic hormone |
| ADAM | a disintegrin and metallopeptidase domain |
| ADP | adenosine diphosphate |
| AFP | alpha-fetoprotein |
| AGR | anterior gradient homolog |
| ALAS | aminolevulinate, delta-, synthase |
| AMACR | alpha-methylacyl-CoA racemase |
| AMP | adenosine monophosphate |
| APC | adenomatous polyposis coli |
| APS | ammonium persulfate |
| apy | APYrase |
| AR | androgen receptor |
| ARA70 | 70 kDa AR-activator |
| ARE | androgen responsive element |
| ATF | activating transcription factor |
| ATP | adenosine triphosphate |
| | |
| Bcl2 | B-cell leukemia/lymphoma 2 |
| BPH | benign prostatic hyperplasia |
| BRCA | breast cancer |
| BrdU | bromodeoxyuridine |
| BSA | bovine serum albumine |
| | |
| Ca | carcinoma |
| CANT | calcium-activated nucleotidase |
| CANX | calnexin |
| CD44 | cluster of differentiation |
| CHOP | CCAAT/enhancer-binding protein homologous protein |
| CMP | cytidine monophosphate |
| CRH | corticotropin-releasing hormone |
| CRPC | castration-resistant prostate carcinoma |
| C-terminus | carboxy-terminus |

| | |
|---|---|
| CTFC | CCCTC-binding Factor |
| CTP | cytidine triphosphate |
| CXCL | chemokine (C-X-C motif) ligand |
| DAG | diacylglycerol |
| DAPI | 4′,6-Diamidino-2-phenylindole dihydrochloride |
| DHEA | dehydroepiandrosterone |
| DHEA-S | DHEA-sulphate |
| DHT | dihydrotestosterone |
| DMSO | dimethylsulfoxid |
| DNA | deoxyribonucleic acid |
| Dol | dolichol |
| DRE | digital rectal examination |
| $E_2$ | estradiol |
| EDEM | ER degradation enhancer, mannosidase alpha-like |
| EDTA | ethylenediaminetetraacetic acid |
| EGF | epidermal growth factor |
| eIF | eukaryotic translation initiation factor |
| ELISA | enzyme-linked Immunosorbent assay |
| ER | endoplasmic reticulum |
| ERAD | ER-associated degradation |
| ERBB | v-erb-b2 erythroblastic leukemia viral oncogene homolog |
| ERE | estrogen responsive element |
| ERSE | ER-stress response element |
| ERα/β | estrogen receptor α/β |
| ETS | avian erythroblastosis virus E26 (v-ets) oncogene homolog |
| FASN | fatty acid synthase |
| FBS | fetal bovine serum |
| FGF | fibroblast growth factor |
| FOX | forkhead box |
| Fuc | fucose |
| G1/2 | gap 1/2-phase |
| Gal | galactose |
| GATA | GATA binding protein |
| GDP | guanosine diphosphate |
| GFP | green fluorescent protein |

| | |
|---|---|
| GH | globular domain of linker histone |
| Glc | glucose |
| GlcA | glucuronic acid |
| GlcNAc | N-acetylglucosamine |
| GM-CSF | granulocyte-macrophage colony-stimulating-factor |
| GMP | guanosine monophosphate |
| GnRH | gonadotropin releasing hormone |
| GOLM | Golgi membrane protein |
| GOLPH | Golgi phosphoprotein |
| GPP130 | 130 kDa Golgi-localized phosphoprotein |
| GSTP | glutathione S-transferase pi |
| HCC | hepatocellular carcinoma |
| Herpud | homocysteine-inducible, endoplasmic reticulum stress-inducible, ubiquitin-like domain member |
| HGF | hepatocyte growth factor |
| HGPIN | high grade PIN |
| $H_n$ | histone n |
| HNF | hepatocyte nuclear factor |
| HPRT | hypoxanthine phosphoribosyltransferase |
| H-score | histochemical score |
| HSP | heat-shock protein |
| HX | homeobox |
| IDP | inosine diphosphate |
| IF | immunofluorescence |
| IGF | insulin-like growth factor |
| IHC | immunohistochemistry |
| IL | interleukin |
| IP | inositol phosphate |
| IRE | inositol-requiring protein |
| ITP | inosine triphosphate |
| IκB | inhibitor of kappa B |
| $K_n$ | lysine n |
| LH | luteinizing hormone |

| | |
|---|---|
| M | metastasis |
| Man | mannose |
| MAPK | mitogen-activated protein kinase |
| $me_n$ | methylated n-times |
| miRNA | microRNA |
| M-phase | mitotic phase |
| mRNA | messenger RNA |
| N | node |
| NDP | nucleoside diphosphate |
| NFκB | nuclear factor kappa-light-chain-enhancer of activated B cells |
| NKn | NKn homeobox |
| NMP | nucleoside monophosphate |
| N-terminus | amino-terminus |
| NTP | nucleoside triphosphate |
| OD | optical density |
| PAP | prostatic acid phosphatase |
| PBS | phosphate buffered saline |
| PCA | prostate cancer antigen |
| pcr | polymerase chain reaction |
| PDGF | platelet-derived growth factor |
| PERK | protein kinase RNA-like endoplasmic reticulum kinase |
| PHA-E | Phaseolus vulgaris Erythoragglutinin |
| PI | propidium iodide |
| PIN | prostatic intraepithelial neoplasia |
| PIP | phosphatidylinositol bisphosphate |
| PK | protein kinase |
| PL | phospholipase |
| PNGase | peptide: N-glycosidase |
| pre-OP | pre-operative |
| PSA | prostate-specific antigen |
| PSGR | prostate-specific G-protein coupled receptor |
| PSMA | prostate-specific membrane antigen |
| pT(NM) | pathological T(NM) |
| PTEN | phosphatase and tensin homolog |
| qRT-PCR | quantitative real-time PCR |

| | |
|---|---|
| RAR | retinoic acid receptor |
| RASSF | Ras association (RalGDS/AF-6) domain family member |
| RNA | ribonucleic acid |
| RPE | radical prostatectomy |
| RPMI | Roswell Park Memorial Institute |
| RT | room temperature |
| SDS | sodium dodecyl sulphate |
| Sia | sialic acid |
| siRNA | small interfering RNA |
| SOX | SRY (sex determining region Y)-box |
| S-phase | synthesis phase |
| SPINK | serine peptidase inhibitor, Kazal type |
| SPP | secreted phosphoprotein |
| T | tumor |
| TARP | T-cell receptor gamma alternate reading frame protein |
| TEMED | tetramethylethylenediamine |
| TGF | transforming growth factor |
| TLE | transducin-like enhancer of split |
| TMA | tissue microarray |
| TMPRSS | transmembrane protease, serine |
| TRIB | tribbles homolog |
| UDP | uridine diphosphate |
| UGGT | UDP-Glc glycoprotein glucosyltransferase |
| UMP | uridine monophosphate |
| unspec | unspecific |
| untr | untreated |
| uPA | u-plasminogen activator |
| uPAR | uPA receptor |
| UPR | unfolded protein response |
| UTP | uridine triphosphate |
| VEGF | vascular endothelial growth factor |
| WB | Western Blot |
| Xyl | xylose |

## 7.2 List of figures

## 7.3 List of tables

## *7.4 Curriculum vitae*

Surname: GERHARDT

Name: Josefine

Date of birth: 17th August 1984

Nationality: German

**Education**

| | |
|---|---|
| since 15th May 2008 | PhD student at the University Zurich<br>• University Hospital Zurich, Institute of Surgical Pathology |
| October 2004-<br>April 2008 | Main studies at the University Heidelberg, Germany<br>• Degree: Diploma (1st April 2008, final mark: 1.0)<br>• Diploma thesis: „Functional interaction of L1-CAM with growth factor receptors“ |
| January 2007-<br>June 2007 | Research fellow at the Karolinska Institute Stockholm, Sweden |
| October 2002-<br>October 2004 | Basic studies at the Technical University of Dresden, Germany<br>• Degree: intermediate diploma (31st August 2004, final mark: 1.4) |
| 1994-2002 | Johannes-Kepler-Gymnasium Chemnitz, Germany<br>• Degree: Abitur (14th June 2002, final mark: 1.2) |

**Publications**

**Gerhardt J***, Montani M*, Wild P, Hermanns T, Müntener M, Kristiansen G. FOXA1 promotes Tumor Progression in Prostate Cancer and represents a novel Hallmark of Castrate Resistant Prostate Cancer. Accepted for publication in Am J Pathol. *These authors contributed equally to the work.

Beer M, Montani M, **Gerhardt J**, Wild PJ, Hany TF, Hermanns T, Müntener M, Kristiansen G. Profiling gastrin-releasing peptide receptor in prostate tissues. Clinical implications and molecular correlates. Prostate 2011.

**Gerhardt J**, Steinbrech C, Büchi O, Behnke S, Bohnert A, Fritzsche F, Liewen H, Stenner F, Wild P, Hermanns T, Müntener M, Dietel M, Jung K, Stephan C, Kristiansen G. The Androgen-Regulated Calcium-Activated Nucleotidase 1 (CANT1) Is Commonly Overexpressed in Prostate Cancer and Is Tumor-Biologically Relevant *in Vitro*. Am J Pathol 2011,178:1847-1860.

Ikenberg K, Fritzsche FR, Zuerrer-Haerdi U, Hofmann I, Hermanns T, Seifert H, Müntener M, Provenzano M, Sulser T, Behnke S, **Gerhardt J**, Mortezavi A, Wild P, Hofstadter F, Burger M, Moch H, Kristiansen G. Insulin-like growth factor II mRNA binding protein 3 (IMP3) is overexpressed in prostate cancer and correlates with higher Gleason scores, BMC Cancer 2010, 10:341.

Tischler V, Fritzsche FR, **Gerhardt J**, Jager C, Stephan C, Jung K, Dietel M, Moch H, Kristiansen G. Comparison of the diagnostic value of fatty acid synthase (FASN) with alpha-methylacyl-CoA racemase (AMACR) as prostatic cancer tissue marker, Histopathology 2010, 56:811-815.

Tischler V, Fritzsche FR, Wild PJ, Stephan C, Seifert HH, Riener MO, Hermanns T, Mortezavi A, **Gerhardt J**, Schraml P, Jung K, Moch H, Soltermann A, Kristiansen G. Periostin is up-regulated in high grade and high stage prostate cancer, BMC Cancer 2010, 10:273.

Kristiansen G, Rose M, Geisler C, Fritzsche FR, **Gerhardt J**, Luke C, Ladhoff AM, Knuchel R, Dietel M, Moch H, Varga Z, Theurillat JP, Gorr TA, Dahl E. Endogenous myoglobin in human breast cancer is a hallmark of luminal cancer phenotype, Br J Cancer 2010, 102:1736-1745.

Fritzsche FR, Stephan C, **Gerhardt J**, Lein M, Hofmann I, Jung K, Dietel M, Kristiansen G. Diagnostic and prognostic value of T-cell receptor gamma alternative reading frame protein (TARP) expression in prostate cancer, Histol Histopathol 2010, 25:733-739.

Riener MO, Pilarsky C, **Gerhardt J**, Grutzmann R, Fritzsche FR, Bahra M, Weichert W, Kristiansen G. Prognostic significance of AGR2 in pancreatic ductal adenocarcinoma, Histol Histopathol 2009, 24:1121-1128.

**Oral presentations**

Joint Annual Meeting of the Swiss and Austrian Society of Pathology, Feldkirch, Austria, 4/11-6/11 2010: Calcium activated Nucleotidase (CANT) 1 and Hepatocyte Nuclear Factor (HNF) 3alpha promote progression of Prostate Carcinomas

94. Jahrestagung der Deutschen Gesellschaft für Pathologie, Berlin, Germany, 27/5 – 30/5 2010: Calcium activated Nucleotidase 1 (CANT1) und Hepatocyte Nuclear Factor 3 alpha (HNF3alpha) fördern die Prostatakarzinomprogression

8th Day of Clinical Research, Zurich, 16/4 2009: Comparative Analysis of Marker Candidates in Prostate Cancer reveals novel Tissue Biomarkers of Malignancy

**Prices**

Posterprice for the best Poster in the field “Cancer” at the 8$^{th}$ Day of Clinical Research, 8/6 2009 in Zurich